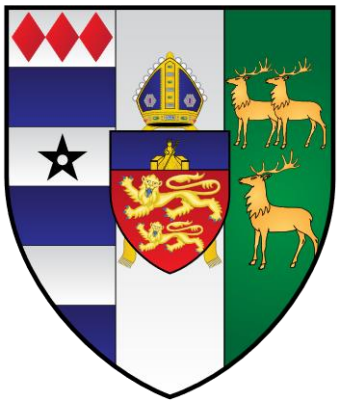
Immunogenicity of protein aldehydes





Lu Li Jovanoska

Lincoln College

Supervisors:

Professor Quentin Sattentau

Professor Anton van der Merwe

A thesis submitted for the degree of

Doctor of Philosophy

Sir William Dunn School of Pathology

The University of Oxford

Michaelmas 2021

Abstract

Protein carbonylation introduces diverse non-enzymatic post-translational modifications (PTMs) containing aldehydes and ketones (reactive carbonyls) during oxidative or glycative stress, and is a hallmark of unhealthy ageing and various neurological, cardiovascular, respiratory, musculoskeletal and metabolic diseases. The activation of innate and adaptive immune responses to carbonylated proteins is thought to trigger or exacerbate these pathologies, although how specific PTMs activate the immune system is not well understood.

In this thesis, the protein hen egg lysozyme (HEL) was modified with glycolaldehyde (GA) as a model to investigate the immunogenicity of protein aldehydes. Mice immunised with HEL GA in the absence of adjuvant produced higher IgG titres to native HEL protein. Chemical reduction of aldehydes to non-reactive alcohol groups maintained equivalent levels of protein cross-linking and mostly abrogated immunogenic responses. Moreover, mice immunised with GA-modified self-homologue mouse lysozyme (ML) produced anti-ML IgG responses to break self-tolerance.

T and B cell adaptive immune responses were investigated to determine their role in GA-mediated immunogenicity. Antigen-specific $CD4^+$ T cell recall responses to native HEL protein were not elevated in mice immunised with HEL GA compared with controls. In contrast, the number of HEL-specific antibody secreting cells (ASCs) was increased in mice after HEL GA immunisation.

Innate immune responses were then considered as potential factors mediating enhanced GA-protein immunogenicity. Binding assays showed that HEL GA had increased mouse C3 degradation product opsonisation compared with controls. Mice depleted of complement C3 using cobra venom factor then immunised with HEL GA suggested greater early anti-HEL IgG responses compared with non-depleted mice. C3 knockout mice immunised with HEL GA also appeared to show increased anti-HEL IgG responses, suggesting an immunoregulatory rather than immunoenhancing role for complement in GA-mediated immunogenicity. Pull-down and co-immunoprecipitation experiments to determine whether GA-modified proteins could engage innate immune factors confirmed increased complement activation and immunoglobulin binding.

In summary, protein aldehydation induced by GA treatment increases IgG antibody responses to native protein and can break self-tolerance in the absence of adjuvant. Protein aldehydes are confirmed to be the immunogenic moiety underlying this immunogenicity because their chemical reduction abrogates most of the ensuing antibody response. Protein aldehydes appear to induce greater B cell activation and differentiation to ASCs, although the GA-enhanced B cell response does not seem to be mediated by $CD4^+$ T helper cells. The mechanism underlying GA-enhanced immunogenicity remains to be determined, although protein aldehydes have altered interactions with various soluble factors including complement and immunoglobulin. This thesis adds to existing knowledge about how protein aldehyde PTMs may activate innate and adaptive immune responses to ultimately lead to unhealthy ageing and associated pathologies.

Acknowledgements

First of all, thank you to my supervisor Quentin Sattentau for his patience, guidance, and encouragement to pursue research in his lab. Thank you also to Amin Moghaddam and Scarlett Harris for their previous work on the project, and my graduate advisor Anton van der Merwe for scientific advice along the way. I am also very thankful to have had the opportunity to discuss my work with viva examiners Mike Dustin and Kevin Marchbank, as well as my other assessors Paul Fairchild, Nicola Ternette and Oliver Bannard.

I am most grateful to all who helped with mass spectrometry (MS), without which half of my thesis would be missing. Thank you to Nicola for expert advice and generous access to MS software; Rod Chalk and Tiago Moreira at the Centre for Medicines Discovery for helpful MS lectures and assistance in using the open access MS facility; Marjorie Fournier of the Advanced Proteomics Facility; Sarah Bonham and Iolanda Vendrell of the Discovery Proteomics Facility; and Lilli Hahn for her advice on analysing MS data.

A huge thank you also goes to the Pathology Support Building staff, without which the other half of my thesis would not exist: Nicky Hamp, Dom Paczoska and Clare Allen for taking care of my mice, and Linda Randall for smooth running of the facility. I am also hugely grateful for the expertise of Robert Hedley, Michal Maj and Line Eriksen of the flow cytometry facility.

Thank you to all our collaborators who generously provided reagents, services, and advice from all over the world, especially Tadashi Ueda from Kyushu University; Naorem Nihesh and Aaron Esser-Kahn from the University of Chicago; Oliver Bannard and Tal Arnon at the University of Oxford; Paul Morgan and Wioleta Zelek at the University of Cardiff; and Kenneth Reid for his invaluable advice on complement biology.

I am very thankful to Quentin, Kristijan Jovanoski, Lachlan Deimel, Maeva Dupont and Anton for providing valuable comments on my thesis, and Kristijan for extensive software troubleshooting.

Thank you to Sattentau lab members past and present for being wonderful colleagues and making the lab a supportive and fun environment: Cherrelle Dacon, Kate Dicker, Lachlan, Linnea Drexhage, Maeva, Niloofar Karaji, Rebecca Moore, Scarlett and Shengpan Zhang. Scarlett and Lachlan, it has been a pleasure to work together during those long mouse protocols and thank you for experimental advice and chats. Xiaochao Xue and Aziz Khan, thank you for putting up with my endless chemistry questions.

I have been privileged to work at the Sir William Dunn School of Pathology. Thank you to all who provided technical advice, especially Adam Harding for ELISpot. I would like to also thank the admin staff, support staff, and cleaning staff for all their efforts behind the scenes, especially for their care and concern during the pandemic.

I sincerely thank Lincoln College for providing me with the opportunity and funding to read my DPhil at the University of Oxford, and the advice from my lovely college advisor Mohammad Mofatteh on personal and professional matters.

Finally, to my parents Bing and Holly, thank you for your unconditional love and support throughout my life. Most of all, to Kristijan, thank you for keeping me sane and fed in the weeks leading up to submission and encouraging me through the most difficult moments of my DPhil. I couldn't have done it without you! You are my rock and inspiration and this thesis is for you.

Table of Contents

Abstract ..... **iii**

Acknowledgements ..... **v**

Table of Contents ..... **vii**

List of Figures ..... **xi**

List of Tables ..... **xvii**

Abbreviations ..... **xix**

1 Introduction **1**

1.1 Immune responses to infection and injury 1

1.2 Protein immunogenicity 4

1.3 Protein carbonylation 7

1.4 Immune consequences of protein carbonylation 16

1.5 Thesis scope and aims 19

2 Materials & Methods **21**

2.1 General 21

2.1.1 Reagents and reaction conditions 21

2.1.2 Enzyme-linked immunosorbent assays (ELISAs) 21

2.2 Protein preparation, modification, and characterisation 22

2.2.1 Peptide reconstitution and quantification 22

2.2.2 Protein reconstitution and quantification 22

2.2.3 Endotoxin removal 23

2.2.4 Murine Toll-like receptor 4 (mTLR4) reporter assay 23

2.2.5 Pattern-associated molecular pattern (PAMP) reporter assay 23

2.2.6 Peptide modification and desalting 24

2.2.7 Protein modification and desalting 24

2.2.8 2,4-Dinitrophenylhydrazine (DNPH) carbonyl assay 25

2.2.9 Biotin hydrazide carbonyl assay 25

2.2.10 Biotin labelling 25

2.2.11 SDS-PAGE 26

2.2.12 Liquid chromatography mass spectrometry (LC-MS) 26

2.2.13 Liquid chromatography tandem MS (LC-MS/MS) 27

2.3 Cellular studies 27

2.3.1 Cell culture conditions 27

2.3.2 Bone marrow-derived dendritic cells (BMDCs) 28

2.3.3 Antigen presentation assays 28
2.3.4 MD4 splenocyte assays 29
2.3.5 Flow cytometry 29
2.4 Animal studies 30
2.4.1 Mouse strains 30
2.4.2 Immunisations 30
2.4.3 Blood sampling 30
2.4.4 Assessing in vivo antibody responses 30
2.4.5 Lymphocyte recall assay 31
2.4.6 ^{3}H thymidine proliferation assay 32
2.4.7 Cytokine ELISAs 32
2.4.8 B cell enzyme-linked immunosorbent spot (ELISpot) assay 32
2.4.9 MD4 adoptive transfer 33
2.4.10 Cobra venom factor (CVF) administration 33
2.5 Complement studies 34
2.5.1 Sera for functional complement assays 34
2.5.2 Complement activation ELISAs 34
2.5.3 Complement C3 ELISA 35
2.5.4 Complement C1q binding ELISA 35
2.5.5 Immunoglobulin binding ELISAs 36
2.6 Proteomics studies 36
2.6.1 Pull-down assay with human sera 36
2.6.2 Co-immunoprecipitation (co-IP) assay with mouse sera 37
2.6.3 On bead and in solution digests 37
2.6.4 Pull-down and co-IP LC-MS/MS 38
2.6.5 LC-MS/MS analysis 39
2.7 Computational and statistical analysis 39
2.7.1 Illustrations 39
2.7.2 Statistical analysis 39
3 Immunogenicity and biochemical characterisation 41
3.1 Background 41
3.1.1 Detecting protein carbonyls 41
3.1.2 Post-translational modifications caused by glycolaldehyde 44
3.1.3 Chapter aims 46
3.2 Results 47
3.2.1 GA-modified HEL elicits IgG responses to native protein 47
3.2.2 Biochemical characterisation of HEL GA and HEL PR 51

3.2.3 Optimising HEL GA treatment for in vivo immunogenicity 55
3.2.4 Lysines are targets of GA modification and K97 is a key residue 68
3.2.5 Breaking self-tolerance with GA-modified mouse lysozyme 73
3.3 Discussion 81
3.3.1 Results summary 81
3.3.2 Challenges with MS characterisation of GA-induced PTMs 82
3.3.3 Variable antibody responses to GA-modified proteins 84
3.3.4 Autoantigen-induced experimental autoimmune disease models 86
3.4 Conclusions 87

4 GA-mediated adaptive immunogenicity 91
4.1 Background 91
4.1.1 Brief overview of adaptive immune activation 91
4.1.2 Potential mechanisms of aldehyde-enhanced adaptive immunity 94
4.1.3 Chapter hypotheses and aims 97
4.2 Results 98
4.2.1 In vitro $HEL_{11–26}$ peptide presentation to $CD4^+$ T cell hybridomas 98
4.2.2 $HEL_{11–25/26}$ peptide treated with GA is modified at the N-terminus 99
4.2.3 Any N-terminal modification to $HEL_{11–25}$ is sufficient 105
4.2.4 GA treatment N-terminally modifies all HEL peptides in vitro 105
4.2.5 GA-modified peptides may induce stronger IgG responses in vivo 111
4.2.6 GA-modified protein does not enhance subdominant epitopes 114
4.2.7 $CD4^+$ T cell responses in HEL GA and ML GA immunised mice 115
4.2.8 Anti-HEL IgG responses appear to be thymus dependent 120
4.2.9 HEL GA immunised mice have more HEL-specific ASCs 123
4.2.10 In vitro and in vivo MD4 B cell proliferation 134
4.3 Discussion 137
4.3.1 Results summary 137
4.3.2 Differences between peptide and protein GA modifications 139
4.3.3 $CD4^+$ T cell memory recall responses in GA-immunised mice 141
4.3.4 Alternative hypotheses for enhanced B cell activation 144
4.4 Conclusions 145

5 GA-mediated innate immunogenicity 147
5.1 Background 147
5.1.1 Pattern recognition in innate immunity 147
5.1.2 Innate immune modulation by protein carbonyls 148
5.1.3 Overview of the complement cascade 150
5.1.4 Complement enhancement of antibody responses 156

5.1.5 Measuring complement activation and opsonisation 158
5.1.6 Chapter hypotheses and aims 159
5.2 Results 160
5.2.1 C1q binding to HEL GA 160
5.2.2 C3 activation and degradation product deposition on HEL GA 164
5.2.3 In vitro MD4 B cell activation with complement from mouse sera 166
5.2.4 IgG responses in C3-depleted mice immunised with HEL GA 171
5.2.5 IgG responses in C3 knockout mice immunised with HEL GA 175
5.2.6 Pull-down MS for HEL GA interaction partners in human sera 180
5.2.7 Co-IP MS for HEL GA interaction partners in mouse sera 193
5.2.8 Validation of immunoglobulin binding 208
5.3 Discussion 213
5.3.1 Results summary 213
5.3.2 Non-specific C1q binding to HEL 213
5.3.3 Complement activation in mice and humans 215
5.3.4 Comparison of pull-down and co-IP experiments 217
5.3.5 Complement activation and immunogenicity 219
5.3.6 Potential protein interactions of interest with HEL GA 220
5.4 Conclusions 222
6 Discussion & Conclusion 225
6.1 Thesis summary 225
6.2 Intermediate aldehydes versus stable end-products 226
6.3 Alternative methods of protein aldehydation 227
6.4 Alternative model proteins 230
6.5 Future prospects 233
Bibliography 235
Appendix 263

List of Figures

Figure 1.1: Relative reactivity of carbonyl groups. 8
Figure 1.2: Oxidative and glycative stress leads to protein carbonylation and ultimately protein cross-linking or other stable end-products. 9
Figure 1.3: Direct oxidation of amino acid side chains can generate protein carbonyls. 10
Figure 1.4: Formation of selected 4-hydroxy-2-nonenal (HNE) PTMs. 11
Figure 1.5: Formation of selected 2-propenal (acrolein) PTMs. 12
Figure 1.6: Formation of selected malondialdehyde (MDA)-based PTMs. 13
Figure 1.7: Protein glycation by glucose and fructose, and selected PTMs arising from the Amadori breakdown product 3-deoxyglucosone (3-DG). 15
Figure 3.1: Commonly used derivatisation reagents for detecting reactive carbonyls (RCs). 43
Figure 3.2: Reaction of glycolaldehyde (GA) with protein. 45
Figure 3.3: Specific PTMs and their monoisotopic mass changes resulting from modification with glycolaldehyde (GA) and its oxidation product glyoxal. 47
Figure 3.4: Sequence (UniProt ID: P00698) and structure of hen egg lysozyme (HEL). 49
Figure 3.5: HEL GA immunisation elicits higher anti-HEL IgG responses compared with HEL mock in female BALB/c mice. 51
Figure 3.6: HEL GA immunisation elicits higher anti-HEL IgG responses compared with HEL mock and HEL PR in female BALB/c mice. 52
Figure 3.7: GA treatment increases HEL carbonylation and oligomerisation, and post-reduction (PR) decreases carbonylation. 53
Figure 3.8: GA treatment causes PTMs and PR treatment selectively reduces RC-containing PTMs. 54
Figure 3.9: DNPH derivatisation of HEL GA identifies three RC-containing peaks. ... 56
Figure 3.10: Carbonylation and oligomerisation increase over time with HEL GA modification. 58
Figure 3.11 HEL GA-modified for 3 h elicits higher IgG titres. 59
Figure 3.12: Increasing GA concentration increases PTMs, while increasing protein concentration decreases the proportion of modified HEL. 60
Figure 3.13: GA modification does not proceed at lower temperatures, and modified protein is best preserved at -80 °C. 62
Figure 3.14: GA modification in acetate buffer is more efficient at higher pH and favours single GA-aldoamine. 63
Figure 3.15: GA modification in citrate buffer is more efficient at higher pH and favours single GA-aldoamine. 64

Figure 3.16: GA modification in phosphate buffer is highly efficient and results in extensive PTMs. 65
Figure 3.17: Selected HEL GA prepared in different buffers then buffer exchanged into PBS for in vivo experiments..... 67
Figure 3.18: HEL GA elicits higher IgG titres compared with HEL PR under several buffer conditions..... 68
Figure 3.19: User-specified PTMs detected by LC-MS/MS for HEL mock..... 70
Figure 3.20: User-specified PTMs detected by LC-MS/MS for HEL GA (3 h). 71
Figure 3.21: User-specified PTMs detected by LC-MS/MS for HEL GA 7 d..... 72
Figure 3.22: K97 is a key residue that increases the extent of GA modification. 75
Figure 3.23: Sequence and structure of mouse lysozyme (ML) compared with HEL. .. 76
Figure 3.24: ML cleaned of endotoxin before immunisation. 77
Figure 3.25: ML GA treatment increases protein carbonylation and oligomerisation, while PR treatment decreases carbonylation. 78
Figure 3.26: ML GA treatment increases PTMs, while PR treatment selectively reduces RC-containing PTMs. 79
Figure 3.27: Mouse lysozyme (self-protein) modified with GA elicits higher IgG responses compared with ML mock and ML PR. 80
Figure 4.1: GA modification of $HEL_{11–26}$ peptide increases presentation, but is not reversed by PR. 100
Figure 4.2: $HEL_{11–25}$ peptides chemically capped to block GA modification on specific amino groups. 102
Figure 4.3: GA modification of $HEL_{11–25}$ peptide is mostly prevented by N-terminal capping. 103
Figure 4.4: $HEL_{11–26}$ GA peptide is predominantly modified on the N-terminus and $HEL_{11–26}$ PR is not reduced. 104
Figure 4.5: Any N-terminal modification on $HEL_{11–25}$ is sufficient to enhance peptide presentation..... 106
Figure 4.6: Peptides require a free N-terminal amine for GA modification..... 109
Figure 4.7: GA-aldoamine compared with acetylation. 111
Figure 4.8: N-terminal (Nt)-acetylation and GA modification have different effects on peptide presentation. 112
Figure 4.9: GA-modified HEL peptides may elicit anti-peptide IgG responses in vivo. 113
Figure 4.10: HEL GA protein presentation to $CD4^+$ T cell hybridomas in vitro does not show selective enhancement of subdominant epitopes. 117
Figure 4.11: Splenocytes from HEL mock and HEL GA immunised mice have similar proliferative responses to HEL peptide stimulation. 118
Figure 4.12: HEL-specific splenocyte proliferation is not enhanced after prime and boost with HEL GA compared with HEL mock and HEL PR. 119

Figure 4.13: Mice repeatedly boosted with ML GA have detectable splenocyte responses. 122
Figure 4.14: Anti-HEL IgG responses to HEL GA immunisation appear to be thymus-dependent. 122
Figure 4.15: ELISpot detection of total antibody-secreting cells (ASCs). 124
Figure 4.16: Biotinylated HEL can be used to detect HEL-specific ASCs. 125
Figure 4.17: HEL-specific ASCs are effectively stimulated by in vivo boosting. 127
Figure 4.18: HEL-specific ASCs can be detected in bone marrow without boosting. 128
Figure 4.19: HEL-specific ASCs are less effectively stimulated in vitro. 129
Figure 4.20: ELISpot images from immunised mice boosted 7 d prior to ELISpot. 132
Figure 4.21: Greater numbers of HEL-specific ASCs detected in HEL GA immunised mice compared with HEL mock and HEL PR. 133
Figure 4.22: No HEL-specific ASCs detected for no-adjuvant HEL-immunised mice after prime. 135
Figure 4.23: Naïve transgenic MD4 splenocytes co-stimulated in vitro with HEL mock have higher responses compared with HEL GA and HEL PR. 136
Figure 4.24: Adoptive transfer of MD4 (HEL-specific) B cells to wild type (WT) congenic hosts. 138
Figure 5.1: The complement cascade. 151
Figure 5.2: Negative regulation of complement activation. 154
Figure 5.3: Cleavage of C4. 155
Figure 5.4: Cleavage of C3. 155
Figure 5.5: C3 activation products and their receptors. 155
Figure 5.6: C1q-biotin binds more strongly to HEL GA compared with HEL mock and HEL PR. 161
Figure 5.7: Human C1q-biotin appears to bind non-specifically to BSA and hIgG1-GAGA negative controls. 162
Figure 5.8: Old C1q stocks bind non-specifically to hIgG1-GAGA negative controls. 163
Figure 5.9: Mouse C1q binds specifically to BSA GA 7 d but does not bind to HEL. 164
Figure 5.10: Complement activation via classical, lectin and alternative pathways differ between sources of normal human sera. 166
Figure 5.11: Mouse C3 activation and degradation product deposition on HEL GA is greater compared with HEL mock and HEL PR. 167
Figure 5.12: 1% normal mouse sera can be added as a source of complement for in vitro assays. 169
Figure 5.13: FBS cannot be substituted with HL-1 chemically-defined supplement for splenocyte proliferation assays. 170
Figure 5.14: Normal mouse sera enhances anti-CD40 co-stimulation but negates LPS co-stimulation. 170

Figure 5.15: Transient depletion of complement C3 has no effect on anti-HEL IgG titres 4 weeks post-prime. 172
Figure 5.16: Transient depletion of complement C3 has early effects on anti-HEL IgG responses. 174
Figure 5.17: Transient depletion of complement C3 has no effect on later anti-HEL IgG titres or splenocyte responses. 176
Figure 5.18: C57BL/6 mice can develop anti-HEL IgG responses from no-adjuvant HEL immunisations with high doses and boosting. 177
Figure 5.19: Bleed and immunisation schedule for the $C3^{-/-}$ experiment. 178
Figure 5.20: $C3^{-/-}$ mice have higher anti-HEL IgG responses compared with WT controls for HEL GA immunisation. 179
Figure 5.21: Magnetic beads become carbonylated after GA treatment. 181
Figure 5.22: Overview of pull-down experiment. 182
Figure 5.23: Less HEL bait is detected by tandem LC-MS in HEL GA pull-down despite being abundant in SDS-PAGE. 183
Figure 5.24: HEL mock and HEL PR pull-downs are more similar than to HEL GA. 185
Figure 5.25: List of 60 proteins enriched (red) or depleted (blue) > 1 FC in HEL GA pull-down compared with HEL mock, HEL PR and beads. 186
Figure 5.26: List of 80 proteins enriched (red) or depleted (blue) with > 1 FC in HEL GA pull-down compared with HEL mock and HEL PR (but not beads). 188
Figure 5.27: Complement proteins are most abundant in HEL GA pull-down. 190
Figure 5.28: Complement activation is generally increased for HEL GA pull-down compared with HEL mock and HEL PR. 191
Figure 5.29: Immunoglobulins (Igs) are more abundant in beads control and HEL GA pull-down. 193
Figure 5.30: Many Ig constant regions are enriched in HEL GA pull-down compared with HEL mock and HEL PR. 194
Figure 5.31: Apolipoproteins are more abundant in beads control and HEL GA pull-down. 195
Figure 5.32: Monoclonal mouse IgG1 anti-HEL antibodies bind similarly to HEL GA and HEL PR. 195
Figure 5.33: HEL immunoprecipitation and elution are more efficient using HyHEL-10 compared with D1.3. 196
Figure 5.34: Co-IP after incubating HEL GA with normal mouse sera captures more proteins. 197
Figure 5.35: Overview of co-IP experiment. 199
Figure 5.36: More proteins are co-immunoprecipitated but less HEL bait is detected by tandem LC-MS for HEL GA eluant compared with HEL mock and HEL PR eluants. 200
Figure 5.37: HEL mock and HEL PR co-IP are more similar compared with HEL GA. 201

Figure 5.38: List of 64 proteins enriched (red) or depleted (blue) > 1 FC in HEL GA co-IP compared with HEL mock, PR, no bait and input controls. 202
Figure 5.39: List of 84 proteins enriched (red) or depleted (blue) > 1 FC in HEL GA co-IP compared with HEL mock and HEL PR, but not relative to no bait or input controls. 204
Figure 5.40: Complement proteins are least abundant in HEL GA co-IP. 205
Figure 5.41: Increased classical or lectin complement activation and amplification in HEL GA co-IP compared with HEL mock and HEL PR. 206
Figure 5.42: Immunoglobulins may be more abundant in no bait control and HEL GA co-IP. 208
Figure 5.43: IgM constant region is enriched in HEL GA co-IP. 209
Figure 5.44: Ribosomal proteins are most abundant in HEL GA co-IP. 210
Figure 5.45: Apolipoproteins are least abundant in HEL GA co-IP. 210
Figure 5.46: Natural IgM from sera may bind better to HEL GA compared with HEL mock and HEL PR. 211
Figure 5.47: IgG from sera may bind better to HEL GA compared with HEL mock and HEL PR. 212
Figure A.1: Overlaid intact LC-MS spectra comparing HEL GA (orange) and HEL PR (green) samples. 263
Figure A.2: Unbiased search for modifications detected with LC-MS/MS for HEL mock. 264
Figure A.3: Unbiased search for modifications detected with LC-MS/MS for HEL GA 3 h. 265
Figure A.4: Unbiased search for modifications detected with LC-MS/MS for HEL GA 7 d. 266
Figure A.5: Anti-ML IgG responses measured in the second ML immunisation experiment. 267
Figure A.6: Splenocytes from HEL mock and HEL GA primed mice have similar cytokine responses after native HEL protein stimulation. 267
Figure A.7: HEL-specific splenocyte proliferation is not enhanced after priming with HEL GA compared with HEL mock and HEL PR, and does not correlate with anti-HEL IgG titre. 268
Figure A.8: Gating strategy for adoptively transferred MD4 B cells ($B220^{+}CD45.1^{+}$) in wild type (WT) B6 congenic hosts. 269
Figure A.9: Setting up conditions for the HEL mock, HEL GA and HEL PR pull-down experiment. 270

List of Tables

Table 3.1: Parameters for user-defined PTMs. 70
Table 3.2: PTMs detected by nano-LC-MS/MS in the Hoffmann lab (Leipzig University). 74
Table 3.3: Lysines present (colour) or mutated to arginine (grey) for seven HEL mutants and HEL WT. 74
Table 3.4: Experimental autoimmune diseases induced by autoantigen immunisation. 88
Table 3.5: Studies on breaking self-tolerance using non-enzymatic chemical modifications. 88
Table 4.1: BALB/c $CD4^+$ T cell hybridomas corresponding to HEL epitopes in vivo.. 99
Table 5.1: ORA of pull-down hits compared with background show significant enrichment of gene ontology (GO) terms. 189
Table 5.2: ORA of pull-down hits compared with background does not show significant enrichment of GO pathways. 190
Table 5.3: Common hits between normal human sera pull-down and normal mouse sera co-IP. 211
Table A.1: Over representation analysis (ORA) of pull-down hits compared with background show significant enrichment of terms and pathways. 271

Abbreviations

•OH	Hydroxyl radical
2-ME	2-Mercaptoethanol
3-DG	3-Deoxyglucosone
^{3}H	Tritium
A_{280}	Absorbance 280 nm
A_{450}	Absorbance 450 nm
AA	Acetaldehyde
AAS	α-Aminoadipic semialdehyde
ACE2	Angiotensin-converting enzyme 2
ACN	Acetonitrile
AGE	Advanced glycation end-products
ALE	Advanced lipoxidation end-products
ALR	AIM2-like receptor
ANOVA	Analysis of variance
AO-DAPI	Acridine orange and 4′,6-diamidino-2-phenylindole
AP-1	Activator protein 1
APC	Antigen-presenting cell
APL	Altered peptide ligand
ARP	Aldehyde-reactive probe, N′-aminooxymethylcarbonylhydrazino-D-biotin
ASC	Antibody secreting cell
ATP	Adenosine triphosphate
B6	C57BL/6
BCA	Bicinchoninic acid
BCR	B cell receptor
BG	Background
BH	Biotin hydrazide
BM	Bone marrow
BMDC	Bone marrow-derived dendritic cell
BMDM	Bone marrow-derived macrophage
BSA	Bovine serum albumin
C1qA	C1q subunit A
C1qB	C1q subunit B
C3aR	C3a receptor
C4BP	C4b-binding protein
C5	Citrate pH 5 buffer
C5aR	C5a receptor
$CaCl_2$	Calcium chloride
Cat	Cathepsin
CD5L	CD5 antigen-like
CFA	Complete Freund’s Adjuvant
CFHR	Complement factor H-related
CFSE	Carboxyfluorescein succinimidyl ester
CHO	Chinese hamster ovary
CI	Confidence interval
CID	Collision-based dissociation
CII	Collagen II

CLR	C-type lectin receptor
CMA	Carboxymethyl arginine
CMC	Carboxymethyl cysteine
CML	Carboxymethyl lysine
CO_2	Carbon dioxide
Co-IP	Co-immunoprecipitation
CPM	Counts per minute
CR	Complement receptor
CR1	Complement receptor 1
CR2	Complement receptor 2
CR3	Complement receptor 3
CR4	Complement receptor 4
CRIg	Complement receptor of the immunoglobulin superfamily
CRIT	C2 receptor inhibitor trispanning
CRP	C-reactive protein
Crry	Complement receptor 1-related protein y
Cu^{2+}	Copper ion
CVF	Cobra venom factor
d	Days
Da	Dalton
DAF	Decay-accelerating factor
DAMP	Damage-associated molecular pattern
DAVID	Database for Annotation Visualisation and Integrated Discovery
DC	Dendritic cell
DDA	Data-dependent acquisition
dH_2O	Distilled water
DMSO	Dimethyl sulfoxide
DNA	Deoxyribonucleic acid
DNPH	2,4-Dinitrophenylhydrazine
EAE	Experimental autoimmune encephalomyelitis
EAGLE	Either advanced glycation or lipoxidation end-products
ECM	Extracellular matrix
EDC	1-Ethyl-3-(3-dimethylaminopropyl)carbodiimide
EDTA	Ethylenediaminetetraacetic acid
EGTA	Egtazic acid
ELISA	Enzyme-linked immunosorbent assay
ELISpot	Enzyme-linked immunosorbent spot
ERK1/2	Extracellular-signal-regulated kinase 1/2
ESI-QTOF	Electrospray ionisation quadrupole time-of-flight
ETD	Electron-based fragmentation
EU	Endotoxin unit
FA	Formaldehyde
FBS	Foetal bovine serum
FC	Fold change
Fc	Fragment crystallisable
FcR	Fragment crystallisable receptor
FDC	Follicular dendritic cell
FDR	False discovery rate
Fe^{3+}	Iron ion
FGE	Formylglycine-generating enzyme

Flt3	FMS-like tyrosine kinase 3
FMO	Fluorescence minus one
Fmoc	Fluorenylmethyloxycarbonyl
FVS	Fixable viability stain
GA	Glycolaldehyde
GC	Germinal centre
GGS	γ-Glutamic semialdehyde
GM-CSF	Granulocyte-macrophage colony-stimulating factor
gMFI	Geometric mean fluorescence intensity
GO	Gene ontology
GPCR	G-protein coupled receptor
h	Hours
H_2O_2	Hydrogen peroxide
H_2SO_4	Sulfuric acid
HCD	Higher-energy collision dissociation
HCl	Hydrochloric acid
HEK293	Human embryonic kidney 293
HEL	Hen egg lysozyme
HEPES	4-(2-Hydroxyethyl)-1-piperazineethanesulfonic acid
HLA	Human leukocyte antigen
HNE	4-Hydroxy-2-nonenal
HOCl	Hypochlorous acid
HPLC	High-performance liquid chromatography
HRP	Horseradish peroxidase
HSA	Human serum albumin
i.d.	Intradiameter
i.p.	Intraperitoneal
i.v.	Intravenous
IFA	Incomplete Freund's Adjuvant
Ig	Immunoglobulin
IL	Interleukin
ILC	Innate lymphoid cell
IP	Immunoprecipitation
KEL	Kell (antigen)
LC-MS	Liquid chromatography mass spectrometry
LC-MS/MS	Liquid chromatography tandem mass spectrometry
LDL	Low-density lipoprotein
LDS	Lithium dodecyl sulphate
LLPC	Long-lived plasma cell
LN	Lymph node
LOX	Lysyl oxidase
LOX-1	Lectin-like oxidised LDL (low-density lipoprotein) receptor 1
Lp1A	Lipoic acid ligase
LPS	Lipopolysaccharide
LTA	Lipoteichoic acid
MAA	Malondialdehyde-acetaldehyde
mAb	Monoclonal antibody
MAC	Membrane attack complex
MARCO	Macrophage receptor with collagenous structure
MASP	MBL-associated serine protease

MBL	Mannose-binding lectin
MBP	Mannose-binding protein
MCO	Metal catalysed oxidation
MCP	Membrane cofactor protein
MDA	Malondialdehyde
MES	2-(N-morpholino)ethanesulfonic acid
$MgCl_2$	Magnesium chloride
MHC	Major histocompatibility complex
MIRL	Membrane inhibitor of reactive lysis
ML	Mouse lysozyme
MOG	Myelin oligodendrocyte glycoprotein
MS	Mass spectrometry
MS/MS	Tandem mass spectrometry
MSA	Mouse serum albumin
MSP1–19	Merozoite surface protein 1 19 kDa
$NaBH_4$	Sodium borohydride
$NaIO_4$	Sodium (meta)periodate
nanoLC	Nano liquid chromatography
NaOH	Sodium hydroxide
NFκB	Nuclear factor-kappa B
NHS	Normal human sera
NK	Natural killer
NLR	Nucleotide-binding and oligomerisation domain-like receptor
NMR	Nuclear magnetic resonance
NMS	Normal mouse sera
ns	Not significant
NSAF	Normalised spectral abundance factor
Nt	N-terminal
Nu	Nucleophile
ONE	4-Oxo-2-nonenal
$ONOO^-$	Peroxynitrite
ORA	Over representation analysis
OVA	Ovalbumin
OxLDL	Oxidised low-density lipoprotein
P6	Phosphate pH 6 buffer
PAMP	Pathogen-associated molecular pattern
PBS	Phosphate-buffered saline
PBS++	Phosphate-buffered saline containing $CaCl_2$ and $MgCl_2$
PBST	Phosphate-buffered saline Tween-20 (0.05%)
PFA	Paraformaldehyde
PFC	Plaque-forming cell
PFR	Peptide flanking region
PFTase	Protein farnesyl-transferase
PMA	Phorbol myristate acetate
pMHC	Peptide-major histocompatibility complex
Poly I:C	Polyinosinic:polycytidylic acid
PR	Post reduced
PRM	Pattern recognition molecule
PRR	Pattern recognition receptor
PSM	Peptide spectrum match

PTM	Post-translational modification
PTX3	Pentraxin 3
PUFA	Polyunsaturated fatty acid
RAGE	Receptor for advanced glycation end-products
RBC	Red blood cell
RC	Reactive carbonyl
RLR	Retinoic acid-inducible gene 1-like receptor
RMSD	Root-mean-square deviation
RNA	Ribonucleic acid
RNAse	Ribonuclease
ROS	Reactive oxygen species
RSA	Rat serum albumin
RSV	Respiratory syncytial virus
RT	Room temperature
s.c.	Subcutaneous
SAA	Serum amyloid A
SAF	Spectral abundance factor
SD	Standard deviation
SDS-PAGE	Sodium dodecyl sulphate polyacrylamide gel electrophoresis
SEAP	Secreted embryonic alkaline phosphatase
SEM	Standard error of the mean
SFB	Succinimidyl 4-formylbenzoate
SLO	Secondary lymphoid organ
SP-40,40	Clusterin
SP-A	Surfactant protein A
sPRR	Soluble pattern recognition receptor
SR	Scavenger receptor
SR-A	Scavenger receptor A
SRCR	Scavenger receptor cysteine-rich
SUSD4	Sushi domain-containing 4
TCEP	Tris(2-carboxyethyl)phosphine
TCR	T cell receptor
TD	Thymus dependent
TFA	Trifluoroacetic acid
T_{FH}	T follicular helper
TGFβ1	Transforming growth factor beta 1
T_H	T helper
TI	Thymus independent
TLR	Toll-like receptor
TMB	3,3′,5,5′-Tetramethylbenzidine
T_{reg}	T regulatory
TSP-1	Thrombospondin 1
TTL	Tubulin tyrosine ligase
UV	Ultraviolet
V	Volts
VBS	Veronal buffered saline
WT	Wild type

Chapter 1

Introduction

1.1 Immune responses to infection and injury

The innate and adaptive immune systems provide protection against infection and injury. Innate immunity is based on germline-encoded molecules recognising conserved patterns related to pathogens and damage, followed by the rapid deployment of non-specific effector functions to form the initial response. In contrast, adaptive immunity is based on the specific recognition of antigen from a diverse repertoire of lymphocytes that is further refined by somatic gene rearrangements. The adaptive immune response takes longer to reach complete maturity, but is highly specific, sensitive, and provides lasting immunological memory against future challenges (Chaplin 2010; Marshall et al. 2018).

The innate immune system detects biomolecular signatures known as pathogen-associated molecular patterns (PAMPs), which indicate infection, or damage-associated molecular patterns (DAMPs), which indicate host stress. PAMPs often have conserved features that are distinct from those of the host, such as peptidoglycan in bacterial cell walls, lipopolysaccharide (LPS) of gram-negative bacteria, lipoteichoic acid (LTA) of gram-positive bacteria, unmethylated CpG from bacterial and viral DNA, and double stranded RNA from viruses (Mogensen 2009). In contrast, DAMPs are molecules related

to cellular stress or tissue injury. Dying or injured cells may release intracellular components such as nucleic acids, actin, uric acid or adenosine triphosphate (ATP), which are recognised as danger signals (Roh and Sohn 2018; Schaefer 2014).

PAMPs and DAMPs are recognised by pattern recognition receptors (PRRs) expressed by innate sensor cells of the myeloid lineage (e.g. macrophages, neutrophils, and dendritic cells) or pattern recognition molecules (PRMs) in the humoral (extracellular) space. PRR recognition of PAMPs and DAMPs triggers the innate immune response by activating effector functions or amplifying the immune response (Janeway and Medzhitov 2002). Effector functions can involve the destruction or neutralisation of pathogen components; for example, the cleavage of bacterial cell walls by lysozyme and defensin, cell lysis mediated by complement, binding by circulating natural antibodies, and ingestion then digestion by phagocytes. The immune response can also be amplified through the release of cytokines and chemokines that promote local inflammation and recruit other circulating effector cells. Innate responses can also be amplified or modulated by the expression of co-stimulatory molecules on innate sensor cells, which activate specific subsets of innate lymphoid cells (ILCs) that secrete their own cytokines and chemokines (Klose and Artis 2020).

If the innate immune response is unable to resolve the infection or injury, adaptive immunity is recruited to provoke a more targeted response. Activated dendritic cells (DCs) bearing digested antigen on major histocompatibility complex (MHC) molecules enter secondary lymphoid organs (SLOs) to initiate the selection and expansion of naïve T and B lymphocyte clones, which display specific reactivity to antigen through their highly variable antigen receptors (Hodgkin, Heath, and Baxter 2007).

T lymphocytes can be broadly classified as $CD8^+$ or $CD4^+$ T cells based on the expressed T cell co-receptor. $CD8^+$ T cells are cytotoxic and can directly lyse infected

cells, whereas $CD4^+$ T cells are helper cells that aid the ongoing immune response. $CD4^+$ T helper 1, 2 and 17 effector cells (T_H1, T_H2 and T_H17) migrate to the site of infection or injury. T follicular helper (T_{FH}) cells remain within the SLOs to promote B cell antibody class switching, affinity maturation and differentiation to antibody-producing plasma cells. T regulatory (T_{reg}) cells suppress T_H cell activity to prevent immune overactivation (Luckheeram et al. 2012).

B lymphocytes secrete antibodies (immunoglobulin, Ig) that enhance adaptive immune responses by antigen neutralisation, opsonisation and fragment crystallisable receptor (FcR)-dependent functions. Antibodies can be classified into five main isotypes (IgM, IgD, IgE, IgA, IgG) based on the antibody heavy chain, which determines antibody distribution and effector functions (Schroeder and Cavacini 2010).

The first isotype secreted by B cells is IgM, which tends to have low affinity but forms pentamers that confer high overall avidity and effectively activate complement. IgD is also expressed on naïve B cells and exists in a secreted form, but its functions are poorly understood. IgE is mostly found bound to FcR on mast cells and facilitates the release of inflammatory mediators such as histamine upon antigen binding. The isotypes IgA and IgG are both fairly effective at neutralisation, opsonisation, and complement activation. IgA is typically found in secretions and mucosal linings, while IgG is the most abundant isotype in blood and extracellular fluid. IgG can be divided further into subclasses IgG1, IgG2, IgG3, IgG4 in humans (Vidarsson, Dekkers, and Rispens 2014) and IgG1, IgG2a/c, IgG2b, IgG3 in mice (Zhang, Goldschmidt, and Salter 2012).

The nature of infection or injury determines the specific PRRs activated and ultimately which immune effector functions are triggered (Fearon and Locksley 1996; McKenzie, Spits, and Eberl 2014). Immune effector module types 1, 2 and 3 each favour specific cytokines, ILC or T cell differentiation programs, and antibody isotypes to deploy

the most suitable response to a particular infection or injury (Annunziato, Romagnani, and Romagnani 2015). Type 1 immunity is initiated in response to intracellular bacteria, viruses, and parasites, and favours the recruitment of natural killer (NK) and $CD8^+$ cytotoxic T cells. Type 2 immunity was traditionally viewed as a response to allergens and helminths, but is now more broadly viewed as regulating tissue homeostasis. Type 2 immunity tends to recruit mast cells, eosinophils and basophils to promote the release of inflammatory mediators. Type 3 immunity targets extracellular bacteria and fungi, and favours neutrophil and monocyte phagocytosis.

Upon the resolution or clearance of infection or injury, T and B lymphocytes undergo clonal contraction, leaving behind a population of memory T cells, memory B cells and antibody-secreting long-lived plasma cells (LLPCs) to protect against subsequent exposures (Ahmed and Gray 1996).

1.2 Protein immunogenicity

Antigens are biomolecules (proteins, carbohydrates, lipids, nucleic acids) that bind specifically to T cell receptors (TCRs) or antibodies. Antigens that elicit an immune response are termed immunogens. Although immunogenicity is a desirable outcome in the context of effective vaccination and protection against infection, unwanted immunogenicity can result in decreased efficacy of biotherapeutics, hypersensitivity to innocuous molecules, or autoimmunity to self-molecules.

Protein immunogens are the most common target of the adaptive immune system and the main focus of this thesis. The factors underlying protein immunogenicity are incompletely understood and can be broadly divided into host, exposure, and antigen-related factors (Kessler, Goldsmith, and Schellekens 2006). Host-related factors include genetic background, age and health status, which influence the strength of the immune

response generated by an individual (Kessler, Goldsmith, and Schellekens 2006). Humans are highly polymorphic at the MHC locus that determines which peptides are presented during T cell priming. Immune responses are generally less robust in older individuals due to immunosenescence (Allen et al. 2020; Crooke et al. 2019), and there are well-described sex differences, with females generally eliciting stronger immunity (Klein and Flanagan 2016).

Exposure-related factors include antigen formulation, route of administration, dose and frequency. Impurities present during the formulation of an antigen may act as adjuvants by providing non-specific stimulation to the innate immune system (Seidl et al. 2012; Pulendran, Arunachalam, and O'Hagan 2021). The effect of administration route, dosage and frequency are less clear, with Schellekens (2005) arguing that the intrinsic characteristics of an antigen are more important in determining immunogenicity.

In general, cutaneous and mucosal routes of administration mimic the route of exposure for infectious agents, are dense with immune cells and are thought to be more immunogenic (Kuriakose, Chirmule, and Nair 2016). A notable exception is exposure via the gut mucosa, which is believed to induce immune unresponsiveness or tolerance (Kuriakose, Chirmule, and Nair 2016). In contrast, intraperitoneal and intravenous routes are thought to be less immunogenic (Kessler, Goldsmith, and Schellekens 2006; Porter 2001). Regarding dose, some have postulated that the immune system is less tolerant to low antigen doses (Kuriakose, Chirmule, and Nair 2016), while others have argued that high doses and repeated administration are more immunogenic because they increase immune exposure to the antigen (Porter 2001).

Intrinsic characteristics of an antigen also influence the immune response. Larger and more complex antigens are generally more immunogenic, because they tend to have more epitopes and features that can be targeted by the adaptive immune system. Antigens

that interact with cell surfaces may be more immunogenic because they are more likely to be taken up for antigen presentation (Harding et al. 2010). An important factor is the phylogenetic similarity of an antigen to the host organism since the immune system is centrally and peripherally tolerant to self-antigens. For instance, animal-derived insulins are more immunogenic in humans compared with human insulin (Schernthaner 1993).

Protein post-translational modifications (PTMs) can alter recognition by creating neoepitopes, inducing conformational changes, or causing aggregation (Hermeling et al. 2004). For example, non-native glycosylation molecules and patterns can create or expose neoepitopes (Kuriakose, Chirmule, and Nair 2016; Gribben et al. 1990). Unstable proteins may more readily degrade to expose previously hidden (cryptic) antigenic epitopes (Josić et al. 1999; Delamarre et al. 2006). PTMs can induce aggregation and protein aggregates are thought to be more immunogenic (Rosenberg 2006; Moore and Leppert 1980) because they are similar to bacterial or viral array structures (Bachmann et al. 1993) or represent damaged self, but the mechanisms of immunogenicity remain unclear.

Haptens are small molecules that induce immune responses only when bound to carrier proteins, and are thought to activate the immune response by providing an antigenic signal in the context of a co-stimulatory signal (Park, Sanderson, and Naisbitt 2007). Haptens tend to be chemically reactive electrophiles (Karlberg et al. 2008; Grace, Roberts, and Walker 2003), are commonly implicated in hypersensitivity (Jones and Leskowitz 1965), and tend to elicit strong IgG1 responses specific to the hapten (Palm and Medzhitov 2009) while reducing the immunogenicity of the carrier protein (Gefen et al. 2015). Interestingly, protein haptenation shares similarities with protein carbonylation, a type of non-enzymatic PTM caused by oxidative and glycative stress.

1.3 Protein carbonylation

Oxidative stress and metabolite imbalances occur when the accumulation of excess reactive oxygen species (ROS) and reactive compounds from exogenous and endogenous sources exceeds their rate of clearance. ROS and other reactive compounds are highly damaging to biomolecules, including macromolecules such as nucleic acids, lipids, carbohydrates and proteins. In particular, spontaneous chemical reactions between electrophilic reactive species and nucleophilic amino acids often result in a variety of physiological non-enzymatic PTMs (Harmel and Fiedler 2018). A common class of PTM arising from oxidative and glycative stress is protein carbonylation.

Protein carbonylation is broadly defined as the introduction of diverse PTMs that contain reactive carbonyl functional groups, and refers specifically to protein-bound aldehydes and ketones not typically found in native proteins (**Figure 1.1**) (Spears and Fascione 2016; Weber, Davies, and Grune 2015; Spicer and Davis 2014). Reactive carbonyls are distinguished from less reactive types of carbonyl groups such as carboxylic acids and amides, which are naturally present in peptide bonds and amino acid side chains.

Reactive carbonyl groups can be introduced onto proteins directly from attacks by free radicals, or indirectly from reactive compounds generated by lipid peroxidation or glycation (**Figure 1.2**). Metal-catalysed oxidation (MCO) generates highly reactive hydroxyl radicals ($^{\bullet}OH$) from hydrogen peroxide (H_2O_2) and reduced transition metal ions such as Fe^{3+} and Cu^{2+}. $^{\bullet}OH$ can directly attack proteins to oxidise amino acid side chains or cleave the protein backbone (Amici et al. 1989; Stadtman and Levine 2000). The most common protein carbonyls generated by MCO are α-aminoadipic semialdehyde (AAS,

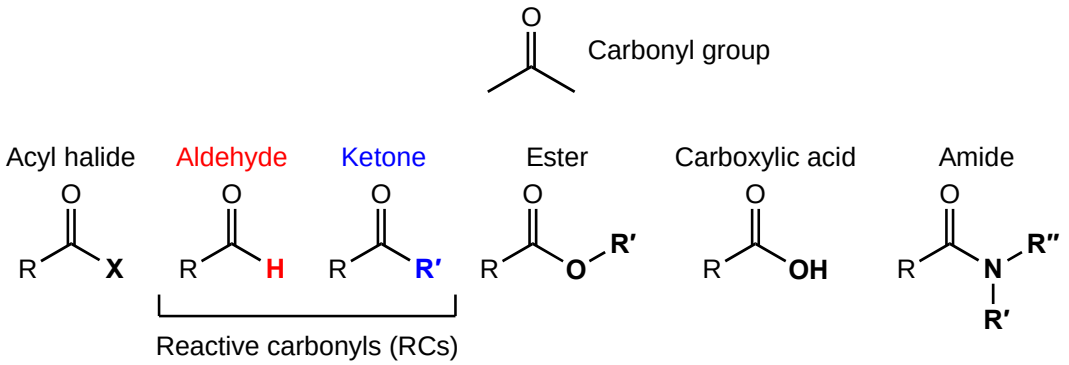


Figure 1.1: Relative reactivity of carbonyl groups. The carbonyl group consists of a carbon atom double-bonded to an oxygen atom. Some carbonyl compounds are displayed and ordered from most to least electrophilic/reactive. Reactive carbonyls include aldehydes (red) and ketones (blue). Protein aldehydes are a particular focus of this thesis. X = halide, R, R′ or R″ = variable alkyl group.

or allysine) from lysine oxidation and γ-glutamic semialdehyde (GGS) from arginine or proline oxidation (**Figure 1.3A−B**). Other amino acid side chains that can be oxidised are threonine and tryptophan, which become 2-amino-3-ketobutryic acid and kynurenine respectively (**Figure 1.3C−D**) (Akagawa 2021; Fedorova, Bollineni, and Hoffmann 2014). Protein backbone cleavage is caused by direct attack of the peptide bond resulting in a ketoacyl group, or by glutamate and aspartate oxidation to form peptides blocked by a pyruvyl group (Stadtman and Levine 2000; Akagawa 2021).

Reactive by-products generated from lipid peroxidation can also introduce protein-bound carbonyls. Oxidation of polyunsaturated fatty acids (PUFAs) produces a variety of highly reactive aldehyde species such as 4-hydroxy-2-nonenal (HNE) (**Figure 1.4**), 2-propenal (acrolein) (**Figure 1.5**), and malondialdehyde (MDA) (**Figure 1.6**) (Pizzimenti et al. 2013). These reactive aldehyde species are potent electrophiles that readily attack nucleophilic amino acids such as cysteine, histidine, lysine, or arginine to form aldehyde-containing Michael adducts (through the carbon-carbon double bond), or

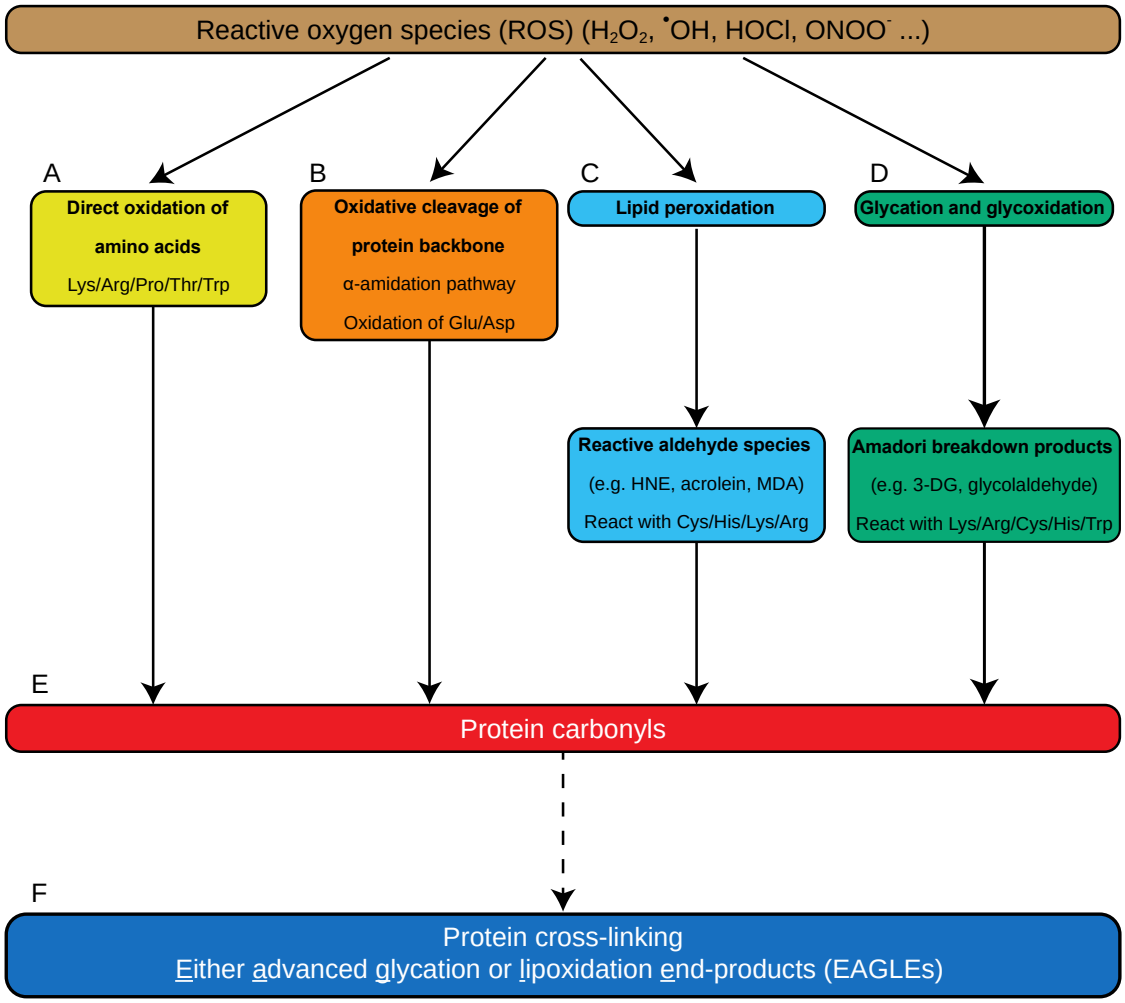


Figure 1.2: Oxidative and glycative stress leads to protein carbonylation and ultimately protein cross-linking or other stable end-products. Protein carbonyls can be introduced directly by reactive oxygen species (ROS) or indirectly through reactive compounds formed by lipid peroxidation or glycation/glycoxidation. A) ROS can introduce protein carbonyls by direct oxidation of amino acid side chains or B) oxidative cleavage of the protein backbone. C) Lipid peroxidation and D) glycation/glycoxidation generate highly reactive breakdown products such as 4-hydroxy-2-nonenal (HNE), 2-propenal (acrolein), malondialdehyde (MDA), 3-deoxyglucosone (3-DG), glycolaldehyde, and many others. The preferred residues and exact post-translational modifications (PTMs) formed are specific to each reactive compound. Moreover, different reactive compounds can combine to form hybrid PTMs. A general feature of oxidative and glycative stress is the introduction of E) protein carbonyls, which are commonly used as a biomarker for unhealthy ageing and disease. Unstable protein carbonyls ultimately form F) stable end-products such as protein cross-links or either advanced glycation or lipoxidation end-products (EAGLEs), which usually no longer retain the reactive carbonyl groups. Adapted from Weber, Davies, and Grune (2015).

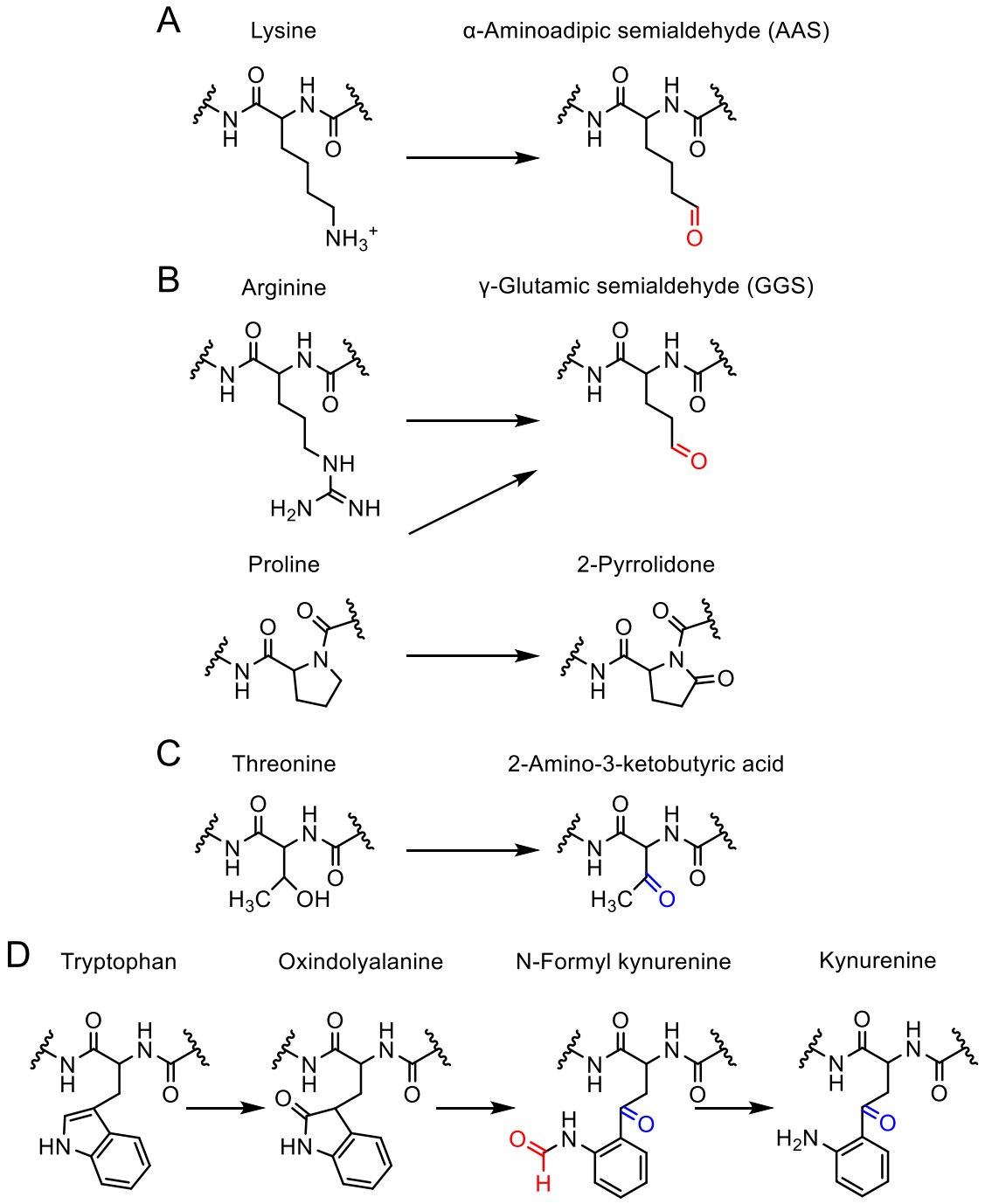


Figure 1.3: Direct oxidation of amino acid side chains can generate protein carbonyls. A) Lysine oxidation to α-aminoadipic semialdehyde (AAS, or allysine). B) Arginine or proline oxidation to γ-glutamic semialdehyde (GGS). Proline oxidation also generates 2-pyrrolidone, which does not contain any reactive carbonyls. C) Threonine oxidation to 2-amino-3-ketobutryic acid. D) Tryptophan oxidation to kynurenine and its isoforms. Aldehydes highlighted in red and ketones in blue. Adapted from Akagawa (2021).

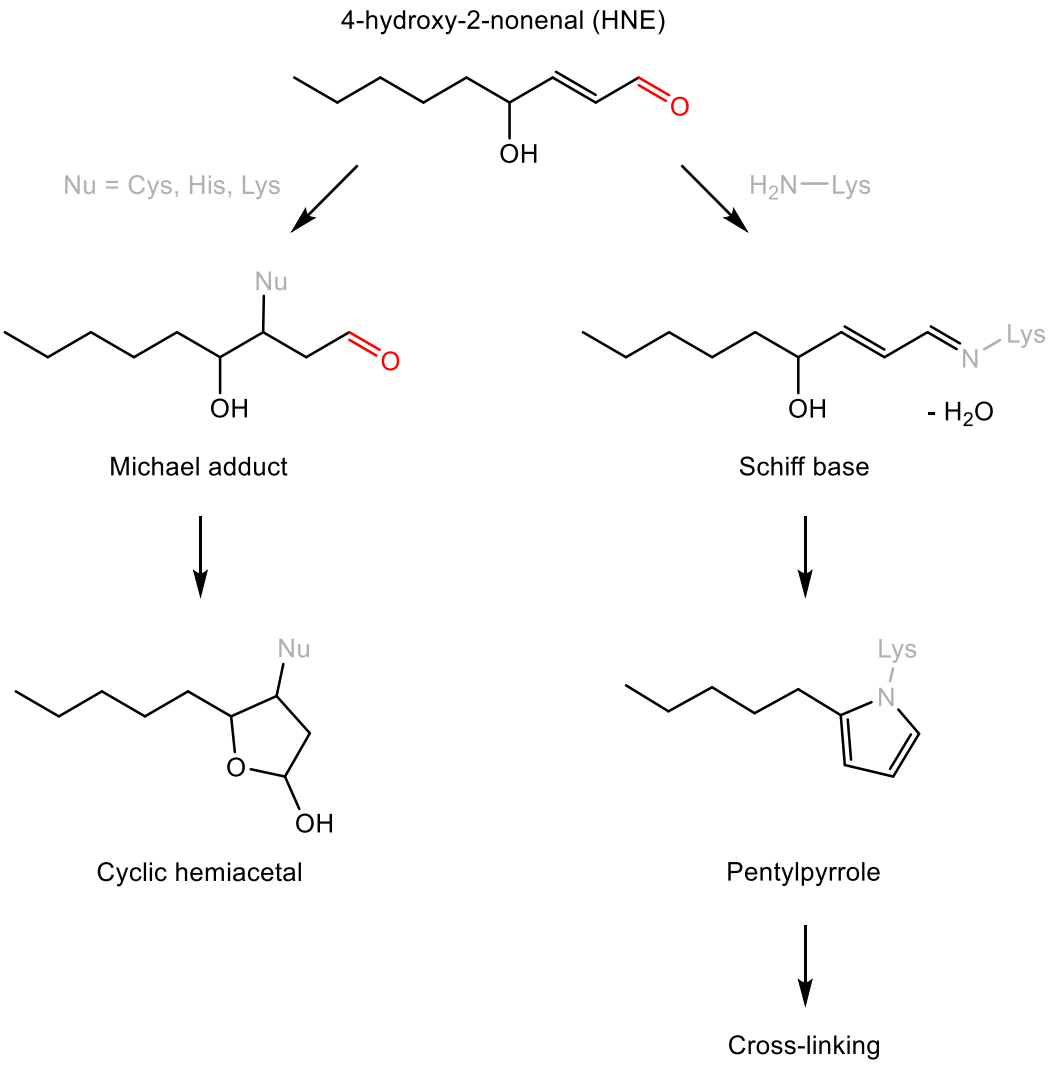


Figure 1.4: Formation of selected 4-hydroxy-2-nonenal (HNE) PTMs. HNE is a reactive α,β-unsaturated aldehyde generated from lipid peroxidation. HNE can form Michael adducts on the side chains of the nucleophilic (Nu) amino acids cysteine, histidine and lysine. Amino acids and their side chains are indicated in grey. The Michael adducts retain a reactive aldehyde group (red) that can cyclise to hemiacetal. Alternatively, HNE can form Schiff bases with lysine residues that cyclise and form protein cross-links. Selected non-cross-linked PTMs shown for clarity. Adapted from Vistoli et al. (2013) and Akagawa (2021).

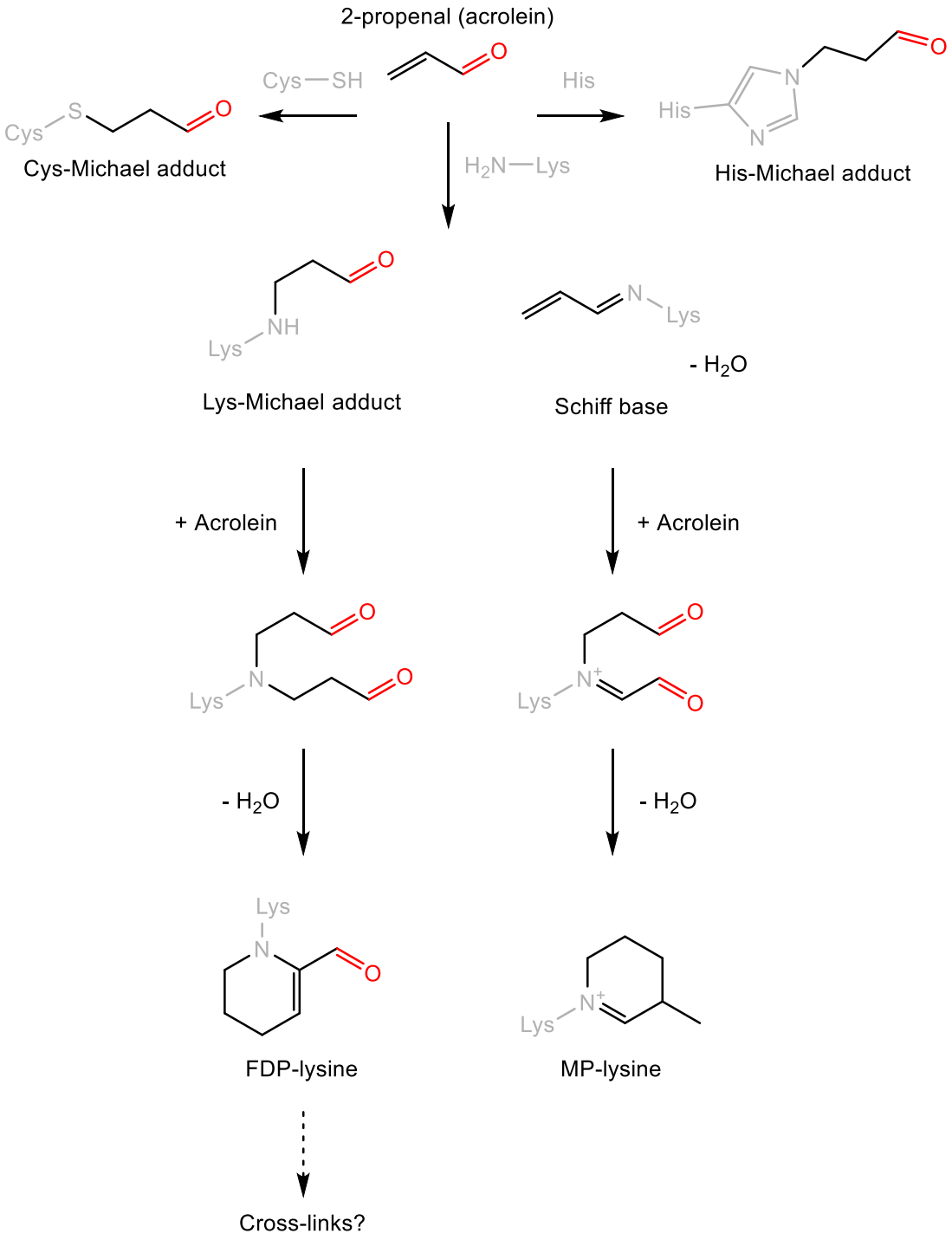


Figure 1.5: Formation of selected 2-propenal (acrolein) PTMs. Acrolein is a reactive α,β-unsaturated aldehyde generated from lipid peroxidation. Acrolein can form Michael adducts with the nucleophilic amino acids cysteine, histidine and lysine. Amino acids and their side chains are indicated in grey. The Michael adducts retain a reactive aldehyde group (red). Acrolein can also form Schiff bases on lysine residues. Both Michael adducts and Schiff base acrolein products on lysine can combine with a second molecule of acrolein to form cyclic PTMs. Note that FDP-lysine (but not MP-lysine) retains an aldehyde group that can undergo further reactions. Selected non-cross-linked PTMs shown for clarity. Adapted from Vistoli et al. (2013) and Akagawa (2021).

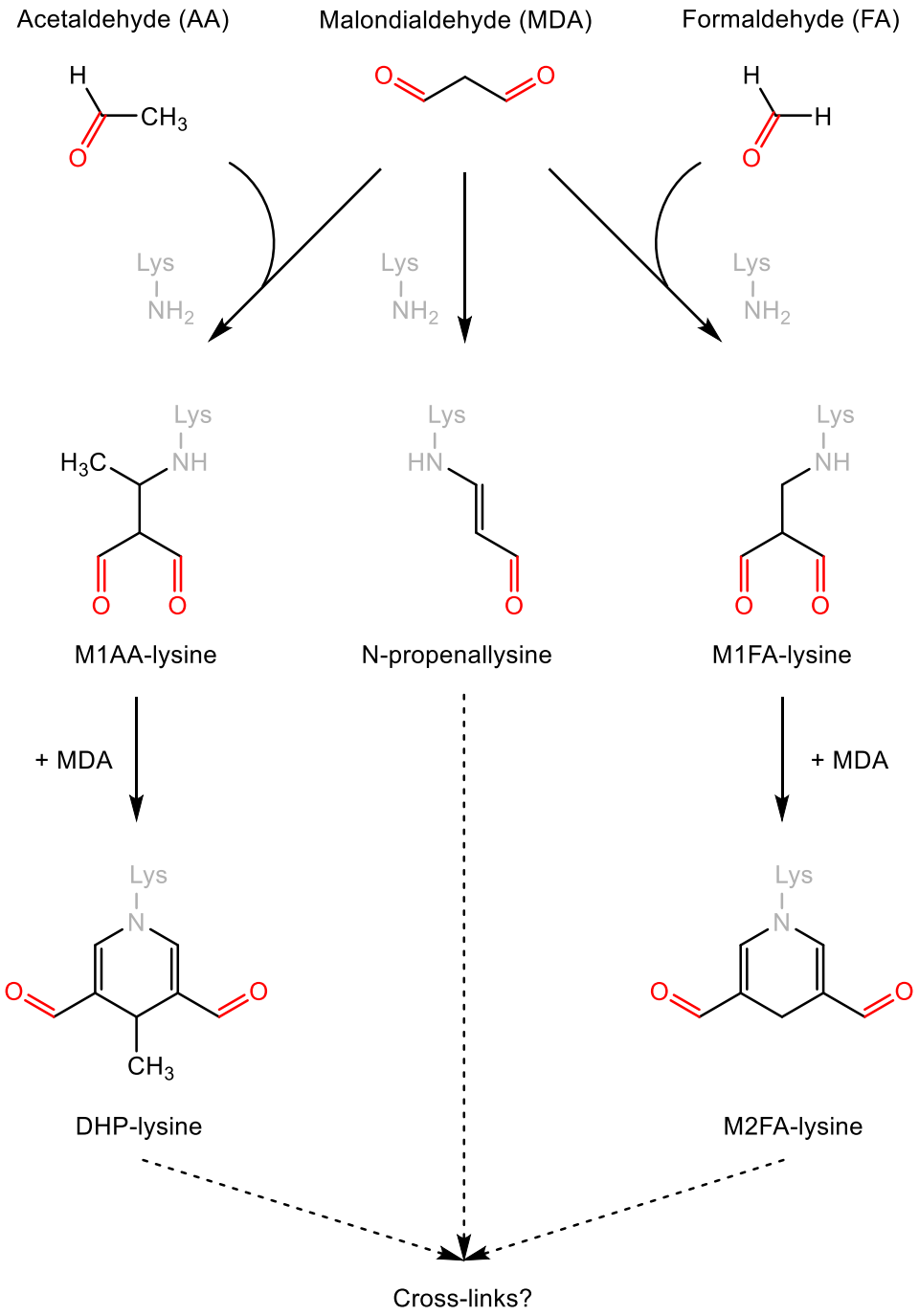


Figure 1.6: Formation of selected malondialdehyde (MDA)-based PTMs. MDA is a reactive di-aldehyde by-product of lipid peroxidation that readily reacts with lysine residues to form N-propenallysine. MDA can also combine with one molecule of acetaldehyde (AA), a by-product of ethanol metabolism, to form M1AA-lysine. Combining with an additional molecule of MDA results in DHP-lysine. Alternatively, one molecule of formaldehyde (FA) from endogenous or exogenous sources can also combine with one molecule of MDA to form M1FA-lysine. Combining with an additional molecule of MDA results in M2FA-lysine. N-propenallysine, DHP-lysine and M2FA-lysine all retain reactive aldehyde groups (red) that can react/rearrange further to form protein cross-links or other stable products. Amino acids and their side chains are indicated in grey. Selected non-cross-linked PTMs shown for clarity. Adapted from Vistoli et al. (2013), Akagawa (2021) and Nakamura et al. (2017).

form transient Schiff bases with lysine residues (through the carbon-oxygen double bond) (e.g. **Figure 1.4**). The preferred residues for attack and the exact products formed are highly specific to each reactive aldehyde species.

The initial PTMs formed after Michael addition or Schiff base formation are intermediates that further react and/or rearrange to form protein cross-links or more stable end-products collectively known as advanced lipoxidation end products (ALEs) (Vistoli et al. 2013). Of the reactive aldehyde species listed, HNE and MDA are the most biologically abundant and therefore the most studied, while acrolein is the most electrophilic but not commonly formed in vivo (Pizzimenti et al. 2013).

Another common route for introducing protein carbonylation is through the Maillard reaction. The initial stage of the Maillard reaction is known as protein glycation, and is caused by the reaction between a reducing sugar (e.g. glucose and fructose, whose aldehyde or ketone functional groups allow them to react as reducing agents) and free amines (e.g. protein N-termini or lysine side chains) (**Figure 1.7**) (Amaya-Farfan and Rodriguez-Amaya 2021). Protein glycation results in a reversible Schiff base that can undergo chemical isomerisation (Amadori rearrangement) to form relatively stable intermediate products containing a ketone or aldehyde group.

During the intermediate stage of the Maillard reaction, Amadori products undergo dehydration, fragmentation and degradation to produce a variety of reactive compounds, which further attack proteins on lysine, arginine, cysteine, histidine and tryptophan residues (Amaya-Farfan and Rodriguez-Amaya 2021). As with lipoxidation by-products, the preferred residues for attack and the exact PTMs formed are specific to each reducing sugar and Amadori breakdown product.

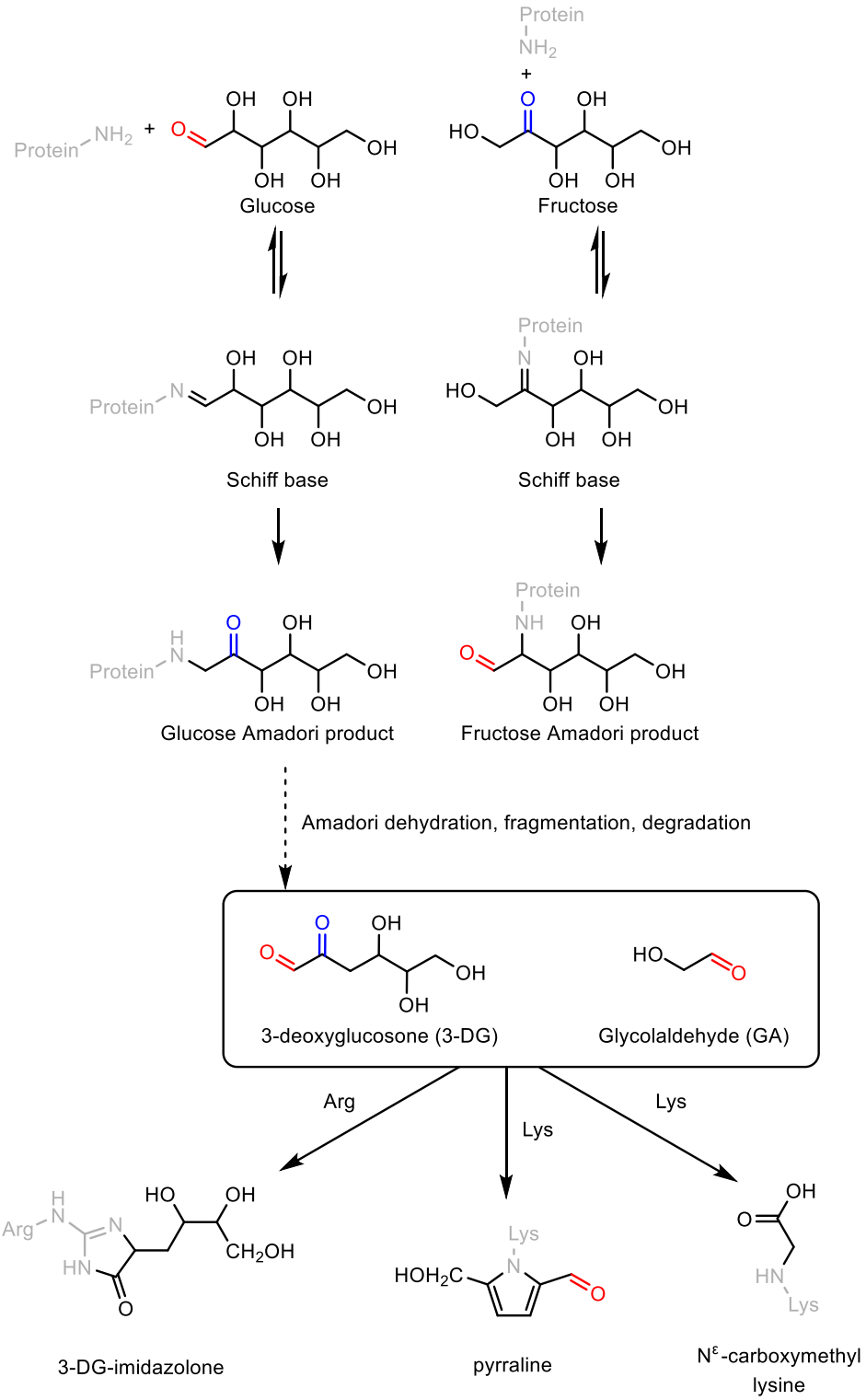


Figure 1.7: Protein glycation by glucose and fructose, and selected PTMs arising from the Amadori breakdown product 3-deoxyglucosone (3-DG). Glucose and fructose are reducing sugars. Glucose contains a reactive aldehyde group (red), while fructose contains a reactive ketone group (blue). Glucose and fructose can react with protein amino groups to form reversible Schiff bases. The Schiff base can undergo irreversible Amadori rearrangement to form Amadori products. Amadori products undergo sugar dehydration, fragmentation and degradation to form reactive compounds such as 3-DG and glycolaldehyde (GA), which attack proteins further. 3-DG tends to react with lysine and arginine to form various PTMs, including the aldehyde-containing pyrraline. Generic proteins, amino acids and their side chains are indicated in grey. Selected non-cross-linked PTMs shown for clarity. Adapted from Vistoli et al. (2013), Akagawa (2021), and Ahmed and Furth (1992).

The end stage of the Maillard reaction is the least well-understood and eventually culminates in the formation of protein cross-links or stable advanced glycation end-products (AGEs) (Amaya-Farfan and Rodriguez-Amaya 2021). 3-deoxyglucosone (3-DG) and glycolaldehyde (GA) are two more well-characterised reactive molecules generated during glucose Amadori product breakdown that react with proteins to introduce protein aldehyde-containing PTMs (**Figure 1.7**).

1.4 Immune consequences of protein carbonylation

As with most PTMs, protein carbonylation can affect protein structure, function and distribution depending on the nature of the PTM and modification site, although carbonylated proteins typically become less active and more unstable after modification (Nyström 2005). The problem arising from protein carbonylation is that the PTMs it generates are generally considered to be chemically irreversible (Stadtman and Levine 2000; Akagawa 2021). Therefore, the main route for the clearance of carbonylated proteins is degradation by lysosomes and the ATP-ubiquitin independent (20S) proteasome (Chondrogianni et al. 2014; Fedorova, Bollineni, and Hoffmann 2014; Nyström 2005).

Protein degradation mechanisms can become overwhelmed under conditions of excess carbonyl stress. Cross-linked and aggregated carbonylated proteins are more resistant to proteolysis (Moheimani et al. 2010), and such proteins can actively inhibit lysosomal and proteasomal activity (Grune et al. 2005). The accumulation of cytotoxic aggregates has deleterious effects on cellular and tissue function, and is especially problematic for long-lived vascular, retinal, and neural proteins (Dalle-Donne et al. 2003). Key cellular pathways involved in homeostasis are especially susceptible to carbonylation, and affected pathways can create a feedback loop that accelerates the burden of protein carbonylation (Baraibar et al. 2012).

Indeed, protein carbonylation has been demonstrated to increase with age, particularly in the last third of an organism's lifespan (Stadtman and Levine 2000). Elevated levels of carbonyl stress have been detected in many human pathologies and often positively correlate with disease progression and severity (Dalle-Donne et al. 2003, 2006). Thus, protein carbonylation is often clinically used as a biomarker of unhealthy ageing and various neurological, cardiovascular, respiratory, musculoskeletal and metabolic diseases (Dalle-Donne et al. 2003; Yan and Forster 2011; Harmel and Fiedler 2018).

Protein carbonylation may be not only a biomarker but also a cause of disease pathogenesis. However, the underlying causal mechanisms are not well-understood because protein carbonylation is a generic marker of oxidative and glycative stress that encompasses a large, chemically heterogeneous, and poorly characterised group of PTMs. The effects of individual PTMs are extremely difficult to isolate and characterise due to the diverse chemistry of reactive species that cause protein carbonylation and the heterogeneity of non-enzymatic modifications. Moreover, PTMs containing aldehydes and ketones are inherently unstable intermediates, and their effects are often conflated with downstream stable either advanced glycation or lipoxidation end-products (EAGLEs) that no longer contain reactive carbonyl groups. Nonetheless, it is thought that the activation of innate and adaptive immune responses to protein carbonyl PTMs and EAGLEs can trigger or exacerbate human pathologies.

Support for the hypothesis that the reactive aldehyde moiety itself can elicit adaptive immune responses was first demonstrated by Allison and Fearon (2000). Aldehyde functional groups were introduced onto various proteins including hen egg lysozyme (HEL), ovalbumin (OVA), heterologous (pigeon) or homologous (rat) cytochrome c, and merozoite surface protein 1 (MSP1-19) by treatment with glycolaldehyde (GA), a reactive by-product of the Maillard reaction (**Figure 1.7**). Mice immunised with GA-modified

proteins in the absence of adjuvant had increased IgG1 antibody responses to native carrier protein by several orders of magnitude. The antibody responses were largely abrogated when protein aldehyde formation was prevented by concurrent treatment with the reducing agent sodium cyanoborohydride ($NaCNBH_3$).

Allison and Fearon also introduced protein aldehydes onto OVA by sodium (meta)periodate ($NaIO_4$) oxidation of the N-linked glycan, which results in two aldehyde groups per monosaccharide (Gahmberg and Andersson 1977). $NaIO_4$ treatment also increased IgG1 antibody responses to native protein, required the N-linked glycan, and was abrogated by subsequent reduction of aldehydes using another reducing agent, sodium borohydride ($NaBH_4$). The enhanced immunogenicity was not caused by protein aggregation because the monomeric fraction of $NaIO_4$-modified OVA was still immunogenic. Moreover, $NaIO_4$-modified OVA co-injected with unmodified HEL only elicited antibody responses to native OVA, suggesting that enhanced immunogenicity was specific to $NaIO_4$-modified protein rather than generally enhancing immune responses as a non-specific adjuvant.

Subsequent studies from our lab performing immunisations in the absence of adjuvant and without contaminating endotoxin extended the observations of Allison and Fearon. Mice immunised with GA-modified OVA produced antibodies that were more reactive to native OVA protein compared with GA-modified OVA, suggesting that the underlying mechanisms were not hapten-specific (Moghaddam 2001). HEL modified with GA, MDA or HNE all increased IgG1 but not IgG2a responses to native protein, and total protein carbonyl content in GA-modified or $NaIO_4$-modified OVA was positively correlated with IgG1 titres (Moghaddam et al. 2011). Antibody responses were eliminated when samples were concurrently modified in the presence of $NaBH_4$ to prevent protein carbonyl formation (Moghaddam et al. 2011).

Interestingly, immune responses to protein carbonyls appear to favour T_H2 responses. Different strains of mice immunised with HEL GA generated IgG1 responses and T_H2 cytokines secreted by $CD4^+$ T cells (Moghaddam et al. 2011). Formalin-inactivation of the respiratory syncytial virus (RSV) vaccine (Moghaddam et al. 2006) and dry-roasting peanuts (Hillson 2013) also increased protein carbonyl content and favoured T_H2 immune responses with functional consequences for hypersensitivity. The T_H2-bias was also observed in MDA-modified proteins (Binder et al. 2004), MDA acetaldehyde (MAA)-modified proteins (Willis et al. 2003) and 3-DG-modified proteins (Heilmann et al. 2014), although other researchers have not specifically linked enhanced immunogenicity to reactive aldehyde groups.

1.5 Thesis scope and aims

The mechanisms by which protein carbonyls enhance the immunogenicity of their native carrier protein remain unknown. In this thesis, I aim to characterise how protein carbonyls, in particular protein aldehydes, modulate the innate and adaptive immune systems to enhance antibody responses to native protein. The hypothesis is that reactive carbonyls drive antibody responses to native protein, and that neutralising the reactive carbonyls abrogates the enhanced antibody responses. Chapter 3 will first characterise the immunogenicity and biochemical nature of glycolaldehyde (GA) modification on the model protein hen egg lysozyme (HEL); Chapter 4 will investigate the effect of HEL GA modification on T and B cell adaptive immune responses; and Chapter 5 will examine the effect of HEL GA modification on complement and other innate immune factors.

Chapter 2

Materials & Methods

2.1 General

2.1.1 Reagents and reaction conditions

Reagents were purchased from Merck unless otherwise indicated. Reagents used for tissue culture and in vivo experiments were cell culture-grade and endotoxin-free. Reactions were carried out at room temperature (20–25 °C, RT) unless otherwise specified. Overnight incubations were 16–20 h unless otherwise indicated.

2.1.2 Enzyme-linked immunosorbent assays (ELISAs)

General conditions for ELISAs were as follows unless otherwise specified. High-bind 96-well plates (SpectraPlate-96 HB, PerkinElmer) were used for ELISAs. Antigens were coated in 100 mM sodium bicarbonate ($NaHCO_3/Na_2CO_3$) buffer pH 9.7 (ELISA coating buffer) at 4 °C overnight. Plates were washed with phosphate-buffered saline (PBS) supplemented with 0.05% Tween-20 (PBST) using a microplate washer (HydroSpeed, Tecan). Blocking was performed with 1% BSA/PBS, dilutions were prepared in 1% BSA/PBST and incubations were at RT for 1 h. Plates were developed with TMB (Ultra TMB-ELISA Substrate Solution, Thermo Fisher Scientific) and allowed to develop for

up to 15 min. Colour development was stopped with 2 N sulfuric acid (H_2SO_4). Absorbance was measured using a SpectraMax M3 or M5 plate reader (Molecular Devices) at wavelengths of 450 nm and 570 nm for background subtraction ($A_{450–570}$).

2.2 Protein preparation, modification, and characterisation

2.2.1 Peptide reconstitution and quantification

Peptides were ordered commercially (ChemPeptide) with at least 95% purity, or synthesised as part of a collaboration with the Esser-Kahn laboratory at the University of Chicago. Lyophilised peptides were reconstituted in distilled water (dH_2O) (Gibco, Thermo Fisher Scientific), 0.22 μm sterile filtered (Costar Spin-X, Corning), aliquoted and stored at –80 °C. Peptides containing aromatic amino acids (Trp, Tyr, Phe) were quantified by measuring absorbance 280 nm (A_{280}) on a NanoDrop 2000c Spectrophotometer.

2.2.2 Protein reconstitution and quantification

Lyophilised hen egg lysozyme (HEL) was purchased from Sigma-Aldrich (L6876) and reconstituted in endotoxin-free Dulbecco's PBS without calcium chloride ($CaCl_2$) or magnesium chloride ($MgCl_2$) (Sigma-Aldrich D8537). Lyophilised mouse lysozyme (ML) was produced as per Tsujihata et al. (2000) and provided as a generous gift (Tadashi Ueda, Kazumasa Yoshida and Manabu Nakazono, Kyushu University). ML contained salts and was thus reconstituted in endotoxin-free dH_2O, then buffer exchanged before use.

Proteins were quantified using A_{280} or bicinchoninic acid (BCA) assay (Thermo Fisher Scientific) according to manufacturer's instructions. Briefly, 25 μL of diluted bovine serum albumin (BSA) standards and protein samples were added to flat-bottomed 96-well plates before adding 200 μL BCA working reagent. Samples were incubated at 37 °C for 30 min before measuring absorbance 562 nm (A_{562}).

2.2.3 Endotoxin removal

Lipopolysaccharide (LPS) contamination was removed using EndoTrap Red Column (Lionex) according to manufacturer's instructions. Briefly, the column was regenerated with the supplied regeneration buffer and equilibrated with 3 column volumes of the supplied equilibration buffer before adding sample reconstituted in 0.5× PBS. Fractions were collected and pooled, then re-tested for successful LPS removal.

2.2.4 Murine Toll-like receptor 4 (mTLR4) reporter assay

Human embryonic kidney 293 (HEK293) cells stably transfected with mTLR4, MD-2 and CD14 (293/mTLR4-MD2-CD14, Invivogen) were cultured and used as per manufacturer's instructions. Briefly, 50,000–100,000 cells were seeded in 100 μL cell media in a flat-bottomed 96-well plate. Ultrapure-LPS (Invivogen) was used as a standard. Samples for testing were added at a final concentration of 20–50 μg/mL. After 20–24 h incubation, 180 μL supernatant was harvested and human interleukin 8 (IL-8) levels were measured using an uncoated ELISA kit (Thermo Fisher Scientific) (Section 2.4.7).

2.2.5 Pattern-associated molecular pattern (PAMP) reporter assay

RAW-Blue cells (Invivogen) stably expressing all TLRs (except TLR5), RIG-I, MDA-5, NOD-1 and NOD-2 were cultured and used as per manufacturer's instructions. Briefly, 50,000–100,000 cells were seeded in 100 μL cell media in a flat-bottomed 96-well plate. Ultrapure-LPS was used as a standard. Samples for testing were added at a final concentration of 20–50 μg/mL. After 20–24 h incubation, 20 μL supernatant was harvested. Secreted embryonic alkaline phosphatase (SEAP) induced by NF-κB and AP-1 activation was measured by adding 180 μL QUANTI-Blue (Invivogen), incubating at 37 °C for 0.5–6 h, then measuring absorbance at 630 nm (A_{630}).

2.2.6 Peptide modification and desalting

Peptides were modified at 0.25 mg/mL with 5 mM glycolaldehyde (GA) dimer (Sigma-Aldrich G-6805) in PBS at 37 °C for 3 h. Excess GA was removed by desalting through a tC18 reversed-phase chromatography gravity column (Sep-Pak WAT054960). Columns were activated with 100% acetonitrile (ACN) then equilibrated with 0.1% formic acid prepared in LC-MS Grade water (Merck). Peptides acidified to 0.1% formic acid were applied to the column, washed with 0.1% formic acid, then eluted in 50% ACN/0.1% formic acid. Eluted peptides were diluted in PBS for in vitro assays or further processing. Alternatively, modified peptides were dialysed into PBS using a Mini Dialysis Kit with 1 kDa cut-off (Sigma-Aldrich) for in vivo experiments.

To post reduce peptides, eluted peptides were incubated with 20 mM sodium borohydride ($NaBH_4$) at 37 °C for 2 h. To remove the fluorenylmethoxycarbonyl protecting group (Fmoc), 20 mg/mL piperazine was added to an equal volume of 1 mg/mL peptide and incubated with shaking at 37 °C for 1 h. To reduce the 6-azido-L-lysine protecting group (azido) to an amino group, 56 mg/mL tris(2-carboxyethyl)phosphine (TCEP) was incubated with an equal volume of peptide with shaking at 37 °C for 16 h. Modified peptides were desalted using a tC18 column, quantified, aliquoted, and stored at –80 °C.

2.2.7 Protein modification and desalting

Proteins were modified at 0.25 mg/mL with 20 mM GA dimer in PBS at 37 °C for 3 h. Excess GA was removed by desalting through an Amicon Ultra Centrifugal Filter with a 10 kDa cut-off, then passed through a 0.22 μm sterile filter. Samples were post-reduced with 10–20 mM $NaBH_4$ at 37 °C for 3–16 h, then excess $NaBH_4$ was removed as for GA above. Modified proteins were quantified, aliquoted, and stored at –80 °C.

2.2.8 2,4-Dinitrophenylhydrazine (DNPH) carbonyl assay

3× to 4× volumes of 10 mM DNPH dissolved in 2 N hydrochloric acid (HCl) was added to samples and derivatised at RT for 1 h with shaking. Samples were neutralised with at least 25× volumes of ELISA coating buffer to 10 μg/mL. ELISA plates were coated with 100 μL/well neutralised DNPH reaction at 4 °C overnight. Biotinylated anti-DNP antibody (Invitrogen A6435) and streptavidin-horseradish peroxidase (strep-HRP, GE Healthcare Life Sciences RPN1051) 1:2000 were used for detection.

2.2.9 Biotin hydrazide carbonyl assay

Biotin hydrazide (BH) was dissolved in dimethyl sulfoxide (DMSO) at 50 mM. 1 μg sample was derivatised with 10 mM BH in PBS at RT for 1 h with shaking. After derivatisation, samples were diluted in ELISA coating buffer to 2.5 μg/mL. ELISA plates were coated with 100 μL/well BH reaction at 4 °C overnight.

2.2.10 Biotin labelling

NHS-LC-Biotin (Thermo Fisher Scientific 21336) was used to biotinylate proteins according to manufacturer's instructions. Briefly, NHS-LC-Biotin was equilibrated to RT and a fresh 10 mM solution was prepared in DMSO. NHS-LC-Biotin was added in 20-fold molar excess to proteins in PBS and incubated at RT for 1 h. The reaction was desalted by dialysis (Slide-A-Lyzer MINI, Thermo Fisher Scientific) or ultrafiltration (Amicon Ultra Centrifugal Filters, Merck) at RT, then 0.22 μm filtered to remove aggregates. To confirm biotinylation and conservation of epitopes, proteins were coated on ELISA plates at 10 μg/mL, then incubated with either strep-HRP 1:2000 or HEL antisera 1:20,000 in 1% BSA/PBST at RT for 1 h.

2.2.11 SDS-PAGE

Peptides were loaded in precast NuPAGE 12% Bis-Tris 1.0 mm gels and proteins were loaded in 4–12% Bis-Tris 1.0 mm gels (both Thermo Fisher Scientific). The ladder used was Novex Sharp pre-stained protein standard (Invitrogen). Samples were heated in 1× lithium dodecyl sulphate (LDS) sample buffer and 1× reducing buffer (both Invitrogen) at 70 °C for 10 min, then run in 1× MES buffer at 100 V. Gels were stained with SimplyBlue SafeStain or SilverQuest Silver Staining Kit (both Invitrogen) according to manufacturer's instructions, or SYPRO Tangerine (Invitrogen) 1:5000 in 10% (v/v) acetic acid with shaking for 30 min.

2.2.12 Liquid chromatography mass spectrometry (LC-MS)

Reversed-phase chromatography was performed in-line prior to mass spectrometry (MS) using an Agilent 1290 uHPLC system (Agilent Technologies). Concentrated protein samples were diluted to 0.02 mg/ml in 0.1% formic acid and 50 µL was injected onto a 2.1 mm × 12.5 mm Zorbax 5 µm 300SB-C3 guard column housed in a column oven set at 40 °C. The solvent system consisted of 0.1% formic acid in ultra-high purity water (Millipore) (solvent A) and 0.1 % formic acid in methanol (LC-MS grade, Chromasolve) (solvent B). Chromatography was performed as follows: initial conditions were 90 % A and 10 % B at a flow rate of 1.0 mL/min. A linear gradient from 10 % B to 80 % B was applied over 35 s. Elution then proceeded isocratically at 95 % B for 40 s followed by equilibration at initial conditions for a further 15 s. Protein intact mass was determined using a 6530 electrospray ionisation quadrupole time-of-flight mass spectrometer (ESI-QTOF, Agilent Technologies). The instrument was configured with the standard ESI source and operated in positive ion mode. The ion source was operated with the capillary voltage at 4000 V, nebulizer pressure at 60 psi, drying gas at 350 °C and drying gas flow

rate at 12 L/min. The instrument ion optic voltages were as follows: fragmentor 250 V, skimmer 60 V and octopole RF 250 V (doi:10.3390/chromatography1040159). Samples were run by myself and Tiago Moreira at the open access Mass Spectrometry Facility, Centre for Medicines Discovery, University of Oxford. Data were analysed in Agilent MassHunter Qualitative Analysis software version B.07.00.

2.2.13 Liquid chromatography tandem MS (LC-MS/MS)

Peptides were prepared in 50% ACN/0.1% formic acid in LC-MS Grade water (Merck). LC-MS/MS analysis was performed by Sarah Bonham of the Kessler laboratory at the Target Discovery Institute using a Dionex Ultimate 3000 coupled to a Q Exactive HF mass spectrometer. Approximately 15 pmol peptide in 0.2 μL volume was injected per sample. Samples were separated on EASY-Spray PepMap RSLC C18 column. MS1 scans were acquired at a resolution of 60,000 at 200 m/z and the top 12 most abundant precursor ions were selected for higher-energy collisional dissociation (HCD) fragmentation. PEAKS Studio software v8.5 was used to search a custom database for GA-associated modifications. Only peptides with intact N-terminal Ala residue and confidently modified (defined as fragmentation before and after the proposed modification site above 5% relative intensity) were included in the analysis.

2.3 Cellular studies

2.3.1 Cell culture conditions

Cell lines were cultured in RPMI 1640 (Sigma-Aldrich) supplemented with 10% foetal bovine serum (FBS), 10 mM HEPES, 2 mM GlutaMAX, and 50 μM 2-mercaptoethanol (2-ME). For mouse primary cells, 1 mM sodium pyruvate and 100 units of Penicillin

G/Streptomycin (Pen-Strep) were added to prevent bacterial growth. Cells were handled under sterile conditions and incubated at 37 °C, 5% CO_2 and 95% humidity.

2.3.2 Bone marrow-derived dendritic cells (BMDCs)

BMDCs were derived from BALB/c mice unless otherwise noted. Bone marrow was extracted from mouse femur and tibia bones and cultured in the presence of 10 ng/mL granulocyte-macrophage colony-stimulating factor (GM-CSF, BioLegend). After 3 d, the culture medium was replaced with fresh cell medium containing 10 ng/mL each of GM-CSF and mouse IL-4 (BioLegend). After 6 d, BMDCs were lifted with 5 mM lidocaine, 12 mM EDTA, pH 7.5 buffer then used in experiments.

In later experiments (indicated in text), GM-CSF BMDCs were derived following the protocol of Lutz et al. (1999). Briefly, on day 0 bone marrow cells were cultured at 0.2×10^6 cells/mL in 100 mm non-tissue culture dishes with 20 ng/mL GM-CSF. On day 3 an equal volume of fresh media was added, on days 6 and 8 the media was half changed with fresh media, and on day 10 immature BMDCs in the non-adherent fraction were harvested. Alternatively, Flt3 BMDCs were derived following Brasel et al. (2000). In brief, on day 0 cells were seeded at 2×10^6 cells/mL in 6-well tissue culture plates with 200 ng/mL murine Flt3 (Peptrotech) and on day 9 non-adherent cells were harvested.

2.3.3 Antigen presentation assays

Antigen-presenting cells (APCs) (10,000 Chinese hamster ovary (CHO) cells, 50,000 A20 cells, or 100,000 BMDCs) were seeded in 96-well plates, antigens were diluted in sterile PBS then added at the desired concentrations, and $CD4^+$ T cell hybridomas (10,000 Ed2, 5000 Ad11, 10,000 Ad23, 10,000 Ad71, 100,000 Ed106) (all gifted from Benny Chain, University of London) were added to a final volume of 200 μL. After 16–24 h

incubation, supernatant was harvested and IL-2 concentration measured using an uncoated ELISA kit (Thermo Fisher Scientific) (Section 2.4.7).

2.3.4 MD4 splenocyte assays

C57BL/6-Tg(IghelMD4)4Ccg/J (MD4, JAX stock #002595) (Mason, Jones, and Goodnow 1992) spleens were kindly provided by Gabriela Pirgova, Tal Arnon lab, University of Oxford. 150,000 MD4 splenocytes (prepared following Section 2.4.5) were added to 96-well plates with 10 μg/mL HEL. Co-stimulation was performed either with 1 μg/mL monomeric anti-CD40 (BioLegend 102907) or 0.1 μg/mL ultrapure-LPS (Invivogen). Alternatively, B cell proliferation was induced using 1 μg/mL each of anti-CD40 and anti-IgM (BioLegend 157102). 1% normal mouse serum (prepared in-house, Section 2.5.1) was optionally added to the assay.

2.3.5 Flow cytometry

Samples were stained in U-bottomed 96-well plates. Cells were washed twice with PBS, then stained with fixable viability stain 780 (FVS780, BD Biosciences) diluted 1:2000 to 1:4000 in PBS at either 37 °C for 5 min or on ice for 30 min. Cells were treated with anti-mouse CD16/CD32 1: 200 (Fc block, BD Biosciences) then stained on ice in the dark for 20 min with B220-eFluor 450 (BioLegend), CD86-PE (BD Biosciences) and CD69-APC (BD Biosciences) all diluted 1:200. After staining, cells were washed with 2% FBS/PBS (flow buffer), fixed with 1.5% paraformaldehyde (PFA) at RT for 10 min, then washed again twice with 2% FBS/PBS. Data were acquired on a flow cytometer (CytoFLEX, Beckman Coulter) and analysed using FlowJo version 10.

2.4 Animal studies

2.4.1 Mouse strains

Wild type (WT) BALB/c and C57BL/6 (B6) mice were bred in-house or ordered from reputable suppliers in the United Kingdom. B6;129S4-C3^{tm1Crr}/J (C3$^{-/-}$) mice (Wessels et al. 1995) were generously provided by Paul Morgan (University of Cardiff). Experiments were set up following a randomised block design. All mice were female unless indicated.

2.4.2 Immunisations

All immunogens were tested and cleaned of LPS to ≤ 0.05 endotoxin units (EU) per μg immunogen. Mice were immunised without anaesthesia while immobilised by scruffing. For subcutaneous (s.c.) immunisations, mice were injected over the left or right flanks using a 29G 12.7 mm insulin needle (BD Biosciences). For hock immunisations, mice were injected as per Kamala (2007). For intraperitoneal (i.p.) immunisations, mice were injected in the lower right quadrant using a 30G 8 mm needle (BD Biosciences).

2.4.3 Blood sampling

Mice were warmed 15 min before blood collection. Lateral tail veins were pricked with a 25G needle (Terumo) and the tail massaged to collect blood in polypropylene tubes. Blood was left to clot at RT for > 30 min then centrifuged at 3000 *g* for 5 min. In earlier experiments, sera were transferred to V-bottomed 96-well plates, diluted 5× or 10× with PBS, then frozen at –20 °C. In later experiments, the sera were frozen undiluted.

2.4.4 Assessing in vivo antibody responses

Antigens were coated on ELISA plates at 5–10 μg/mL in 50 μL ELISA coating buffer at 4 °C overnight, RT for 2–4 h, or 37 °C for 1 h. Plates were washed with 0.05% PBST and

blocked with 100 μL 1% BSA/PBS at RT for 1 h. Sera dilutions were prepared in 1% BSA/PBST and 50 μL/well of diluted sera were incubated at RT for 1 h. Antibodies present in sera were detected using HRP-conjugated anti-mouse Ig antibodies: anti-IgG 1:20,000 (Bio-Rad STAR120P), anti-IgG1 1:5000 (BD Biosciences 559626), anti-IgG2a 1:2000 (BD Biosciences 553391), anti-IgG2b 1:5000 (Southern Biotech 1091-05), anti-IgG2c 1:10,000 (Bethyl Laboratories A90-236P), anti-IgG3 1:5000 (Serotec STAR136P), and anti-IgM 1:1000 (BD Biosciences 550588). The cut-off value for responders was set at 2× absorbance of no sera or naïve sera controls. To calculate endpoint titres, data were fitted with a variable-slope Hill function with 4 parameters and the endpoint titre was interpolated based on the cut-off value.

2.4.5 Lymphocyte recall assay

Mice were culled using a rising concentration of carbon dioxide (CO_2) and cervical dislocation. The spleen and draining lymph nodes were aseptically excised and transferred to ice-cold supplemented RPMI. Tissues were gently mashed through a 70 μm or 100 μm cell strainer using the plunger end of a 1 mL syringe and flushed through with ice-cold supplemented RPMI. In earlier experiments, cells were then manually counted using trypan blue and a haemocytometer. In later experiments, cells were pelleted at 300 *g* for 5 min, incubated with red blood cell (RBC) lysis buffer (Red Blood Cell Lysing Buffer Hybri-Max, Sigma) for 3–4 min, diluted with 20 mL RPMI, centrifuged at 300 *g* for 8 min, resuspended in 5–10 mL supplemented RPMI and re-filtered to remove clumps if needed. AO-DAPI (Solution 13, ChemoMetec) was added 1:20 for automated counting (NucleoCounter NC-3000, ChemoMetec). 0.5–1 × 10^6 cells/well were added to U-bottomed 96-well plates to a final volume of 200 μL/well either in the absence of presence of 50 μg/mL antigen stimulation. Splenocytes were then incubated for 3 d before measuring proliferation and cytokine secretion, except for IL-4, which was measured after 1 d.

2.4.6 ^{3}H thymidine proliferation assay

1 μCi/well methyl-^{3}H thymidine (Perkin Elmer NET027) in 20 μL supplemented RPMI was added to cells and incubated for a further 6–24 h. Cells were then transferred and lysed on glass fibre filtermats using a Micro96 Cell Harvester (Skatron Instruments). Betaplate Scint (Perkin Elmer) was added to the filtermats before measuring scintillation using a MicroBeta Trilux Liquid Scintillation Counter (Wallac Oy).

2.4.7 Cytokine ELISAs

Mouse IL-2, IL-4, IL-5, IL-6, IL-21, IFNγ and human IL-8 were quantified using uncoated ELISA kits (Thermo Fisher Scientific) according to manufacturer's instructions. Briefly, capture antibody was coated onto ELISA plates overnight, plates were blocked with diluent, diluted standards and supernatants were incubated for 2 h, and biotinylated detection antibody plus strep-HRP were used for detection.

2.4.8 B cell enzyme-linked immunosorbent spot (ELISpot) assay

Mice were boosted 7 d prior to the ELISpot assay. 1 d before the assay, ELISpot plates (Millipore) were activated with 35% ethanol, washed five times with ultrapure water, then coated with 50 μL anti-mouse IgG capture antibody (Mabtech) at 15 μg/mL in PBS and incubated at 4 °C overnight. The following day, ELISpot plates were washed five times with PBS then blocked with 200 μL supplemented RPMI for at least 1 h. The spleen, draining lymph nodes, and bone marrow were harvested from mice and a single cell suspension was prepared (Section 2.4.5). Cells were plated and incubated for 12–16 h and removed by washing five times with PBS. Biotinylated probes (1 μg/mL anti-mouse IgG detection antibody (Mabtech), 5 μg/mL HEL-LC-biotin or 5 μg/mL OVA-LC-biotin; Section 2.2.10) were diluted in 2% FBS/PBS and incubated at RT for 2 h. Plates were washed

five times with PBS then incubated with strep-HRP (Mabtech) at RT for 1 h. Plates were again washed five times with PBS and TMB-ELISpot (Mabtech) substrate added for 3–10 min until spots were visible by eye. Plates were left to dry upside down on tissue culture hood vents for 1 h, then imaged on an ELISpot reader (AID) and analysed using software version 8.0.

2.4.9 MD4 adoptive transfer

C57BL/6-Tg(IghelMD4)4Ccg/J (MD4, JAX stock #002595) (Mason, Jones, and Goodnow 1992) spleens from two female mice were kindly provided by Gabriela Pirgova, Tal Arnon lab, University of Oxford. Splenocytes were prepared (Section 2.4.5) then stained with 5 μM carboxyfluorescein succinimidyl ester (CFSE) at 37 °C in the dark for 15 min and the reaction was quenched with FBS. CFSE-stained splenocytes were washed with warm supplemented RPMI, then resuspended in PBS for adoptive transfer. Approximately 2×10^6 B cells (determined by flow cytometry staining, Section 2.3.5) were transferred into congenic WT C57BL/6J female mice by the intravenous (i.v.) route. 24 h later, mice were immunised s.c. on the left and right flanks with 100 μg unmodified or modified HEL. 3 d after immunisation, the spleen and lymph nodes (inguinal and axillary on both sides) were harvested and prepared as single cell suspensions for flow cytometry analysis (Section 2.3.5). Cells were stained using the following panel of antibodies: B220-eFluor 450 1:100 (BioLegend), CD45.1-BV650 1:50 (BD Biosciences), IgMα-PerCP/Cy5 1:50 (BioLegend), CD86-PE 1:100 (BD Biosciences), CD69-APC 1:100 (BD Biosciences).

2.4.10 Cobra venom factor (CVF) administration

20 μg CVF (Quidel) in 100 μL PBS was administered i.p. in the lower right quadrant of mice. This was equivalent to an 800 μg/kg dose in an adult mouse weighing 25 g. Sera

harvested at various time points were processed (Section 2.4.3) and frozen immediately at –80 °C until measuring complement C3 levels (Section 2.5.3).

2.5 Complement studies

2.5.1 Sera for functional complement assays

Human sera were commercially purchased: plasma-derived sera from male AB donors (Sigma H4522), off-the-clot sera from male AB donors (Sigma H6914), off-the-clot sera from a mixed pool of four donors (TCS Bioscience CR100), and sterile-filtered off-the-clot sera from a mixed pool of donors (TCS Biosciences CS100). Additionally, in-house human sera were prepared and pooled from three fully-consenting volunteers. Blood was aseptically collected in silica-coated vacutainer tubes (BD Biosciences) and allowed to clot at RT for 30 min, then centrifuged at 3000 *g* for 5 min. The serum fraction was transferred into sterile tubes and centrifuged again at 20,000 *g* for 2 min. Clarified sera were pooled, aliquoted and immediately frozen at –80 °C until use.

Mice sera were obtained from naïve individuals that were culled using a rising concentration of CO_2 and cervical dislocation. Blood was collected by cardiac puncture using a 25G needle and transferred to sterile tubes. Sera were prepared and stored as for in-house human sera. Samples with excessive haemolysis were discarded.

2.5.2 Complement activation ELISAs

Targets were coated on 96-well ELISA plates at 10–20 μg/mL in 50 μL ELISA coating buffer either at 4 °C overnight or at 37 °C for 1 h. Plates were washed with 0.05% PBST then blocked with 100 μL 1% BSA in Veronal-buffered saline (VBS) at RT for 1 h. Sera dilutions were prepared in 0.1% BSA/VBS and 50 μL/well incubated at 37 °C for 1 h. Anti-human C3d 1:10,000 (Abcam ab17453, mouse monoclonal IgG1 [7C10]) and anti-

mouse C3d 1:250 (R&D Systems AF2655, polyclonal goat IgG) diluted in 0.1% BSA/VBS and incubated at RT for 1 h. The corresponding HRP-conjugated secondary antibodies were incubated for 1 h before developing the ELISAs: anti-mouse IgG1 HRP 1:2000 (BD Biosciences 559626) and anti-goat IgG HRP 1:5000 (Jackson ImmunoResearch 705-035-147).

2.5.3 Complement C3 ELISA

Mouse complement C3 was measured using a commercial ELISA kit (Abcam ab157711) as per the manufacturer's instructions. Briefly, sera were thawed and immediately diluted 1:5000 to 1:7500 in 1× diluent. 100 µL/well diluted sera were added to pre-coated plates and incubated at RT for 20 min. Plates were manually washed four times with 300 µL 1× wash buffer. Anti-C3-HRP was diluted 1:100 in 1× diluent, added to plates, then incubated at RT in the dark for 20 min. Plates were again washed before adding 100 µL/well chromogen substrate at RT in the dark for 10 min. 100 µL/well stop solution was added to terminate the reaction.

2.5.4 Complement C1q binding ELISA

ELISA plates were coated with targets at 1–10 µg/well. Plates were blocked for 1 h with 1% BSA/PBS. Native human C1q (Abcam) or mouse C1q (ComplementTech) were reconstituted to 1 mg/mL in dH_2O, diluted in 0.1% BSA/VBS and added to blocked plates at RT for 1 h. Otherwise, diluted normal human or mouse sera were used as sources of C1q and incubated at 37 °C for 1 h. Native C1q was detected using an anti-C1q-biotin antibody 1:50 (Abcam clone [JL-1]) plus strep-HRP 1:2000. Alternatively, human and mouse C1q were biotinylated (Section 2.2.10). Biotinylated C1q was detected using strep-HRP 1:2000.

2.5.5 Immunoglobulin binding ELISAs

ELISA plates were coated with targets at 1–10 μg/well. Plates were blocked for 1 h with 1% BSA/PBS. Normal human and mouse sera were serially diluted in 1% BSA/PBST and incubated at 37 °C for 1 h. HRP-conjugated antibodies diluted in 1% BSA/PBST were used to detect bound antibodies: rat anti-mouse IgM HRP 1:1000 (BD Biosciences 550588), rat anti-mouse IgG HRP 1:1000 (Thermo Fisher Scientific 04-6020), goat anti-human IgM HRP 1:10,000 (Abcam ab97205), or goat anti-human IgG HRP 1:10,000 (Jackson ImmunoResearch 709-035-149).

2.6 Proteomics studies

2.6.1 Pull-down assay with human sera

Pre-modified HEL was conjugated to Dynabeads M-270 Carboxylic Acid (Invitrogen) as per manufacturer's instructions. Briefly, beads were washed twice with 10 mM sodium hydroxide (NaOH) followed three times with ultrapure water. Beads were activated using 100 mM EDC at RT for 30 min with rotation. Beads were quickly washed with cold ultrapure water, then with 50 mM MES pH 5. Beads were incubated with ligands at 0.6 mg/mL in 50 mM MES pH 5 buffer at RT for 30 min with rotation. After conjugation, beads were quenched with 50 mM Tris pH 7.4 and washed four times with VBS.

The amount of protein conjugated to the beads was quantified by BCA assay (Section 2.2.2) and carbonylation amount was confirmed by DNPH assay (Section 2.2.8). For the pull-down assay, HEL-conjugated beads were added to human plasma-derived sera diluted 10× in VBS and incubated at RT for 1 h on a rotating wheel. After the incubation, beads were washed three times with VBS and used in downstream experiments.

2.6.2 Co-immunoprecipitation (co-IP) assay with mouse sera

Dynabeads Co-Immunoprecipitation Kit (Life Technologies) was used to conjugate antibody to Dynabeads M-270 Epoxy beads according to manufacturer's instructions. Briefly, HyHEL-10 (Absolute Antibody) was centrifuged at 16,000 *g* for 10 min at 4 °C to remove aggregates. Beads were washed and activated with C1 buffer, then 7 μg antibody per mg of beads was resuspended in C1 plus C2 buffer and mixed by gentle pipetting. The reaction was incubated on a rotating wheel at 37 °C for 24 h. Antibody-conjugated beads were washed with HB, LB, and SB buffers provided, then stored in PBS until co-IP.

For co-IP, fresh sera were harvested and pooled from two naïve female BALB/c mice (Section 2.5.1). Mouse sera were diluted 10× in PBS containing $CaCl_2$ and $MgCl_2$ (Life Technologies 14140, PBS++). Unmodified and modified HEL proteins were added to diluted sera and incubated at 37 °C for 1 h. HyHEL-10 conjugated beads were subsequently added and incubated at RT for 1 h with rotation. Beads were then isolated and washed by gentle pipetting four times with PBS++. Bound HEL was eluted from HyHEL-10 using 100 mM glycine pH 2.5 incubated at RT for 10 min, then neutralised with one tenth volume of 1 M Tris pH 8.5. The eluted co-IP samples were then used for downstream experiments, including in solution digest for LC-MS/MS (Section 2.6.3).

2.6.3 On bead and in solution digests

0.3 mg beads were resuspended in 8 M urea in 100 mM ammonium bicarbonate buffer and incubated at RT for 10 min. Cysteines were reduced with 10 mM TCEP at RT for 30 min, then alkylated with 50 mM 2-chloroacetamide at RT in the dark for 30 min. Samples were pre-digested with 50–100 ng endoproteinase Lys-C at 37 °C for 2 h. Urea was diluted to 2 M with 100 mM ammonium bicarbonate buffer. $CaCl_2$ was added to a final concentration of 2 mM, then 50–100 ng trypsin added for digestion at 37 °C for 16–20 h.

Trypsin digestion was stopped with 5% formic acid and the sample was centrifuged at 20,000 *g* for 30 min to remove aggregates and beads. The digestion reaction was desalted using homemade C18 membrane tips that were first activated using 100% acetonitrile. Samples were loaded, washed with 0.1% trifluoroacetic acid (TFA), then eluted with 50% ACN/0.1% TFA. The eluted sample was dried overnight on a SpeedVac (Thermo Fisher Scientific) and stored at –20 °C until MS injection.

2.6.4 Pull-down and co-IP LC-MS/MS

Peptides were separated by nano liquid chromatography (nanoLC) (Ultimate RSLC 3000 for pull-down, Easy-nLC 1000 for co-IP, both Thermo Fisher Scientific) coupled in line to a Q Exactive mass spectrometer equipped with an Easy-Spray source (Thermo Fisher Scientific). Peptides were trapped onto a C18 PepMac100 precolumn (300 µm i.d. × 5 mm, 100 Å, Thermo Fisher Scientific) using Solvent A (0.1% formic acid, HPLC grade water). The peptides were further separated onto an Easy-Spray RSLC C18 column (75 µm i.d., 50 cm length, Thermo Fisher Scientific) using a linear gradient of 30 min for pull-down or 60 min for co-IP (15% to 35% solvent B, 0.1% formic acid in ACN) at a flow rate of 200 nL/min. The raw data were acquired on the mass spectrometer in a data-dependent acquisition mode (DDA). Full-scan MS spectra were acquired in the Orbitrap (scan range 350–1500 m/z, resolution 70,000; AGC target, 3e6, maximum injection time, 50 ms for pull-down or 100 ms for co-IP). The 10 most intense peaks were selected for higher-energy collision dissociation (HCD) fragmentation at 30% of normalised collision energy. HCD spectra were acquired in the Orbitrap at resolution 17,500, AGC target 5e4, maximum injection time 120 ms with fixed mass at 180 m/z. Charge exclusion was selected for unassigned and 1+ ions. The dynamic exclusion was set to 20 s for pull-down or 5 s for co-IP. Samples were run by Marjorie Fournier at the Advanced Proteomics Facility, University of Oxford.

2.6.5 LC-MS/MS analysis

LC-MS/MS data from the Advanced Proteomics Facility was filtered to remove contaminants and false discovery rate (FDR) of < 1 % then exported to Microsoft Excel by Marjorie Fournier. I performed the remaining analysis in Microsoft Excel, Perseus software version 1.6.15.0 (Tyanova et al. 2016), ConsensusDBPath (Kamburov et al. 2011), and DAVID functional annotation (Jiao et al. 2012).

2.7 Computational and statistical analysis

2.7.1 Illustrations

Diagrams and illustrations were drawn in ChemDraw version 20.1, BioRender.com, and Adobe Illustrator version 23.1. Protein models were rendered with PyMOL version 2.1.

2.7.2 Statistical analysis

Statistical analyses were performed using GraphPad Prism version 9.3. Data were typically shown with the mean ± standard error of the mean (SEM) unless otherwise indicated. Power analyses were performed with G*Power version 3.1. All relevant information about the statistical tests used for each experiment can be found in the corresponding figure captions. The threshold for statistical significance was set at $p \leq 0.05$.

Chapter 3

Immunogenicity and biochemical characterisation

3.1 Background

3.1.1 Detecting protein carbonyls

Protein carbonyl detection generally relies on derivatising reactive aldehyde and ketone functional groups using specific chemical probes. Reagents containing free amino groups such as amines, hydrazines and hydroxylamines are commonly used for derivatisation and form corresponding imines, hydrazones and oximes respectively (Fritzsche et al. 2018). Derivatisation reagents can be coupled to other molecules to facilitate enrichment, detection or quantification: for example, biotin can be conjugated for affinity purification, fluorescent molecules for direct visualisation, or Girard reagents for enhancing mass spectrometry (MS) sensitivity (for reviews, see Yan and Forster 2011; Fedorova, Bollineni, and Hoffmann 2014).

The standard and most widely used method for global detection of protein carbonylation was developed in the 1970s (Fields and Dixon 1971) and uses 2,4-dinitrophenylhydrazine (DNPH) for derivatisation. The reaction of DNPH with reactive carbonyls (RCs) yields DNP-hydrazone, which absorbs ultraviolet (UV) light at 360–390 nm with a molar

extinction coefficient of 22,000 $M^{-1}cm^{-1}$ (Levine et al. 1990), and can be measured by spectrophotometry and quantified using the Beer-Lambert law (Braslavsky 2007). Since commercial anti-DNP-hydrazone monoclonal antibodies are widely available (Rogowska-Wrzesinska et al. 2014), DNP-hydrazone can also be detected by various immunoassays such as immunoblotting (Shacter et al. 1994) and enzyme-linked immunosorbent assay (ELISA) (Buss et al. 1997).

Other commonly used probes for protein carbonyl detection include biotin hydrazide (BH) (Yoo and Regnier 2004) and aldehyde-reactive probe (ARP, N′-aminooxymethylcarbonylhydrazino-D-biotin) (**Figure 3.1**) (Chavez et al. 2006), which are commonly used for enriching carbonylated proteins from complex samples followed by MS. The efficiency and specificity of labelling depends on the type of protein carbonyl, chemical properties of the probe and derivatisation conditions (Chand Bollineni, Fedorova, and Hoffmann 2013; Ugur, Coffey, and Gronert 2012). For instance, the spacer length affects label stability (Ugur, Coffey, and Gronert 2012), derivatisation is usually more efficient at lower pH (Chand Bollineni, Fedorova, and Hoffmann 2013), and aldehydes and ketones have different labelling efficiencies (Chand Bollineni, Fedorova, and Hoffmann 2013). The development of improved probes to improve labelling efficiency and specificity is an ongoing area of research (for example in Fritzsche et al. 2018).

Another chemistry that can be exploited to detect protein carbonyls is the reduction of RCs to alcohol using mild reducing agents such as sodium borohydride ($NaBH_4$) (Levine et al. 1990). Reduction using tritiated $NaBH_4$ incorporates radioactive tritium (^3H), which can be detected by liquid scintillation counting (Levine et al. 1990). However, one disadvantage is that $NaBH_4$ also reduces Schiff bases, which do not contain RCs (Levine et al. 1990; Floor et al. 2006).

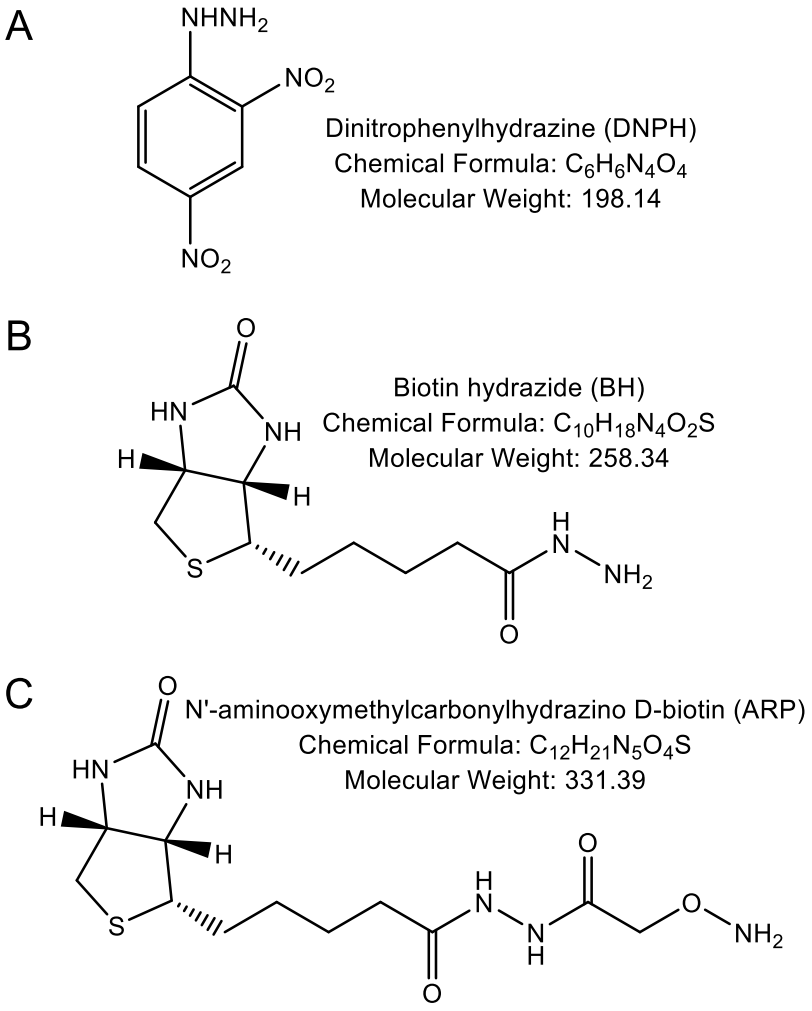


Figure 3.1: Commonly used derivatisation reagents for detecting reactive carbonyls (RCs). A) Dinitrophenylhydrazine (DNPH), B) biotin hydrazide (BH) and C) aldehyde-reactive probe (ARP).

Analytical techniques used for PTM detection, mapping, and characterisation can also be used for label-free analysis of protein carbonyls, depending on their longevity and stability. Some protein carbonyls may be particularly difficult to detect because they are very short-lived or lost during MS fragmentation (Fedorova, Bollineni, and Hoffmann 2014). In this workflow, proteins, peptides or free amino acids are modified with reactive compounds, then separated using high-performance liquid chromatography (HPLC) based on spectroscopic characteristics such as absorbance and fluorescence. The eluted fractions can be analysed by MS to determine molecular mass, tandem MS for site-specific mapping, nuclear magnetic resonance (NMR) for structural determination, or

competition ELISA to determine immunoreactivity of monoclonal antibodies raised against the modification. These approaches have been used to characterise protein carbonyls and other PTMs resulting from HNE (Crabb et al. 2002; Ishii et al. 2003), acrolein (Furuhata et al. 2003) and MDA modification (Uchida et al. 1997; Ishii et al. 2006).

3.1.2 Post-translational modifications caused by glycolaldehyde

Glycolaldehyde can be used to introduce protein carbonyls, specifically protein aldehydes, to various proteins (Acharya and Manning 1983; Allison and Fearon 2000). Glycolaldehyde (GA, $HOCH_2CHO$) is a highly reactive short-chain (two-carbon) sugar generated in vivo as a by-product of Maillard reaction sugar fragmentation (**Figure 1.7**) (Namiki and Hayashi 1975; Glomb and Monnier 1995), free amino acid conversion by myeloperoxidase-hydrogen peroxide (H_2O_2)-chloride activated phagocytes (Anderson et al. 1997), polyunsaturated fatty acid (PUFA) peroxidation (Chikazawa et al. 2020) and oxidative degradation of vitamin C (Mlakar et al. 1996; Argirov et al. 2003).

The reaction between GA and proteins appears to be a Maillard reaction, which occurs between reducing sugars and amino acids (Section 1.3) (**Figure 3.2**). GA mainly reacts with primary amino groups (NH_2) on the protein N-terminus and lysine side chains (Acharya and Manning 1983). The aldehyde group of GA first forms a reversible Schiff base with primary amino groups, which confers an additional mass of +42. The Schiff base can undergo Amadori rearrangement to form an Amadori product (also +42), which for GA is "GA-aldoamine", so called because it is both an aldehyde and amine (Acharya and Manning 1983). In contrast, the Amadori products of most other reducing sugars are ketoamines (containing ketone and amine), which are less reactive (**Figure 1.7**). The GA-aldoamine modification increases protein carbonylation, or more specifically protein aldehydation, as measured by derivatisation with reagents such as DNPH.

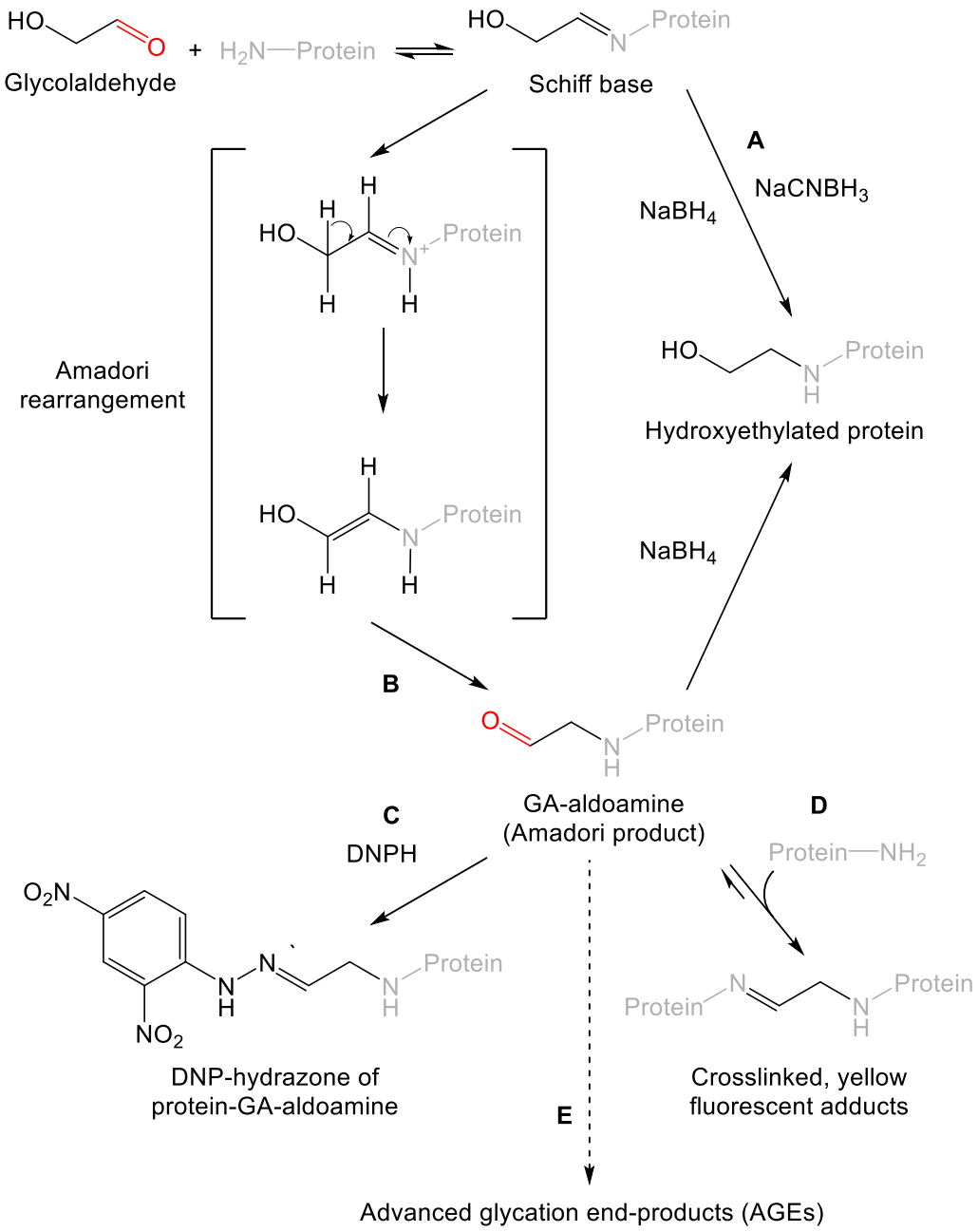


Figure 3.2: Reaction of glycolaldehyde (GA) with protein. The aldehyde group of GA reacts with primary amino groups (NH_2) on the protein N-terminus or lysine side chains to form a reversible Schiff base (imine). A) The Schiff base can be stabilised by sodium cyanoborohydride ($NaCNBH_3$) or sodium borohydride ($NaBH_4$) to form hydroxyethylated protein. B) The Schiff base may undergo irreversible Amadori rearrangement to form the Amadori product GA-aldoamine, which contains a protein aldehyde function. In contrast to Schiff bases, Amadori products can only be reduced by $NaBH_4$. GA-aldoamine can C) be derivatised (e.g. by DNPH), D) react with other primary amino groups to form intra- or inter-molecular protein cross-links, or E) undergo further fragmentation, degradation, and oxidation to form advanced glycation end-products (AGEs). Aldehydes are indicated in red. Generic protein and its amino group are indicated in grey. Adapted from Acharya and Manning (1983).

Due to its reactive aldehyde function, GA-aldoamine can react with other free amines to form covalent Lys-Lys cross-links. Alternatively, GA-aldoamine can undergo

further reactions to form advanced glycation end-products (AGEs), primarily GA-pyridine (+108) formed from the condensation and rearrangement of three GA molecules (Nagai et al. 2002). Other modifications that have been detected on lysines after GA modification include the well-known AGE N^{ε}-carboxymethyllysine (CML, +58) (Glomb and Monnier 1995) and the recently characterised N^{ε}-pyrrolelysine (GA-pyrrole, +50 and not pyrrolysine the amino acid) (Chikazawa et al. 2020), although both PTMs are formed after oxidation of either GA or its reaction products (**Figure 3.3**) (Glomb and Monnier 1995; Klaus, Rau, and Glomb 2018; Vistoli et al. 2013).

Aside from lysines, GA has been reported to react with free cysteines to form thiohemiacetal intermediates that can oxidise to carboxymethyl cysteine (CMC) (Adrover et al. 2008). In contrast, GA has limited reactivity with the guanidino group of arginine (Acharya and Manning 1983; Cho, Okitani, and Kato 1986). Our chemistry collaborators have shown that GA may also react with histidine, tyrosine and serine under certain conditions, but these PTMs have not been documented or characterised in the literature (Naorem Nihesh, personal communication).

3.1.3 Chapter aims

In this chapter, I aimed to:

a) Verify whether protein aldehydes introduced by GA modification of model protein HEL increases IgG responses to native protein;
b) Characterise HEL modification by GA, in particular using MS approaches;
c) Understand the relationship between in vitro modification and the in vivo antibody response; and
d) Determine whether self-tolerance to mouse lysozyme (ML), a homologous extracellular protein, can be broken by protein aldehydation.

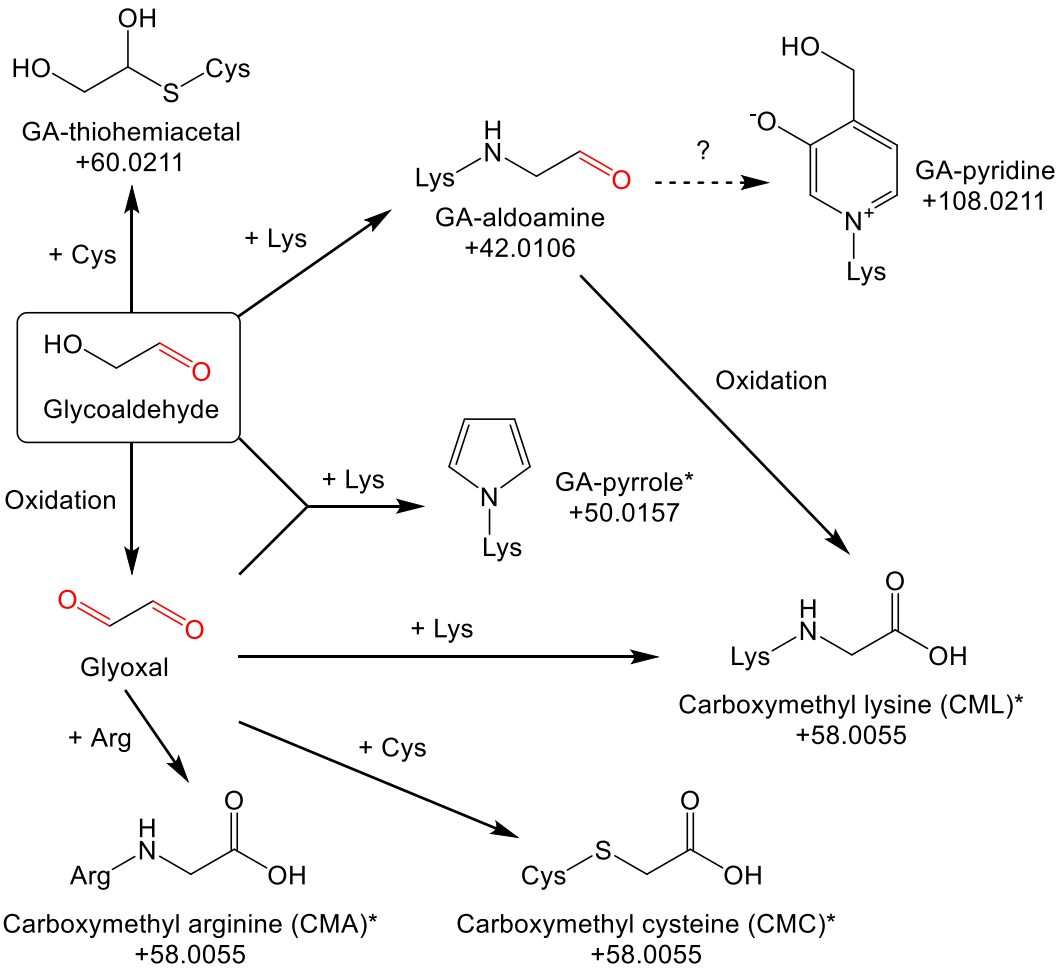


Figure 3.3: Specific PTMs and their monoisotopic mass changes resulting from modification with glycolaldehyde (GA) and its oxidation product glyoxal. GA-aldoamine (Acharya and Manning 1983) and GA-pyridine (Nagai et al. 2002) form on lysine residues. GA can also react with free cysteines to form thiohemiacetal (Adrover et al. 2008). Other PTMs require the oxidation of GA to glyoxal, or direct oxidation of the PTMs (Spanneberg et al. 2010). These PTMs are indicated with asterisks and include carboxymethylated lysine, cysteine and arginine (Vistoli et al. 2013). GA-pyrrole is thought to be formed from one molecule of GA and one of glyoxal (Chikazawa et al. 2020). Aldehydes are indicated in red.

3.2 Results

3.2.1 GA-modified HEL elicits IgG responses to native protein

Lysozyme is a secreted anti-microbial enzyme that forms part of the innate immune system, whose main function is to cleave peptidoglycan found in bacterial cell walls to facilitate lysis. Hen egg lysozyme (HEL, UniProt ID: P00698) is a major component of egg white (approximately 3.5% of the total protein content) (Weth, Schroeder, and Buxtorf

1988) that was first described over a century ago (Laschtschenko 1909). Since then, it has been extensively studied as a model protein, and its anti-microbial properties have been highly useful in food and pharmaceutical industrial applications (Abeyrathne, Lee, and Ahn 2013). HEL has 129 amino acids (Canfield 1963), a predicted molecular weight of 14305 Daltons (Da) when folded (Expasy), no naturally occurring PTMs (UniProt), eight cysteines forming four disulphide bonds, and six lysines (plus an additional amino group at the N-terminus) (**Figure 3.4**). Its relatively small size and simplicity make it a useful model for studying the effect of protein modifications on immunogenicity.

To repeat previous studies, HEL was modified at 0.25 mg/mL with 20 mM GA at 37 °C for 3 h (HEL GA), then buffer exchanged into phosphate-buffered saline (PBS) to remove excess GA. These "standard" reaction conditions were identical to Allison and Fearon (2000) and minimised protein cross-linking while being optimal for anti-HEL IgG responses (Moghaddam 2001). HEL incubated without GA was concurrently prepared as a control (HEL mock). Additionally, to remove the effects of GA-aldoamine, Allison and Fearon (2000) performed GA modification in the presence of reducing agents to directly modify proteins with hydroxyethyl, which is the reduced form of GA-aldoamine (**Figure 3.2A**). In contrast, our lab modified this protocol to post-reduce HEL GA with 20 mM sodium borohydride ($NaBH_4$) (HEL PR) so that protein carbonyls would be specifically reduced while maintaining all other non-carbonyl modifications such as protein cross-linking (Moghaddam et al. 2011) (**Figure 3.2B**). Thus, HEL PR serves as a negative control to verify that observed effects resulting from HEL GA modification are specific to GA-aldoamine rather than other chemical modifications.

Allison and Fearon (2000) immunised mice (strain and sex not specified) with proteins in PBS without adjuvant via the subcutaneous (s.c.) route at the base of the tail.

KVFGRCELAA AM**K**RHGLDNY RGYSLGNWVC
AA**K**FESNFNT QATNRNTDGS TDYGILQINS
RWWCNDGRTP GSRNLCNIPC SALLSSDITA
SVNCA**KK**IVS DGNGMNAWVA WRNRC**K**GTDV
QAWIRGCRL

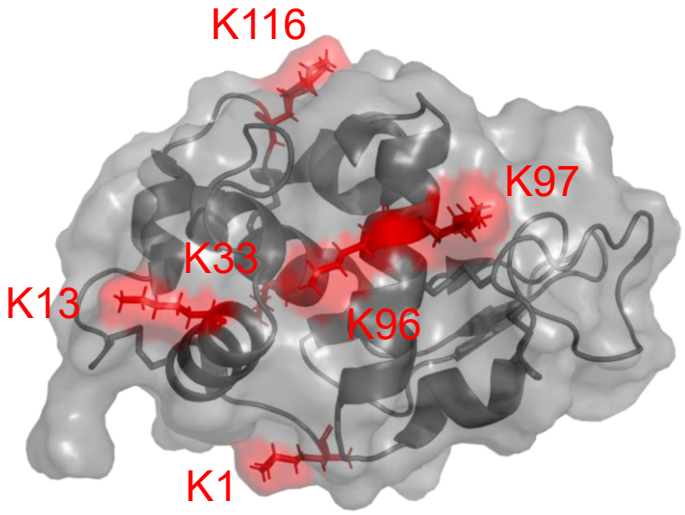


Figure 3.4: Sequence (UniProt ID: P00698) and structure of hen egg lysozyme (HEL). Lysines indicated in red within the sequence and structure. K33 is on the other side of the molecule in this orientation. PDB ID: 2VB1 (J. Wang et al. 2007)**.**

In our lab, HEL protein is additionally tested and cleaned of endotoxin (data not shown) because endotoxin contamination can activate or modulate immune responses non-specifically as a pattern-associated molecular pattern (PAMP) (Section 1.1). Immunisations in our lab are typically performed on female BALB/c mice because females generally have greater immunological responsiveness compared with males (Terres, Morrison, and Habicht 1968) and to avoid complications arising from fighting in male mice. Our lab generally immunises non-anaesthetised mice subcutaneously (s.c.) in the flank but previous experiments have suggested that s.c. flank immunisation may produce highly variable anti-HEL IgG responses. To test whether other immunisation routes were less variable or more immunogenic, I immunised female BALB/c mice with (10 μg) HEL mock, HEL

GA or HEL PR in PBS s.c. in the flank, intraperitoneally (i.p.), or s.c. in the hock (a more refined version of the footpad injection) (Kamala 2007) (**Figure 3.5A**).

Four weeks after priming, IgG antibody responses against native HEL were measured from sera (**Figure 3.5B**). Mice immunised in the flank with HEL GA had one low responder and two high responders, and no responders for mice immunised with HEL mock. In contrast, for hock immunisations, HEL GA immunised mice had lower anti-HEL IgG responses compared with flank as well as one responder in the HEL mock immunised group. Interestingly, HEL GA i.p. immunisations also produced lower responses than immunisations in the flank but with less variation. Based on these results, I decided to keep using s.c. flank immunisation because it seemed to be the most immunogenic route overall for HEL GA. Although sample sizes for this experiment were small, HEL GA nevertheless generally elicited higher anti-HEL IgG responses compared with HEL mock, regardless of immunisation route.

Next, I tested whether I could reproduce with greater statistical power the observation of Allison and Fearon (2000) that mice immunised with HEL GA and without extrinsic adjuvant had increased anti-HEL IgG responses. Furthermore, I examined whether increased responses could be abrogated by HEL PR, which was not used by Allison and Fearon, but had been successfully used in our lab (Moghaddam et al. 2011). Based on previous protocols in the lab, I performed seven separate experiments with 10 μg prime followed six weeks later with a 5 μg homologous boost, and pooled together the anti-HEL IgG endpoint titres post-prime and post-boost. I observed that HEL GA was indeed significantly more immunogenic than HEL mock and HEL PR after priming, and after priming plus boosting (**Figure 3.6**).

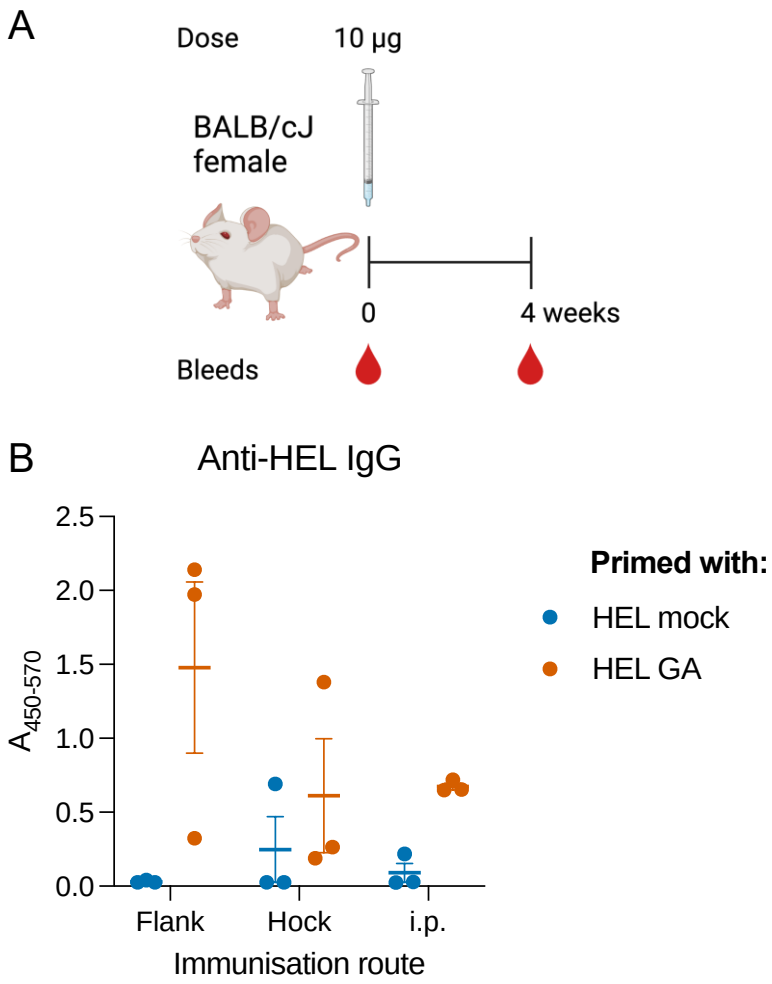


Figure 3.5: HEL GA immunisation elicits higher anti-HEL IgG responses compared with HEL mock in female BALB/c mice. A) Bleed and immunisation schedule. B) Anti-HEL IgG responses after priming. Sera were diluted 1:50. Data are mean ± SEM.

3.2.2 Biochemical characterisation of HEL GA and HEL PR

Following the in vivo experiments, I biochemically characterised the changes caused by GA modification of HEL. As previously shown in our lab (Moghaddam et al. 2011), GA modification of HEL increased protein carbonylation (**Figure 3.7A**) and caused some HEL to oligomerise (**Figure 3.7B**).

I also analysed HEL GA by intact liquid chromatography mass spectrometry (LC-MS) (**Figure 3.8**). A majority of HEL protein remained unmodified but many new peaks

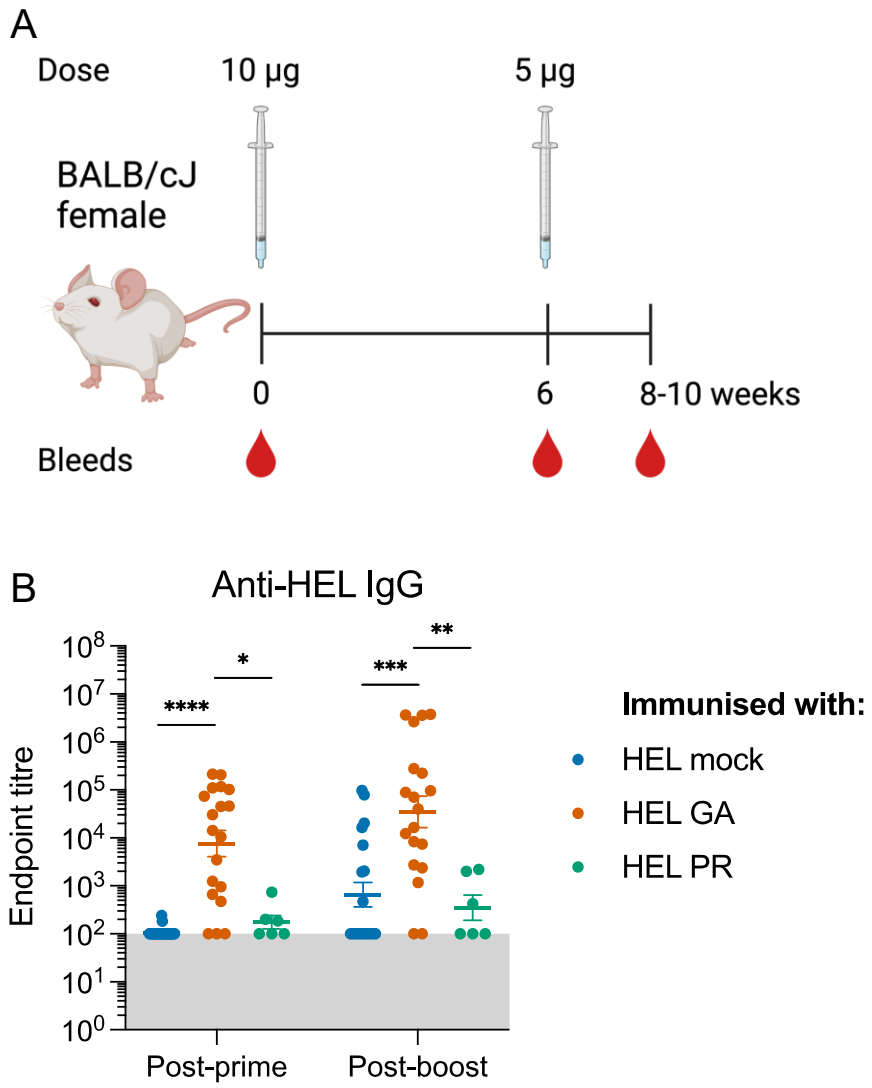


Figure 3.6: HEL GA immunisation elicits higher anti-HEL IgG responses compared with HEL mock and HEL PR in female BALB/c mice. A) Bleed and immunisation schedule. B) Endpoint titres after prime and boost. 6–25 mice were analysed for post-prime and 6–19 mice were analysed for post-boost across 5 independent experiments. Data are mean ± SEM (*p ≤ 0.05, **p ≤ 0.01, ***p ≤ 0.001, ****p ≤ 0.0001; Kruskal-Wallis then Dunn's multiple comparison test). Sera were serially diluted starting at 1:100 and non-responding mice were plotted at the limit of detection (shaded in grey).

appeared after GA treatment, representing a heterogeneous mix of modifications. Based on previously assigned PTMs (Moghaddam et al. 2011), I identified GA-aldoamine (+42) and GA-pyridine (+108). GA-pyridine appeared to be the most abundant modification (41% relative to unmodified) followed by GA-aldoamine (25% relative to unmodified). However, I was unable to identify CML (+58) unambiguously, since the only peak in that region was +61. I also did not find any evidence for GA-pyrrole (+50).

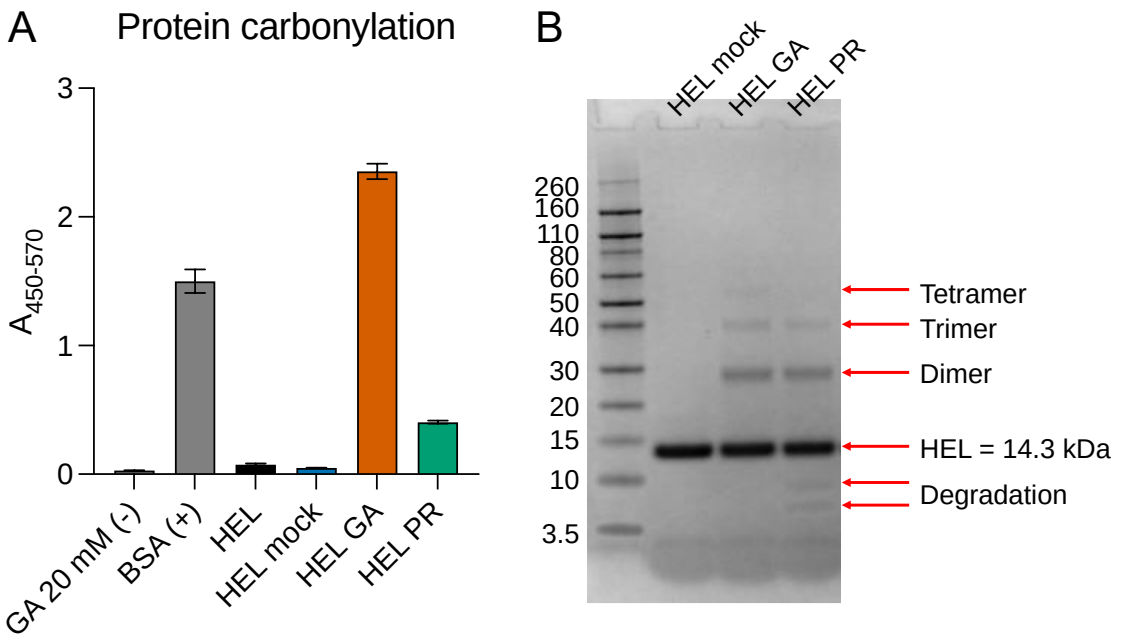


Figure 3.7: GA treatment increases HEL carbonylation and oligomerisation, and post-reduction (PR) decreases carbonylation. HEL was GA-modified at 0.25 mg/mL with 20 mM GA at 37 °C for 3 h, and post-reduced with 20 mM $NaBH_4$ at 37 °C for 3 h. A) Protein carbonylation measured by DNPH ELISA. Data are mean ± SD of 3 technical replicates. B) Reducing SDS-PAGE gel. 1 µg protein was loaded in each lane of a 4–12% Bis-Tris gel. Representative experiment shown from one of four batches of modified HEL.

HEL PR had lower levels of protein carbonylation compared with HEL GA but higher compared with HEL mock, suggesting that $NaBH_4$ did not reduce all RCs (**Figure 3.7A**). Post-reduction also caused a small amount of protein degradation (**Figure 3.7B**). Otherwise, HEL PR retained most modifications resulting from GA treatment, as seen by overlaying the intact LC-MS spectra (**Figure 3.8B**). However, the GA-aldoamine peak (+42) increased by mass +2, suggesting that it was mostly reduced to non-reactive hydroxyethyl (**Figure 3.2B**). In contrast, the GA-pyridine peak (+108) did not seem to change, whereas the potential CML peak at +61 disappeared and a few other unidentified peaks also shifted.

The shifting of numerous previously unassigned peaks post-reduction suggested that the peaks could actually be HEL modified with multiple GA-aldoamines. Indeed, I

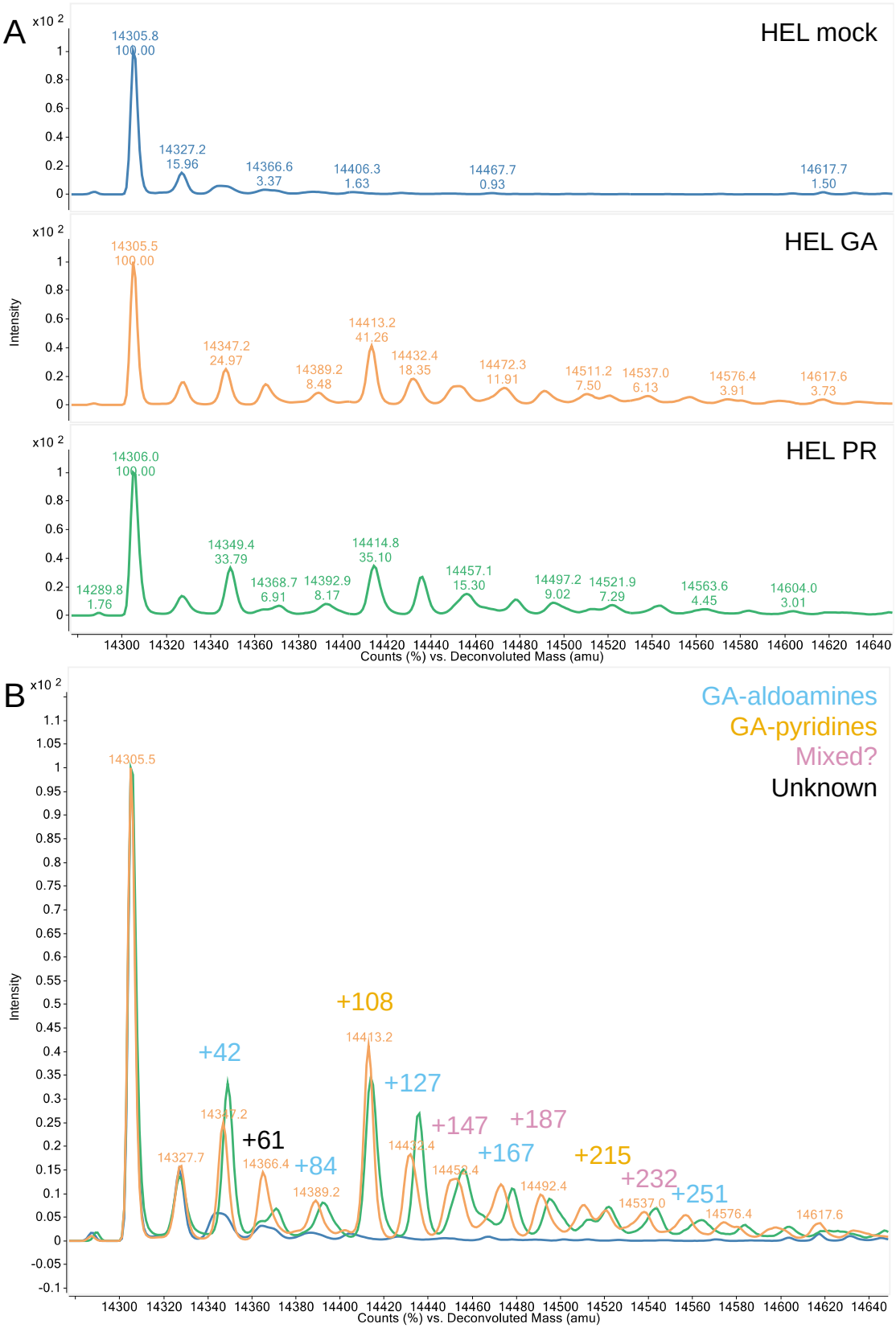


Figure 3.8: GA treatment causes PTMs and PR treatment selectively reduces RC-containing PTMs. HEL was GA modified at 0.25 mg/mL with 20 mM GA at 37 °C for 3 h, followed by PR with 20 mM $NaBH_4$ at 37 °C for 3 h. A) Offset and B) overlaid intact LC-MS spectra. Peaks are annotated with deconvoluted mass and abundance percent relative to the largest peak.

identified mass shifts for HEL GA that were close to multiples of +42, corresponding to HEL modified with two (+84), three (+127), four (+167) and six (+251) GA-aldoamines (**Figure 3.8B**, light blue). There was also a small peak that corresponded to HEL modified with two GA-pyridines (+215, orange). Some peaks could have been HEL modified with GA-pyridine plus additional GA-aldoamines, but I was less confident about these assignments since the observed masses differed from expected by 3 to 5 Da (**Figure 3.8B**, pink). Many new peaks after GA modification appeared to have been modified with at least one GA-aldoamine, and thus GA-aldoamine rather than GA-pyridine may be the most abundant PTM. Previous interpretations of the LC-MS data (Moghaddam et al. 2011) are therefore likely to have underestimated the GA-aldoamine content of GA-modified HEL.

Post-reduction of GA-aldoamine with $NaBH_4$ theoretically changes mass by only +2, and this small shift was difficult to detect unambiguously. Therefore, I also tried derivatising HEL GA with DNPH to label RC-containing peaks. Derivatisation of RCs with DNPH (MW = 198.14, **Figure 3.1A**) is a condensation reaction (i.e. loss of H_2O, MW = 18) and should result in an overall mass change of +180. LC-MS of HEL GA derivatised with DNPH revealed five potential new peaks (**Figure 3.9**), although the mass shifts for some were too far from the expected +180 to be DNPH. The GA-aldoamine peak (peak 1) indeed appeared to be derivatised by DNPH, while peak 3 was tentatively assigned as three GA-aldoamine and peak 4 as GA-pyridine plus GA-aldoamine.

3.2.3 Optimising HEL GA treatment for in vivo immunogenicity

I observed that IgG antibody responses after HEL GA immunisation were often variable (**Figure 3.5**) and hypothesised that this may be due to the heterogenous modifications caused by GA (**Figure 3.8**). Previous work established a significant correlation between

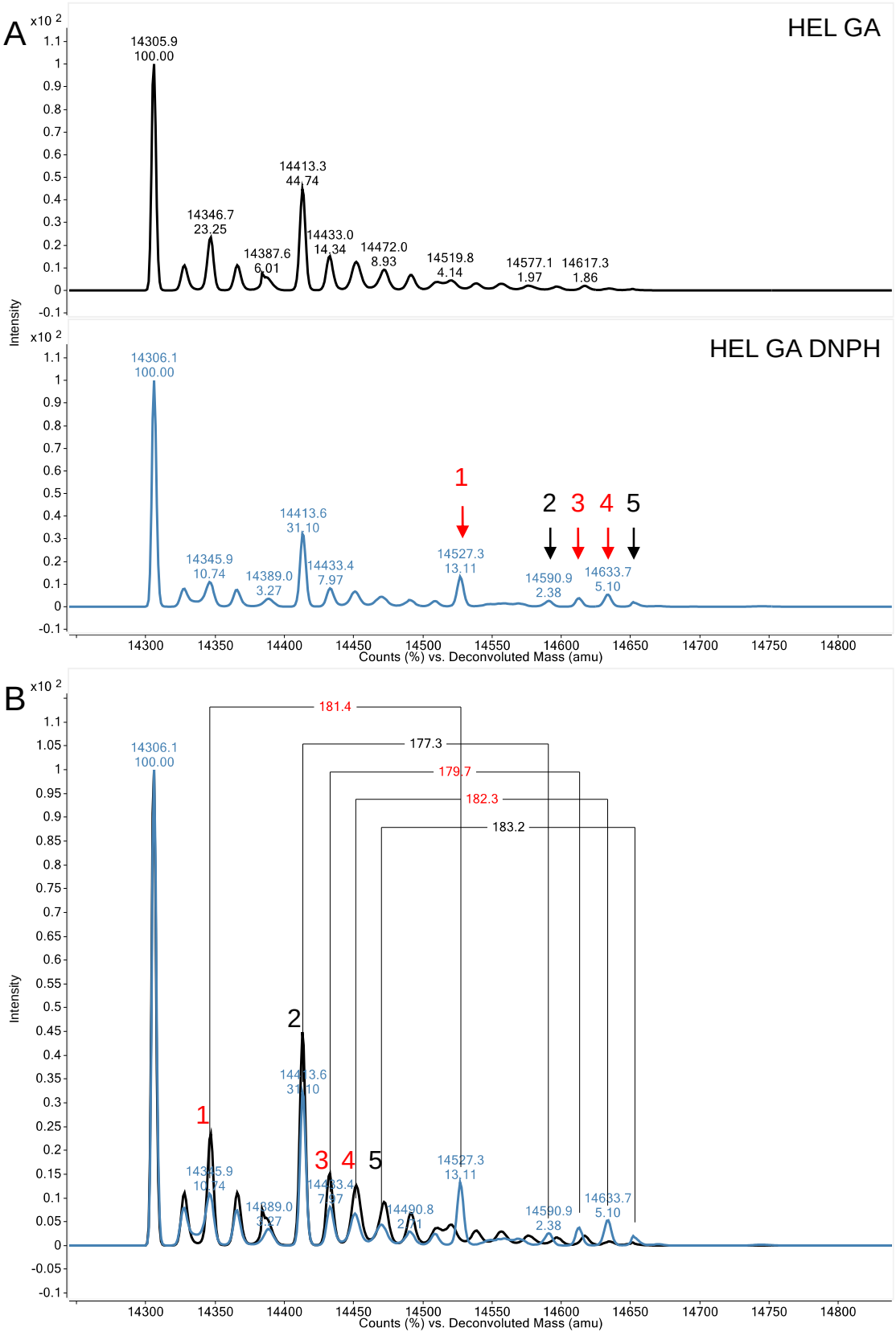


Figure 3.9: DNPH derivatisation of HEL GA identifies three RC-containing peaks. DNPH derivatisation results in a mass change of +180. A) Offset intact LC-MS spectra. New peaks that appear post-derivatisation are indicated with arrows. B) Overlaid intact LC-MS spectra. Callipers show three peaks that were derivatised (red) and two other peaks that may not correspond with derivatised species (black). Peaks are annotated with deconvoluted mass and abundance percent relative to the largest peak.

the amount of protein carbonylation (measured in moles carbonyl / moles purified protein) (Levine et al. 1990) and IgG1 antibody titres against native protein (Moghaddam et al. 2011). Thus, I investigated whether HEL GA immunogenicity could be enhanced or made less variable by altering reaction conditions to a) increase overall protein aldehydation while b) preventing the formation of non-aldehyde PTMs, so that protein aldehydes could be exclusively linked to increased immunogenicity.

First, I set up HEL GA modifications 0, 0.5, 1, 2 and 3 h long, then buffer exchanged the reactions into PBS for analysis. Longer incubations with GA increased HEL protein carbonylation (**Figure 3.10A**) but also oligomerisation (**Figure 3.10B**). After 0.5 h incubation, protein carbonylation was higher than background (**Figure 3.10A**) and GA-aldoamine (+42) could already be detected by intact LC-MS (**Figure 3.10C**). In contrast, GA-pyridine (+108) was only detected after 2 h, and became the most abundant modified peak by 3 h.

Female BALB/c mice were then primed with 10 μg HEL mock, HEL GA (3 h) or HEL GA modified for 1 h, and homologously boosted with 5 μg six weeks later (**Figure 3.11A**). Anti-HEL IgG responses were measured six weeks post-prime and four weeks post-boost (**Figure 3.11B**). After priming, four out of six HEL GA 3 h immunised mice and two out of six HEL GA 1 h immunised mice had detectable anti-HEL IgG titres, while no responses were seen in HEL mock immunised mice. After homologous boosting, the four responders in the HEL GA 3 h group had even higher titres, and an additional responder was detected in the HEL GA 1 h group. These results suggested that immunogenicity may be positively correlated with the amount of protein carbonylation.

I next investigated the effect of other variables such as GA concentration, protein concentration and temperature, keeping all other conditions standard. Since there were

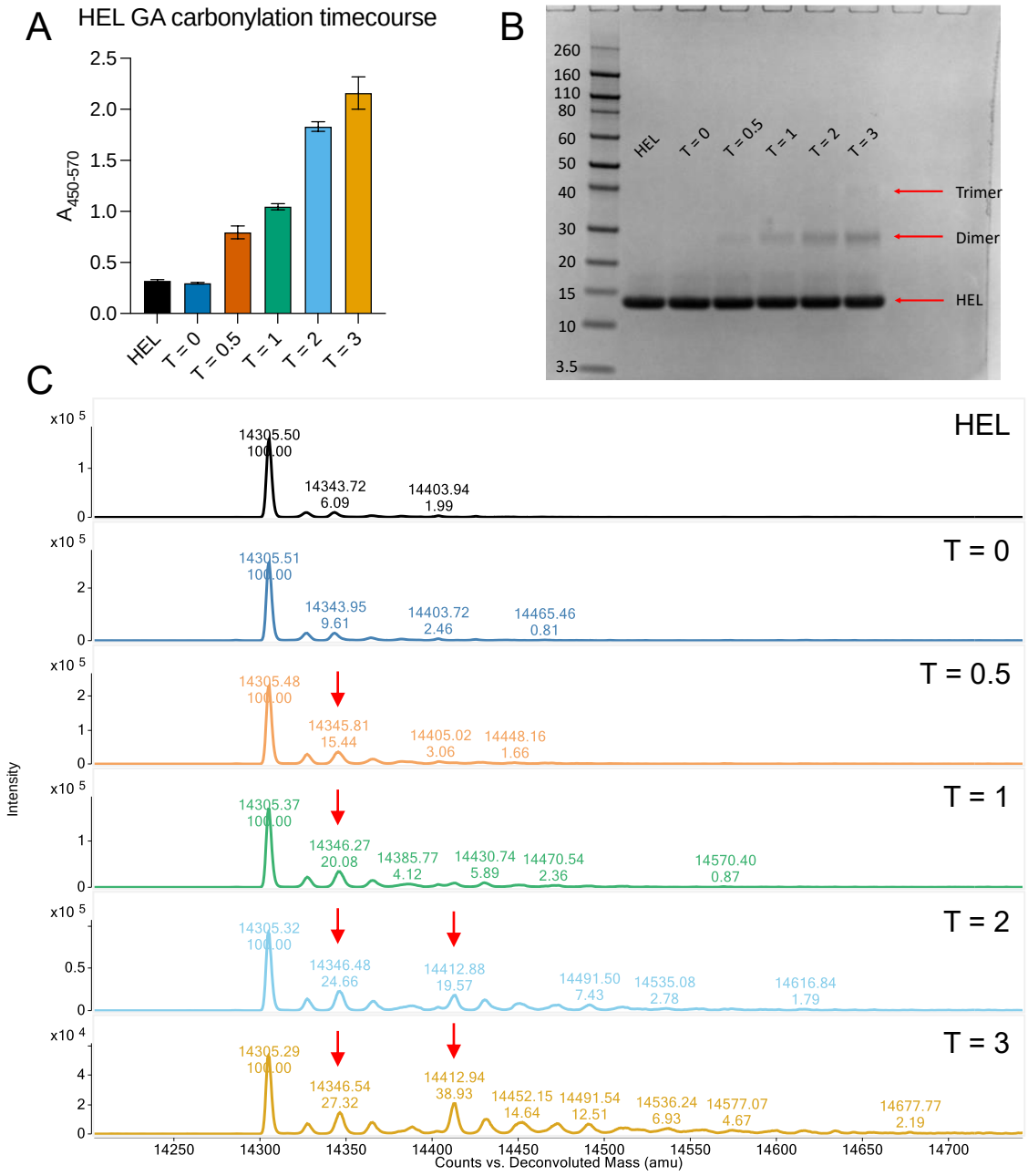


Figure 3.10: Carbonylation and oligomerisation increase over time with HEL GA modification. HEL was buffer exchanged into PBS after modification. A) Protein carbonylation measured by DNPH ELISA. Data are mean ± SD of 3 technical replicates. B) Reducing SDS-PAGE gel. 2 µg protein was loaded in each lane of a 4–12% Bis-Tris gel. C) Intact LC-MS spectra. Red arrows indicate new peaks. Peaks are annotated with deconvoluted mass and abundance percent relative to the largest peak.

many conditions to test, I ran samples on intact LC-MS on the same day without buffer exchanging into PBS to increase throughput. As expected, lower GA concentrations resulted in fewer modifications during the 3 h incubation (**Figure 3.12A**). No new peaks

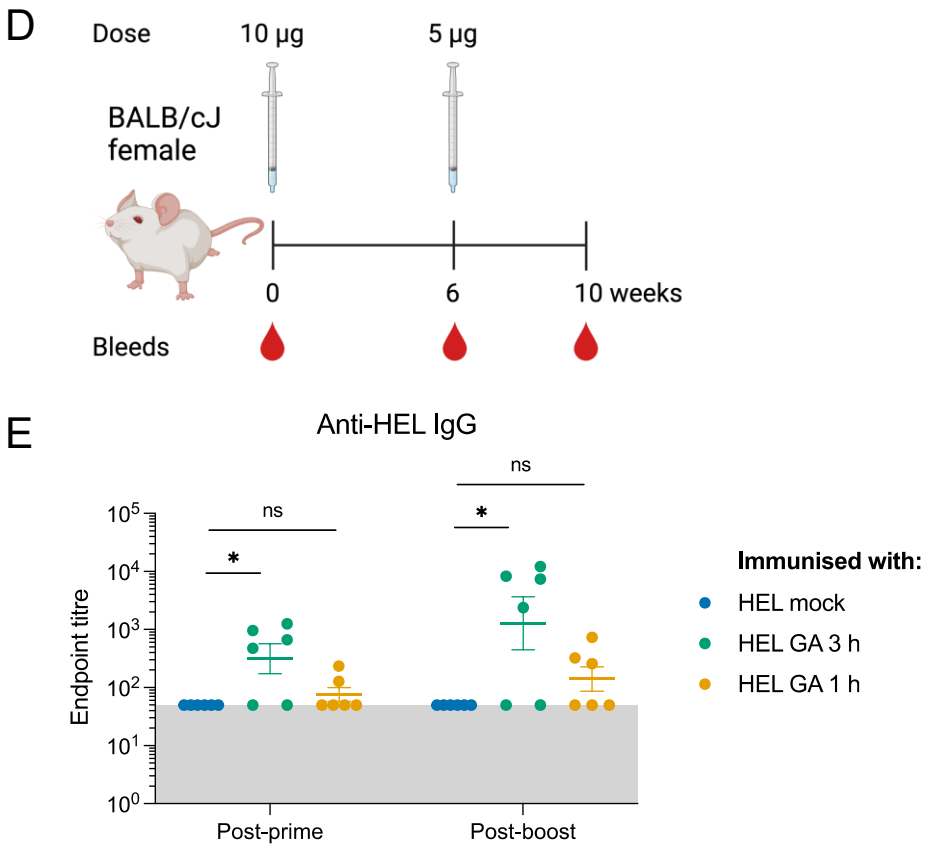


Figure 3.11: HEL GA-modified for 3 h elicits higher IgG titres. A) Bleed and immunisation schedule. B) Anti-HEL IgG responses of immunised female BALB/c mice primed with 10 µg and homologously boosted with 5 µg protein six weeks later. Data are mean ± SEM (*$p \leq 0.05$; Kruskal-Wallis then Dunn's multiple comparison test). Sera were serially diluted starting at 1:50 and non-responding mice were plotted at the limit of detection (shaded in grey).

were detected with only 1 mM GA treatment. GA-aldoamine was detected starting from 5 mM GA, GA-pyridine from 20 mM GA, and extensive modifications (with visible aggregation indicative of protein cross-linking) at 50 mM GA.

I expected to see increased cross-linking in reactions with higher HEL protein concentrations due to the increased likelihood of intermolecular interactions. Although aggregation was visibly noticeable in the tube when incubated for extended periods, none was seen within 3 h. Instead, higher protein concentrations seemed to decrease the overall proportion of modified HEL, in particular HEL with GA-pyridine (**Figure 3.12B**).

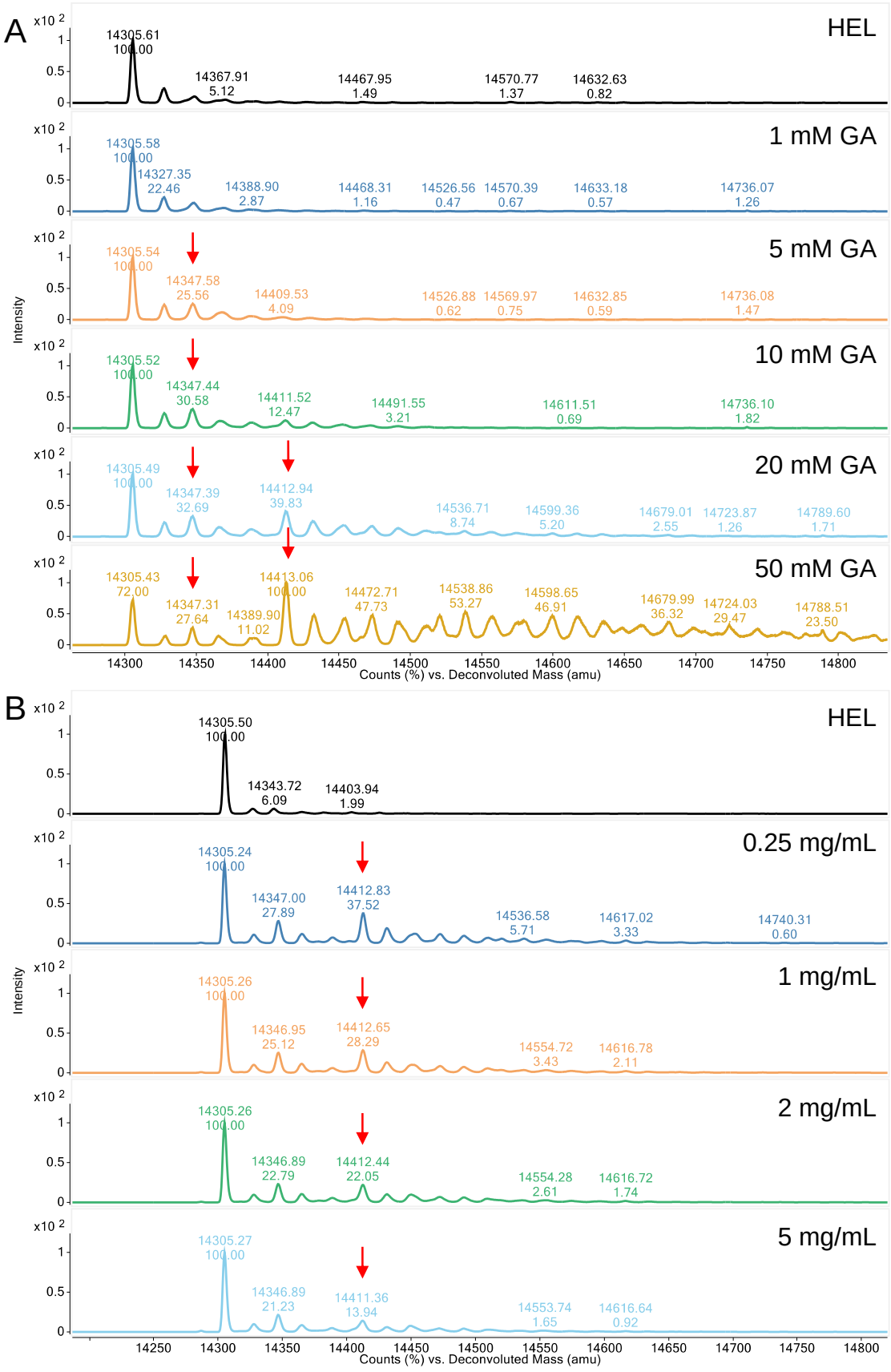


Figure 3.12: Increasing GA concentration increases PTMs, while increasing protein concentration decreases the proportion of modified HEL. HEL was not buffer exchanged into PBS but placed immediately on ice at the end of the reaction and intact LC-MS run on the same day. Intact LC-MS spectra showing the effect of A) GA concentration and B) protein concentration.

Lower incubation temperatures at 4 °C (on ice) and even 21 °C (RT) appeared to slow the chemical reaction substantially, and after 3 h barely any new PTMs were formed (**Figure 3.13A**). This suggested that leaving reactions or buffer-exchanged products on ice for short periods of time was acceptable. In contrast, after excess GA was removed by buffer exchange, I found that GA-aldoamine levels decreased. Immediately after GA modification, the relative proportion of HEL modified with GA-aldoamine was 28% compared with unmodified HEL (**Figure 3.13B**). After only 5 d at 4 °C, this decreased to 18% and further to 14% after 6 weeks. However, more GA-aldoamine was preserved (24%) if samples were aliquoted and stored at -80 °C soon after buffer exchange. I also noted that the relative abundance of HEL modified with GA-pyridine increased from 38% to more than 50% after all methods of storage.

So far, I was unable to increase GA-aldoamine content without also introducing GA-pyridine. Chen et al. (2017) increased the efficiency of peptide aldehyde modification by optimising their use of buffers and pH. I considered whether a similar strategy could be successfully applied to GA-modified proteins. I tested acetate (**Figure 3.14**), citrate (**Figure 3.15**), and phosphate buffers (**Figure 3.16**) at a range of pH values and found that both composition and pH influenced HEL GA modification. Acetate and citrate buffers seemed to favour the formation of a single GA-aldoamine rather than GA-pyridine, which was largely absent. In contrast, GA modification in phosphate buffer was very efficient and resulted in extensive modification. For all buffers, reactions at higher pH resulted in more modification than reactions at lower pH in the same buffer.

I selected two buffer conditions for further experiments: a) citrate pH 5 (C5) as it had a high proportion of HEL modified with single GA-aldoamine (61% relative to unmodified) (**Figure 3.15A**, green), and b) phosphate pH 6 (P6) (**Figure 3.16A**, blue), in

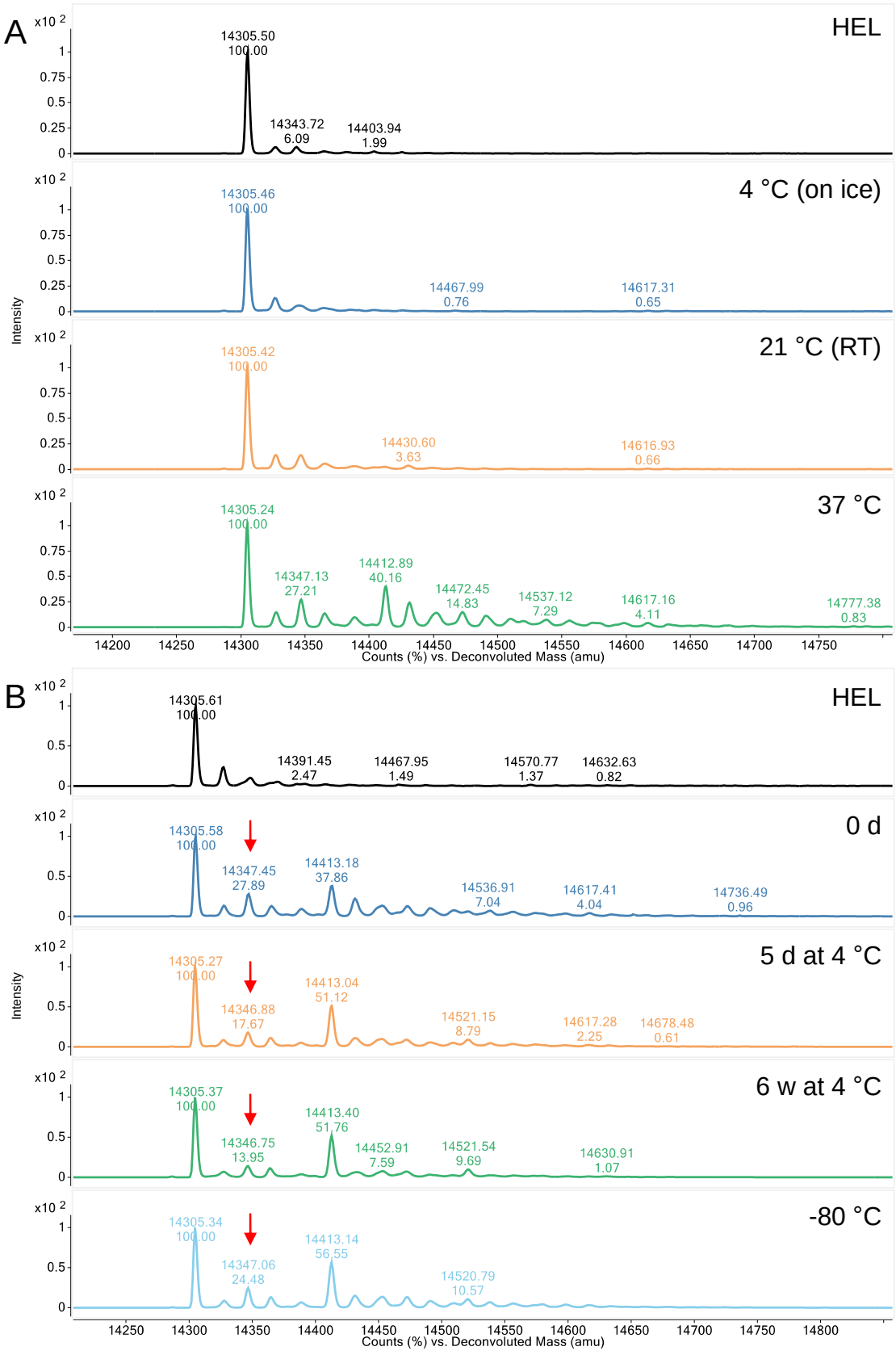


Figure 3.13: GA modification does not proceed at lower temperatures, and modified protein is best preserved at -80 °C. Intact LC-MS spectra showing the effect of A) reaction temperature and B) storage conditions.

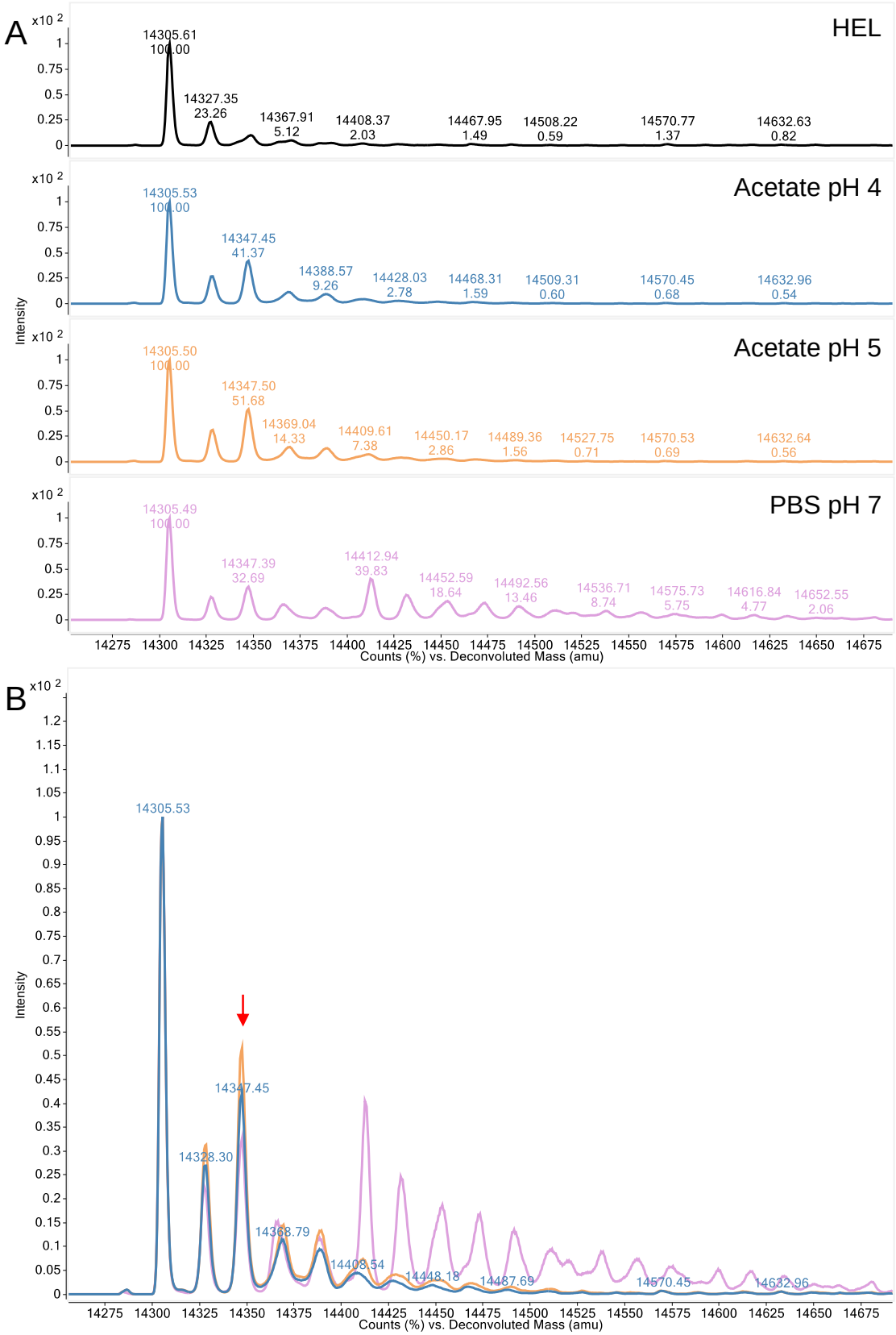


Figure 3.14: GA modification in acetate buffer is more efficient at higher pH and favours single GA-aldoamine. HEL was not buffer exchanged into PBS but placed immediately on ice at the end of the reaction and intact LC-MS run on the same day. Intact LC-MS spectra A) offset and B) overlaid. Red arrow indicates single GA-aldoamine peak.

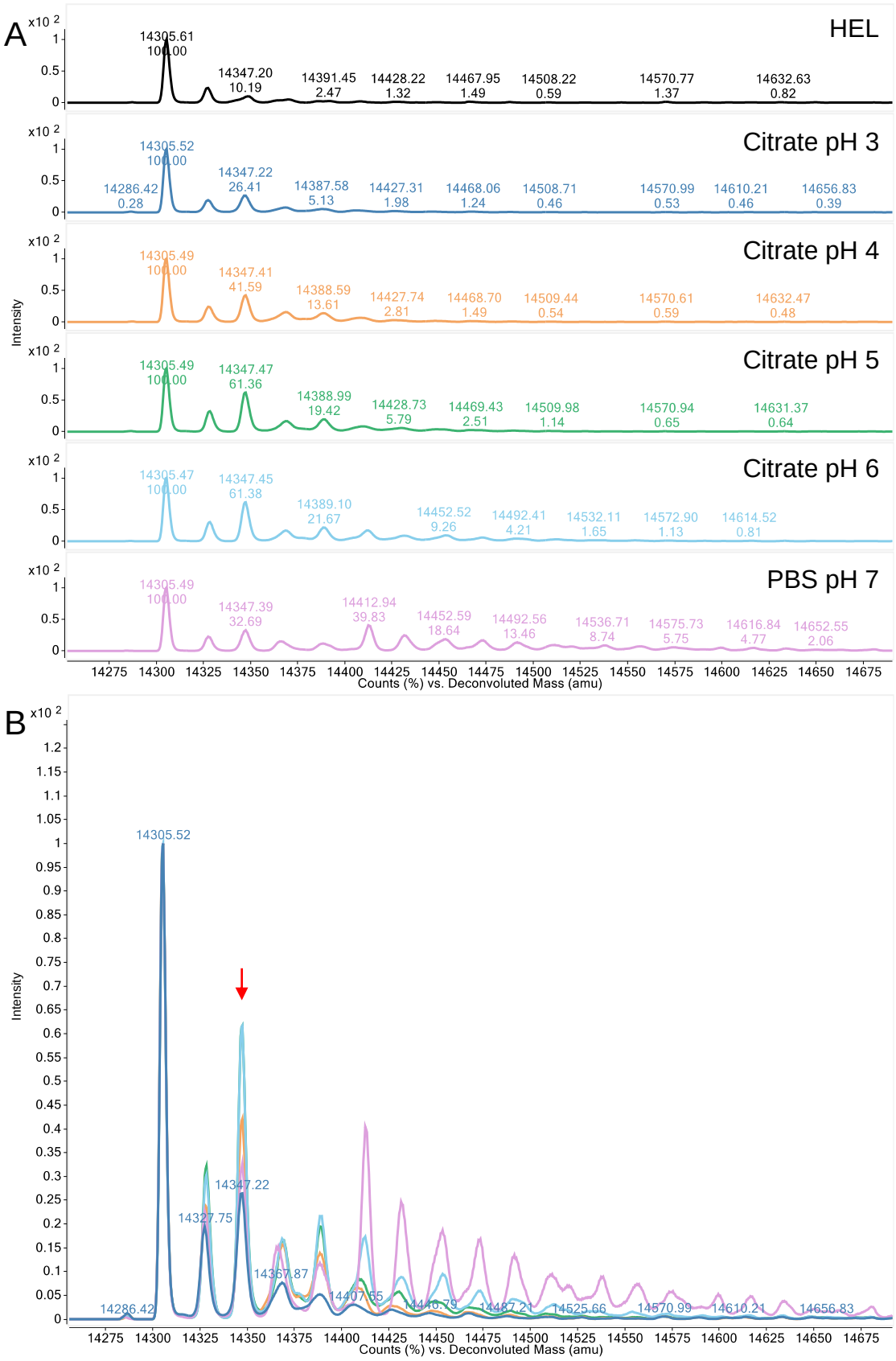


Figure 3.15: GA modification in citrate buffer is more efficient at higher pH and favours single GA-aldoamine. HEL was not buffer exchanged into PBS but placed immediately on ice at the end of the reaction and intact LC-MS run on the same day. Intact LC-MS spectra A) offset and B) overlaid. Red arrow indicates single GA-aldoamine peak.

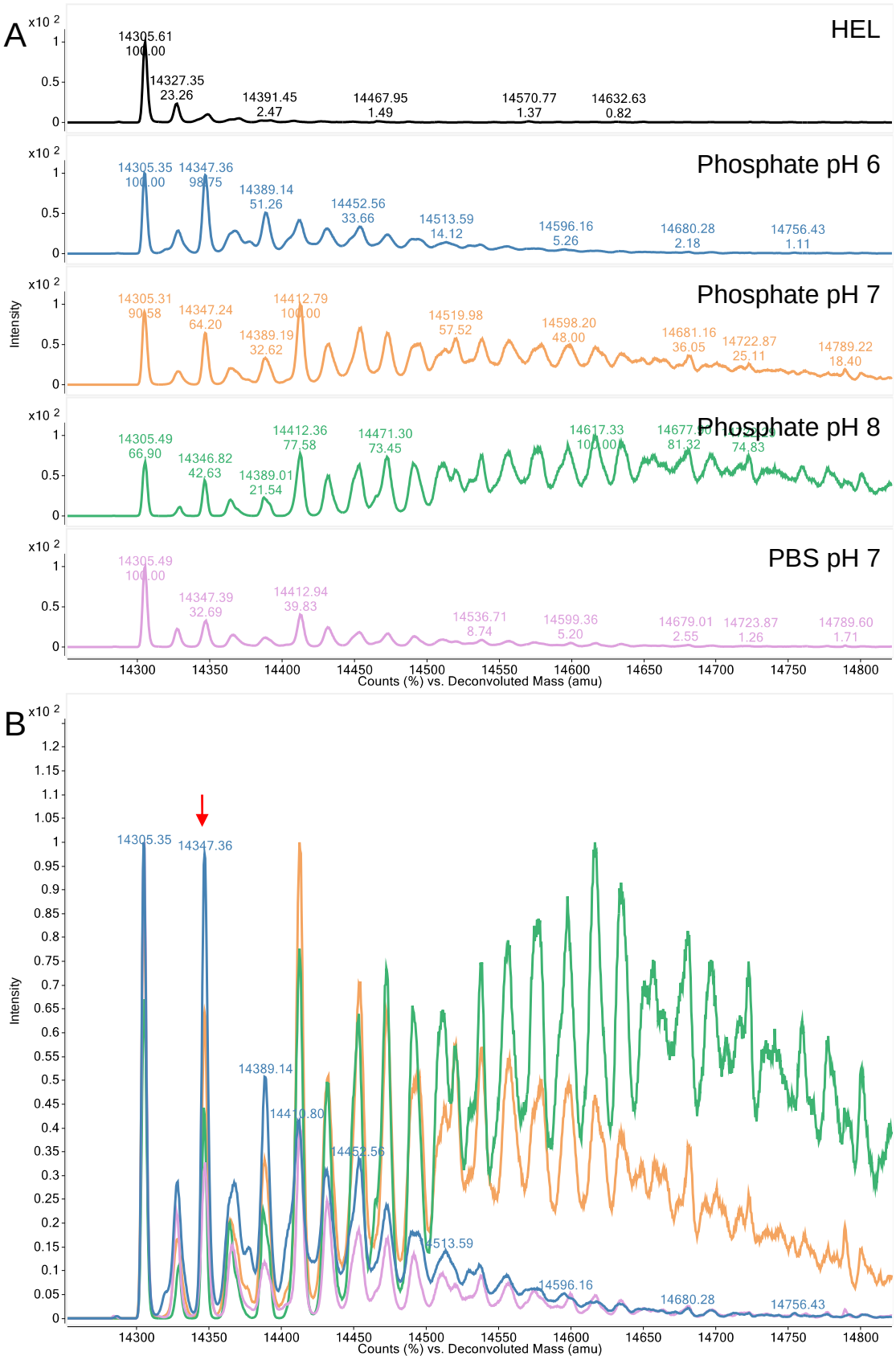


Figure 3.16: GA modification in phosphate buffer is highly efficient and results in extensive PTMs. HEL was not buffer exchanged into PBS but placed immediately on ice at the end of the reaction and intact LC-MS run on the same day. Intact LC-MS spectra A) offset and B) overlaid. Red arrow indicates single GA-aldoamine peak.

which HEL was more modified than HEL GA PBS. After buffer exchanging into PBS for immunisations, both HEL GA C5 and HEL GA P6 surprisingly lost much of their GA-aldoamine content, down to 32% and 46% respectively (**Figure 3.17**). Nonetheless, the DNPH assay suggested that HEL GA P6 had the highest carbonyl content, followed by HEL PBS GA, then HEL C5 GA (**Figure 3.18A**). These samples were post-reduced, and overlaying intact LC-MS spectra again suggested that GA-aldoamine peaks shifted while GA-pyridine remained unchanged (**Figure A.1**). I also checked the samples on reducing SDS-PAGE (**Figure 3.18B**). As before, I found that HEL GA samples were oligomerised (although HEL modified in C5 buffer was less so), and HEL PR samples were slightly degraded.

To test in vivo immunogenicity, female BALB/c mice were immunised with HEL GA modified in PBS, C5, and P6 buffers, plus their post-reduced samples (**Figure 3.18C**). Six weeks after priming, HEL GA PBS immunisations elicited the highest anti-HEL IgG titres, followed by HEL GA P6, then HEL GA C5 (**Figure 3.18D**). Interestingly, HEL GA C5, which had lower overall carbonylation but a relatively homogeneous population of HEL modified with GA-aldoamine, elicited anti-HEL IgG responses that were completely abrogated by post-reduction. In contrast, HEL GA P6 seemed slightly less immunogenic than HEL GA PBS, even though it had slightly higher levels of carbonylation.

Since I could not increase protein carbonylation without also introducing additional modifications, I used the original HEL GA PBS reaction conditions for the remainder of the thesis. At least when compared with the C5 and P6 reaction conditions, HEL GA PBS elicited the highest response and was the most physiological buffer.

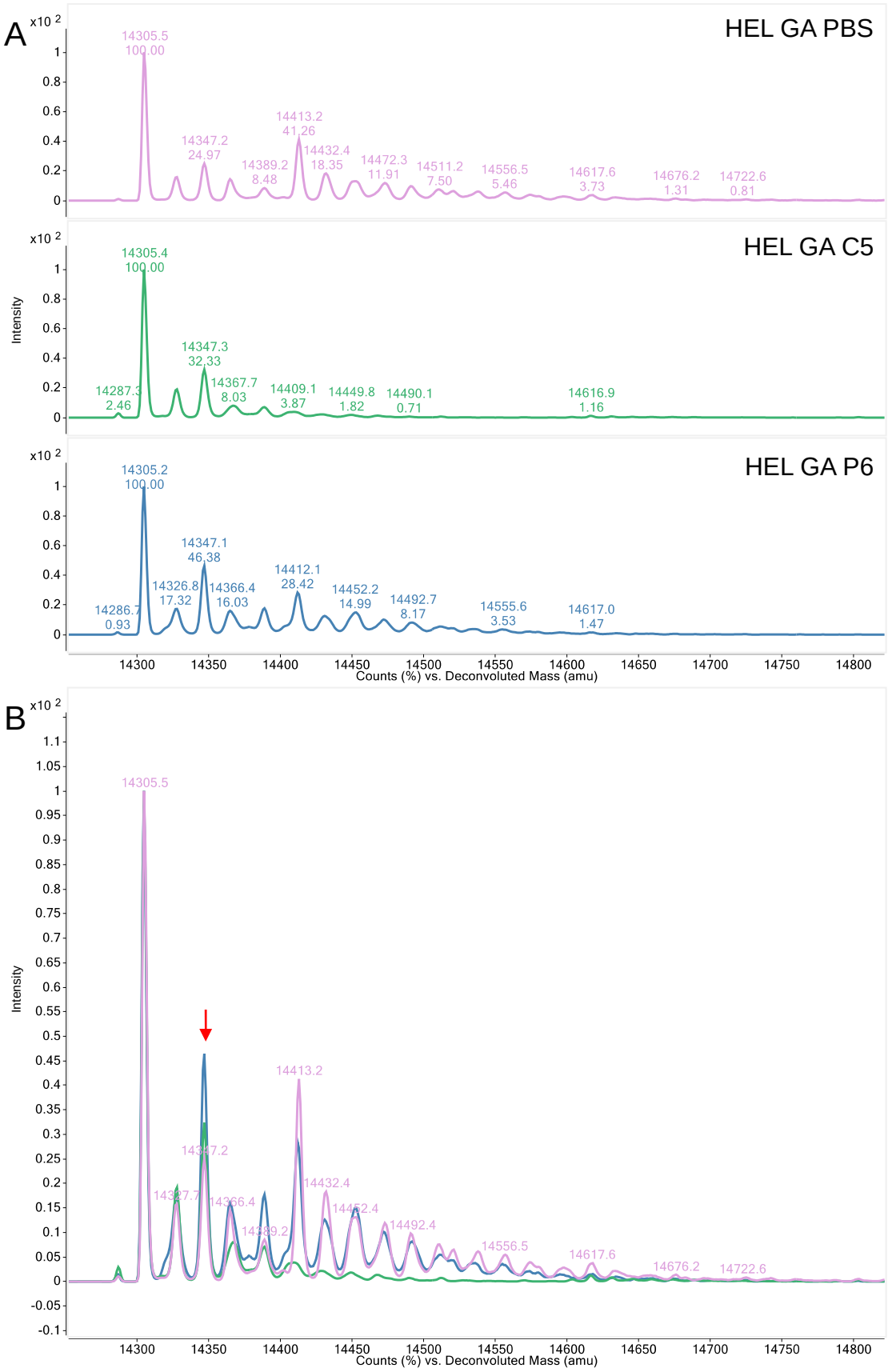


Figure 3.17: Selected HEL GA prepared in different buffers then buffer exchanged into PBS for in vivo experiments. A) Offset and B) overlaid intact LC-MS spectra. Note that the extent of modification has decreased after buffer exchange into PBS. Red arrow indicates single GA-aldoamine peak.

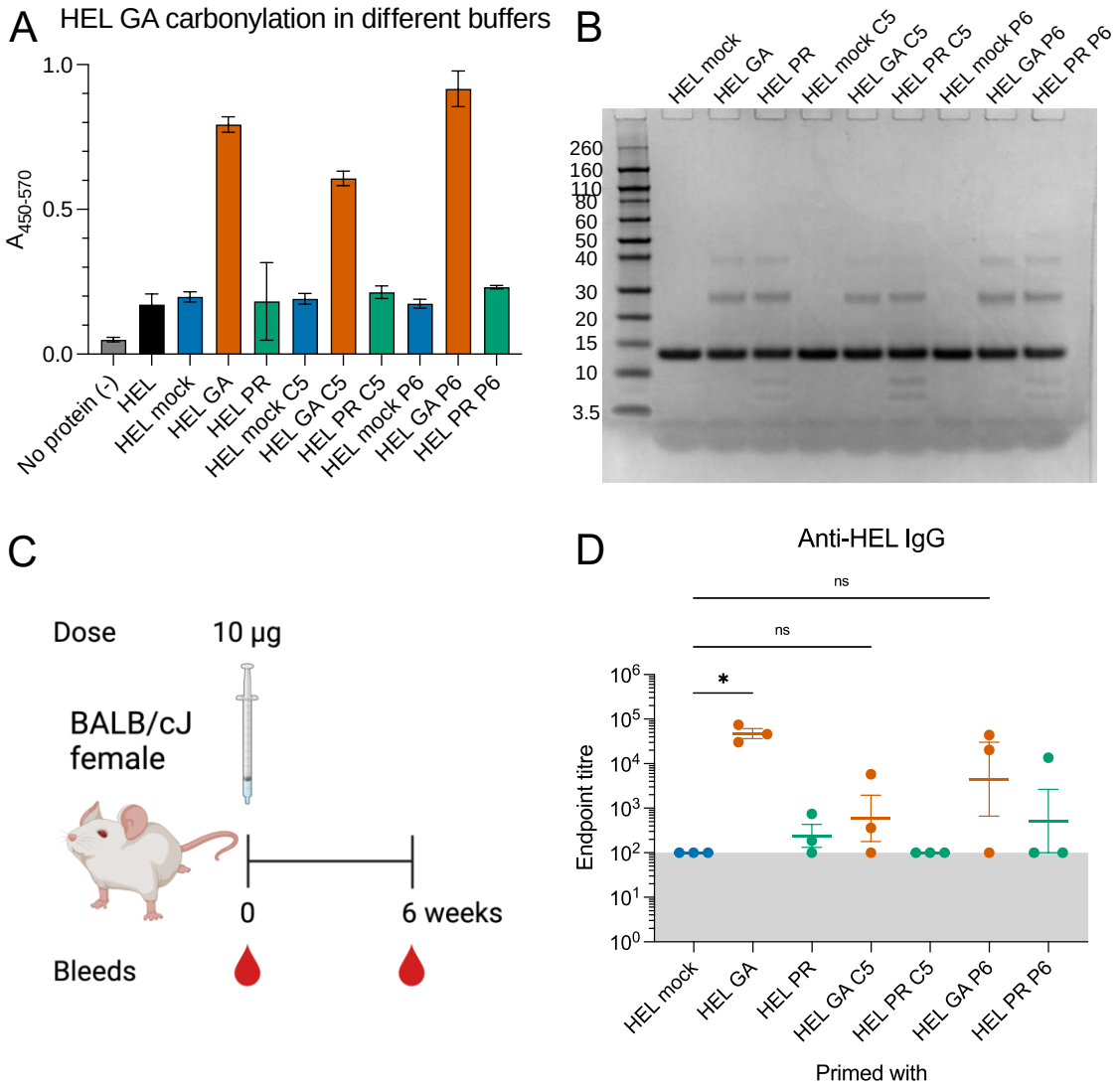


Figure 3.18: HEL GA elicits higher IgG titres compared with HEL PR under several buffer conditions. A) Protein carbonylation measured by DNPH ELISA. Data are mean ± SD of 3 technical replicates. B) Reducing SDS-PAGE gel. 1 µg protein was loaded in each lane of a 4–12% Bis-Tris gel. C) Bleed and immunisation schedule. D) Anti-HEL IgG responses of primed female BALB/c mice. Data are mean ± SEM (*p ≤ 0.05; Kruskal-Wallis then Dunn's multiple comparison test). Sera were serially diluted starting at 1:100 and non-responding mice were plotted at the limit of detection (shaded in grey).

3.2.4 Lysines are targets of GA modification and K97 is a key residue

Tandem MS (also termed MS/MS) can map protein modification sites, and I investigated whether GA indeed modified lysines and if particular sites were favoured. Previously, Marie-Laetitia Thézénas (Discovery Proteomics Facility, University of Oxford) did not detect any GA-pyridine or GA-aldoamine on HEL mock, HEL GA (3 h) and HEL GA 7 d samples (prepared by Amin Moghaddam) that were run on LC-MS/MS (data not

shown). These LC-MS/MS observations were unexpected because my intact LC-MS results suggested that both GA-pyridine or GA-aldoamine should be relatively abundant.

Therefore, together with Iolanda Vendrell (Discovery Proteomics Facility, University of Oxford), I re-analysed the LC-MS/MS data with new search parameters (**Table 3.1**) using PEAKS X software. I corrected the monoisotopic mass for GA-pyridine from 109.0289 to 108.0211 (an extra hydrogen atom had been included), searched for the recently described GA-pyrrole PTM (Chikazawa et al. 2020), and restricted the search to residues known to have the particular modifications.

The re-analysed HEL mock sample had basal levels of carboxymethylation, with 9 unique peptides detected with the modification on K1, K97, R61, or R68 (**Figure 3.19**). Surprisingly, there were also 3 unique peptides detected with GA-aldoamine (labelled "glycolaldehyde") on K96 and K116.

In contrast, the HEL GA sample had a much greater proportion of uniquely modified peptides detected for GA-pyridine (52), carboxymethylation (17), GA-aldoamine (10) and GA-pyrrole (6) (**Figure 3.20**). The lysine-specific modifications were mostly clustered on K1, K96, K97 and K116, although some modifications were still detected on K13 and K33. Carboxymethylation was often found on various arginines and tryptophans.

HEL modified with GA for 7 d was even more extensively modified (**Figure 3.21**), with most lysines modified with GA-pyridine and increased carboxymethylation on lysine, arginine and tryptophan. Furthermore, an unbiased search for both user-specified and Unimod PTMs (Han et al. 2011) returned results consistent with the user-directed search (**Figure A.2 to Figure A.4**).

Table 3.1: Parameters for user-defined PTMs. Monoisotopic mass and searched residues shown.

PTM	Old Parameters	New Parameters
GA-aldoamine	42.01, CRHK	42.0106, K
Carboxymethyl	58.06, CRHK	58.0055, KRW
GA-pyridine	109.0289, HRK	108.0211, K
GA-pyrrole	-	50.0157, K

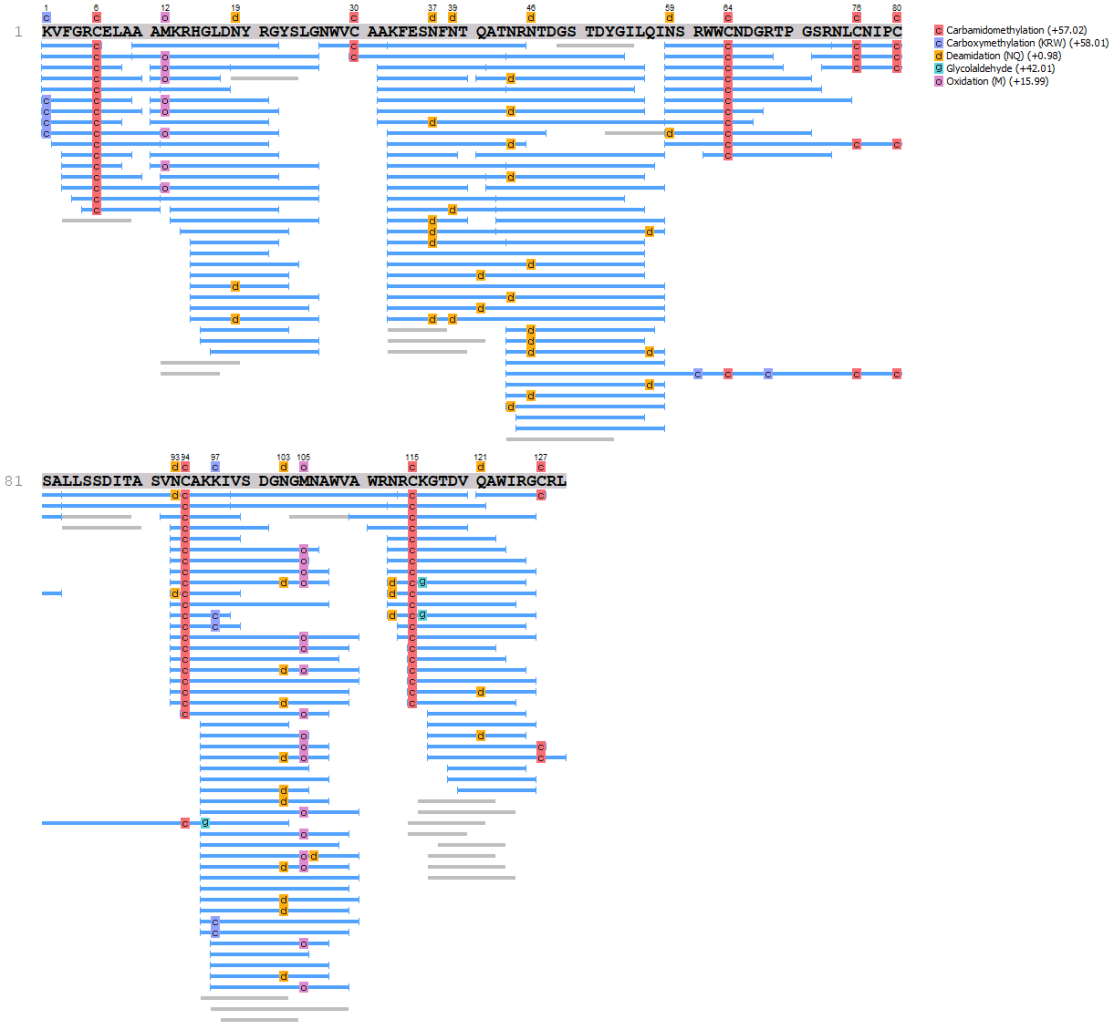


Figure 3.19: User-specified PTMs detected by LC-MS/MS for HEL mock. PEAKS database search tool was run to find user-specified PTMs. Blue lines represent unique peptide spectrum matches (PSMs). Detected PTMs are indicated on the blue lines. Confidently mapped PTMs appear above the protein sequence and their amino acid position is indicated. Amin Moghaddam prepared the samples, which I re-analysed together with Iolanda Vendrell.

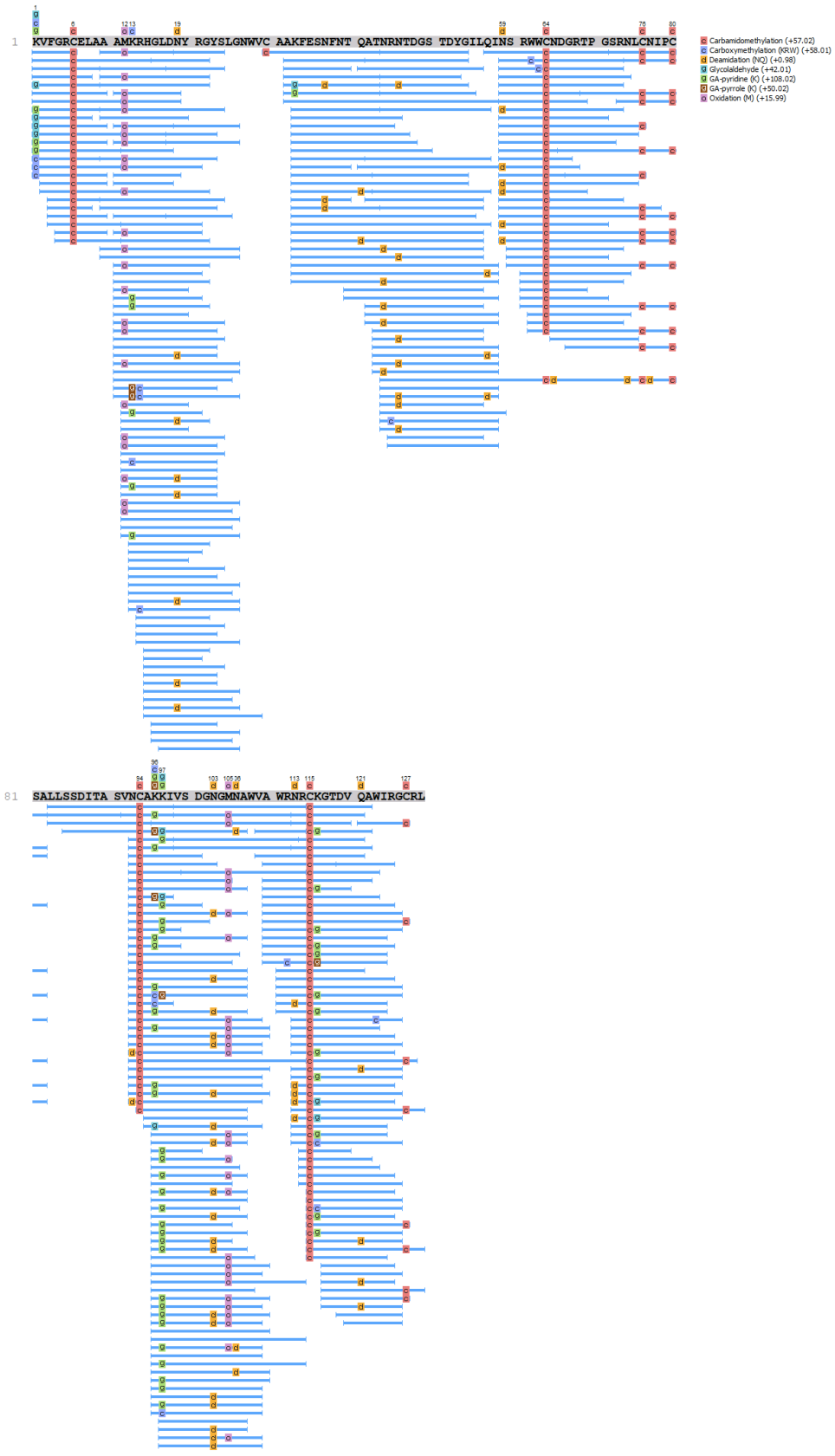


Figure 3.20: User-specified PTMs detected by LC-MS/MS for HEL GA (3 h). PEAKS database search tool was run to find user-specified PTMs. Blue lines represent unique peptide spectrum matches (PSMs). Detected PTMs are indicated on the blue lines. Confidently mapped PTMs appear above the protein sequence and their amino acid position is indicated. Amin Moghaddam prepared the samples, which I re-analysed together with Iolanda Vendrell.

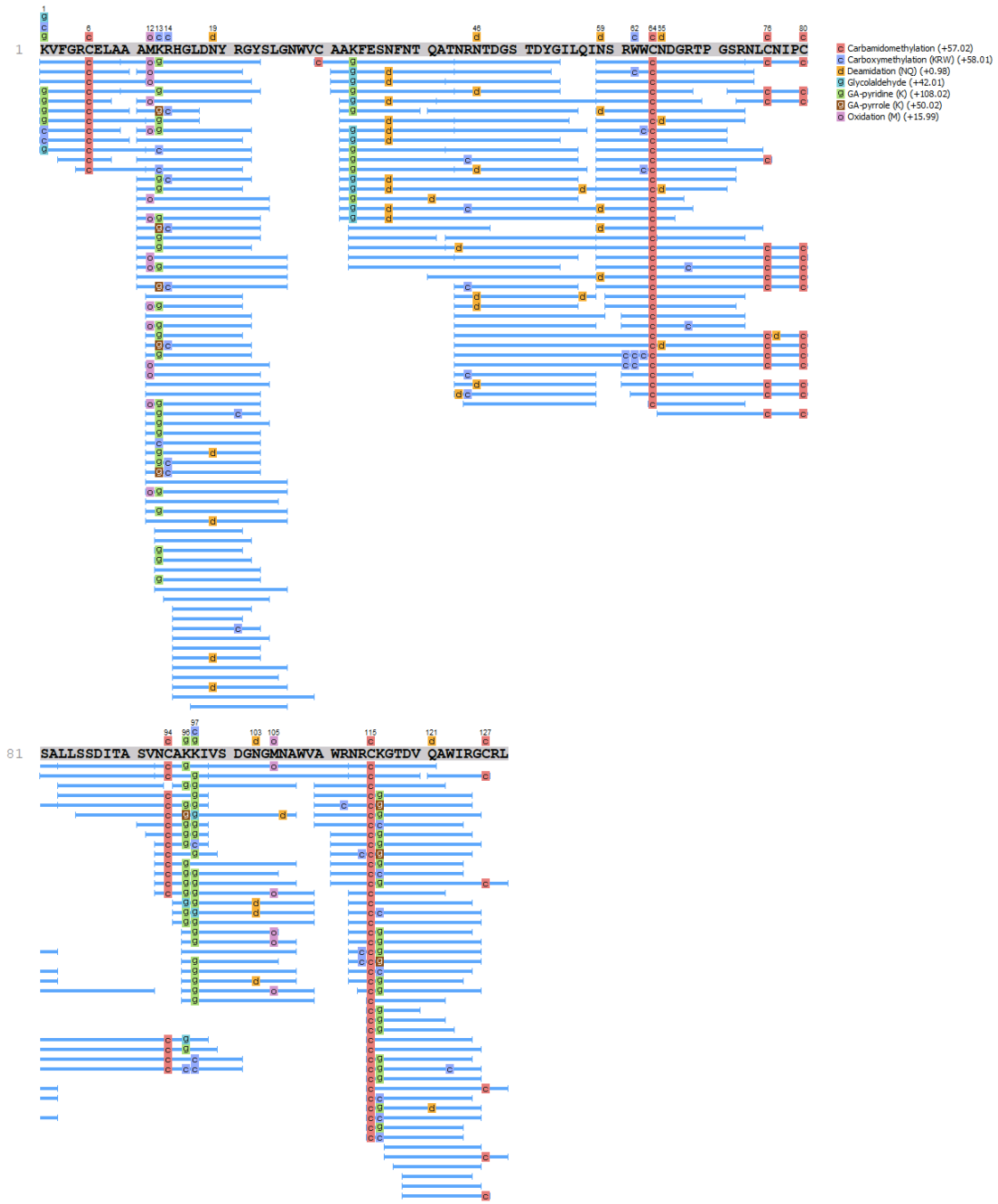


Figure 3.21: User-specified PTMs detected by LC-MS/MS for HEL GA 7 d. PEAKS database search tool was run to find user-specified PTMs. Blue lines represent unique peptide spectrum matches (PSMs). Detected PTMs are indicated on the blue lines. Confidently mapped PTMs appear above the protein sequence and their amino acid position is indicated. Amin Moghaddam prepared the samples, which I re-analysed together with Iolanda Vendrell.

Concurrently, I contacted the Ralf Hoffman lab (Leipzig University), which specialises in mapping protein carbonyls. Sanja Milkovska-Stamenova ran and analysed my HEL mock, HEL GA and HEL PR samples using nano-LC-MS/MS. She detected GA-aldoamine (and its reduced form) on K97 and K116, and GA-pyridine on K97 (**Table 3.2**). She also unambiguously identified carboxymethyl on K13, K97, K116 and R5.

As an alternative to tandem MS, I analysed whether mutating lysines affected GA modification. Xiaochao Xue and Lachlan Deimel from our lab designed and produced six HEL mutants with various lysines mutated to arginine (**Table 3.3**). In HEL without any lysines (0×Lys), proteins treated with GA were minimally modified with unknown PTMs of +59 (potentially CML) and +82 (**Figure 3.22**). Adding back K97 (1×Lys) resulted in GA-aldoamine and GA-pyridine PTMs, and potential modifications at other residues. In contrast, restoring only K13 and K96 (2×Lys) did not have much effect and had a similar mass spectrum to 0×Lys HEL. Further evidence suggesting a key role for K97 in GA modification was seen in its removal (5×Lys) from wild type (WT) HEL (6×Lys), which drastically decreased GA-pyridine and RC-containing peaks at +42, +84 and +126. However, even without K97, the other five lysines still contributed to GA modification in 5×Lys HEL. While the other five lysines did not affect GA modification as much as K97, their presence still increased the overall amount of modification, as seen by comparing 3×Lys with 4×Lys, or 1×Lys with a different 3×Lys termed 3×Lys Distal.

3.2.5 Breaking self-tolerance with GA-modified mouse lysozyme

Mouse lysozyme (ML, UniProt ID: P08905) is the mouse self-homologue of HEL, with which it shares 57.8% sequence identity (Clustal Omega) (**Figure 3.23**). It is 14812 Da when folded (Expasy) and has four instead of six lysines: K1, K13, K96 (also found in

Table 3.2: PTMs detected by nano-LC-MS/MS in the Hoffmann lab (Leipzig University). Sample run and analysis performed by Sanja Milkovska-Stamenova.

Residue	PTM
K1	–
R5	Carboxymethyl
K13	Carboxymethyl
K33	–
K96	–
K97	GA-aldoamine GA-pyridine Carboxymethyl
K116	GA-pyridine Carboxymethyl

Table 3.3: Lysines present (colour) or mutated to arginine (grey) for seven HEL mutants and HEL WT. Mutants that share the same colour scheme only differ from one another by one residue.

HEL	K1	K13	K33	K96	K97	K116
0×Lys						
1×Lys						
2×Lys						
3×Lys						
3×Lys Distal						
4×Lys						
5×Lys						
WT						

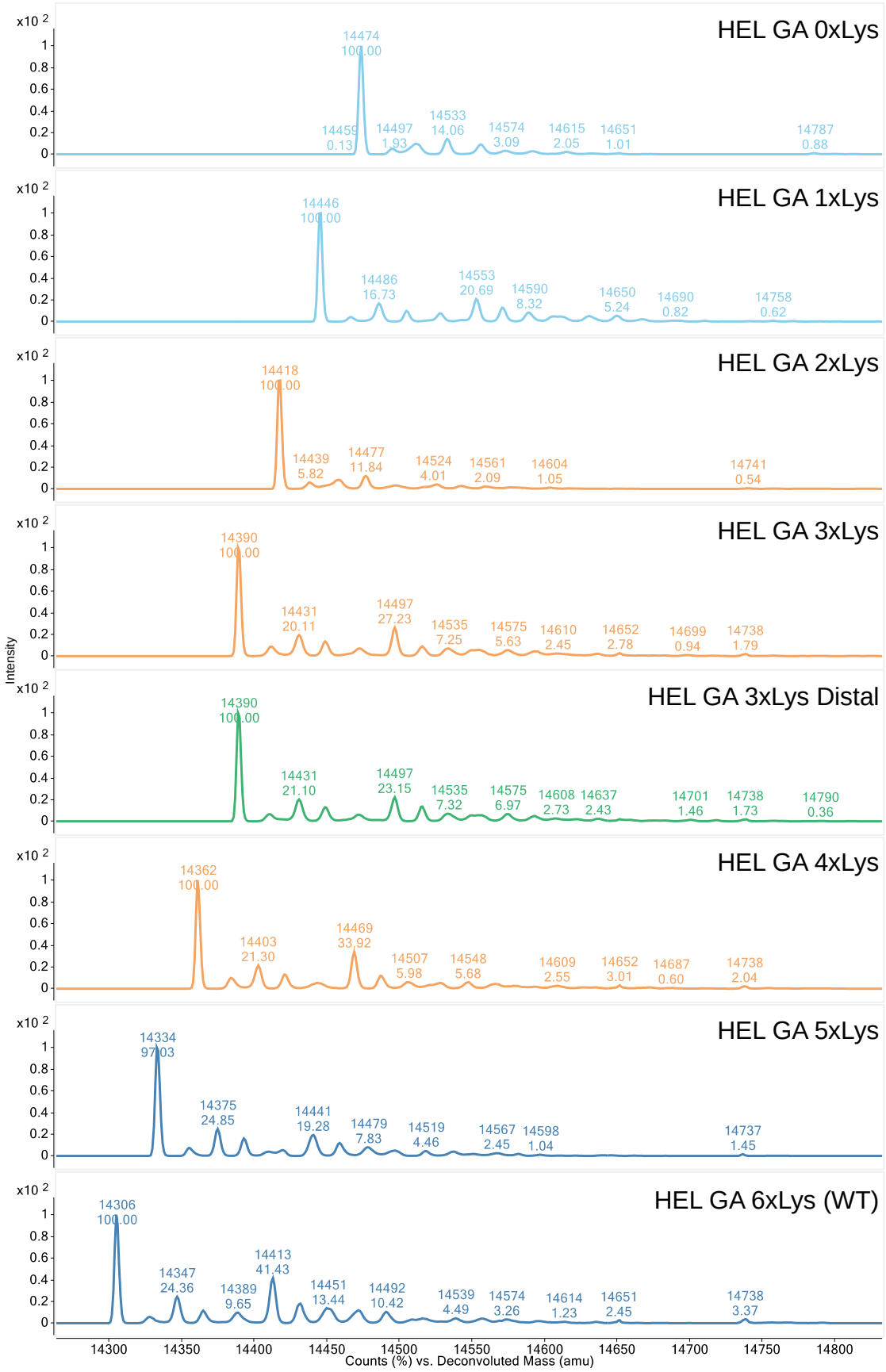


Figure 3.22: K97 is a key residue that increases the extent of GA modification. Intact LC-MS spectra comparing all GA-modified HEL mutants. Mutants that share the same colour scheme only differ from one another by one residue.

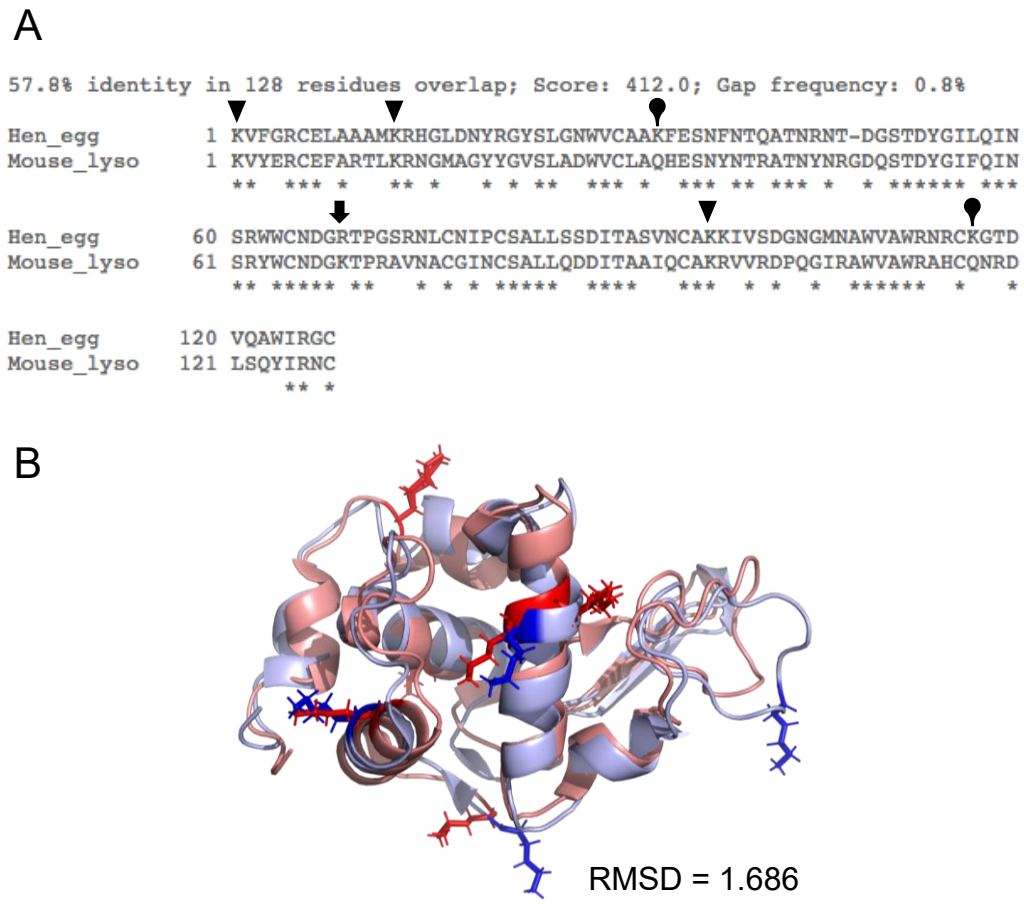


Figure 3.23: Sequence and structure of mouse lysozyme (ML) compared with HEL. A) Sequence alignment of HEL and ML (UniProt ID: P08905). Triangles: identical lysines. Arrow: a lysine found only in ML. Teardrops: lysines only present in HEL. B) Structural overlay of HEL and ML. The root-mean-square deviation (RMSD) was calculated to be 1.686 in PyMOL. ML PDB ID: 1IVM (Obita, Ueda, and Imoto 2003).

HEL), and K69 (only present in ML). ML is present in the blood serum of BALB/c mice at a concentration of approximately 5.6 to 8.4 µg/mL (Hook, Carey, and Muschel 1960). Batches of ML were produced by our collaborators (Tadashi Ueda, Kazumasa Yoshida and Manabu Nakazono, Kyushu University) (Tsujihata et al. 2000), which I then modified as before with GA and $NaBH_4$ for female BALB/c mouse immunisations. Prior to modification, ML was tested for various pattern recognition receptor (PRR) agonists and cleaned of endotoxin (**Figure 3.24**).

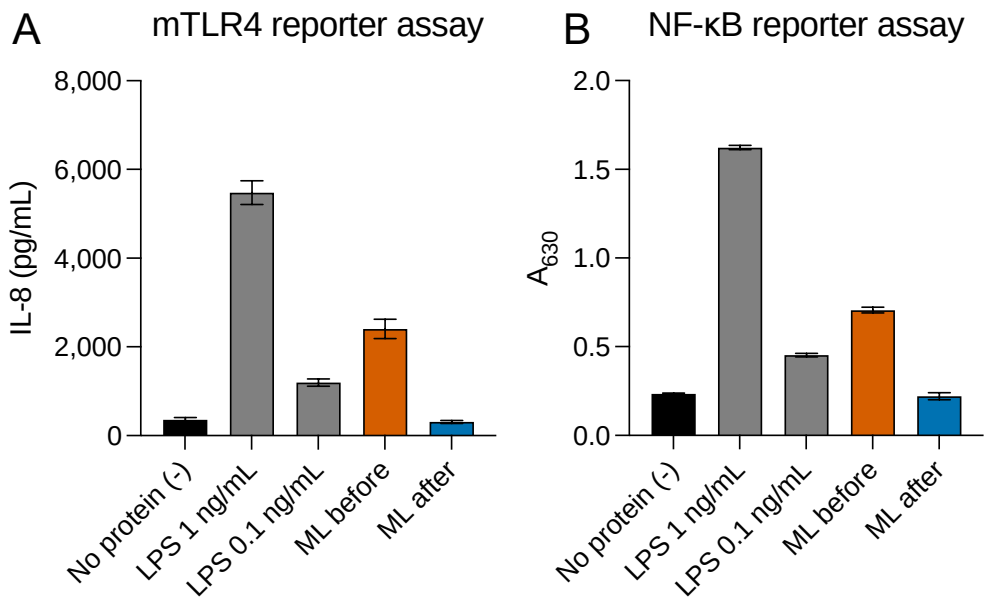


Figure 3.24: ML cleaned of endotoxin before immunisation. Representative of four batches of ML. A) mTLR4 and B) NF-κB cell reporter assays for LPS and PRRs respectively.

As with HEL, GA treatment of ML increased protein carbonylation and oligomerisation (**Figure 3.25**). Intact LC-MS showed that ML could be modified with one to four GA-aldoamines, which was consistent with the number of available lysines (**Figure 3.26**). After PR treatment, protein carbonylation decreased to a level similar to ML mock (**Figure 3.25A**) while cross-linking (**Figure 3.25B**) and most PTMs remained (**Figure 3.26B**). Intact LC-MS suggested that GA-pyridine was unaffected, but the 3x and 4x GA-aldoamine peaks were slightly increased in mass and likely to be reduced to non-reactive alcohol. As with HEL, an unknown peak at +60 from GA modification completely disappeared after post-reduction.

Female BALB/c mice were immunised a total of four times with 30–45 μg each time and at least 4 weeks between immunisations (**Figure 3.27A**). This prolonged schedule was chosen due to wait times in receiving ML batches and to maximise the dosage from limited amounts of protein. The experiment was performed twice in total.

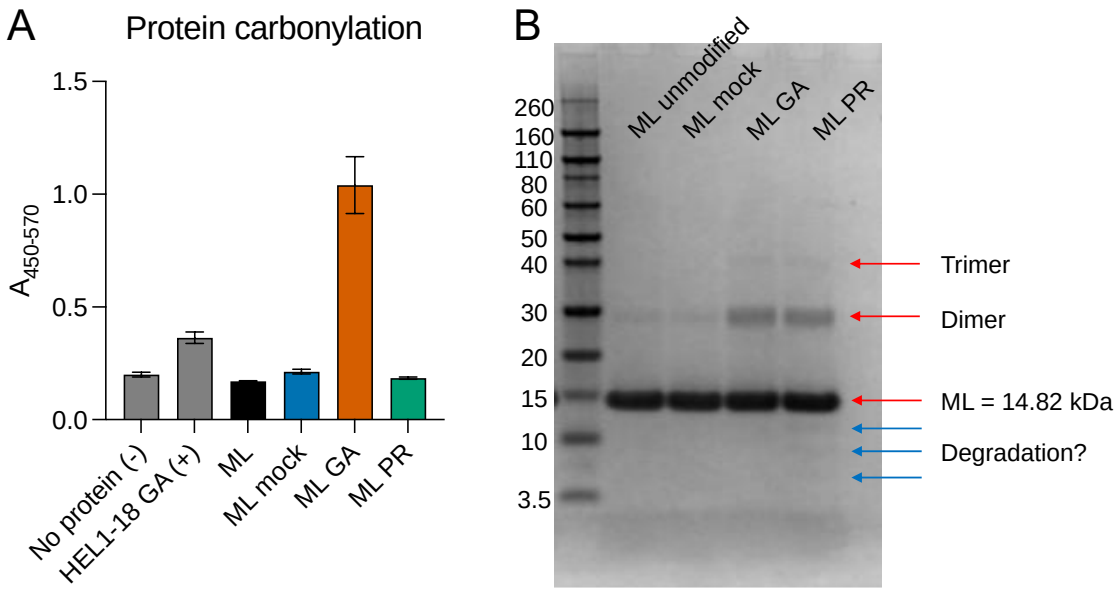


Figure 3.25: ML GA treatment increases protein carbonylation and oligomerisation, while PR treatment decreases carbonylation. ML was GA modified at 0.25 mg/mL with 20 mM GA at 37 °C for 3 h, followed by PR with 20 mM $NaBH_4$ at 37 °C for 3 h. A) Protein carbonylation measured by DNPH ELISA. Data are mean ± SD of 3 technical replicates. B) Reducing SDS-PAGE gel. 2 µg protein was loaded in each lane of a 4–12% Bis-Tris gel.

Unfortunately, during the first experiment some ML PR sample was lost during preparation, so there was not enough to give the mice a fourth immunisation in that group.

After tracking the levels of anti-ML IgG over time, I observed that the high dose of ML emulsified in a strong adjuvant such as complete Freund's adjuvant (CFA) for prime and incomplete Freund's adjuvant (IFA) for boosts sufficed to break self-tolerance after one or two injections (**Figure 3.27B**). Only one out of nine mice did not produce any anti-ML IgG response to ML Freund's immunisation by the end of the experiment. In contrast, anti-ML IgG responses for no adjuvant immunisations were not seen until at least after the third injection, mostly in the ML GA immunisation group (**Figure 3.27C**). One mouse in the ML mock group had detectable anti-ML IgG responses in baseline sera and mounted a strong anti-ML IgG response after three injections (**Figure A.5**) and was excluded from analysis. Anti-ML IgG responses fluctuated in individual mice over time,

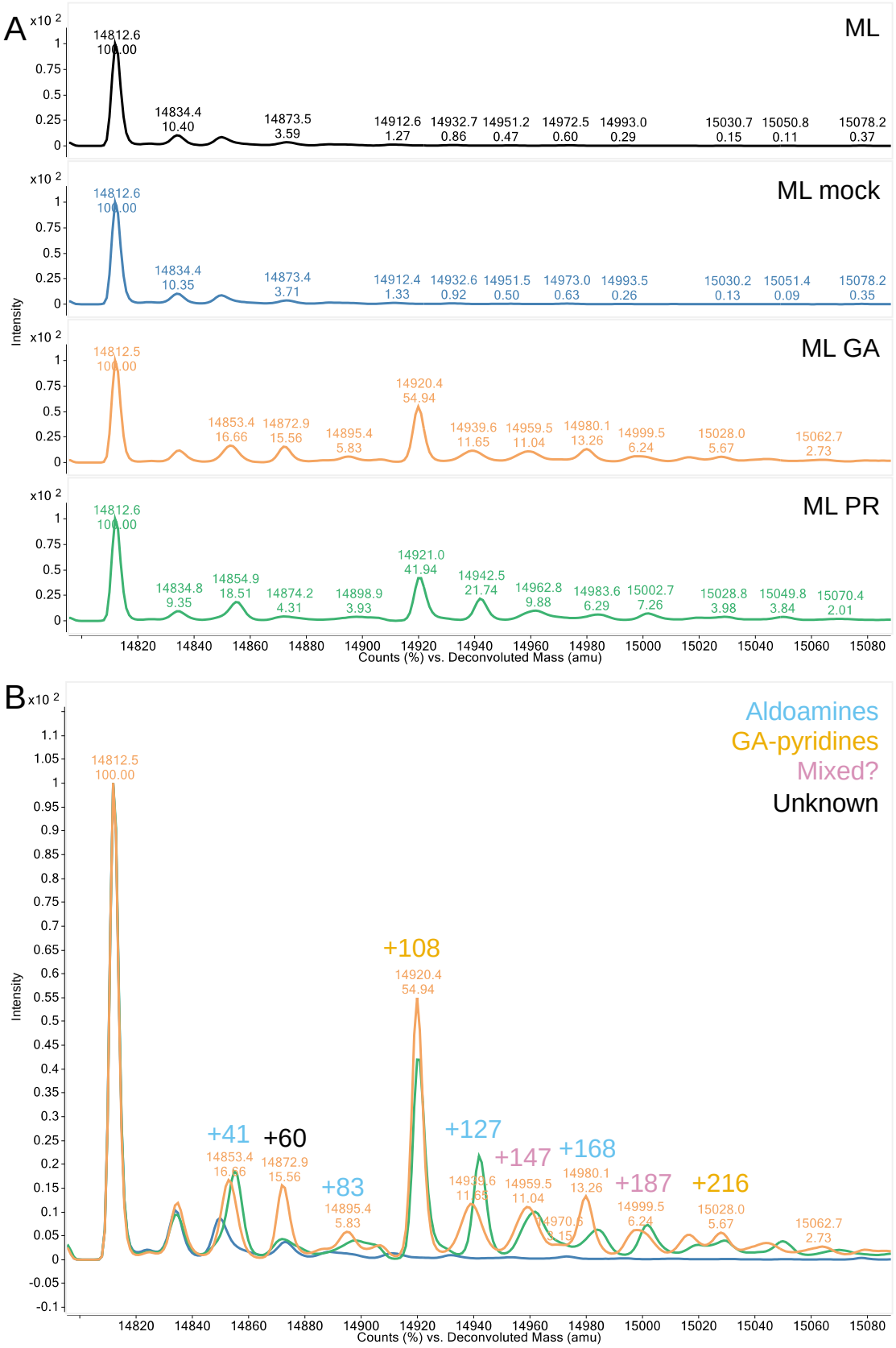


Figure 3.26: ML GA treatment increases PTMs, while PR treatment selectively reduces RC-containing PTMs. ML was GA modified at 0.25 mg/mL with 20 mM GA at 37 °C for 3 h, followed by PR with 20 mM $NaBH_4$ at 37 °C for 3 h. A) Offset and B) overlaid intact LC-MS spectra. Peaks are annotated with deconvoluted mass and abundance percent relative to the largest peak. Predicted modifications annotated on selected peaks.

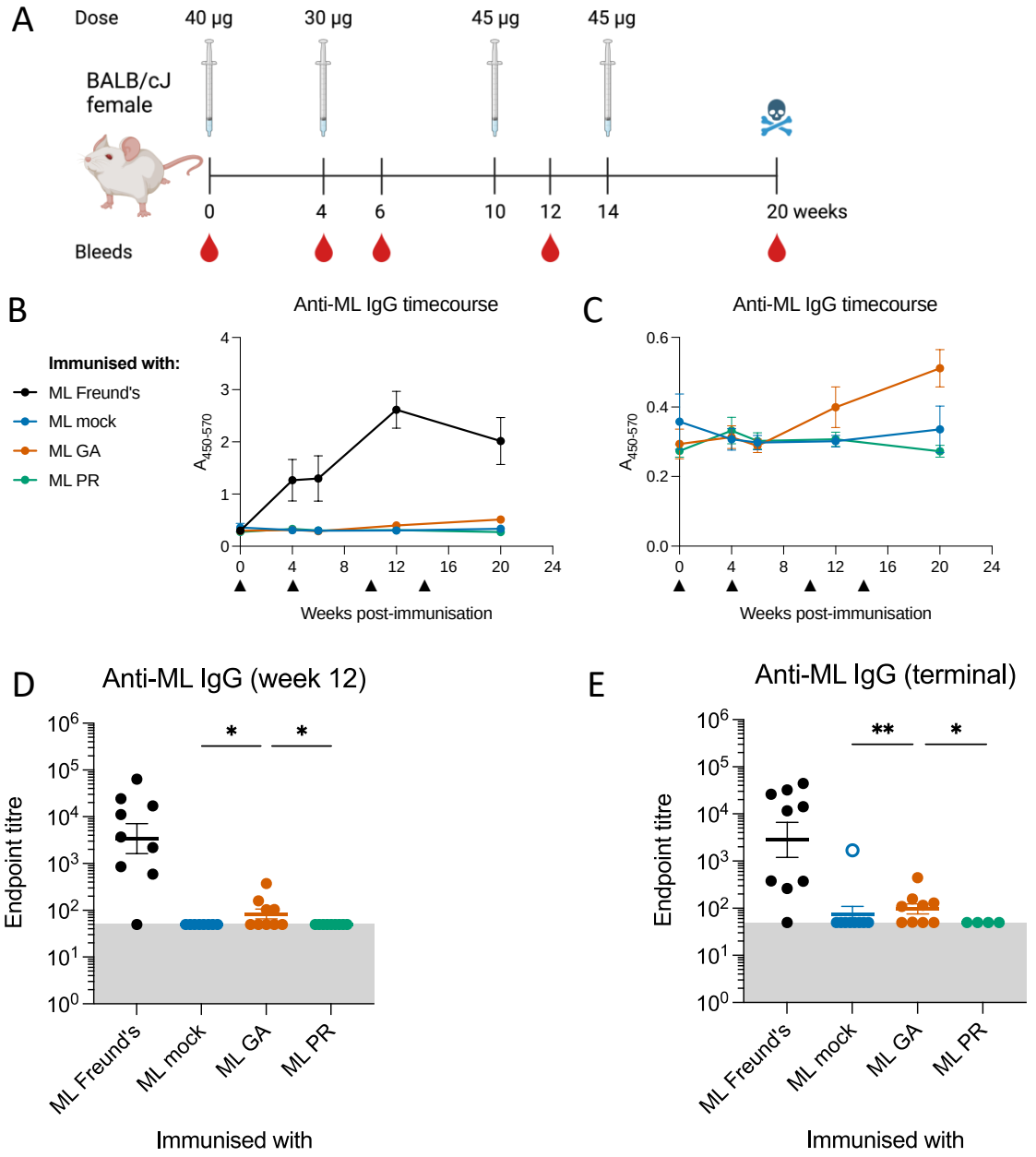


Figure 3.27: Mouse lysozyme (self-protein) modified with GA elicits higher IgG responses compared with ML mock and ML PR. A) Bleed and immunisation schedule. B) Anti-ML IgG responses measured during the experiment. Sera were diluted 1:50. C) Same as B but without ML Freund's group. Triangles indicate when immunisations were given. D) Anti-ML IgG endpoint titres measured in week 12. E) Terminal anti-ML IgG endpoint titres. Empty circle: outlier mouse with baseline anti-ML IgG response, which was included in plots but excluded from analysis. Data are mean ± SEM of 9 mice across 2 independent experiments, except PR group where n = 4 for terminal timepoint (*$p \leq 0.05$; Kruskal-Wallis then Dunn's multiple comparison test with ML Freund's excluded from statistical analysis). Sera were serially diluted starting at 1:50 and non-responding mice were plotted at the limit of detection (shaded in grey).

possibly from reacting with self-protein in vivo. Mice with detectable anti-ML IgG titres did not show any visible signs of autoimmunity, such as overgrooming, weight loss or behavioural distress.

Nonetheless, pooled anti-ML IgG endpoint titres after three injections at week 12 revealed significant differences between ML GA immunised mice compared with ML mock and ML PR (**Figure 3.27D**). This was similarly the case for the terminal timepoint at week 20 (**Figure 3.27E**) when the ML mock outlier was excluded.

3.3 Discussion

3.3.1 Results summary

In this chapter, I confirmed that modification of HEL with GA, which introduces protein aldehydes, elicited greater IgG responses to native HEL protein in immunised female BALB/c mice. HEL GA was more immunogenic compared with HEL mock and HEL PR in the absence of endotoxin and extrinsic adjuvant, and when administered by different immunisation routes. Anti-HEL IgG responses were mostly decreased after post-reduction with $NaBH_4$, which reduces protein aldehydes to non-reactive alcohols. Furthermore, mice immunised with GA-modified ML generated autoantibodies to native ML, demonstrating that GA modification can also break tolerance to self-proteins.

Characterisation of HEL and ML GA modifications showed expected increases in protein carbonylation and cross-linking. Intact LC-MS revealed that GA modification produced a heterogeneous population of unmodified and modified proteins. I detected previously described PTMs such as GA-aldoamine (+42) and GA-pyridine (+108), and potentially CML (+58). In contrast with previous peak assignments (Moghaddam et al. 2011), I found that proteins were modified with GA-aldoamine at multiple sites and

therefore more abundant than previously thought. $NaBH_4$ treatment decreased global protein carbonylation as measured by DNPH and slightly shifted the mass of GA-aldoamine peaks, although some non-reduced protein aldehydes seemed to remain.

Tandem MS mapping showed that most GA modifications occurred on lysine, in agreement with previous work (Section 3.1.2). Any of the six lysines could be modified with GA-aldoamine or GA-pyridine, although some lysines (K1, K96, K97, K116) were preferentially modified over others (K13, K33). Results from different MS facilities confirmed GA-aldoamine and GA-pyridine on K97 of HEL GA. Experiments with GA-modified HEL lysine mutants indicated that the extent of modification depended on lysine composition and that K97 was a key residue facilitating HEL modification.

To further understand the link between protein aldehydes and in vivo immunogenicity, I altered the extent of GA modification using different reaction conditions. I found that lower overall carbonylation generally resulted in lower anti-HEL IgG responses. HEL with lower levels of carbonylation was predominantly modified with GA-aldoamine and no GA-pyridine, yet was still immunogenic, providing further evidence that protein aldehydes cause immunogenicity.

3.3.2 Challenges with MS characterisation of GA-induced PTMs

Intact LC-MS provides a useful overview of the extent of protein modification. However, mass accuracy can be a limiting factor depending on the size of the protein and PTM shifts, signal to noise ratio, and asymmetric peaks. Some PTMs, especially those of low abundance, can differ from expected values by up to 2 Da (Rod Chalk, Centre for Medicines Discovery, personal communication). Thus, it was challenging to confidently identify certain PTMs with LC-MS, especially small shifts after post-reduction of GA-aldoamine (+2). Other examples of ambiguous peak assignments include whether +60

was CML (+58), and whether +167 was four GA-aldoamines (+168) or GA-pyridine plus CML (+166). Although CML was unambiguously detected by tandem MS, previous experiments from the lab using a monoclonal antibody for CML detection suggested that the modification is not abundant in GA-modified proteins (Harris 2020).

A disadvantage of relying solely on MS for PTM identification is that it is based on mass changes and does not provide structural information. GA-aldoamine has a mass change of +42, but so does the reversible Schiff base product (**Figure 3.2**). Therefore, the amount of GA-aldoamine may be overestimated, and could explain the apparent decrease in GA-aldoamine during storage. Moreover, NMR studies performed by our collaborators on GA-modified peptides suggested that +42 may instead be a ring-structured epoxide (Naorem Nihesh, University of Chicago, personal communication) rather than the previously postulated aliphatic aldehyde (Acharya and Manning 1983). Epoxides are also derivatised by hydrazines in acidic aqueous conditions (although the reaction is more efficient in organic solvents) (H. J. C. Chen and Chung 1996; Zalan, Lazar, and Fulop 2010), and would therefore be detected based on the conditions used in our DNPH assay.

The transient or labile nature of some GA modifications also presented issues for detection and site mapping using tandem MS. GA-aldoamine was detected, but with lower abundance than expected from intact LC-MS results. Protein aldehyde intermediates are inherently unstable due to their propensity to react with other chemical groups. To overcome this, GA-aldoamine can be stabilised by derivatisation prior to MS analysis, and I successfully used DNPH derivatisation to identify GA-aldoamine peaks with intact LC-MS (**Figure 3.9**). Another explanation for the low abundance is that GA-aldoamines may become detached during classical collision-induced dissociation (CID) in bottom-up proteomics. A top-down MS approach combined with less harsh electron-based

fragmentation (ETD) may be a better technique for mapping labile GA-aldoamines (Joseph Gault, Carol Robinson lab, personal communication).

3.3.3 Variable antibody responses to GA-modified proteins

The route of immunisation appeared to affect the consistency and magnitude of HEL GA immunogenicity. A pilot experiment suggested that subcutaneous immunisations were most immunogenic but most variable, while intraperitoneal injections were less immunogenic but also less variable, and hock injections were somewhere in between (**Figure 3.5B**). These results were similar to a study by Thiele et al. (1998), in which female BALB/c mice were immunised with malondialdehyde and acetaldehyde (MAA)-modified albumin, which introduces the aldehyde-containing PTM known as DHP-lysine (**Figure 1.6**). The authors found that the subcutaneous and intraperitoneal routes were most immunogenic (and variable), followed by footpad injection, while intravenous immunisation was not immunogenic at all. Subcutaneous injections may be more variable because they are more prone to leakage, although intraperitoneal injections can also be misplaced (Steward et al. 1968). There are no definitive conclusions in the literature about the effect of immunisation routes on immunogenicity, which is highly dependent on antigen, adjuvant, and organism (Chapter 1). However, it is generally thought that the most to least immunogenic routes are intradermal, subcutaneous, intramuscular, intraperitoneal then intravenous, due to the higher concentration of immune cells in skin and mucosa (W. Wang et al. 2012).

Another explanation for high levels of in vivo variability could be related to the heterogeneity of GA modification (**Figure 3.8**), occurring both within the same molecule and between different molecules. Most protein remained unmodified after standard GA treatment (**Figure 3.8**). Given that protein carbonylation is significantly correlated with

IgG1 antibody titres (Moghaddam et al. 2011), the protein samples may not be sufficiently carbonylated to elicit a robust response in all mice. Similarly, Willis et al. (2002) demonstrated that immunogenicity correlated with the number of aldehyde-containing DHP-lysine PTMs. I did not perform a correlation analysis between protein carbonylation and antibody titres because our DNPH assay measured relative protein carbonyl content and thus could not be pooled across different experiments. Measuring absolute protein carbonyls is a laborious process requiring protein precipitation and there are no universally accepted protein carbonylation standards (Rogowska-Wrzesinska et al. 2014).

Nonetheless, less extensively modified HEL GA 1 h and HEL GA C5 samples were immunogenic but elicited lower anti-HEL IgG antibody responses (**Figure 3.11B and Figure 3.18D**). However, HEL GA C5 responses were eliminated after post-reduction, which supports a role for protein aldehydes in increasing immunogenicity, although the sample size for the experiment was small.

On the other hand, I was unable to increase the proportion of GA-aldoamine modified HEL without introducing other PTMs such as GA-pyridine, which is a stable end-product formed from three GA molecules (Nagai et al. 2002). Reaction conditions such as concentration and temperature affected the rate of reaction, and accelerating the reaction appeared to favour GA-pyridine formation. The presence of both GA-aldoamine and GA-pyridine in HEL GA samples is an issue because it is difficult to discern the individual effects of each PTM. This is illustrated by in vivo anti-HEL IgG responses to HEL GA (3 h) compared with HEL GA 1 h (**Figure 3.12**). HEL GA (3 h) was more immunogenic but this could be due to increased protein carbonylation or the presence of GA-pyridine. Similarly, HEL GA P6 had higher levels of protein carbonylation but seemed to be less immunogenic than HEL GA (PBS) (**Figure 3.18**). HEL GA (PBS) had a higher proportion of GA-pyridine (**Figure 3.17**), which could also contribute to immunogenicity.

That HEL PR is still slightly immunogenic after post-reduction (**Figure 3.5 and Figure 3.18)** suggests that GA-pyridine, or some other non-aldehyde modification such as cross-linking, could also have an immunomodulatory effect. Indeed, it is well-known that protein aggregation can increase immunogenicity (Ratanji et al. 2014; W. Wang et al. 2012). GA-pyridine also mediates uptake through scavenger receptor A (SR-A) (Nagai et al. 2000) while GA-aldoamine does not (Takata et al. 1988). However, GA treatment of HEL for 7 d mostly modifies HEL with GA-pyridines (**Figure 3.21**) (Mariño et al. 2017) and in our lab elicited much lower anti-HEL IgG responses in immunised mice compared with HEL GA 3 h (Harris 2020). Since HEL GA is significantly more immunogenic than HEL PR (**Figure 3.6**), protein aldehydes are therefore the key driver of immunogenicity.

An alternative explanation for residual immunogenicity is that GA-aldoamine is not completely reduced, an interpretation supported by the DNPH assay (**Figure 3.7A**) and intact LC-MS data (**Figure 3.8**). Post-reduction should result in a mass shift of +2 for every GA-aldoamine, but often the change actually observed was smaller. Higher $NaBH_4$ concentrations could not be used to ensure complete post-reduction, because such concentrations caused high levels of protein degradation (data not shown), which can also affect immunogenicity.

3.3.4 Autoantigen-induced experimental autoimmune disease models

Allison and Fearon (2000) demonstrated that IgG autoantibodies could be generated against GA-modified rat cytochrome c, which is identical to mouse cytochrome c (UniProt). Cytochrome c is a mitochondrial protein not normally found in the extracellular space, and thus may have a lower threshold for breaking self-tolerance compared with secreted proteins. My experiments show that IgG autoantibodies could also be produced

against GA-modified ML (**Figure 3.27**), an extracellular protein that is likely to have a higher threshold for breaking self-tolerance. Future studies could investigate the potential pathogenic role of anti-ML antibodies, for example in immune-mediated glomerulonephritis by measuring circulating creatinine and immune complex deposition in the kidneys (Davis, Marder, and West 1981)

Following my experiments with ML, I planned to investigate whether GA-mediated breaking of self-tolerance was relevant in a disease model. A number of studies have demonstrated that mice produce autoantibodies after being injected with non-enzymatically modified autoantigens (**Table 3.4**). However, most of these studies used adjuvants and did not test for endotoxin contamination. Moreover, heterologous proteins from rat and chicken rather than true self-proteins from mouse were often used and did not always relate to experimental autoimmune diseases (**Table 3.5**). The choice of protein was likely influenced by the difficulties and expense of sourcing milligram quantities of mouse protein required to break self-tolerance for a sufficiently-powered study.

One disease model I am currently pursuing is experimental autoimmune encephalomyelitis (EAE), using the outer membrane portion of myelin oligodendrocyte glycoprotein (MOG_{1-125}). I acquired constructs to produce mouse rather than rat MOG (Steve Kerfoot lab, Western University, Canada), and am currently producing MOG_{1-125} for future experiments.

3.4 Conclusions

In this chapter, I confirmed that GA modification increases IgG antibody responses to native protein. This was demonstrated for both HEL and its self-homologue ML. To my knowledge, this is the first demonstration of breaking self-tolerance to an abundant extracellular protein in the absence of endotoxin contamination or adjuvants.

Table 3.4: Experimental autoimmune diseases induced by autoantigen immunisation. Adapted from Yu and Petersen (2018).

Experimental Autoimmune Disease	Autoantigen
Encephalomyelitis	Myelin oligodendrocyte glycoprotein
Myocarditis	Myosin
Myasthenia gravis	Acetylcholine receptor
Rheumatoid arthritis	Collagen II
Uveitis	S-arrestin, retinoid-binding protein 3
Goodpasture syndrome	Collagen IV
Pemphigus vulgaris	Desmoglein 3
Bullosa acquisita	Collagen VII
Bullous pemphigoid	Collagen XVII

Table 3.5: Studies on breaking self-tolerance using non-enzymatic chemical modifications. MOG = myelin oligodendrocyte glycoprotein; MSA = mouse serum albumin; CII = collagen II; RSA = rat serum albumin; EAE = experimental autoimmune encephalomyelitis; $ONOO^-$ = peroxynitrite; HOCl = hydrochlorous acid; GA = glycolaldehyde; MDA = malondialdehyde; HNE = 4-hydroxynonenal; CFA = Complete Freund's Adjuvant.

"Self" Protein	Disease Model	Modification	Adjuvant	Reference
Mouse MOG	EAE	$ONOO^-$	CFA + pertussis toxin	Warnecke et al. (2017)
MSA	NA	HOCl	LPS	Walczewska et al. (2015)
Rat MOG	EAE	MDA	CFA	Wållberg et al. (2007)
Rat CII	Arthritis	HOCl	CFA	Westman, Lundberg, and Erlandsson Harris (2006)
RSA	NA	HOCl	CFA	Westman and Harris (2004)
Chick CII	Arthritis	HOCl	CFA	Marcinkiewicz et al. (2004)
Rat (= mice) cytochrome c	NA	GA	PBS	Allison and Fearon (2000)
MSA	NA	MDA, HNE	CFA	Wuttge, Bruzelius, and Stemme (1999)

GA modification heterogeneously modifies proteins primarily on lysine residues with early-stage protein aldehydes (GA-aldoamines), stable AGEs (GA-pyridine and potentially CML) and cross-linking. Lysine composition, particularly the presence of K97 in HEL, affects the extent of modification. Moreover, certain lysines (K1, K96, K97, K116) are favoured for modification. The specific reaction conditions used also determine the extent of modification.

Protein aldehydes contribute greatly to protein immunogenicity because reducing them to non-reactive alcohols mostly decreased IgG antibody responses. However, since modification produces a heterogeneous sample, it is possible that other modifications such as GA-pyridine and protein cross-linking also have immunomodulatory effects. Different modifications may act through different immune pathways and could explain the variability of in vivo responses.

Despite its limitations for producing homogeneous samples for characterisation and immunisation, GA modification results in protein aldehydation that can evoke strong immune responses and break self-tolerance without extrinsic adjuvant. The focus of subsequent chapters will be to investigate mechanistically how protein aldehydes resulting from GA-modification interact with and enhance the immune response.

Chapter 4

GA-mediated adaptive immunogenicity

4.1 Background

4.1.1 Brief overview of adaptive immune activation

Hen egg lysozyme (HEL) modified with glycolaldehyde (GA) introduced protein aldehydes, which significantly increased IgG antibodies against native HEL (Chapter 3). Increased IgG antibody production suggests enhanced antigen-specific T and B cell responses. Therefore, this section provides a brief overview of adaptive immune activation before considering how protein aldehydes may modulate the adaptive immune response.

The activation or "licensing" of conventional dendritic cells (DCs) by innate signalling is a critical step in the induction of adaptive immunity because DCs are the key antigen-presenting cells (APCs) involved in priming naïve T cells (Théry and Amigorena 2001). Immature DCs actively acquire antigens for presentation by phagocytosis, endocytosis and macropinocytosis, and express many different pattern recognition receptors (PRRs) that recognise various pathogen-associated or damage-associated molecular patterns (PAMPs or DAMPs) to induce innate immune activation (Reis E Sousa 2004). DC activation and maturation upregulates co-stimulatory molecules and promotes migration

to secondary lymphoid organs (SLOs) for antigen presentation to naïve T cells (Théry and Amigorena 2001).

Our lab previously investigated if protein aldehydes could increase DC activation and antigen uptake. HEL GA did not induce conventional activation of bone marrow-derived DCs (BMDCs) based on CD40, CD80 and CD86 surface marker expression (Moghaddam et al. 2011). Transcriptomic analysis of BMDCs pulsed with HEL mock and HEL GA did not show significant differences in individual gene expression, although enrichment analysis identified 146 affected pathways relating to translation and metabolism (Harris 2020). However, there were no consistent changes in cytokine secretion and BMDC uptake was not increased for HEL GA compared with HEL mock and HEL PR (Harris 2020). Thus, I investigated the effect of protein aldehydes on T and B cell priming.

Naïve lymphocytes are activated when they receive two signals: the first from specific recognition of the antigen and the second from co-stimulatory molecules (Bretscher and Cohn 1970). Naïve T cells receive both signals from activated DCs in the SLOs. The first signal is propagated through T cell receptor (TCR) recognition of peptides bound to major histocompatibility complex (MHC) classes I and II, and is assisted by the T cell co-receptors CD8 or CD4 respectively (Wang and Reinherz 2002). The second signal is derived from DC co-stimulatory molecules that enhance T cell survival and proliferation, such as ligation of DC-expressed B7 molecules to T cell-expressed CD28 (Chen and Flies 2013). Additionally, cytokines secreted by DCs can direct differentiation of $CD4^+$ T helper cell subsets, which have different effector functions in the immune response (Kapsenberg 2003).

Antigens also drain into SLOs by afferent lymph or blood, where they are presented on follicular dendritic cells (FDCs) or subcapsular sinus macrophages to naïve B

cells (Okada and Cyster 2006; Batista and Harwood 2009). Antigen recognition by the B cell receptor (BCR) provides the first signal for activation, and is enhanced by the B cell co-receptor complex comprised of CD19, CD21 (CR2) and CD81 (TAPA-1) (Fearon and Carter 1995). Antigens are taken up and presented as peptide-MHC-II complexes on the B cell surface to elicit co-stimulation from activated $CD4^+$ T follicular helper (T_{FH}) cells recognising the same antigen (Crotty 2014). T_{FH} cells promote survival and differentiation of B cells through ligation of CD40L (CD154) to B cell-expressed CD40, and secretion of IL-21 plus other cytokines to promote antibody isotype switching (Crotty 2014).

After priming, B cells proliferate and differentiate into antibody secreting cells (ASCs) such as plasmablasts and terminally differentiated plasma cells (PCs). Some of these cells migrate to the outer follicle regions to form a primary focus (Okada and Cyster 2006). The remaining B cells migrate into the follicle with their associated T_{FH} cells to form a germinal centre (GC), where they undergo affinity maturation and isotype switching to produce high affinity antibodies (McHeyzer-Williams, Malherbe, and McHeyzer-Williams 2006). The end of the GC reaction results in memory B cells that circulate in the lymphoid compartments, or long-lived plasma cells (LLPCs) that persist in the bone marrow for at least several years secreting high-affinity antibodies (Radbruch et al. 2006).

The scenario above describes the activation of naïve B cells in a thymus-dependent (TD) manner, which is the case for most protein antigens that require T cell help to produce high affinity antibodies and immunological memory (Parker 1993). Naïve B cells can also be activated in a thymus-independent (TI) manner and such antigens fall into two classes: TI-1 and TI-2 (Coutinho and Möller 1973). TI-1 antigens are often B cell mitogens that induce mitosis by Toll-like receptor (TLR) activation, for example lipopolysaccharide (LPS), bacterial DNA (CpG) or polyinosinic:polycytidylic acid (poly I:C). At low concentrations, TI-1 antigens bind to both BCR and TLR to produce specific antibody

responses, while at higher concentrations TI-1 antigens stimulate polyclonal B cell activation. TI-2 antigens are usually highly repetitive structures (e.g. bacterial polysaccharides) that can crosslink a cluster of 10–20 BCRs (Vos et al. 2000) to stimulate low affinity IgM production. Further cytokine signals secreted by other immune cells can also induce isotype switching for TI-2 antigens (Mond et al. 1995) or even induce robust primary immune responses (Obukhanych and Nussenzweig 2006).

4.1.2 Potential mechanisms of aldehyde-enhanced adaptive immunity

Protein carbonylation is a type of non-enzymatic PTM (Chapter 1). Non-enzymatic PTMs can be antigenic, meaning that they are directly recognised by TCRs or BCRs in a hapten-specific manner. For example, immunisation of mice with malondialdehyde (MDA)- or 4-hydroxy-2-nonenal (HNE)-modified (see **Figure 1.5** and **Figure 1.6**) mouse serum albumin (MSA) generated T cells specific for PTMs but not native MSA (Wuttge, Bruzelius, and Stemme 1999). Antibodies have been produced specifically against PTMs formed by MDA (Koji Uchida et al. 1997; Ishii et al. 2006), HNE (K. Uchida et al. 1993; Ishii et al. 2003), acrolein (Furuhata et al. 2003), and many other reactive species (Nagai et al. 2016).

In disease, activated $CD4^+$ T cells and antibodies recognising protein aldehyde PTMs are common. For example, malondialdehyde-acetaldehyde (MAA)-adducts (**Figure 1.6**) have been detected in atherosclerotic plaques (Palinski et al. 1990; Yla-Herttuala et al. 1994), alcohol-induced liver disease (Rolla et al. 2000), and synovial tissue of rheumatoid arthritis patients (Thiele et al. 2015). In contrast, the focus of this chapter (and thesis) is on how protein aldehydes modulate immune responses to native protein, rather than direct responses specifically to PTMs.

Previous work from our lab suggested that mice immunised with HEL GA had stronger $CD4^+$ memory T cell recall responses to native HEL (Moghaddam et al. 2011).

In this study, an elevated secretion of T_H2 cytokines corresponded with an increase in isotype-switched IgG1 antibody responses. Thus, this section will consider the mechanisms by which protein aldehyde PTMs could influence $CD4^+$ T cell priming and activation, which is central to the formation of class-switched IgG antibody responses.

Immune responses are often dominated by T cell (or B cell) responses to particular epitopes, a phenomenon known as immunodominance. Epitopes generated from the same antigen form a relative hierarchy of immunodominant, subdominant, and cryptic epitopes. Many factors determine which epitopes will become immunodominant in a given protein, including antigen processing, peptide binding to MHC, and the presence of T cells bearing the appropriate TCR in the repertoire of an individual (Sercarz et al. 1993; Kim and Sadegh-Nasseri 2015).

During antigen processing, APCs internalise antigens to be unfolded and digested by a cocktail of reductases and proteases. PTMs can mask or create new sites of enzymatic activity to alter the patterns of cleavage and the generated peptide repertoire. For example, the enzymatic PTM citrullination was shown to alter the cleavage pattern of cathepsin L (CatL) in the rheumatoid arthritis-associated protein vimentin (Scally et al. 2013), and spontaneous deamidation of asparagine is known to mask a tetanus toxin C endopeptidase cleavage site (Moss et al. 2005). PTMs can also induce local and global conformational changes to antigen structure and stability (Xin and Radivojac 2012), which could affect sensitivity to lysosomal proteolysis and in vivo immunogenicity (Delamarre et al. 2006).

The peptides generated by antigen processing bind to and form a complex with MHC class II (pMHC-II), which is recognised by $CD4^+$ T cells. Peptides bind to MHC-II via a minimal motif of nine amino acids known as the peptide core or register. Anchoring residues at positions 1, 4, 6/7 and 9 hold the peptide within an open-ended MHC-II

groove, while TCR contact residues are usually at positions 2, 3, 5 and 8 (Wieczorek et al. 2017). Residues outside the peptide core are known as peptide flanking residues (PFRs), and play an important role in MHC-II and TCR interactions (Holland, Cole, and Godkin 2013). Additionally, the non-classical MHC molecules human leukocyte antigen HLA-DM and HLA-DO are gatekeepers of peptide loading (Mellins and Stern 2014).

The differences in mass and charge conferred by PTMs can change steric or electrostatic interactions between peptides and MHC-II. This can alter the stability or binding conformation of existing epitopes, or cause new cryptic epitopes to bind to MHC-II. In the context of disease, PTMs that promote binding of cryptic epitopes to MHC-II are well-documented. In humans, citrullination of rheumatoid arthritis peptides (Hill et al. 2003) and deamidation of α-gliadin gluten peptides (Quarsten et al. 1999) have been shown to promote binding to MHC-II risk alleles.

PTMs can also diminish or abrogate binding of existing immunogenic peptides. C57BL/6 mice immunised with peroxynitrite ($ONOO^-$)-modified myelin oligodendrocyte glycoprotein (MOG) did not develop experimental autoimmune encephalomyelitis (EAE) because tyrosine nitrotyrosination at an anchoring residue decreased the binding affinity of the peptide to MHC-II (Warnecke et al. 2017). Ultimately, the interaction between peptides and MHC-II determine which peptides are displayed and their relative abundance on the APC surface that are available for interactions with $CD4^+$ T cells.

PTMs on amino acids that directly contact the TCR can be recognised in a hapten-specific manner. In addition, PTMs not directly located on TCR contact residues can still cause significant changes in $CD4^+$ T cell binding and function. Subtle changes to pMHC-II stability and binding demonstrated by altered peptide ligands (APLs) can alter TCR binding kinetics (Madura et al. 2015; Insaidoo et al. 2011; Borbulevych et al. 2007) and

lead to altered $CD4^+$ proliferation, cytokine secretion, or polarisation (Jensen, Sercarz, and Gabaglia 2009).

4.1.3 Chapter hypotheses and aims

Unpublished findings from our lab suggested that the increased $CD4^+$ memory T cell recall response to HEL GA immunisation arose from the selective enhancement of particular epitopes, rather than a global increase in all epitope responses (Amin Moghaddam, personal communication). BALB/c mice (MHC-II haplotype I-A^d and I-E^d), immunised with HEL typically show the strongest $CD4^+$ T cell recall responses to $HEL_{106–116}$, which is considered to be the immunodominant epitope (Gammon et al. 1991; Drakesmith et al. 1998). In contrast, mice immunised with HEL GA appeared to have increased $CD4^+$ T cell responses to $HEL_{11–25}$, which is usually a subdominant epitope (Gammon et al. 1991; Schneider et al. 2000; Peters, Hamilton, and Bretscher 2005).

The enhancement of $CD4^+$ T cell responses to $HEL_{11–25}$ and not $HEL_{106–116}$ in mice immunised with HEL GA suggested that GA-induced PTMs could alter antigen processing, pMHC-II binding, and/or $CD4^+$ T cell priming. GA-aldoamine on K13 was hypothesised to enhance $HEL_{11–25}$ presentation in BALB/c mice, while GA-aldoamine on K116 was thought to have no effect or decrease $HEL_{106–120}$ presentation.

In this chapter, I aimed to:

a) Confirm whether GA-modified HEL peptides increase antigen presentation to $CD4^+$ T cell hybridomas, and compare this with GA-modified HEL protein;
b) Verify whether HEL GA immunised BALB/c mice have greater $CD4^+$ memory T cell recall responses;
c) Test whether HEL GA immunised mice have more HEL-specific ASCs; and
d) Determine whether HEL GA can enhance B cell activation.

4.2 Results

4.2.1 In vitro $HEL_{11–26}$ peptide presentation to $CD4^+$ T cell hybridomas

Our lab had previously established a reductionist in vitro model using the BALB/c B cell lymphoma A20 cell line as APCs, HEL peptides corresponding to BALB/c $CD4^+$ T cell epitopes, and BALB/c $CD4^+$ T cell hybridomas (gifted from Benny Chain, University College London) for antigen presentation assays (**Table 4.1**). Hybridomas are immortalised antigen-specific activated T cells, and the amount of interleukin-2 (IL-2) secreted provides a readout for the level of activation.

Using reaction conditions previously established in the lab for peptides, $HEL_{11–26}$ (sequence shown in **Figure 4.1A**, synthesised by Robert Vallée, Ben Davis lab, University of Oxford) was GA-modified with 5 mM GA for 3 h at 37 °C ($HEL_{11–26}$ GA) or mock modified without GA ($HEL_{11–26}$ mock). At the end of the reaction, $HEL_{11–26}$ mock and $HEL_{11–26}$ GA were directly added for an overnight incubation to A20 cells and Ad11 $CD4^+$ T cell hybridomas, which recognise $HEL_{11–26}$ bound to mouse $I\text{-}A^d$ (**Table 4.1**).

Pooling together the results from three independent repeats, I found $HEL_{11–26}$ GA had a significantly lower 50% maximal effective concentration (EC_{50}) compared with $HEL_{11–26}$ mock, but a similar maximal response (**Figure 4.1B**). Moreover, $HEL_{11–26}$ peptide added with 5 mM free GA did not increase peptide presentation, suggesting that enhancement depends on GA-modified peptide rather than free GA itself.

To verify that the enhanced presentation was not caused by free GA, I used a tC18 reversed-phase chromatography gravity column to remove excess GA and eluted the peptides into 50% acetonitrile. Next, a post-reduced (PR) sample was prepared by treating

Table 4.1: BALB/c CD4⁺ T cell hybridomas corresponding to HEL epitopes in vivo. BALB/c CD4⁺ T cell hybridomas (gifted from Benny Chain, University College London), their corresponding 15mer HEL peptide epitopes, monoisotopic mass of the 15mer HEL peptides, MHC-II haplotype binder, predicted binding register and rank, and in vivo immunodominance. HEL epitopes reported in the literature (Drakesmith et al. 1998; Peters, Hamilton, and Bretscher 2005) are provided in brackets, but 15mer peptides were used for most experiments to minimise differences based on peptide length. MHC-II binding registers and ranks were bioinformatically predicted by NetMHCIIpan 4.0 (Reynisson et al. 2020). In vivo immunodominance as reported in (Schneider et al. 2000).

CD4⁺ T Cell Hybridoma	Ed2	Ad11	Ad23	Ad71	Ed106
HEL Epitope	1–15 (2–16)	11–25 (11–25)	21–35 (23–32)	71–85 (71–85)	106–120 (106–116)
Monoisotopic Mass	1716	1780	1700	1547	1775
MHC-II	I-E^d	I-A^d	I-A^d	I-A^d	I-E^d
15mer with Predicted MHC-II Binding	KVFGR CELAA AMKRH	AMKRH GLDNY RGYSL	RGYSL GNWVC AAKFE	GSRNL CNIPC SALLS	NAWVA WRNRC KGTDV
Binder Rank (%)	19.00	85.00	29.00	21.00	0.04
Immuno-dominance	Cryptic	Sub-dominant	Sub-dominant	Cryptic	Dominant

$HEL_{11–26}$ GA with $NaBH_4$ for 2 h at 37 °C, and removing excess reagent as before ($HEL_{11–26}$ PR). I measured peptide carbonylation using biotin hydrazide (BH) due to technical issues detecting signal with DNPH (data not shown), and observed increased carbonylation for $HEL_{11–26}$ GA compared with $HEL_{11–26}$ mock and $HEL_{11–26}$ PR (**Figure 4.1C**). When I repeated the $HEL_{11–26}$ peptide presentation with desalted peptides, I again observed that $HEL_{11–26}$ GA had a lower EC_{50} compared with $HEL_{11–26}$ mock, but the decrease was not reversed by PR (**Figure 4.1D**).

4.2.2 $HEL_{11–25/26}$ peptide treated with GA is modified at the N-terminus

The K13 side chain was hypothesised to be the site of GA modification for the $HEL_{11–26}$ peptide. However, the free amine group on the peptide N-terminus could also be modified.

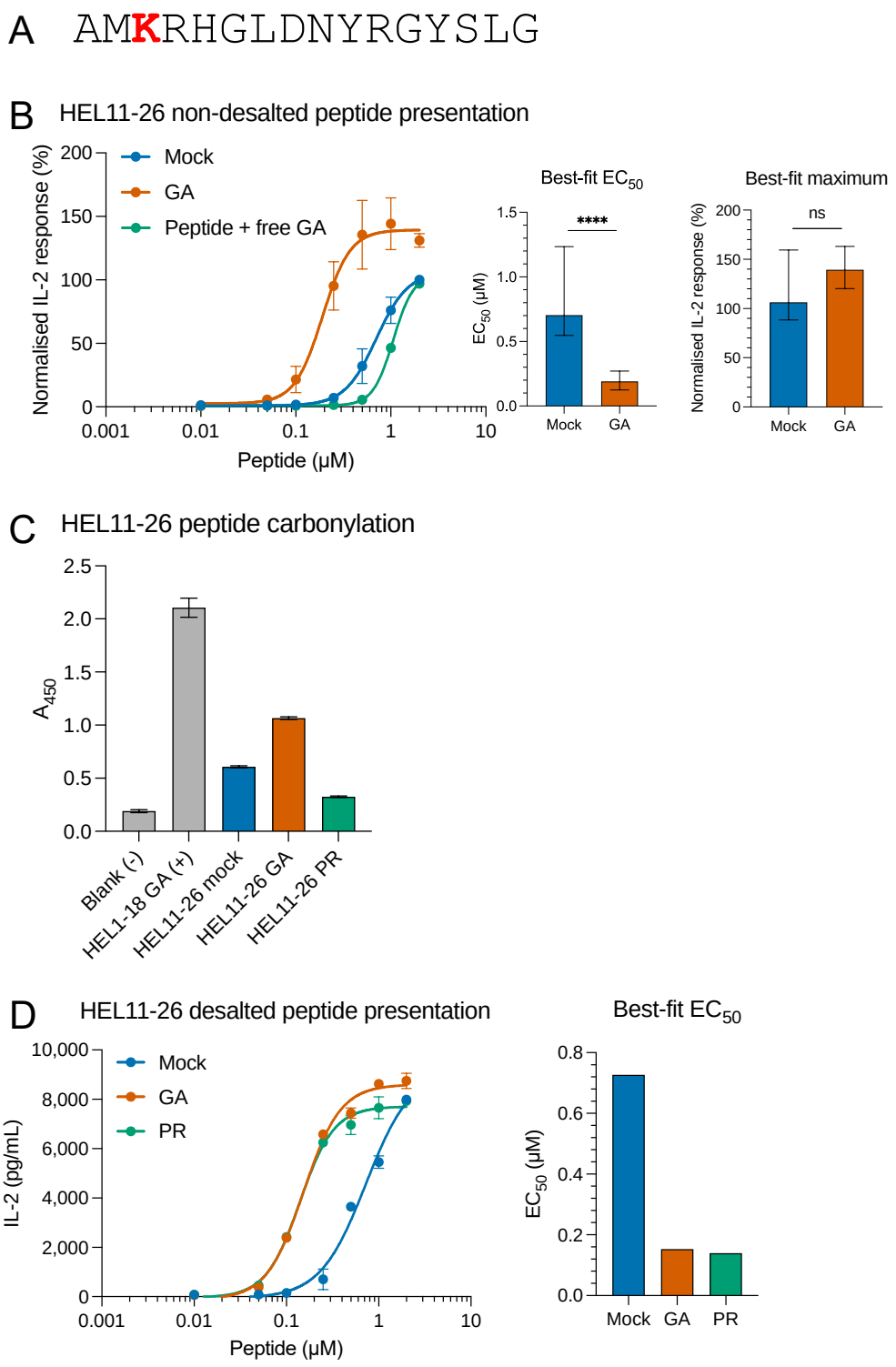


Figure 4.1: GA modification of $HEL_{11–26}$ peptide increases presentation, but is not reversed by PR. $HEL_{11–26}$ peptide was GA modified at 0.25 mg/mL with 5 mM GA at 37 °C for 3 h. PR was performed with 20 mM $NaBH_4$ at 37 °C for 2 h. A) Sequence of $HEL_{11–26}$. B) $HEL_{11–26}$ non-desalted presentation on A20 to Ad11 $CD4^+$ T cell hybridomas. Responses were normalised to 2 μM $HEL_{11–26}$ mock and pooled. Data are mean ± SEM of 3 independent experiments (except for Peptide + free GA). EC_{50} and maximum best-fit values with 95% CI based on fitted variable-slope Hill function with 4 parameters. A global fit curve and F-test were used to test whether the fitted curves differed significantly in their best-fit values. C) Peptide carbonylation measured by biotin hydrazide (BH) ELISA. Data are mean ± SD of 3 technical replicates. D) $HEL_{11–26}$ desalted presentation on A20 to Ad11 $CD4^+$ T cell hybridomas. EC_{50} best-fit values based on fitted variable-slope Hill function with 4 parameters. Data are mean ± SD of 2 technical replicates.

I investigated the modification site using two approaches: chemically-protected peptides and tandem liquid chromatography mass spectrometry (LC-MS).

For the first approach, I used $HEL_{11–25}$ unmodified peptide (**Figure 4.2A**) or variants that were chemically protected either at the N-terminus with a fluorenylmethyloxycarbonyl (Fmoc) protecting group (**Figure 4.2B**) or at the K13 side chain with a 6-azido-L-lysine (azido) protecting group (**Figure 4.2C**) (synthesised by Naorem Nihesh, Aaron Esser-Kahn lab, University of Chicago). I modified the $HEL_{11–25}$ peptides with GA (or mock), chemically removed the protecting groups, and measured peptide carbonylation. The carbonylation assay showed that the peptide with a free N-terminus was modified to a similar extent as unmodified peptide, while the peptide with a free K13 side chain was barely carbonylated (**Figure 4.3A**). I also analysed the peptides using intact LC-MS, which confirmed GA-aldoamine (+42) modifications in the unmodified and free N-terminus peptides, but not the free K13 peptide (**Figure 4.3B**).

Tandem LC-MS results of desalted $HEL_{11–26}$ peptides also provided evidence that GA modification occurred at the N-terminus. Virtually no PTMs were detected on $HEL_{11–26}$ mock (**Figure 4.4A**). For $HEL_{11–26}$ GA, approximately 40% of all detected peptides were modified with GA-aldoamine at the N-terminal alanine (A1), while less than 5% was modified with GA-aldoamine at the K13 side chain (K3) (**Figure 4.4B**). Surprisingly, $HEL_{11–26}$ PR still had about 30% of detected peptides modified with GA-aldoamine at A1, and no evidence of GA-aldoamine reduction to hydroxyethyllysine (+44) (**Figure 4.4C**). The result for $HEL_{11–26}$ PR was unexpected since $NaBH_4$ is supposed to be an effective reducing agent and the carbonylation assay suggested that GA-aldoamine was successfully reduced. Due to the uncertain effects of post-reduction in peptides, PR samples were not prepared or included as controls for subsequent experiments.

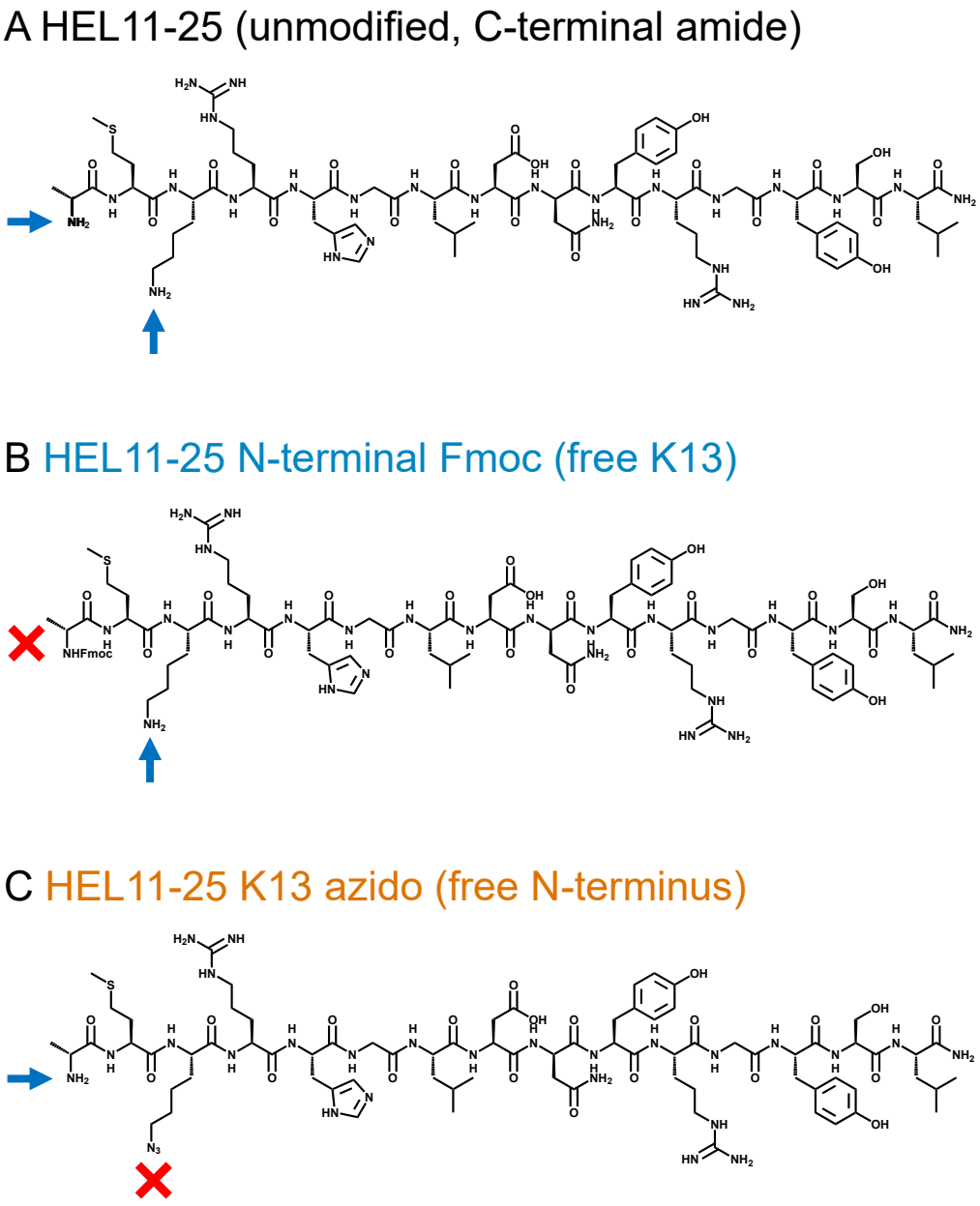


Figure 4.2: $HEL_{11–25}$ peptides chemically capped to block GA modification on specific amino groups. A) Unmodified $HEL_{11–25}$ with two available modification sites at the N-terminus and K13 side chain. B) $HEL_{11–25}$ capped at the N-terminus with a fluorenylmethyloxycarbonyl (Fmoc) group, with K13 free for modification. C) $HEL_{11–25}$ capped at the K13 side chain with a 6-azido-L-lysine (azido) group, with the N-terminus free for modification. Peptides synthesised by Naorem Nihesh (Esser-Kahn lab, University of Chicago) with a C-terminal amide.

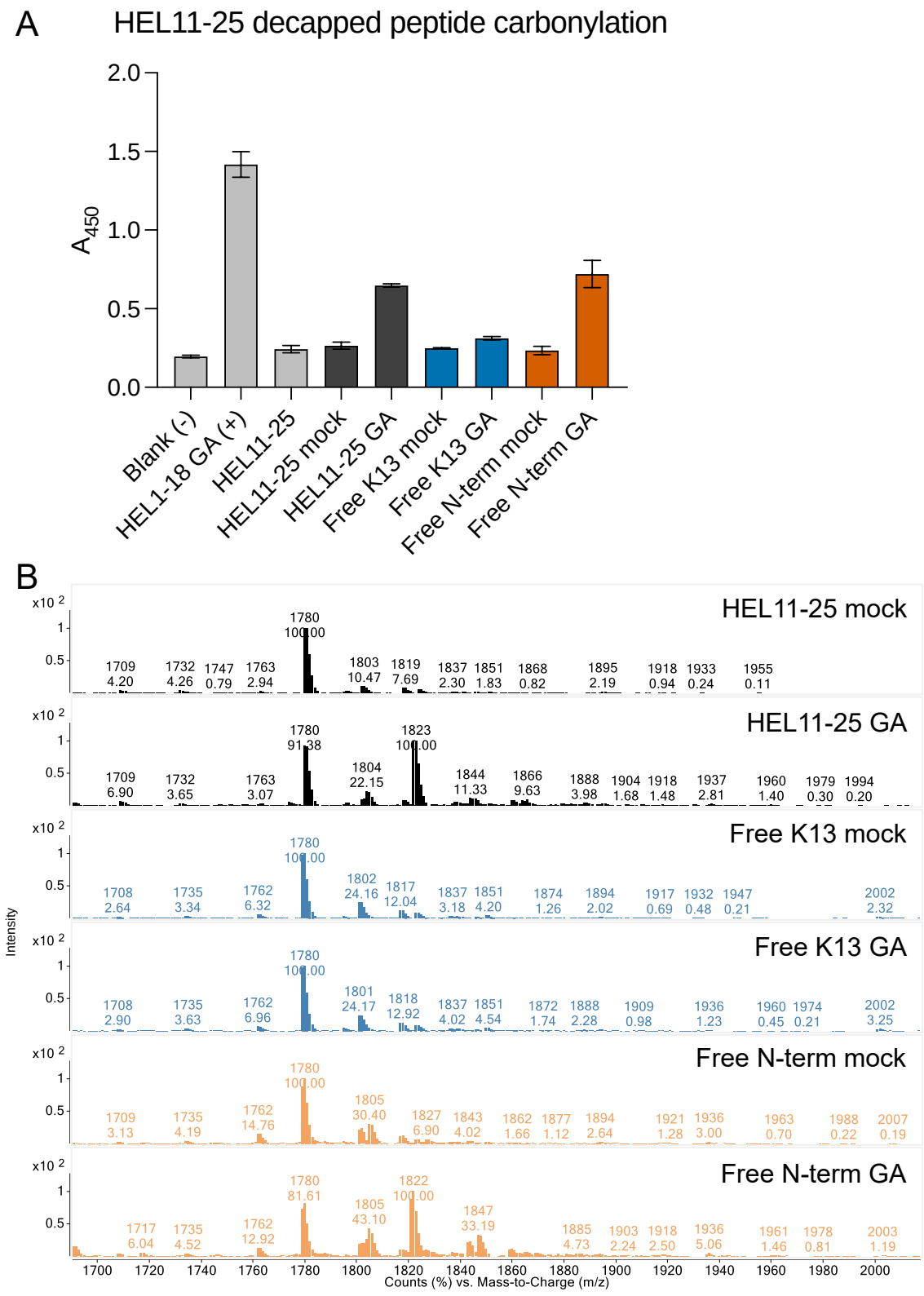


Figure 4.3: GA modification of HEL$_{11–25}$ peptide is mostly prevented by N-terminal capping. Variants of HEL$_{11–25}$ in Figure 4.2 were mock or GA modified then decapped to remove protective groups. A) Peptide carbonylation measured by BH ELISA. Data are mean ± SD of 3 technical replicates. B) Intact MS spectra. Peaks are annotated with deconvoluted mass and abundance percentage relative to the largest peak.



Figure 4.4: $HEL_{11–26}$ GA peptide is predominantly modified on the N-terminus and $HEL_{11–26}$ PR is not reduced. LC-MS-MS results for $HEL_{11–26}$ A) mock, B) GA and C) PR peptides. Data were analysed using PEAKS SPIDER, which quantified the amount of modified peptide (red) compared to unmodified peptide (blue) for all user-defined PTMs: GA-aldoamine (a, +42), hydroxyethyllysine (h, +44), and GA-pyridine (g, +108). For example, for $HEL_{11–26}$ GA at position A1, approximately 40% of peptides are modified with GA-aldoamine (A1a $HEL_{11–26}$ GA in panel B).

4.2.3 Any N-terminal modification to $HEL_{11–25}$ is sufficient

I observed that presentation of $HEL_{11–25}$ N-terminal Fmoc (**Figure 4.2B**) appeared to decrease EC_{50} and increase the maximal response compared with unmodified $HEL_{11–25}$ (**Figure 4.5A**). This suggested that the N-terminal modification may not have to be GA-aldoamine to enhance peptide presentation. Thus, I investigated whether any N-terminal modification could increase $HEL_{11–25}$ peptide presentation to Ad11.

$HEL_{11–25}$ peptides with different N-terminal modifications (Nt-acetyl, Nt-formyl, or Nt-pyroglutamate from ChemPeptide Limited) were presented on Chinese hamster ovary (CHO) cells stably transfected with I-A^d (gifted from Andrea Sant, University of Rochester) to Ad11 hybridomas. I observed that each type of N-terminal modification significantly decreased EC_{50} but did not significantly increase maximal responses (**Figure 4.5B**). Since CHO cells cannot internalise peptides for processing, the effects seen were likely related to increased MHC-II binding of the N-terminally modified peptides.

4.2.4 GA treatment N-terminally modifies all HEL peptides in vitro

Since the exposed N-terminal amine was the preferred site of $HEL_{11–25/26}$ for GA modification, I next considered whether other HEL peptide epitopes would be similarly modified by GA at the N-terminus. I designed a set of 15mer HEL peptides (Chempeptide Limited) corresponding to the BALB/c HEL $CD4^+$ T cell epitopes (**Table 4.1**) with and without Nt-acetylation to determine if blocking the N-terminus would inhibit GA modification. Using intact LC-MS, I observed that all peptides without Nt-acetylation, including the much longer $HEL_{1–32}$ peptide, were predominantly modified with GA-aldoamine (**Figure 4.6**). For 15mer peptides without Nt-acetylation, those that had at least one lysine were modified proportionally more than $HEL_{71–85}$, which did not contain any lysines.

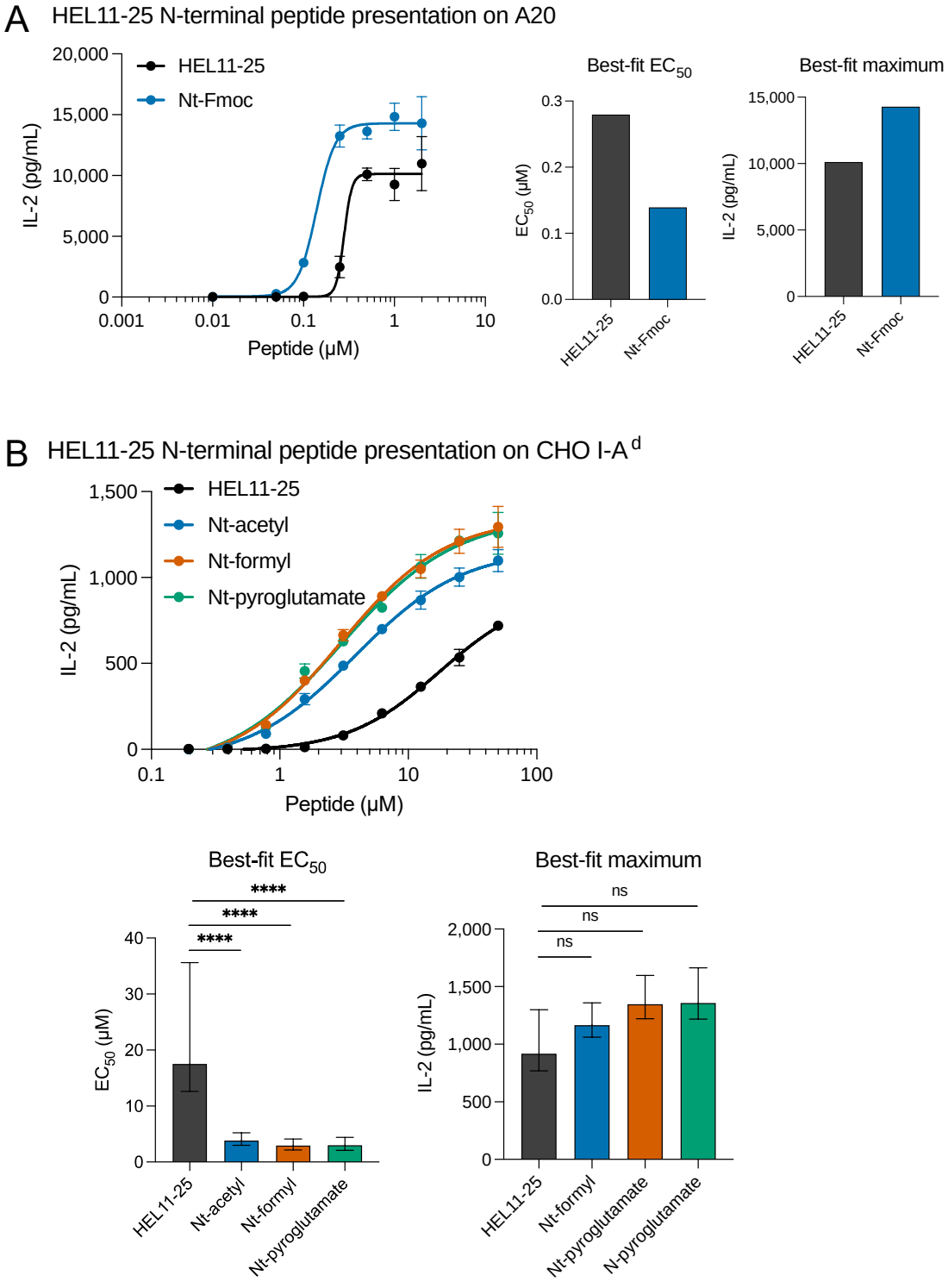
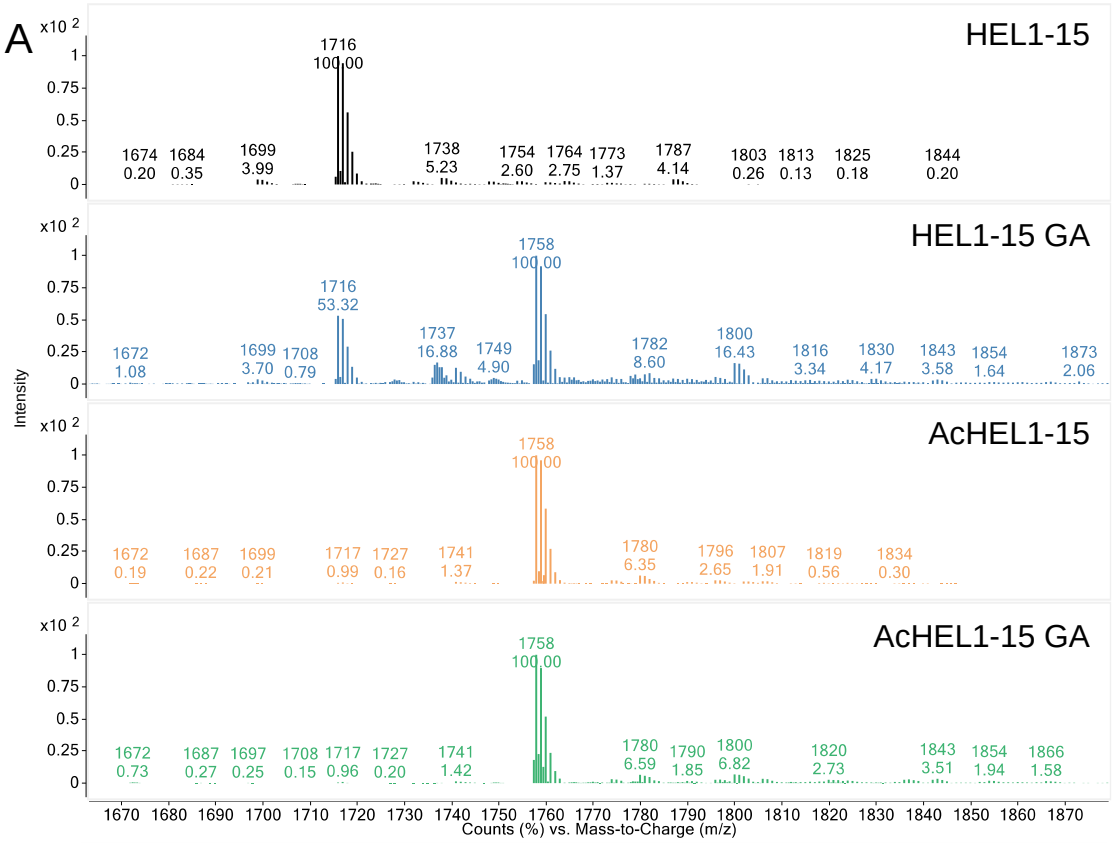
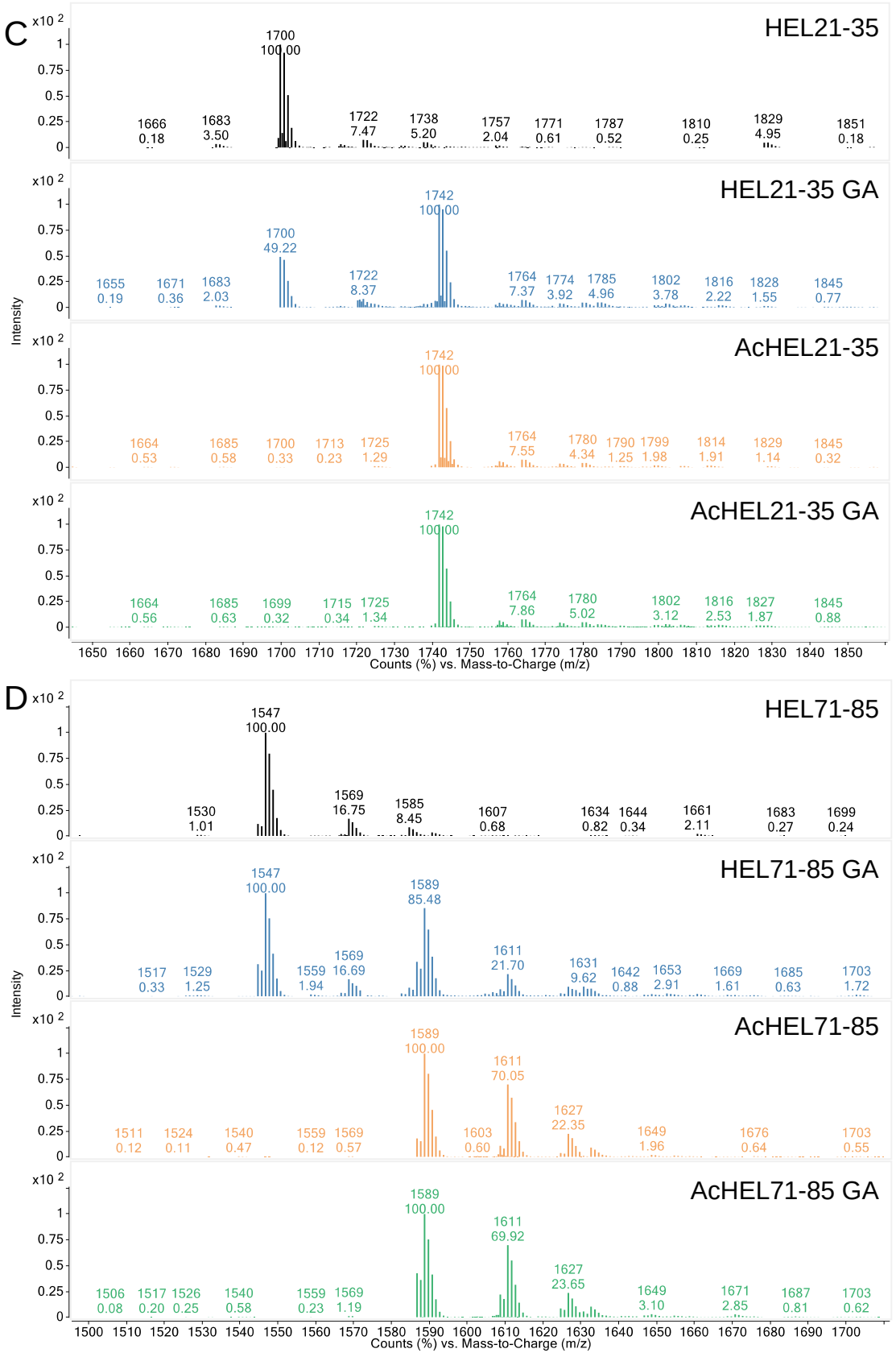


Figure 4.5: Any N-terminal modification on $HEL_{11–25}$ is sufficient to enhance peptide presentation. $HEL_{11–25}$ N-terminally (Nt) modified peptides presented to Ad11 $CD4^+$ T cell hybridomas. A) Nt-Fmoc modification of $HEL_{11–25}$ increases peptide presentation on A20. Data are mean ± SD of 2 technical replicates. EC_{50} and maximum best-fit values based on fitted variable-slope Hill function with 4 parameters. B) Nt modification of $HEL_{11–25}$ increases peptide presentation on CHO I-A^d, which do not internalise peptides for processing. Data are mean ± SEM of 3 independent repeats. EC_{50} and maximum best-fit values with 95% CI based on fitted variable-slope Hill function with 4 parameters. A global fit curve and F-test were used to test whether the fitted curves differed significantly in their best-fit values.



(continued over next page)



(continued over next page)

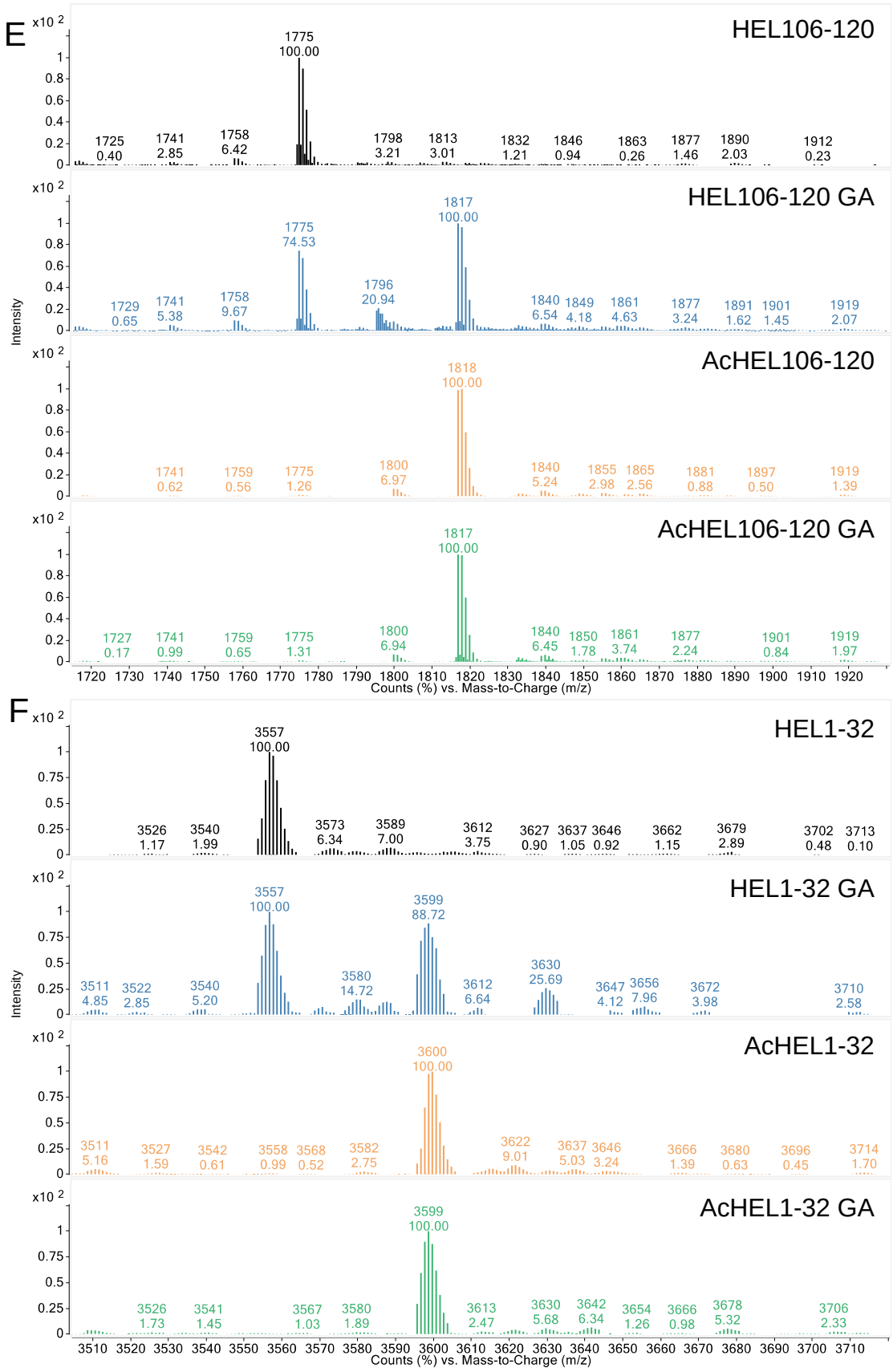


Figure 4.6: Peptides require a free N-terminal amine for GA modification. 15mer HEL peptides with either a free N-terminal amine (HEL) or Nt-acetylation (AcHEL) were GA modified and analysed by intact LC-MS. A) $HEL_{1–15}$, B) $HEL_{11–25}$, C) $HEL_{21–35}$, D) $HEL_{71–85}$, E) $HEL_{106–120}$, F) $HEL_{1–32}$ (32mer peptide).

In contrast, all Nt-acetylated peptides were unchanged after GA treatment. Therefore, the N-terminal amine group facilitates or is the principal site of peptide GA modification.

Next, I tested whether GA modification increased HEL peptide presentation to their corresponding $CD4^+$ T cell hybridomas. Unfortunately, during routine testing I found that all of the hybridomas were mycoplasma positive, so I treated them with ciprofloxacin for two weeks and confirmed they were still mycoplasma negative two weeks after stopping treatment. The hybridomas also did not have selection markers and lost CD3 and CD4 expression over time, which seemed to cause variable IL-2 responses. Thus, I sorted, expanded, and froze down $CD3^+CD4^+$ double positive hybridomas to use in peptide presentation assays (data not shown).

The use of immortalised APCs such as A20 provide a convenient format for comparing hybridoma responses to different peptides and their modified forms. To interrogate a more physiologically relevant type of APC, I derived granulocyte-macrophage colony-stimulating factor (GM-CSF) BMDCs to compare the effect of GA modification and Nt-acetylation on peptide presentation. Both GA-aldoamine and acetylation add C_2H_2O and increase mass by +42, but have different chemical structures and properties (**Figure 4.7**).

While Nt-acetylation increased peptide presentation for $HEL_{1–15}$, $HEL_{11–25}$ and $HEL_{21–35}$, it decreased peptide presentation for $HEL_{71–85}$ and $HEL_{106–120}$ (**Figure 4.8A–E**). In contrast, GA modification increased peptide presentation for both $HEL_{11–25}$ and $HEL_{106–120}$ (**Figure 4.8F–G**). These results suggested that a) N-terminal modification in general (e.g. Nt-acetylation) does not necessarily increase peptide presentation in vitro and b) N-terminal GA-aldoamine can enhance peptide presentation for peptides other than subdominant $HEL_{11–25}$.

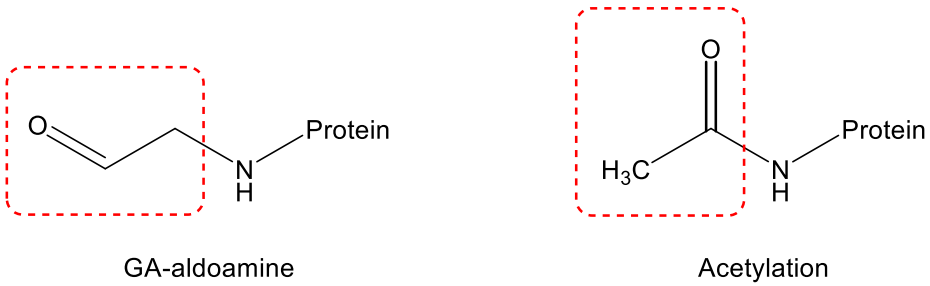


Figure 4.7: GA-aldoamine compared with acetylation. Both PTMs add C_2H_2O and +42 in mass, but have different chemical properties.

4.2.5 GA-modified peptides may induce stronger IgG responses in vivo

HEL peptides modified at the N-terminus with GA-aldoamine were better presented on BMDCs to $CD4^+$ T cell hybridomas. I investigated whether increased presentation of GA-modified peptides to $CD4^+$ T cell hybridomas in vitro corresponded with increased $CD4^+$ T cell responses and anti-peptide IgG titres in vivo.

BALB/c mice were immunised with 10 μg $HEL_{106–120}$ or $HEL_{11–25}$ peptides that were either mock or GA-treated, followed by a homologous 5 μg boost at week 4 (**Figure 4.9A**). B cell epitopes typically recognise three-dimensional structures and may not recognise short linear T cell peptides. Therefore, as a positive control for anti-peptide IgG responses, peptides were also emulsified in Complete Freund's Adjuvant (CFA) for priming and Incomplete Freund's Adjuvant (IFA) for boosting.

At the termination of the experiment in week 6, all three mice immunised with $HEL_{106–120}$ in CFA/IFA generated strong IgG responses to peptide, compared with only one mouse for $HEL_{11–25}$ CFA/IFA immunisation (**Figure 4.9B**). This indicated that it was possible to generate IgG antibodies against the $HEL_{106–120}$ peptide, but not so easily against the $HEL_{11–25}$ peptide. Interestingly, one of three mice immunised with $HEL_{106–120}$ GA had weak but detectable antibody responses to peptide that were absent in mice

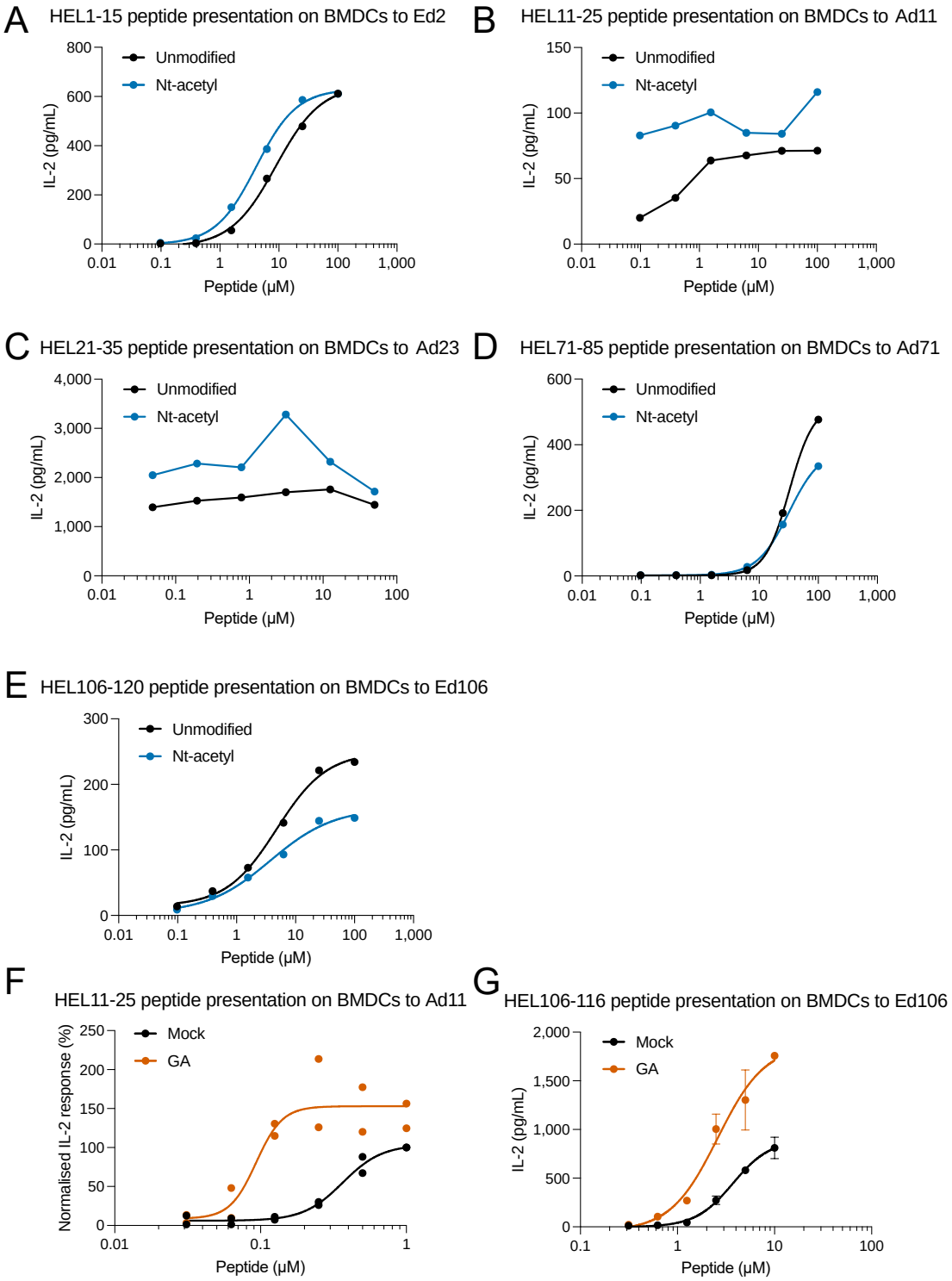


Figure 4.8: N-terminal (Nt)-acetylation and GA modification have different effects on peptide presentation. Unmodified/mock, Nt-acetylated and GA-modified peptide presentation on BALB/c-derived BMDCs to $CD4^+$ T cell hybridomas. Nt-acetylated peptide presentation for A) $HEL_{1–15}$, B) $HEL_{11–25}$, C) $HEL_{21–35}$, D) $HEL_{71–85}$ and E) $HEL_{106–120}$. GA-modified peptide presentation for F) $HEL_{11–25}$. IL-2 responses normalised to mock 1 μM and pooled from 2 independent experiments. G) $HEL_{106–120}$. Data are mean ± SD of 2 technical replicates.

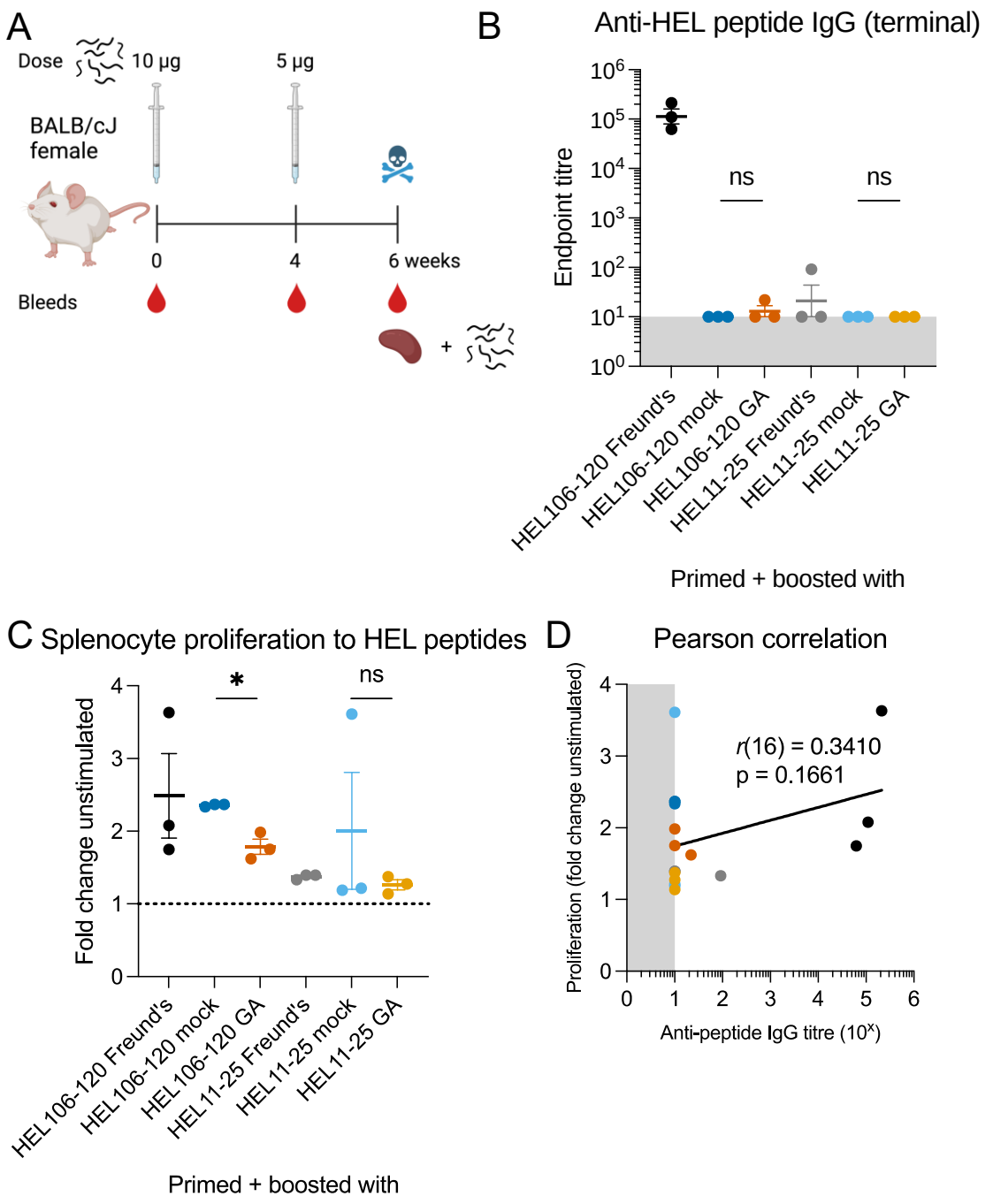


Figure 4.9: GA-modified HEL peptides may elicit anti-peptide IgG responses in vivo. A) Bleed, immunisation and harvest schedule. B) Anti-HEL peptide IgG endpoint titres and C) splenocyte proliferation after stimulation with unmodified HEL peptide expressed as fold change over unstimulated (media only) splenocytes. Data are mean ± SEM (*p ≤ 0.05; unpaired t test). D) Pearson correlation analysis of splenocyte proliferation versus anti-HEL peptide IgG titre of all mice in this experiment (n = 18). Each dot represents a single mouse. Sera were serially diluted starting at 1:10 and non-responding mice were plotted at the limit of detection (shaded in grey).

immunised with $HEL_{106–120}$ mock. In contrast, splenocyte stimulation with $HEL_{106–120}$ showed stronger proliferative responses in mice immunised with $HEL_{106–120}$ mock than in mice immunised with $HEL_{106–120}$ GA (**Figure 4.9C**). Pearson correlation analysis suggested that splenocyte proliferation and anti-HEL peptide IgG titres were not correlated (**Figure 4.9D**).

GA-modified peptide may elicit higher IgG antibody responses to native peptide, but this does not seem to be caused by increased peptide presentation or $CD4^+$ T cell responses. Thus, GA-mediated peptide immunogenicity may be driven by other components of the immune system.

4.2.6 GA-modified protein does not enhance subdominant epitopes

GA modification of HEL peptide occurs on the N-terminus, whereas for HEL protein GA generally modifies lysine side chains. HEL mutated to have no lysines did not appear to be modified with GA-aldoamine (Section 3.2.4, **Figure 3.22**). Given that GA modification may be different for peptides compared with proteins, I performed antigen presentation using GA-modified proteins to determine whether selected $CD4^+$ T cell hybridomas had enhanced responses.

First, I optimised the protocol for deriving BMDCs in our lab: bone marrow cells were incubated with GM-CSF and IL-4, and adherent cells were harvested after 6 d. However, BMDCs are typically found in the non-adherent fraction and left to differentiate for a much longer period (Lutz et al. 1999; Brasel et al. 2000). Therefore, I tested two standard protocols: a) Lutz et al. (1999) differentiated with GM-CSF for 10 d, and b) Brasel et al. (2000) used FMS-like tyrosine kinase 3 (Flt3) for 9 d. Both protocols harvested non-adherent cells at the end of incubation. After comparing the three methods, I found that Flt3 BMDCs had high expression of the DC marker CD11c, upregulated activation

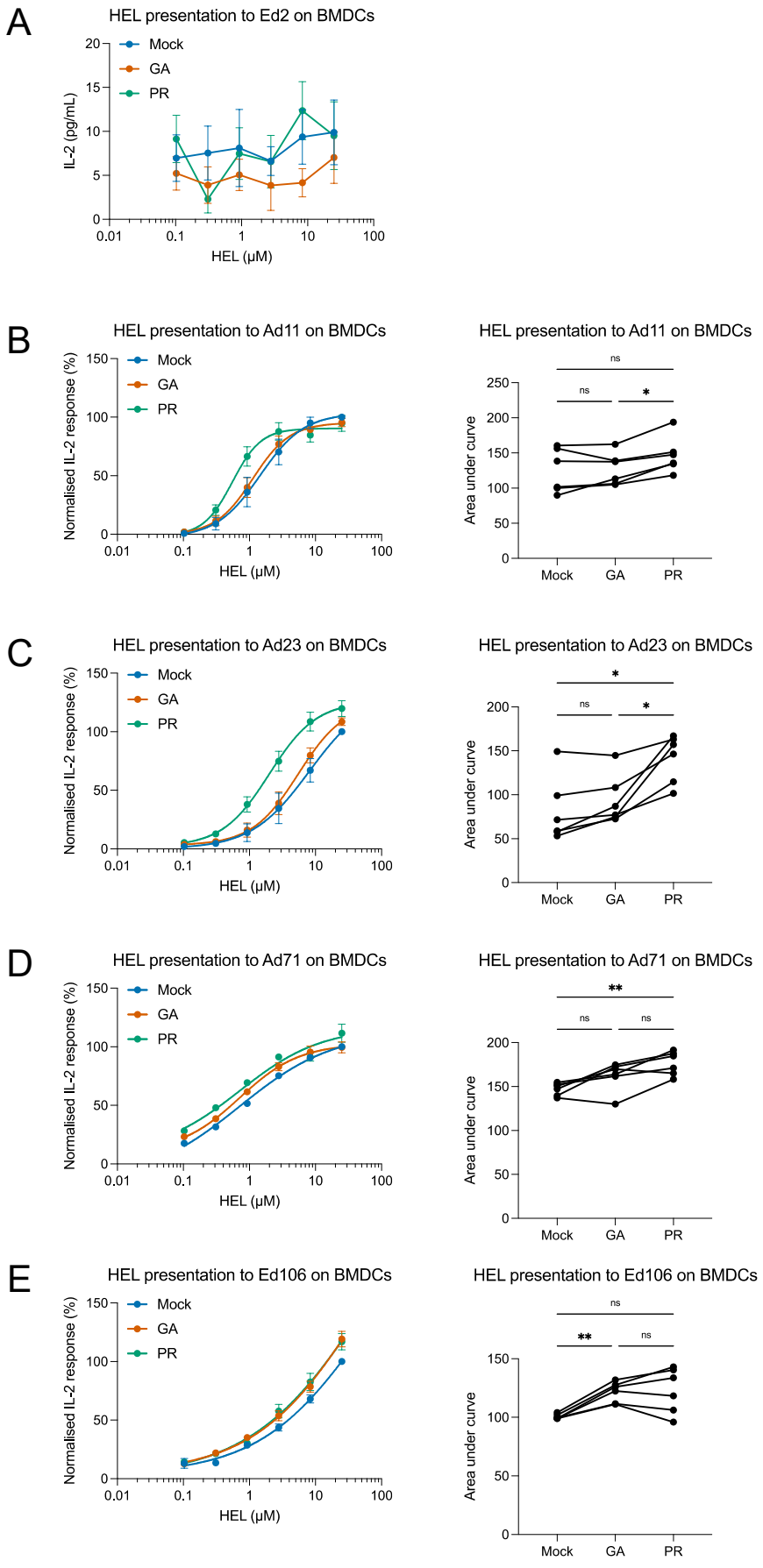
markers (CD40 and CD86) after LPS stimulation, and good antigen presentation (data not shown). Therefore, I proceeded with the protocol by Brasel et al. (2000).

Flt3 BMDCs derived from six female BALB/c mice were used as APCs across two independent experiments. The selective epitope enhancement hypothesis predicts that HEL GA should elicit higher responses than HEL mock and HEL PR for at least one hybridoma recognising a subdominant epitope (Ed2, Ad11, Ad23, Ad71) but not the hybridoma recognising the immunodominant epitope (Ed106) (**Table 4.1**). HEL GA presentation was not significantly enhanced for Ed2, Ad11, Ad23 or Ad71 (**Figure 4.10A–D**). Moreover, HEL GA presentation to Ed106 was significantly higher compared with HEL mock and not diminished by HEL PR (**Figure 4.10E**). Therefore, these data do not support the hypothesis that protein GA modification selectively enhances $CD4^+$ T cell responses to subdominant ($HEL_{11–25}$) and not immunodominant ($HEL_{106–120}$) epitopes.

4.2.7 $CD4^+$ T cell responses in HEL GA and ML GA immunised mice

Based on previous work in the lab, increased in vivo immunogenicity of HEL GA was hypothesised to be caused by selective enhancement of $CD4^+$ T cell epitopes. However, I did not find evidence for selective epitope enhancement using in vitro antigen presentation assays with $CD4^+$ T cell hybridomas. Therefore, I repeated the in vivo experiments on which the hypothesis was based.

Based on a lab protocol used for $CD4^+$ memory T cell epitope mapping, BALB/c mice were immunised s.c. in the flank with 10 μg prime followed by 5 μg boost 6 weeks later, and the spleen was harvested 2–4 weeks post-boost (**Figure 4.11A**). Spleen cells (splenocytes) comprise mostly red blood cells (RBCs), T and B cells, with a small population of DCs, macrophages, neutrophils and natural killer (NK) cells (Hensel et al. 2019).



(caption on next page)

(figure on previous page)

Figure 4.10: HEL GA protein presentation to CD4$^+$ T cell hybridomas in vitro does not show selective enhancement of subdominant epitopes. HEL mock, HEL GA and HEL PR protein presentation on Flt3 BMDCs to CD4$^+$ T cell hybridomas. A) Ed2 (epitope $HEL_{1–15}$), B) Ad11 (epitope $HEL_{11–25}$), C) Ad21 (epitope $HEL_{21–35}$), D) Ad71 (epitope $HEL_{71–85}$), and E) Ed106 (epitope $HEL_{106–120}$). BMDCs were derived from 6 mice from 2 independent experiments. Ed2 did not respond to HEL protein presentation ($HEL_{1–15}$ peptide positive control not shown). Responses were normalised to HEL mock 25 μM and pooled to show mean ± SEM. Data were fitted with a variable-slope Hill function with 4 parameters but best-fit values could not be obtained for incomplete dose-response curves. Instead, the area under the curve for each mouse was calculated and shown as a connected line (*$p \leq 0.05$, **$p \leq 0.01$; repeated measures one-way ANOVA followed by Holm-Šídák's multiple comparison test).

Peptides and proteins added to splenocytes can be presented by autologous APCs to antigen-specific memory cells, which undergo clonal expansion and secrete cytokines that can be used as a readout of lymphocyte memory. In our lab, splenocyte proliferative responses are typically used as a proxy for CD4$^+$ memory T cell responses and measured using tritiated (^{3}H) thymidine incorporation.

Splenocytes from HEL mock or HEL GA immunised mice stimulated with 15mer HEL peptides representing known BALB/c CD4$^+$ T cell epitopes (**Table 4.1 and Figure 4.11A**) did not proliferate much compared with unstimulated splenocytes, since the fold change in proliferation was on average close to one (**Figure 4.11B**). Moreover, there were no significant differences in fold change proliferation between HEL mock and HEL GA immunised mice. Therefore, I was unable to confirm the hypothesis that in vivo CD4$^+$ memory T cell responses to the $HEL_{11–25}$ subdominant epitope were selectively enhanced.

Similarly, for mice immunised with HEL mock, HEL GA or HEL PR (**Figure 4.12A)**, splenocyte proliferation after stimulation with native HEL protein was also low compared with unstimulated splenocytes (**Figure 4.12B**). Moreover, there were no significant differences in fold change proliferation between any of the immunisation groups.

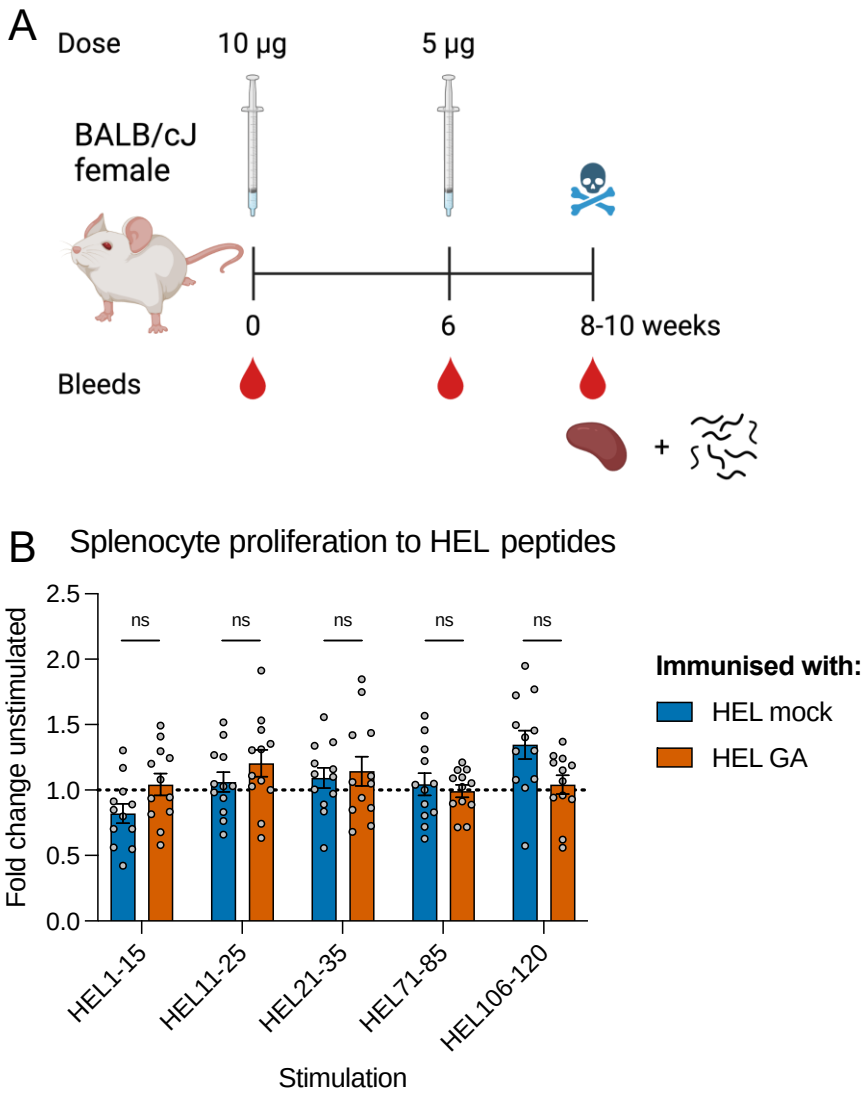


Figure 4.11: Splenocytes from HEL mock and HEL GA immunised mice have similar proliferative responses to HEL peptide stimulation. A) Bleed, immunisation and harvest schedule. Splenocytes from mice homologously primed and boosted with HEL mock or HEL GA were stimulated with HEL peptides corresponding to known $CD4^+$ T cell epitopes, or left unstimulated with media only. B) Splenocyte proliferation as measured by ^3H thymidine incorporation, expressed as fold change over unstimulated splenocytes. Data are mean ± SEM from 12 mice across 2 independent experiments (unpaired t tests between HEL mock and HEL GA for each peptide corrected for multiple comparisons using Holm-Šídák's method).

The weak HEL-specific splenocyte proliferation in mice immunised with HEL GA was surprising given the robust anti-HEL IgG titres seen after prime and boost (**Figure 3.6**). Cytokine analysis on a limited number of splenocyte supernatants also suggested no significant differences between mice immunised with HEL GA and HEL mock, although mice immunised with HEL GA tended to have higher levels of IL-5 (**Figure A.6**).

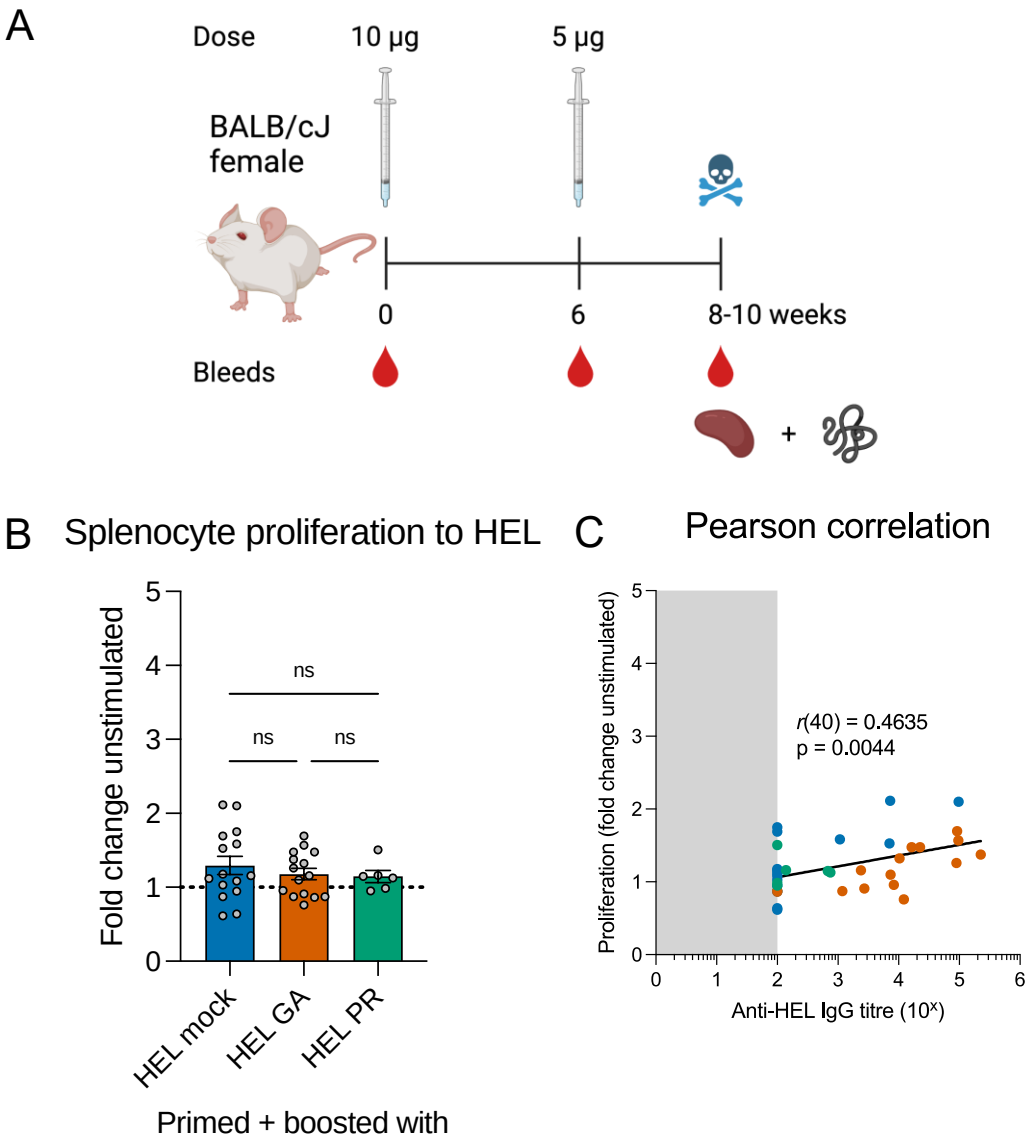


Figure 4.12: HEL-specific splenocyte proliferation is not enhanced after prime and boost with HEL GA compared with HEL mock and HEL PR. A) Bleed, immunisation and harvest schedule. Splenocytes from mice homologously primed and boosted with HEL mock, HEL GA, or HEL PR were stimulated with native HEL protein, or left unstimulated with media only. B) Splenocyte proliferation as measured by ^{3}H thymidine incorporation, expressed as fold change over unstimulated splenocytes. Data are mean ± SEM from 6–15 immunised mice across 3 independent experiments (one-way ANOVA followed by Holm-Šídák's multiple comparisons test). C) Pearson correlation analysis of splenocyte proliferation versus anti-HEL IgG titre of all mice in B). Each dot represents a single mouse. Anti-HEL IgG titres based on Figure 3.6. Sera were serially diluted starting at 1:100 and non-responding mice were plotted at the limit of detection (shaded in grey).

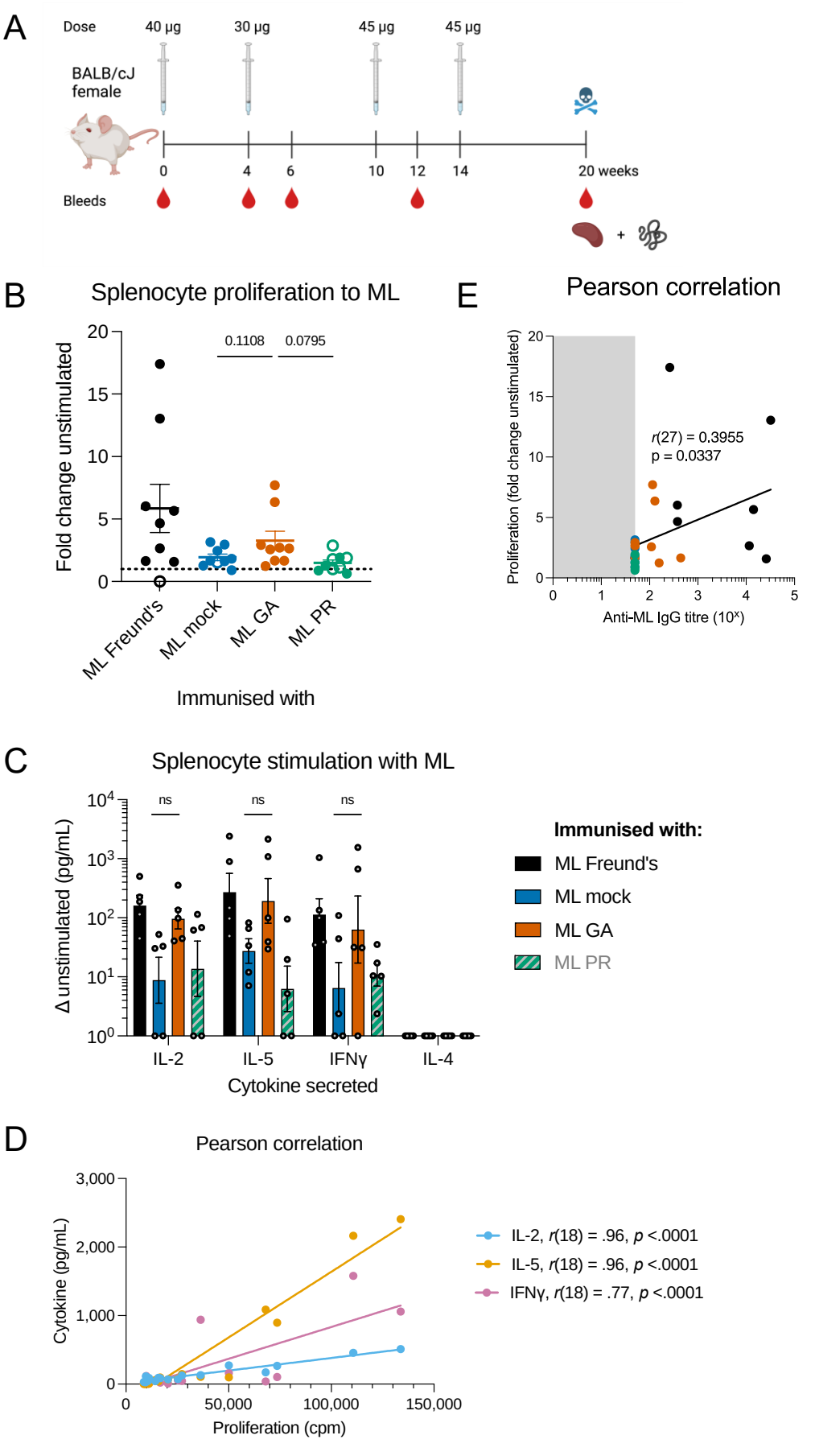
Pearson correlation analysis suggested that there was a significant medium-strength positive association between splenocyte proliferation and anti-HEL IgG titres (**Figure 4.12C**). Notably, the significant association was absent in mice that received only one dose of antigen (**Figure A.7**).

In contrast to prime and boost immunisations with HEL, after four high dose immunisations with mouse lysozyme (ML) (**Figure 4.13A**), splenocyte proliferation and cytokines were slightly higher in ML GA compared with ML mock and ML PR immunised mice (**Figure 4.13B–C**). Moreover, I found that splenocyte proliferation expressed in counts per minute (CPM) significantly and linearly correlated with total cytokine production for IL-2 and IL-5 (**Figure 4.13D**). Similar to HEL prime and boost immunisations, Pearson correlation showed a significant medium-strength positive association between splenocyte proliferation and anti-ML IgG titres (**Figure 4.13E**).

4.2.8 Anti-HEL IgG responses appear to be thymus dependent

$CD4^+$ memory T cell responses to HEL GA immunisation were weak, raising the possibility that despite the presence of antibody isotype switching to IgG, antibody responses might be partially thymus-independent. Therefore, I measured anti-HEL IgG and anti-HEL IgM responses over time for mice immunised with HEL mock or HEL GA in two separate experiments.

The anti-HEL IgG responses appeared typical of thymus-dependent antigens. Anti-HEL IgG was not detected 1 week post-prime (**Figure 4.14A**), and was only detectable in HEL GA immunised mice starting from 2 weeks post-prime (**Figure 4.14A–B**). Anti-HEL IgG then steadily increased to a maximum level between 4–6 weeks post-prime. The production of IgG class-switched antibody is a typical feature of $CD4^+$ T cell help. Moreover, the secondary antibody response after homologous boosting with HEL GA was rapid (**Figure 4.14B**), indicating the presence of memory $CD4^+$ T cells. Thymus-independent antigens directly stimulate B cells and tend to rapidly produce IgM antibodies. However, there was no evidence that anti-HEL IgM was elevated in mice immunised with HEL GA compared with HEL mock (**Figure 4.14C–D**).



(caption on next page)

(figure on previous page)

Figure 4.13: Mice repeatedly boosted with ML GA have detectable splenocyte responses. Bleed, immunisation and harvest schedule. Splenocytes from immunised mice were stimulated with native ML protein, or left unstimulated with media only. B) Splenocyte proliferation as measured by ^{3}H thymidine incorporation, expressed as fold change over unstimulated splenocytes. Data are mean ± SEM from 4–9 mice across 2 independent experiments (one-way ANOVA followed by Holm-Šídák's multiple comparisons test, p-values stated). Excluded mice indicated with empty circles due to various technical issues (described in text). C) Cytokines secreted by ML-stimulated splenocytes measured for mice from one experiment. ML PR group only received three instead of four immunisations and is greyed out. Data analysed with multiple unpaired t tests corrected for multiple comparisons using Holm-Šídák's method. D) Pearson correlation analysis of cytokine secretion versus splenocyte proliferation shows a significant correlation with all cytokines, and a linear relationship for IL-2 and IL-5. E) Pearson correlation analysis of splenocyte proliferation versus anti-ML IgG titre of mice from B) except those previously excluded. Each dot represents a single mouse. Anti-ML IgG titres based on Figure 3.27. Sera were serially diluted starting at 1:50 and non-responding mice were plotted at the limit of detection (shaded in grey).

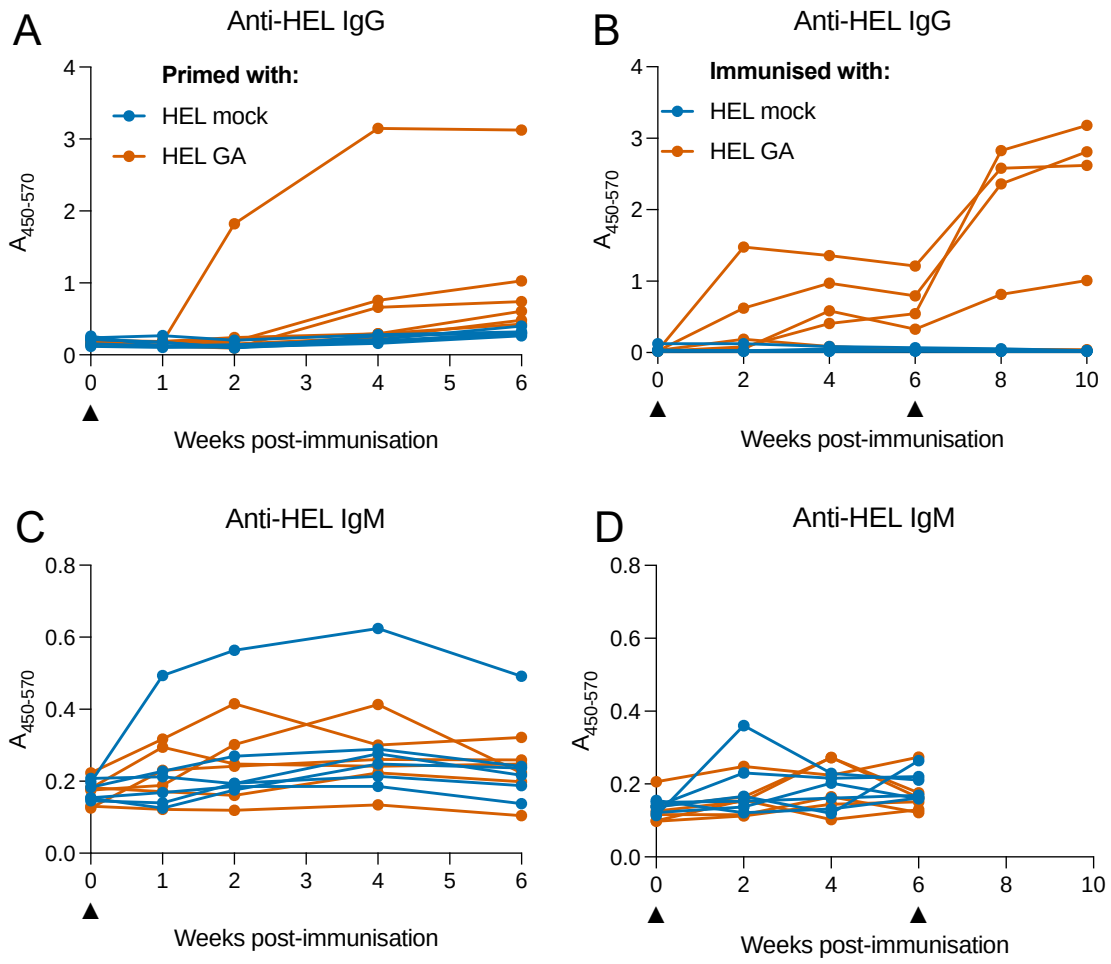


Figure 4.14: Anti-HEL IgG responses to HEL GA immunisation appear to be thymus-dependent. Anti-HEL IgG responses over time for A) mice primed with 10 µg HEL mock or HEL GA or B) mice primed with 10 µg HEL mock or HEL GA and homologously boosted with 5 µg. Anti-HEL IgG responses are detected starting from week 2. C) and D) are anti-HEL IgM responses for A) and B) respectively. Each line represents a single mouse (n = 6 for each experiment). Sera were diluted 1:100.

Taken together, these results suggest that anti-HEL IgG responses to HEL GA immunisation are thymus-dependent rather than thymus-independent. While $CD4^+$ T cells appear to be required for GA-mediated protein immunogenicity, this does not necessarily mean that they mediate enhanced immune responses, as highlighted by the lack of significant differences in $CD4^+$ memory T cell responses between mice immunised with HEL mock, HEL GA and HEL PR (**Figure 4.12B**). Higher $CD4^+$ T cell responses did not translate into higher IgG responses, which suggested that GA-mediated immunogenicity was mediated by other components of the immune system.

4.2.9 HEL GA immunised mice have more HEL-specific ASCs

$CD4^+$ T cells appear to be required but not sufficient for anti-HEL IgG responses after HEL GA immunisation. GA-aldoamine may instead enhance B cell activation to increase the numbers of antibody secreting cells (ASCs) and antibody production. ASCs had not been assayed before in the lab, and I aimed to determine whether HEL-specific ASCs were more numerous in HEL GA compared with HEL mock and HEL PR immunised mice. To detect ASCs, I used enzyme-linked immunosorbent spot (ELISpot) rather than flow cytometry because ELISpot is thought to be more sensitive, and antigen-specific cells after no-adjuvant immunisations were likely to be rare.

Since ELISpot had not been established in our lab, I first tested whether I could detect total IgG ASCs. I stimulated naïve splenocytes with R848 and mouse interleukin-2 (mIL-2) for 4 d to induce polyclonal B cell stimulation, then plated the cells on anti-mouse IgG capture antibody-coated ELISpot plates overnight, and detected captured cells with anti-mouse IgG horseradish peroxidase (HRP). The number of spots titrated with cell number and there were few small spots in the unstimulated splenocytes control, showing that detection of active total ASCs was successful (**Figure 4.15**).

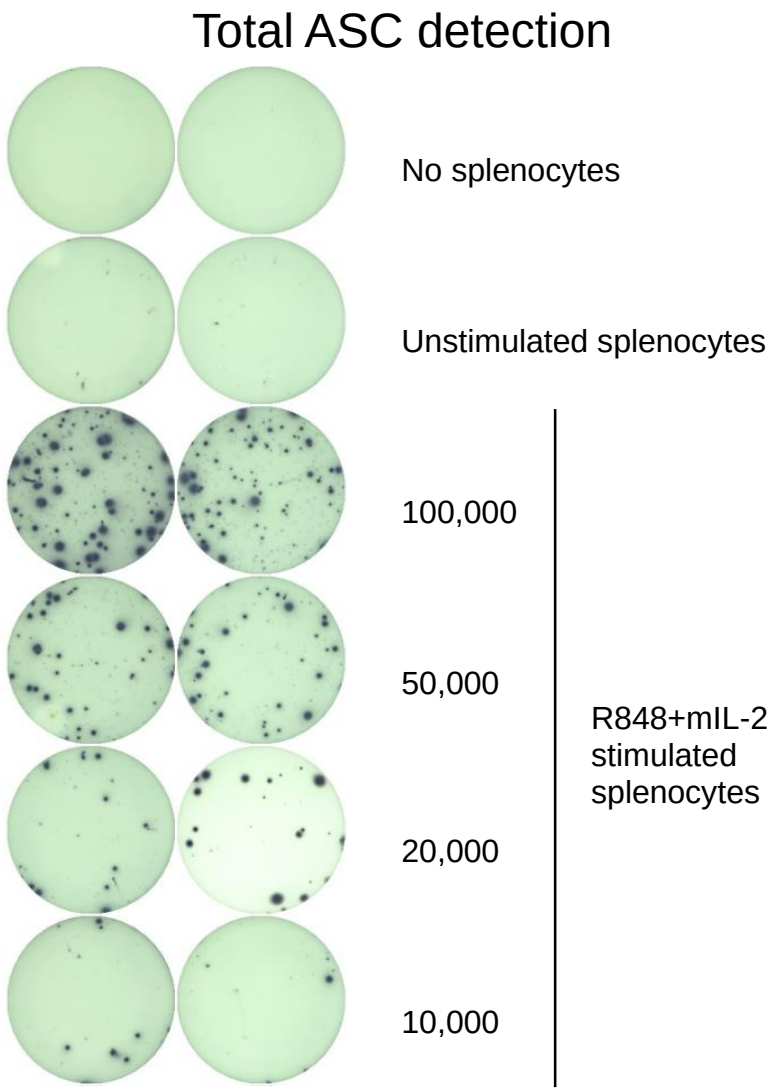


Figure 4.15: ELISpot detection of total antibody-secreting cells (ASCs). Naïve splenocytes were polyclonally stimulated with R848 and mIL-2 for 4 d, then added to ELISpot plates coated with anti-mouse IgG capture antibody. After an overnight incubation, total ASCs were detected with anti-mouse IgG biotinylated detection antibody. Numbers indicate splenocytes added per well.

Next, I tested whether I could detect HEL-specific IgG ASCs. I prepared biotinylated HEL and OVA proteins (**Figure 4.16A**) and confirmed that HEL antibodies from antisera could recognise biotinylated HEL (**Figure 4.16B**). A mouse previously primed with HEL CFA was boosted with HEL IFA to stimulate the differentiation of memory B cells into ASCs. I harvested splenocytes 7 d later, and compared HEL-specific ASC detection between HEL-coated ELISpot plates and the biotinylated HEL probe. I observed that the biotinylated HEL probe produced larger and more distinct spots (**Figure 4.16C**).

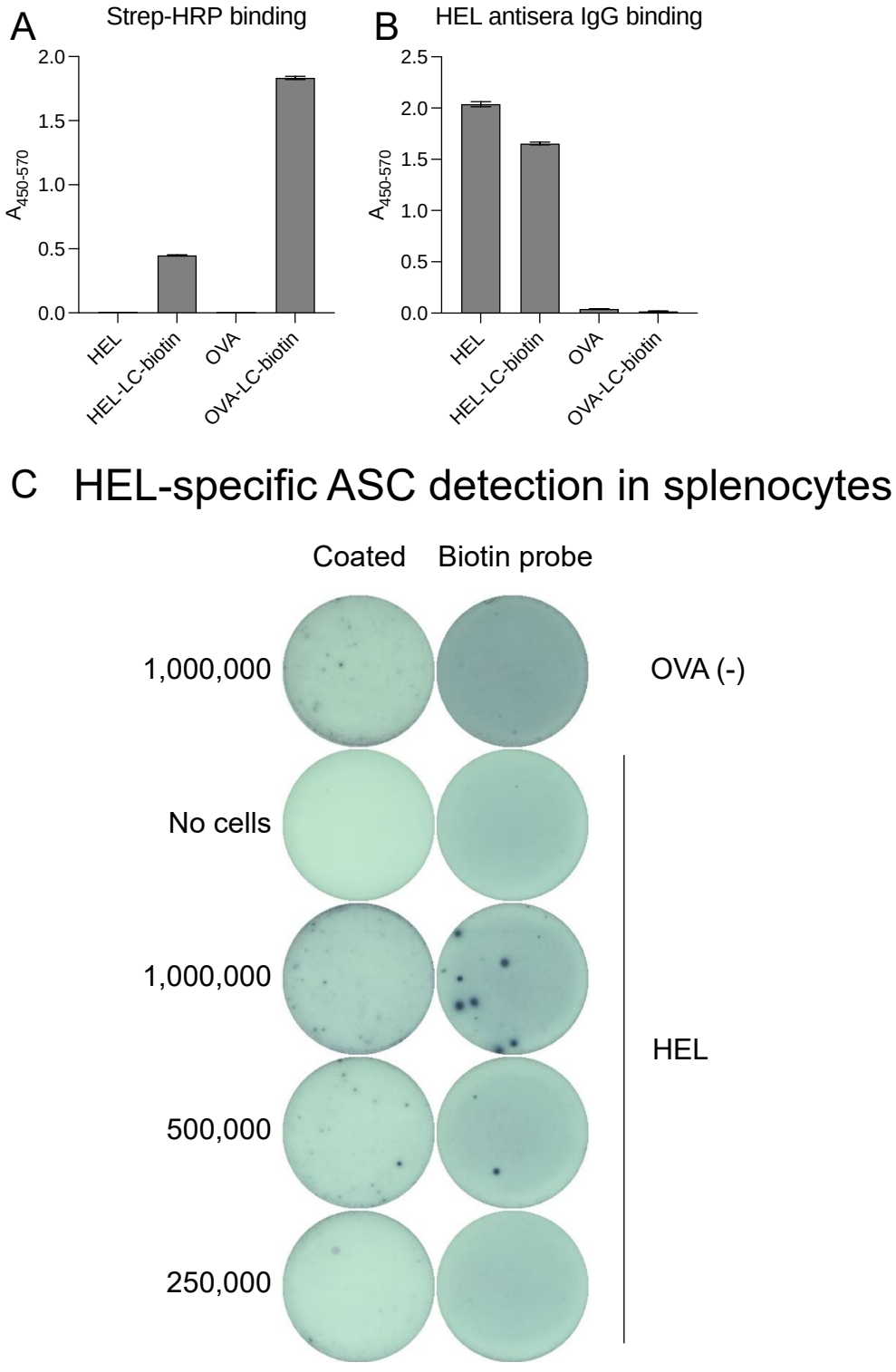


Figure 4.16: Biotinylated HEL can be used to detect HEL-specific ASCs. Splenocytes from one mouse primed with HEL CFA then boosted with HEL IFA 7 d after boosting. A) Strep-HRP binding to proteins coated on ELISA plates. Data are mean ± SD of 3 technical replicates. B) HEL antisera IgG binding to proteins coated on ELISA plates. Data are mean ± SD of 3 technical replicates. C) Detection of HEL-specific ASCs with OVA (negative control) or HEL, direct coating on ELIspot plates compared with HEL biotinylated probe. ASCs are larger and darker spots. Numbers indicate splenocytes plated per well.

I then compared the number of HEL-specific ASCs in the spleen, draining lymph nodes (LNs) and bone marrow (BM) compartments. An irrelevant biotinylated protein (OVA-LC-biotin) was included as a negative control to verify that ASCs were HEL-specific, and total IgG ASCs were detected as a positive control. The highest number of HEL-specific ASCs were detected in BM, followed by LNs, then spleen (**Figure 4.17**).

I also tested whether HEL-specific IgG ASCs could be produced from ex vivo mitogen expansion rather than in vivo boosting. I harvested spleen, LNs, and BM cells from another mouse previously primed and boosted with HEL in CFA/IFA, and measured HEL-specific ASCs 0 d and 5 d after polyclonal B cell stimulation. Some HEL-specific ASCs were detected in BM without any in vitro stimulation (**Figure 4.18**). However, I did not detect any HEL-specific ASCs 5 d post-stimulation, even though there were many total ASCs (**Figure 4.19**). Although polyclonal stimulation expanded total ASCs, there was also a high amount of cell death that may have eliminated HEL-specific clones. Therefore, the in vivo boosting protocol was chosen for subsequent experiments.

After establishing the ELISpot assay, I investigated if there were differences in the numbers of HEL-specific ASCs between mice immunised with HEL mock, HEL GA, or HEL PR via one of three immunisation routes: subcutaneously (s.c.) in the flank, intraperitoneally, or s.c. in the hock. Mice were homologously boosted 7 d prior to harvest to stimulate differentiation of HEL-specific memory B cells to ASCs. HEL-specific ASCs were generally more abundant in HEL GA immunised mice compared with HEL mock and HEL PR, except for one responder mouse immunised in the hock with HEL mock (**Figure 4.20** and **Figure 4.21A–C**). Terminal anti-HEL IgG responses post-boost were also generally higher in HEL GA immunised mice, except for the HEL mock responder (**Figure 4.21D–F**). Pearson correlation analysis suggested a significant strong positive association between anti-HEL IgG responses and HEL-specific ASCs (**Figure 4.21G**).

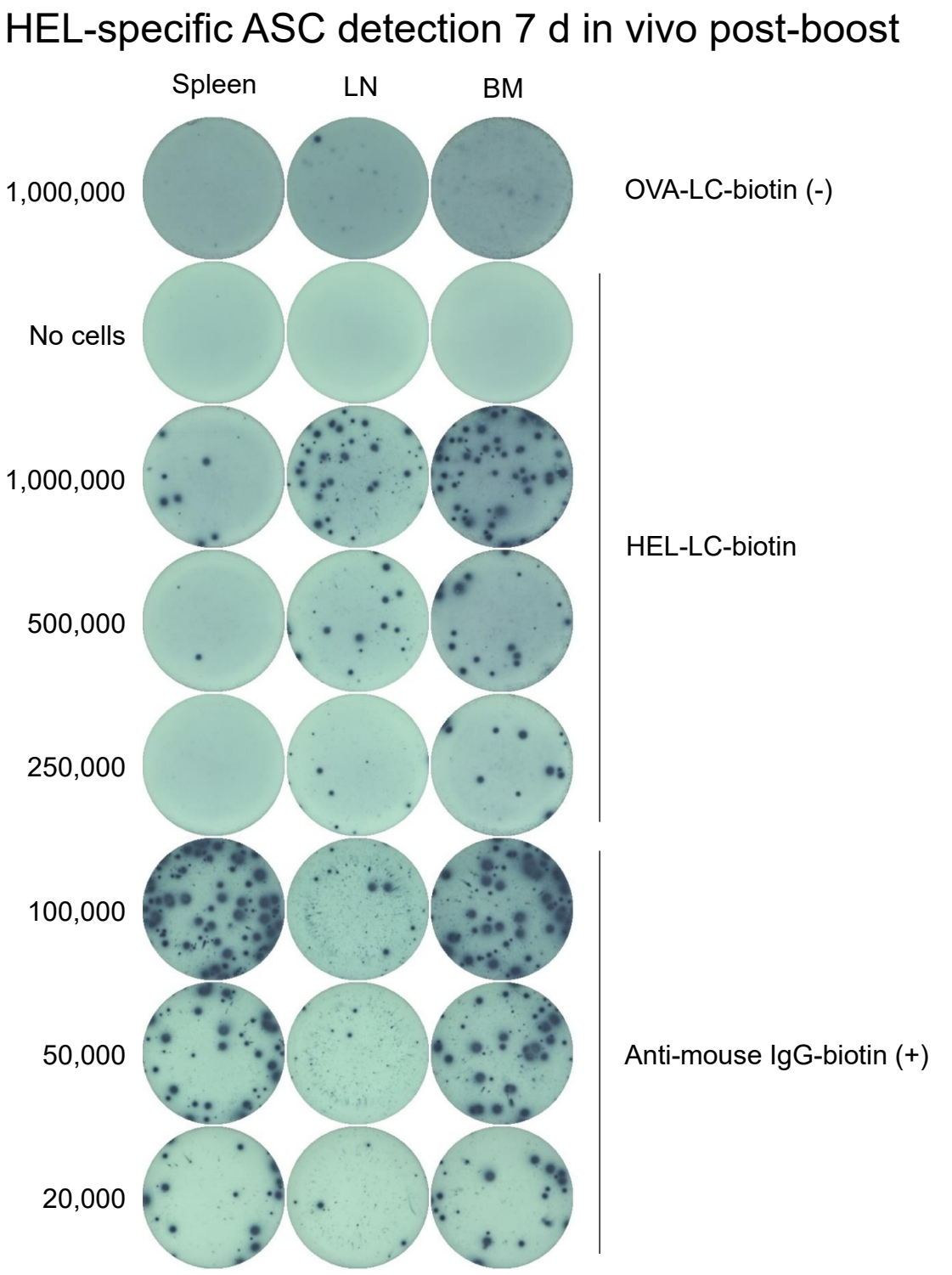


Figure 4.17: HEL-specific ASCs are effectively stimulated by in vivo boosting. Cells from one mouse primed with HEL CFA then boosted with HEL IFA 7 d after boosting (same mouse as in Figure 4.16). OVA-LC-biotin and anti-mouse IgG-biotin included as negative and positive controls respectively. Numbers indicate splenocytes plated per well. LN = draining lymph node cells, BM = bone marrow cells.

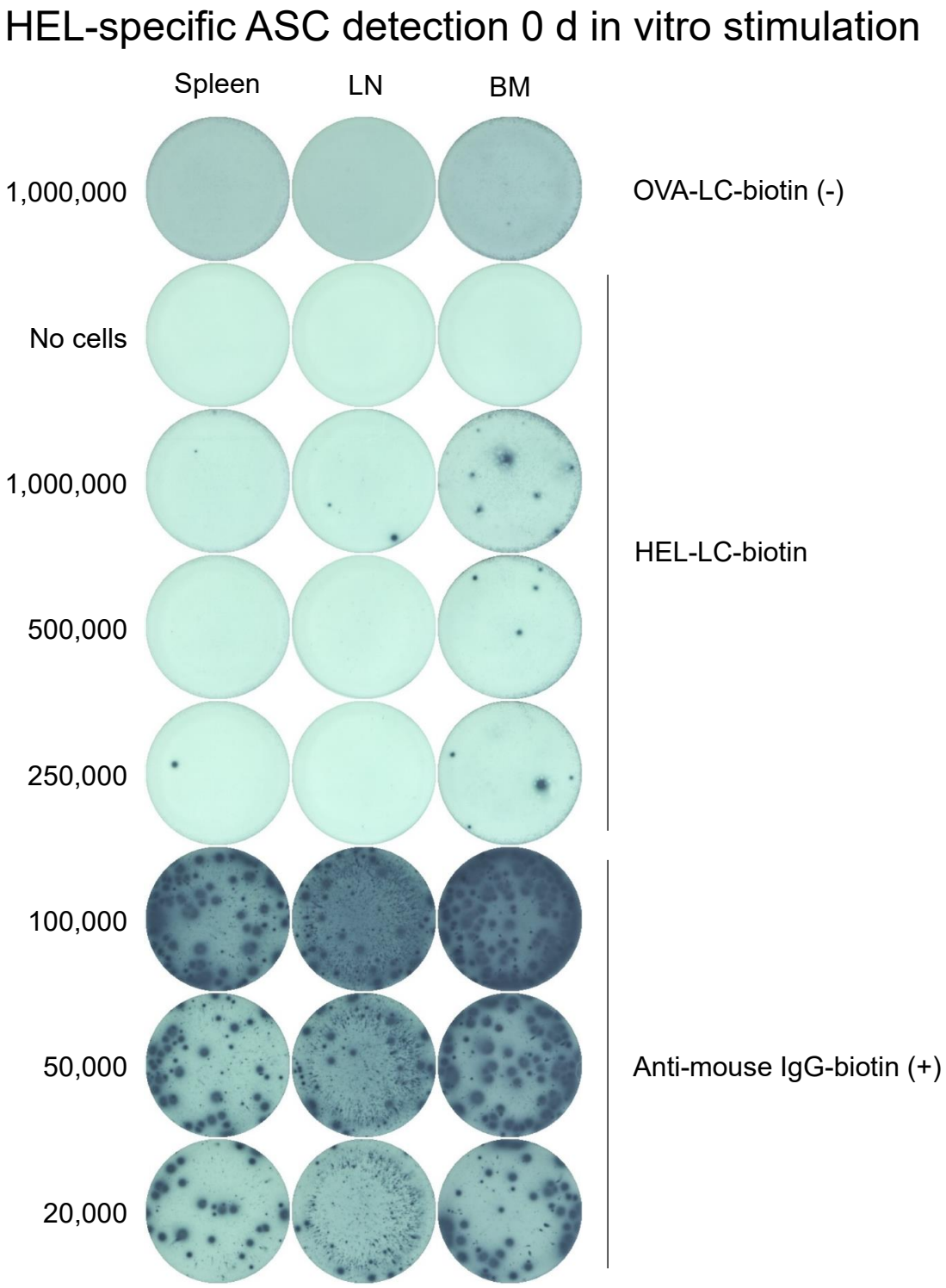


Figure 4.18: HEL-specific ASCs can be detected in bone marrow without boosting. Cells from a mouse primed with HEL CFA then boosted with HEL IFA 6 weeks prior to harvest, without additional in vitro stimulation. OVA-LC-biotin and anti-mouse IgG-biotin included as negative and positive controls respectively. Numbers are splenocytes plated per well. LN = draining lymph node cells, BM = bone marrow cells.

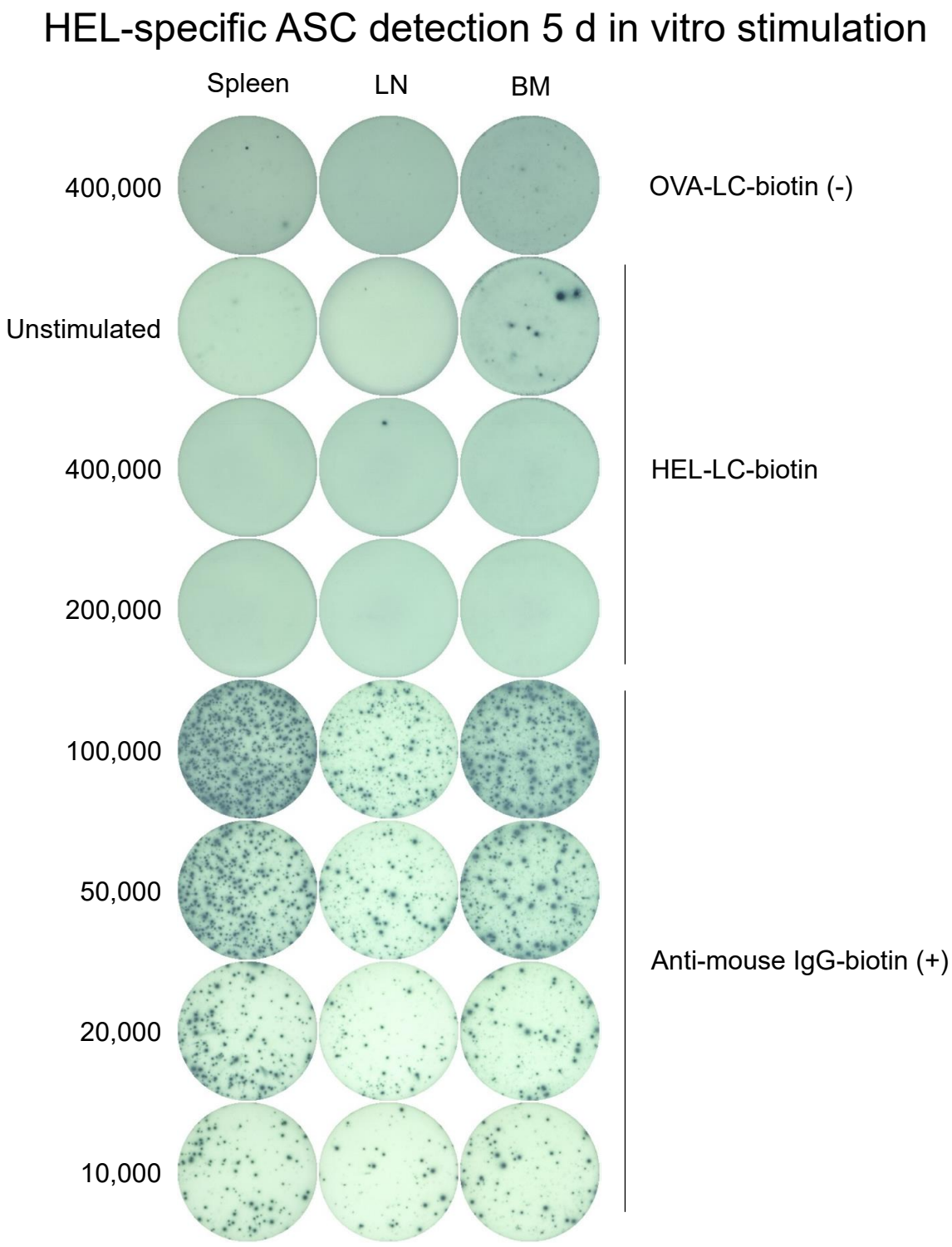
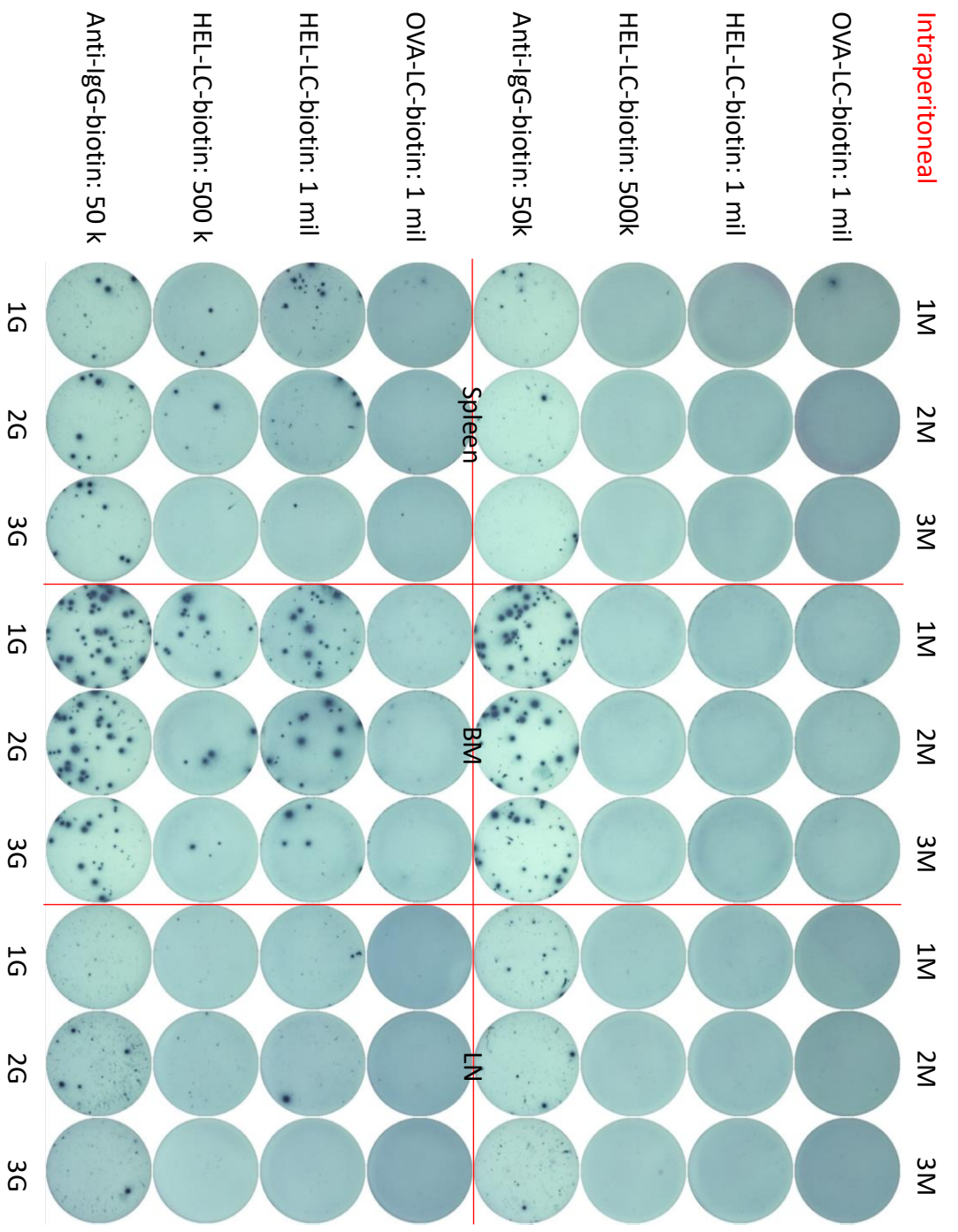


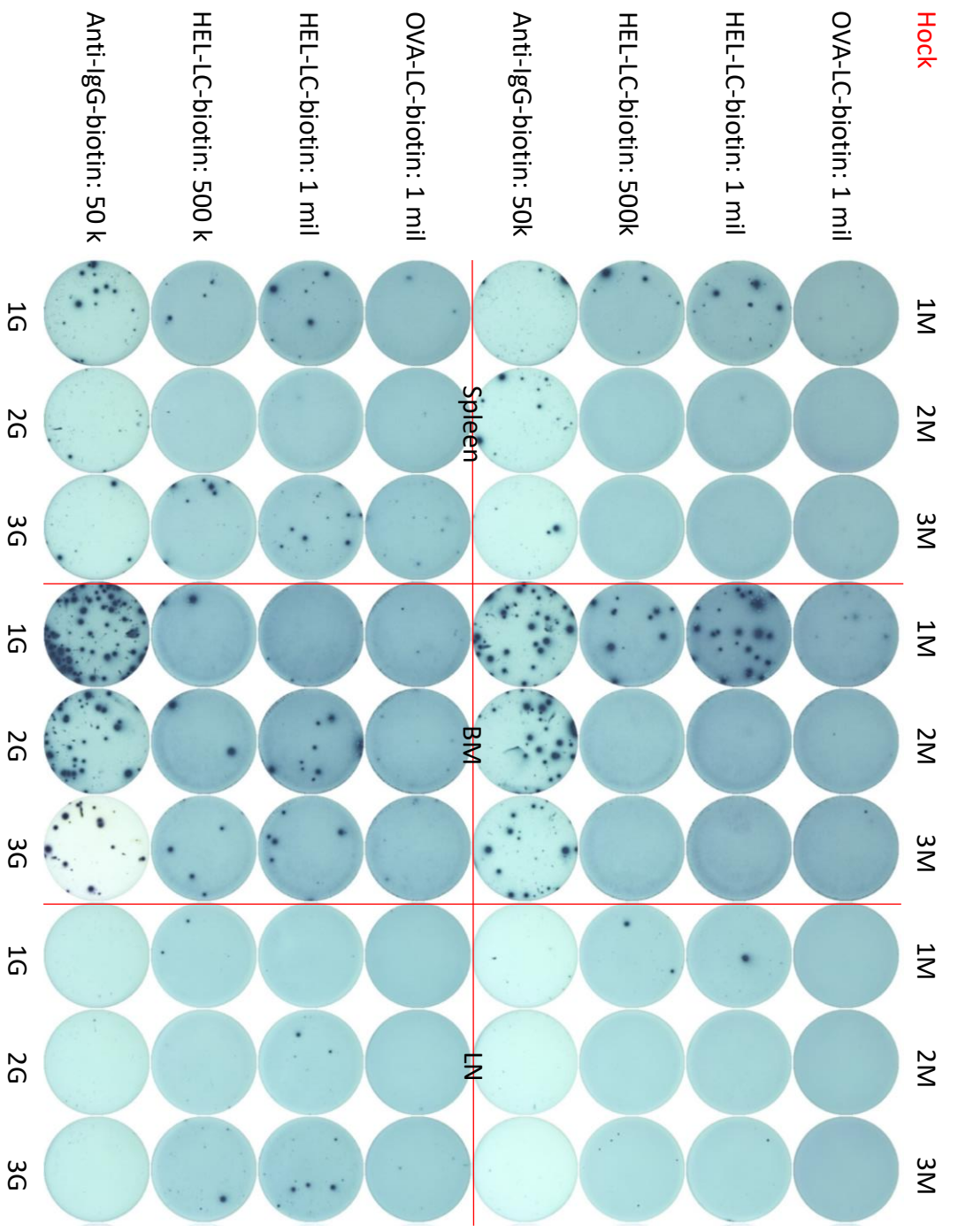
Figure 4.19: HEL-specific ASCs are less effectively stimulated in vitro. Cells from a mouse primed with HEL CFA then boosted with HEL IFA 6 weeks prior to harvest (same mouse as in Figure 4.18), after 5 d in vitro stimulation with R848 and mIL-2. Note the smaller sized spots of stimulated splenocytes and lack of HEL-specific BM cells after stimulation. OVA-LC-biotin and anti-mouse IgG-biotin included as negative and positive controls respectively. Numbers are splenocytes plated per well. LN = draining lymph node cells, BM = bone marrow cells.

A



(continued over next page)

B



(continued over next page)

C

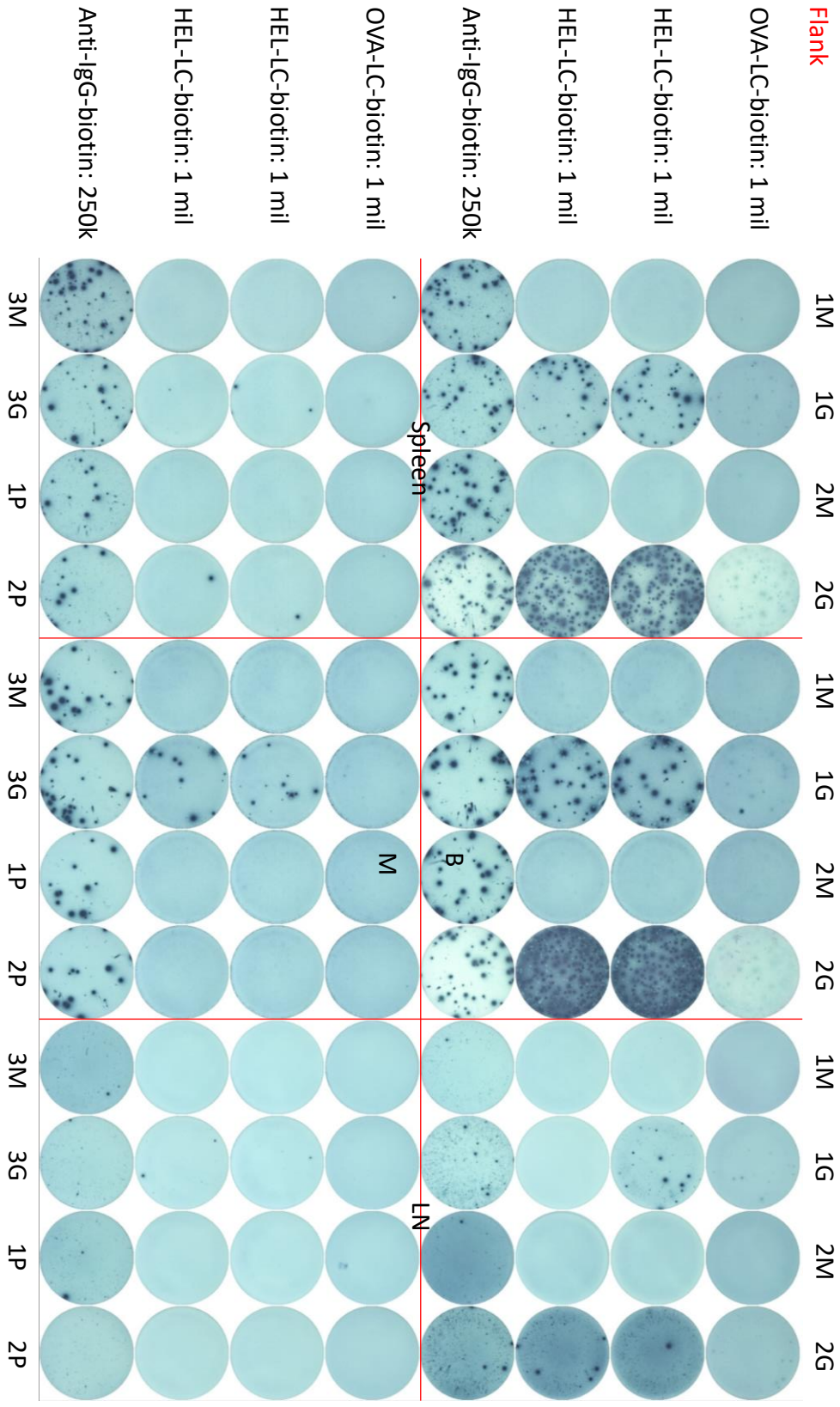


Figure 4.20: ELISpot images from immunised mice boosted 7 d prior to ELISpot. Mice immunised A) i.p., B) s.c. in the hock, C) s.c. in the flank. M = HEL mock, G = HEL GA, P = HEL PR.

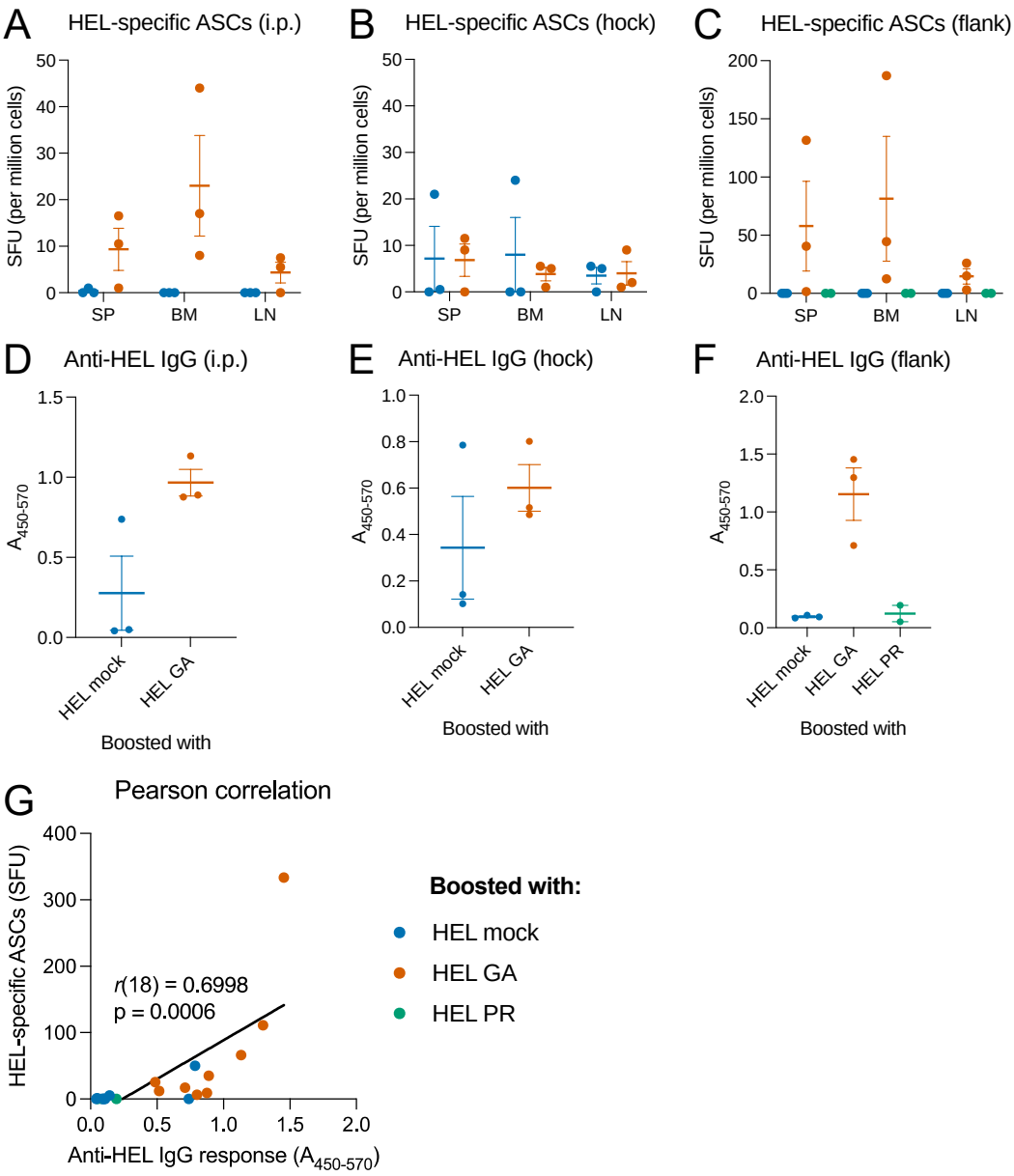


Figure 4.21: Greater numbers of HEL-specific ASCs detected in HEL GA immunised mice compared with HEL mock and HEL PR. Mice were primed with 10 µg HEL mock, HEL GA or HEL PR, then homologously boosted with 5 µg 7 d before harvesting cells. Number of HEL-specific ASCs detected after different routes of immunisation: A) intraperitoneal, B) s.c. hock, and C) s.c. flank. Data are mean ± SEM. ELISpot images in Figure 4.20. Anti-HEL IgG responses for the terminal bleed: D) intraperitoneal, E) s.c. hock, and F) s.c. flank. Data are mean ± SEM. Sera were diluted 1:50. G) Pearson correlation analysis of HEL-specific ASCs versus anti-HEL IgG responses of all mice. Each dot represents a single mouse.

HEL-specific ASCs after prime and boost immunisations were very rare, and usually at fewer than 50 spots per million cells (<0.01%) (**Figure 4.21A–C**). Even the mouse with the highest number of ASCs had no more than 200 spots per million cells (<0.02%), which would have been difficult to detect using flow cytometry without enrichment.

In a separate experiment, I could not detect any HEL-specific ASCs 10 d post-prime, except in one of three HEL CFA immunised mice (**Figure 4.22A**), even though anti-HEL IgG was already present in sera by this time in multiple mice (**Figure 4.22B**). Therefore, ELISpot without enrichment is sufficiently sensitive to detect B cell responses post-boost, but not post-prime.

4.2.10 In vitro and in vivo MD4 B cell proliferation

Since I could detect expansion of HEL-specific ASCs after HEL GA prime-boost immunisations, I investigated whether GA-aldoamine could induce or enhance B cell activation and proliferation. Because antigen-specific clones are extremely rare in a naïve wild type (WT) mouse, I used immunoglobulin (Ig) transgenic mice MD4 (on C57BL/6 background), in which over 90% of B cells express the heavy and light chains of HEL-specific IgG1 HyHEL-10 antibody (Smith-Gill et al. 1984) as functional IgM and/or IgD (Mason, Jones, and Goodnow 1992).

First, I determined whether HyHEL-10 showed different binding to HEL mock, HEL GA and HEL PR by ELISA. HEL mock, HEL GA, and HEL PR were coated on ELISA plates and incubated with HyHEL-10 antibody, which was detected using HRP-conjugated anti-mouse IgG1. Both the amount of HyHEL-10 (**Figure 4.23A**) and coated protein (**Figure 4.23B**) were titrated, and showed that HyHEL-10 binding to HEL GA and HEL PR were stronger compared with HEL mock.

Next, I determined appropriate conditions for the MD4 splenocyte proliferation assay. I titrated HEL on MD4 splenocytes to assess proliferation in response to antigen stimulation alone (**Figure 4.23C**). As expected for naïve B cells, HEL alone was insufficient to stimulate proliferation except at high concentrations of at least 800 μg/mL.

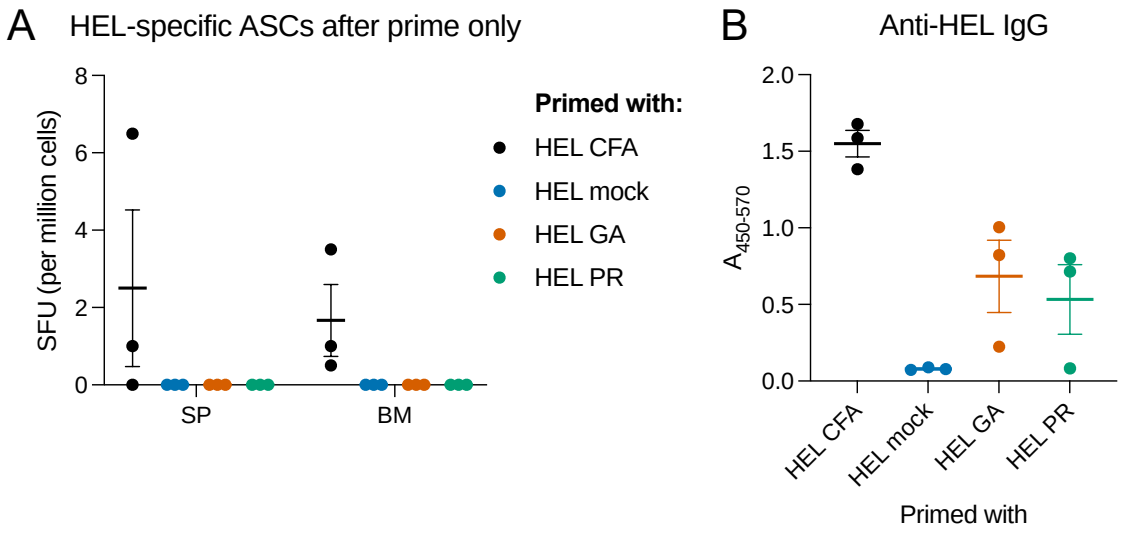


Figure 4.22: No HEL-specific ASCs detected for no-adjuvant HEL-immunised mice after prime. Mice primed with 10 μg HEL CFA, HEL mock, HEL GA, or HEL PR. A) ASCs and B) anti-HEL IgG responses measured 10 d post-prime. Mean with SEM. Sera were diluted 1:20.

The proliferation observed may not even be HEL-specific, as I observed a similar phenomenon with non-transgenic naïve BALB/c splenocytes (data not shown). HEL mock, HEL GA and HEL PR were similarly unable to stimulate naïve MD4 splenocytes (**Figure 4.23D**). In contrast, B cell activators such as LPS (a thymus-independent mitogen) and monomeric anti-CD40 (to mimic thymus-dependent co-stimulation) were each able to induce MD4 splenocyte proliferation, with even higher responses in combination with a low concentration of HEL (5 μg/mL) (**Figure 4.23E–F**). Therefore, I proceeded to use HEL co-stimulation with LPS or anti-CD40 for the MD4 splenocyte proliferation assay.

I compared the ability of HEL mock, HEL GA, and HEL PR to promote MD4 splenocyte proliferation when combined with B cell co-stimulation (**Figure 4.23G**). Preliminary results from one mouse suggested that with LPS or anti-CD40 co-stimulation, HEL mock induced the most proliferation, followed by HEL PR, then HEL GA. This result was the opposite of the trend expected if GA modification could enhance B cell proliferation in the presence of a costimulatory signal.

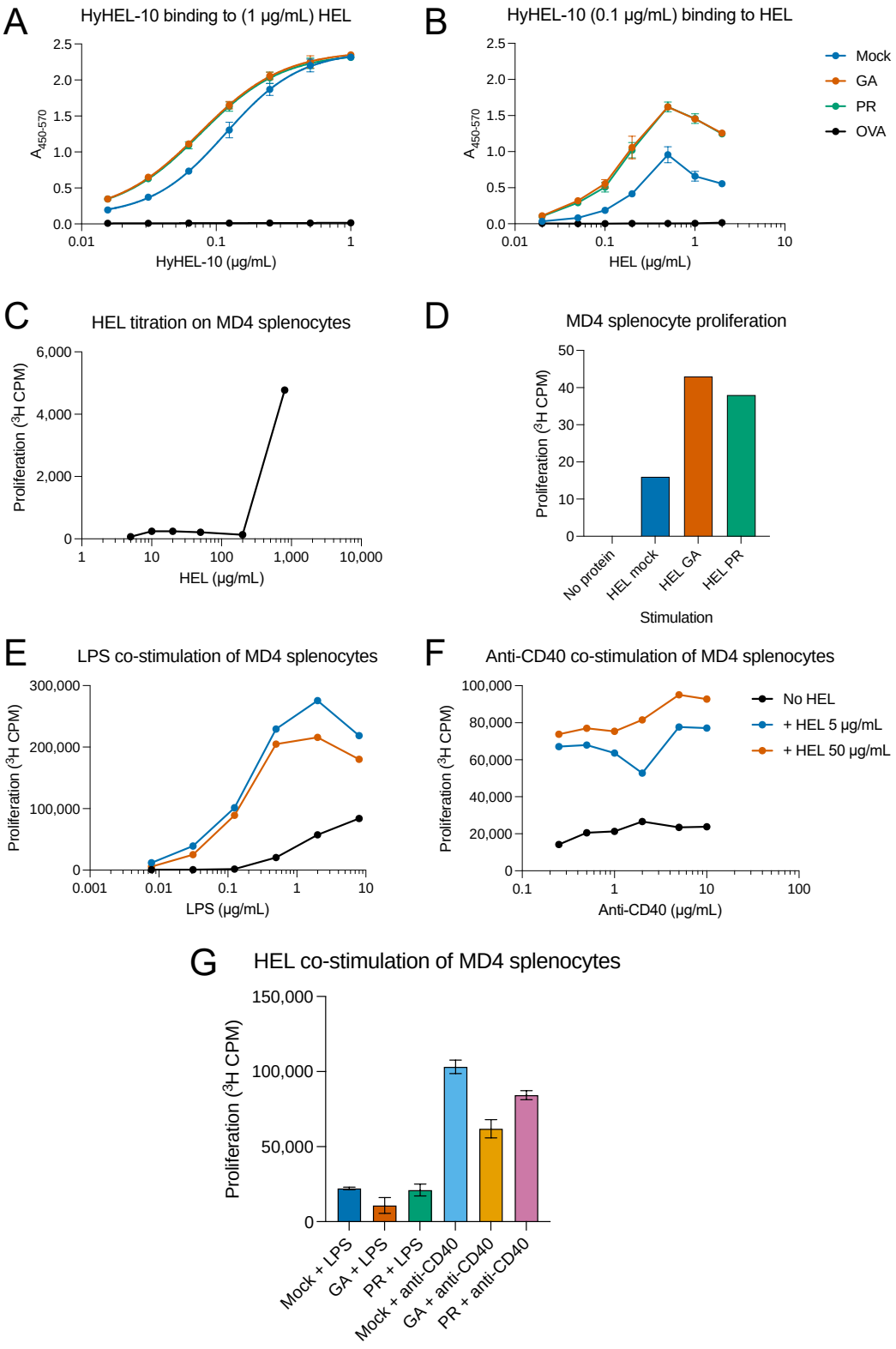


Figure 4.23: Naïve transgenic MD4 splenocytes co-stimulated in vitro with HEL mock have higher responses compared with HEL GA and HEL PR. A) and B) HyHEL-10 (HEL-specific antibody) binding to HEL mock, HEL GA, HEL PR or OVA (negative control) measured by ELISA. Data are mean ± SD of 3 technical replicates. Naïve MD4 splenocytes stimulated with C) unmodified HEL or D) 10 µg/mL modified HEL, E) LPS co-stimulation, F) anti-CD40 co-stimulation. G) Naïve MD4 splenocytes stimulated with HEL mock, HEL GA or HEL PR with LPS or anti-CD40 co-stimulation. Data are mean ± SD of 2 technical replicates. Splenocyte proliferation as measured by ^{3}H thymidine incorporation, expressed as counts per minute (CPM).

Since the in vitro MD4 splenocyte proliferation assay may not reflect B cell activation in vivo, I attempted an adoptive transfer experiment to measure B cell proliferation in vivo. I transferred carboxyfluorescein succinimidyl ester (CFSE)-stained MD4 splenocytes (containing approximately 2 million B cells) to congenic WT hosts via the intravenous (i.v.) route, immunised mice s.c. in the flank the following day, then harvested the LNs and spleen 3 d later.

I detected a small but distinct MD4 B cell population ($CD45.1^+B220^+$) in the spleen and LNs (**Figure A.8**), which was on average 0.036% of live single cells for eleven adoptively transferred mice (**Figure 4.24A**). However, this only translated to a 3.6% park rate, well below the 10-15% rate for a successful adoptive transfer (Moon et al. 2009). Of the MD4 B cells detected, there seemed to be a small amount of CFSE proliferation in all immunisation groups except for the negative control mice immunised with PBS (**Figure 4.24B–C**). However, given the small numbers of MD4 B cells and indistinct CFSE proliferation peaks, this experiment requires further optimisation.

4.3 Discussion

4.3.1 Results summary

In this chapter, the role of T and B cell adaptive immune responses in GA-mediated immunogenicity was investigated. The effect of GA modification on antigen presentation was initially studied using an in vitro model of APC presentation to $CD4^+$ T cell hybridomas. GA-treated HEL peptides increased $CD4^+$ T cell hybridoma responses, but HEL peptides were modified on N-terminal amines and could not be post-reduced. In contrast, GA-treated HEL protein modified on lysine side chains enhanced the hybridoma response to the immunodominant epitope only, but this enhancement was not reversed by HEL PR.

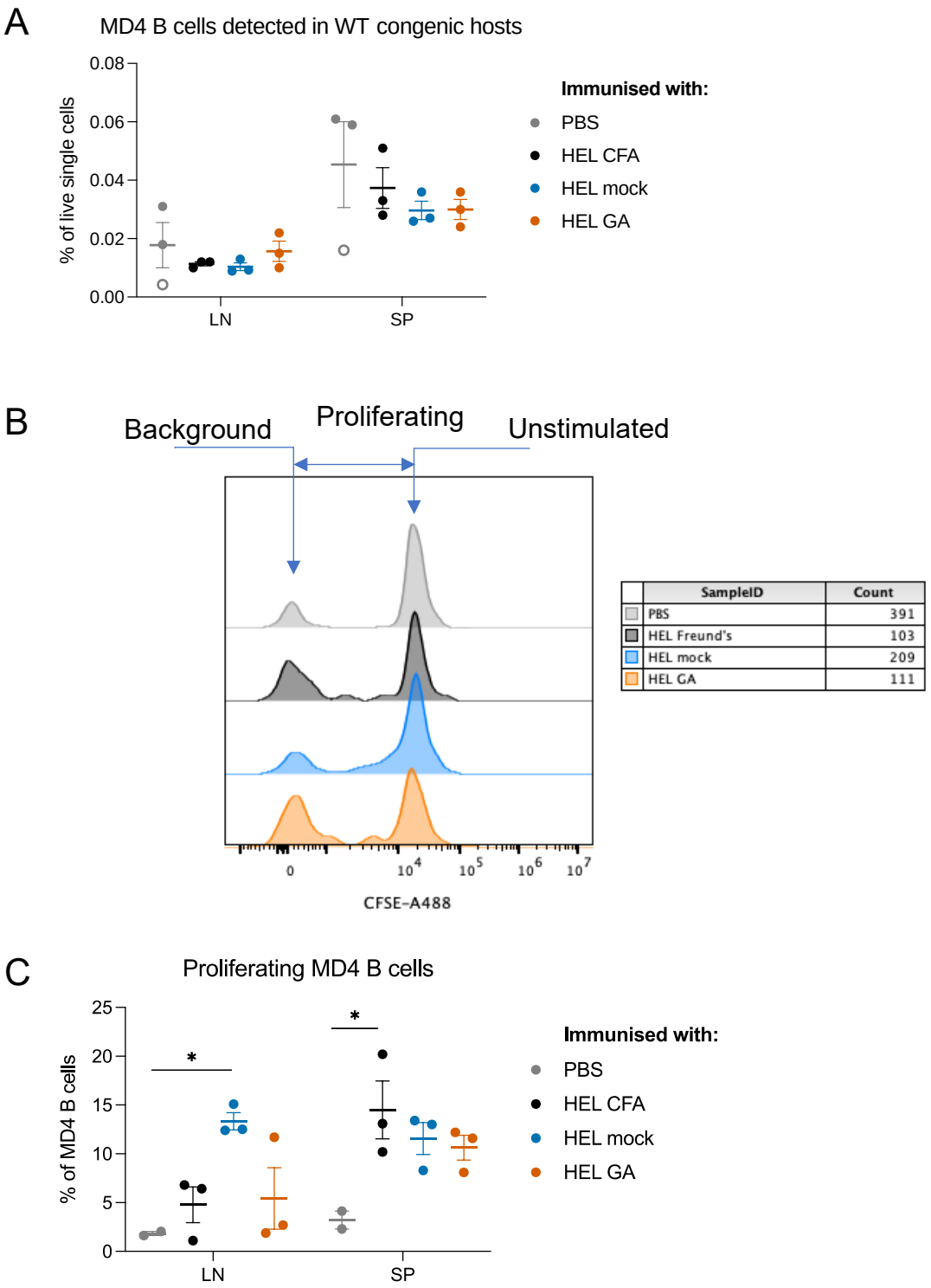


Figure 4.24: Adoptive transfer of MD4 (HEL-specific) B cells to wild type (WT) congenic hosts. 2×10^6 MD4 B cells were adoptively transferred intravenously (i.v.) into wild-type (WT) congenic C57BL/6 mice. Mice were immunised 1 d later with 10 µg HEL CFA, HEL mock, HEL GA or the equivalent volume of PBS as a negative control. Draining lymph nodes (LNs) and spleen (SP) were harvested 3 d post-immunisation and analysed by flow cytometry. A) MD4 B cells ($CD45.1^+B220^+$) detected as a percentage of live single cells. Failed adoptive transfer indicated with open circles. B) CFSE expression in MD4 B cells. Background autofluorescence and unstimulated cells determined by CFSE fluorescence minus one (FMO) control and PBS immunised mice controls respectively. The area between background autofluorescence and unstimulated was defined as proliferating cells. C) Percentage of MD4 B cells determined to be proliferating based on B). Data are mean ± SEM. The gating strategy for MD4 B cells is shown in Figure A.8.

In BALB/c mice primed and boosted with HEL mock, HEL GA or HEL PR, $CD4^+$ memory T cell recall responses stimulated by native HEL protein were weak compared with unstimulated control. $CD4^+$ memory T cell recall responses were also not elevated in mice immunised with HEL GA compared with HEL mock and HEL PR. Therefore, $CD4^+$ T cells may not drive GA-enhanced anti-HEL IgG responses. Nonetheless, antibody responses in HEL GA immunised mice are likely to be thymus-dependent because anti-HEL IgM was not elevated, anti-HEL IgG responses are evidence of class-switching, and the rapid secondary response after boosting suggested immunological memory. Moreover, BALB/c mice immunised with HEL GA had higher B cell memory recall responses compared with HEL mock and HEL PR, which was indicated by increased numbers of HEL-specific ASCs after boosting.

In vitro and in vivo assays to measure B cell activation were attempted using transgenic HEL-specific B cells from MD4 mouse spleens. However, in vitro stimulation with HEL GA alone was insufficient to trigger B cell activation, and HEL GA co-stimulation with LPS or anti-CD40 proliferated the least compared with HEL mock or HEL PR. Similarly, adoptively transferred MD4 B cells appeared to proliferate more in mice immunised with HEL mock compared with HEL GA.

4.3.2 Differences between peptide and protein GA modifications

Originally, it was assumed that GA treatment modified lysine side chains similarly on peptides and proteins, and thus HEL peptides could be used as a simplified model of HEL protein for in vitro antigen presentation. This assumption was disproved since all peptides tested were preferentially GA-modified at their N-terminus with +42 rather than on lysine side chains (**Figure 4.6**).

The difference in GA modification site was not unusual given that the extent and sites of modification are heavily determined by target sequence (Chapter 3) and three-dimensional structure. In linear peptides, the N-terminal amino group is more exposed and preferentially modified because its pK_a value (6.8–9.1) is lower than that of lysine side-chain amino groups (pK_a = 10.5) (Oregioni et al. 2017). Indeed, for chemical synthesis, many selective N-terminal modifications take advantage of the pK_a difference between amino groups on the N-terminus and lysine side chains (Chen et al. 2017).

In contrast, the N-terminus of HEL protein is less exposed and does not appear to be modified by GA (Section 3.2.4, **Figure 3.22**). Since N-terminally modified peptides are unlikely to be generated from the digestion of GA-modified protein, GA-modified peptides and proteins should be considered as distinct models. Although GA modification of peptides increased their presentation to $CD4^+$ T cell hybridomas (**Figure 4.8**), such a phenomenon may only be applicable in vivo to short peptidic molecules rather than more complex protein immunogens.

There also appeared to be differences between post-reduction of GA-modified peptides and proteins. BH derivatisation of $HEL_{11–26}$ peptides suggested that carbonylation was decreased after $NaBH_4$ treatment (**Figure 4.1B**), yet tandem LC-MS suggested that peptide GA-aldoamine was not reduced to hydroxyethyllysine (+44) (**Figure 4.4C**). Moreover, $HEL_{11–26}$ GA and $HEL_{11–26}$ PR peptide presentation were identical (**Figure 4.1C**), which was also demonstrated by other peptide-hybridoma pairs (HEL_{1-18} presentation to 2G7.1 hybridoma, data not shown). These data suggest that peptide post-reduction may not be possible.

Indeed, nuclear magnetic resonance (NMR) studies by our collaborators suggested that the +42 PTM on GA-modified peptides may be a ring-structured epoxide

rather than an aliphatic GA-aldoamine (Naorem Nihesh, University of Chicago, personal communication). Epoxides are not reduced by $NaBH_4$ alone without additional catalysts (Yakabe 2010), so it was unclear why the BH carbonyl assay suggested $HEL_{11–26}$ PR was reduced (**Figure 4.1B**). DNPH derivatisation was not used for measuring peptide carbonylation in this chapter because signals were low and inconsistent. I later discovered that the poor signals were caused by insufficient neutralisation of highly acidic DNPH derivatisation conditions (2 M hydrochloric acid, HCl), which prevented peptide adsorption onto ELISA plates. Future experiments could measure peptide carbonylation using the DNPH assay to determine whether the results are consistent with the BH assay or tandem LC-MS.

4.3.3 $CD4^+$ T cell memory recall responses in GA-immunised mice

HEL GA immunised mice had higher anti-HEL IgG antibody titres compared with HEL mock and HEL PR (**Figure 3.6**). Therefore, it was surprising that splenocyte memory recall responses in HEL GA immunised mice were a) not elevated compared with HEL mock and HEL PR immunised mice (**Figure 4.12**) and b) not significantly elevated compared with unimmunised mice (**Figure A.7B**) and unstimulated splenocyte controls.

The weak splenocyte memory recall responses in HEL GA immunised mice suggest that increased antibody responses may not be driven by $CD4^+$ T cells, which appears to contradict previous reports showing that protein carbonylation can enhance $CD4^+$ T cell activation. BMDCs pulsed with 3-deoxyglucosone (3-DG)-modified (**Figure 1.7**) OVA induced greater proliferation and cytokine responses in OVA-specific naïve $CD4^+$ T cells purified from OT-II transgenic mice (Heilmann et al. 2014). Similarly, splenocytes from TCR transgenic 2D2 mice containing MOG-specific $CD4^+$ T cells proliferated more when stimulated in vitro with MDA-modified MOG compared with unmodified MOG

(Warnecke et al. 2017). However, in those studies it was unclear whether protein carbonylation also enhanced in vivo $CD4^+$ T cell responses because adjuvants were used during immunisation.

Other studies demonstrated that aldehydated proteins could increase non-naïve $CD4^+$ T cell hybridoma responses. GA-modified HEL presented on BMDCs or peritoneal macrophages (Allison and Fearon 2000) and GA-modified OVA presented on splenic DCs (Moghaddam et al. 2011) both stimulated greater $CD4^+$ T cell hybridoma proliferation compared with unmodified protein. These results were consistent with the increased response of Ed106 to HEL GA compared with HEL mock presented on Flt3 BMDCs, although presentation of HEL PR was not decreased (**Figure 4.10E**). Enhanced responses of non-naïve $CD4^+$ T cell hybridomas may not apply to $CD4^+$ T cell priming, but could be relevant in the context of improved $CD4^+$ T cell help provided to other effector cells.

One possible interpretation for weak splenocyte memory recall responses is that HEL GA antibody responses are thymus-independent. However, this explanation is unlikely because the antibody responses have class-switched to IgG isotype, and are rapidly boosted after a second exposure (**Figure 4.14A–B**). Both class switching and rapid secondary immune responses typically require $CD4^+$ T cell help (Stavnezer 1996; Jaigirdar and MacLeod 2015). Further evidence suggesting that protein carbonyl-driven antibody responses are thymus-dependent come from experiments showing a lack of antibody responses in athymic nude mice that had been immunised with MDA-modified albumins (Wuttge, Bruzelius, and Stemme 1999).

If HEL GA-induced antibody responses are indeed thymus-dependent, then there are a number of reasons why $CD4^+$ memory T cell recall responses may be weak despite detectable antibody responses. There could be technical issues relating to the splenocyte

recall assay itself. ^{3}H thymidine is a highly sensitive technique for detecting cellular proliferation (Messele et al. 2000), but this reagent can suffer from batch-to-batch variation. In my initial experiments, proliferation was inadvertently measured using a batch of ^{3}H thymidine that yielded low counts because of partial degradation. To account for batch-to-batch variation, I expressed proliferation as fold change over unstimulated rather than subtracting background counts, which was the previous approach in the lab. Moreover, long processing times for large numbers of mice decreased cell viability and could have led to diminished splenocyte responses. Both technical issues were addressed in later experiments, yet HEL GA splenocyte recall responses remained weak.

A more likely explanation may be that the immunisation protocol used did not induce sufficiently strong CD4^{+} memory T cell responses. Other studies that have measured CD4^{+} T cell recall responses of mice immunised with carbonylated proteins typically use adjuvants, high antigen doses, repeated boosting, and often do not check for endotoxin contamination. For example, Wållberg et al. (2007) immunised DBA/1 mice with 100 μg unmodified or MDA-modified rat MOG in CFA. Lymph nodes were harvested 5 d later and incubated with bone marrow-derived macrophages (BMDMs) pulsed with 50 μg unmodified MOG. Lymphocytes from mice immunised with unmodified MOG proliferated 6-fold compared with unstimulated controls, while lymphocytes from mice immunised with MDA-modified MOG proliferated 8-fold compared with unstimulated controls, which were much stronger than proliferative responses observed in my experiments (**Figure 4.11B**).

Apart from two reports from our lab (Moghaddam et al. 2006, 2011), to my knowledge only one other study has measured ex vivo CD4^{+} T cell responses in mice immunised with aldehydated protein in the absence of adjuvant. Willis et al. (2003) immunised female BALB/c mice i.p. with 25 μg unmodified or MAA-modified HEL every

week for 5 weeks. The authors used up to 800 μg/mL HEL for ex vivo splenocyte stimulation, and differences between the immunisation groups were only apparent when stimulated with at least 100 μg/mL HEL. In contrast, I followed the protocol from Moghaddam et al. (2011) to repeat previous experiments from the lab. I immunised mice subcutaneously with only 10 μg prime and 5 μg boost, then stimulated splenocytes with only 50 μg/mL HEL. With this protocol, splenocyte proliferation were usually no more than 2-fold above unstimulated (**Figure 4.11B**).

Further evidence that the immunisation protocol could be optimised to detect adjuvant-free $CD4^+$ T cell recall responses can be seen from my experiments with ML. Mice repeatedly boosted with higher 30–45 μg doses of ML GA had higher levels of splenocyte proliferation and cytokine secretion despite ML being a self-antigen (**Figure 4.13**). It is possible that a different immunisation protocol for HEL GA might also reveal higher $CD4^+$ T cell responses. Alternatively, cytokines could be a better readout for splenocyte responses (Peters, Hamilton, and Bretscher 2005) because some memory $CD4^+$ T cells may primarily secrete cytokines rather than proliferate upon antigen recall. However, since I demonstrated that splenocyte proliferation and the secretion of certain cytokines are significantly correlated (**Figure 4.13D**), it seems unlikely to be the issue underlying low splenocyte responses.

4.3.4 Alternative hypotheses for enhanced B cell activation

HEL GA immunised mice have increased anti-HEL IgG antibody titres and more HEL-specific ASCs, suggesting enhanced B cell activation. However, how HEL GA enhances B cell activation remains unclear, since HEL GA did not induce or enhance proliferation of HEL-specific MD4 B cells compared with HEL mock and HEL PR (**Figure 4.23**).

Besides a lack of statistical power in these preliminary experiments, there may be other limitations with using the MD4 model to assess B cell activation. First, MD4 B cells already recognise HEL with high affinity, and thus may not accurately reflect immunisation in naïve mice, where the BCR repertoire is likely to have much lower affinity to novel antigens. Heterologous duck or turkey egg lysozymes, or HEL containing three point mutations (HEL3×), all have lower affinity to HyHEL-10 and may be more suitable antigens for MD4 studies. Second, MD4 B cells are derived from C57BL/6 mice, which are low responders to HEL immunisation due to poor T cell responsiveness (Jang, Mikszta, and Kim 1994). Thus, it may be difficult to stimulate adoptively transferred MD4 B cells in C57BL/6 hosts. The adoptive transfer protocol also requires further optimisation to increase donor cell parking and recovery rates.

Future experiments could investigate other potential mechanisms of B cell activation, which is controlled and modulated by many signals (Sicard, Kassardjian, and Julien 2020). For example, the antigen-BCR signal can be enhanced by its co-receptor complex containing CD21, otherwise known as complement receptor 2 (CR2), which links the innate and adaptive immune systems (Rickert 2005). B cell activation can also be enhanced by TLR engagement (Pasare and Medzhitov 2005), which provides another link between innate and adaptive immunity.

4.4 Conclusions

In summary, in vitro and in vivo models were used to investigate the role of T and B cell responses in GA-mediated immunogenicity. HEL peptides were initially used as a simplified model to test the effect of GA modification on antigen presentation. However, HEL peptides were found to be modified at a different site and perhaps with different chemistry to that of modified intact HEL protein. Nonetheless, immunisation with GA-

modified peptide $HEL_{106–120}$ may elicit increased antibody responses to native peptide compared with immunisation with unmodified $HEL_{106–120}$.

BALB/c mice primed and boosted with HEL mock, HEL GA and HEL PR had weak HEL-specific splenocyte recall responses that were not elevated in HEL GA immunised mice. However, the splenocyte recall response may be intrinsically weak due to the low dose no-adjuvant immunisation protocol rather than a lack of $CD4^+$ T cell help, which is likely to be required for the antibody response to protein aldehydes.

In contrast, BALB/c mice immunised with HEL GA had increased numbers of HEL-specific ASCs after boosting, which was indicative of higher B cell memory recall responses. Preliminary experiments with HEL-specific MD4 cells did not provide further insight into the mechanisms of enhanced B cell activation. However, B cell activation could instead be enhanced through innate immune modulation, which will be the focus of the next chapter.

Chapter 5

GA-mediated innate immunogenicity

5.1 Background

5.1.1 Pattern recognition in innate immunity

Pattern recognition is central to the induction of innate immunity. Pattern recognition receptors (PRRs) are proteins that detect and respond to pathogen-associated and damage-associated molecular patterns (PAMPs and DAMPs). There are many different types of PRRs, which can be classified by localisation, domain homology, ligand recognition, or function (Li and Wu 2021; Takeuchi and Akira 2010).

The first PRRs to be discovered and characterised were the Toll-like receptors (TLRs) (Lemaitre et al. 1996). TLRs are membrane receptors characterised by extracellular leucine-rich repeats that activate proinflammatory pathways such as nuclear factor-kappa B (NF-κB) and activator protein 1 (AP-1) (Oda and Kitano 2006). Other membrane-bound PRRs include C-type lectin receptors (CLRs), which also modulate a wide range of signalling functions and are characterised by calcium-dependent carbohydrate recognition domains (Brown, Willment, and Whitehead 2018). Cytoplasmic PRRs include NOD-like receptors (NLRs), RIG-l-like receptors (RLRs) and AIM2-like receptors

(ALRs), which recognise bacterial components, viral RNA, and double stranded DNA respectively to form proinflammatory cytoplasmic multiprotein complexes termed inflammasomes (Li and Wu 2021; Takeuchi and Akira 2010).

Scavenger receptors (SRs) are a highly diverse superfamily of PRRs that promiscuously bind multiple ligands to promote their removal or degradation and to date been divided into twelve different classes ranging from SR-A to SR-L (PrabhuDas et al. 2017). Scavenger receptor A (SR-A1 and isoform SR-A1.1), macrophage receptor with collagenous structure (MARCO, or SR-A6), CD36 (SR-B2), lectin-like oxidised low-density lipoprotein (oxLDL) receptor-1 (LOX-1, or SR-E1), the receptor for advanced glycation end-products (RAGE, or SR-J1) and other SRs have been linked to the recognition of advanced lipoxidation end-products (ALEs) (Miller et al. 2011; Binder, Papac-Milicevic, and Witztum 2016) and advanced glycation end-products (AGEs) (Toda et al. 2019).

A more expansive definition of PRRs includes soluble PRRs (sPRRs) (Smole, Kratzer, and Pickl 2020), which are localised in the extracellular space rather than within cells and also called pattern recognition molecules (PRMs). PRMs form part of innate humoral immunity and include complement proteins, natural immunoglobulin M (IgM), pentraxins (ring-shaped multimers formed from five monomers), collectins (collagen-containing C-type lectins), and ficolins (fibrinogen-like and collagen-like containing lectins) (Smole, Kratzer, and Pickl 2020).

5.1.2 Innate immune modulation by protein carbonyls

Modifications resulting from oxidative and glycative stress can be detected by the innate immune system as DAMPs (Miller et al. 2011; Binder, Papac-Milicevic, and Witztum 2016). Proteins modified by malondialdehyde (MDA) have enhanced uptake by SR-A1 (Shechter et al. 1981), CD36 and LOX-1 (Duryee et al. 2005) and bind complement

proteins such as factor H (Weismann et al. 2011) and C3a anaphylatoxin (Veneskoski et al. 2011). Proteins modified by 4-hydroxy-2-nonenal (HNE) bind to LOX-1 and stimulate nitric oxide production, enhance uptake, and increase extracellular-signal-regulated kinase 1/2 (ERK1/2) and NF-kB signalling (Kumano-Kuramochi et al. 2012). AGE interaction with RAGE upregulates the immunoproteasome to increase proteolysis of damaged proteins (Grimm et al. 2012; Johnston-Carey, Pomatto, and Davies 2016). Low-density lipoprotein (LDL) extensively modified with glycolaldehyde (GA) increases uptake in peritoneal macrophages and foam cell formation (Jinnouchi et al. 1998). Similarly, bovine serum albumin (BSA) extensively modified with aldehydes, particularly GA, increases uptake by SR-A1 in sinusoidal liver cells (Horiuchi et al. 1986) and peritoneal macrophages (Nagai et al. 2000), and downregulates leptin in adipocytes through CD36 (Unno et al. 2005).

Our lab has previously investigated the role of innate immunity in mediating GA-enhanced immunogenicity. Treatment of RAW-Blue and THP1-Blue reporter cell lines expressing TLRs, NLRs and RLRs with GA-modified proteins did not induce NF-κB or AP-1 activation (Amin Moghaddam, personal communication). Moreover, C57BL/6 (B6) mice with a gene knockout for MyD88, a critical adaptor protein downstream of the TLRs (except TLR3) (Muzio et al. 1997; Wesche et al. 1997; Medzhitov et al. 1998), generated higher anti-HEL IgG responses after immunisation with HEL GA compared with mice that were immunised with HEL mock or HEL PR (Amin Moghaddam, personal communication). This suggested that TLR signalling pathways were not essential for GA-enhanced immunogenicity. Similarly, B6 mice with gene knockouts for the scavenger receptors SR-A1, MARCO or RAGE did not have impaired anti-HEL IgG responses after HEL GA immunisation compared with wild type (WT) B6 controls (Harris 2020), suggesting that individual SRs did not mediate GA-enhanced immunogenicity.

Chikazawa et al. (2016) demonstrated that the collagen-like region of complement C1q could directly bind via electrostatic interactions to BSA modified for 7 d with various aldehydes including GA. Notably, C1q seemed to bind directly to modified BSA without antibody intermediaries and appeared to induce complement activation. Preliminary follow-up experiments in our lab revealed that HEL GA also showed increased binding to C1q and enhanced C3 opsonisation compared with HEL mock and HEL PR (Harris 2020). Thus, the remaining sections will introduce the complement cascade and its known roles in enhancing humoral immune responses.

5.1.3 Overview of the complement cascade

The complement cascade is an evolutionarily ancient part of the innate immune system and consists of many inactive precursor serum proteins and membrane-bound complement receptors (CRs) expressed on a wide variety of cells. Activation of the complement cascade initiates sequential rounds of proteolytic cleavage to form new products and complexes that aid in the elimination of pathogens and damaged self-molecules by promoting inflammation, direct lysis, and opsonisation effector functions.

The complement cascade can be initiated through three main pathways: the classical pathway, the lectin pathway, and the alternative pathway (**Figure 5.1**) (Walport 2001). The classical pathway is canonically activated when the recognition molecule C1q, contained in the C1 complex, binds to immune complexes containing IgM or IgG. C1q can also recognise a wide range of other self and non-self ligands, including C-reactive protein (CRP), pentraxin 3 (PTX3), altered-self elements, and bacterial or viral molecules (Reid 2018). The lectin pathway is activated by carbohydrate-recognising mannose-binding lectin (MBL), collectins and ficolins (Garred et al. 2016).

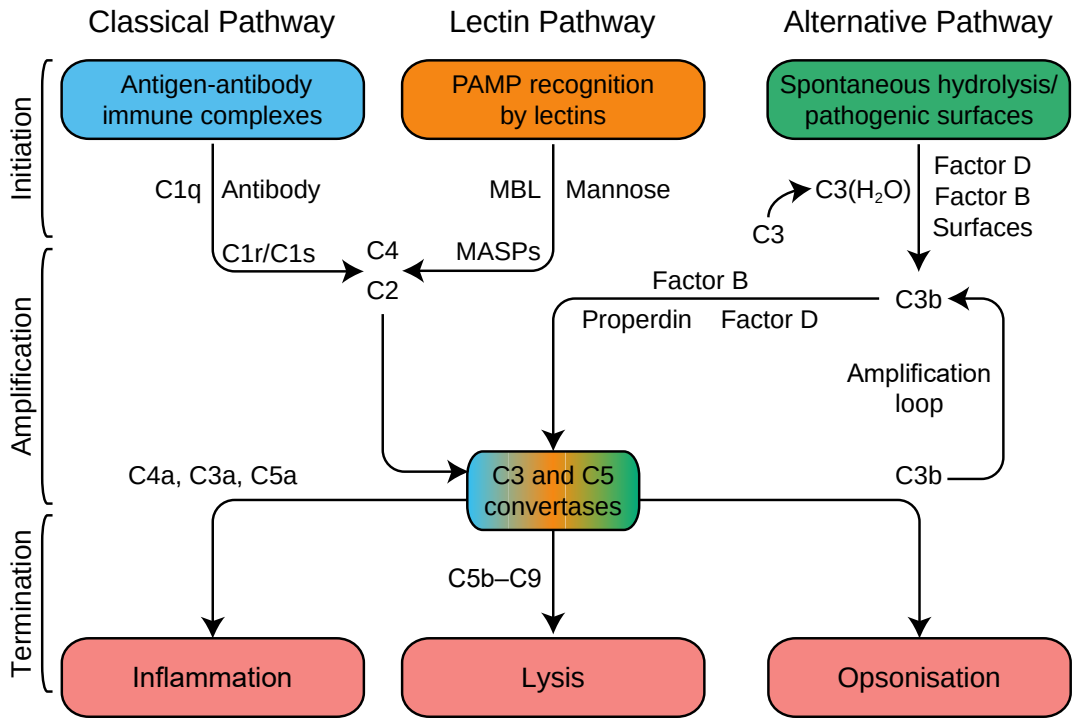


Figure 5.1: The complement cascade. The complement cascade can be initiated through three main pathways: classical, lectin, or alternative. Classical pathway activation is initiated by C1q binding, typically to antigen-antibody immune complexes. C1q binding results in a conformation change in the C1 complex that activates the C1r and C1s serine proteases. Lectin pathway activation is initiated by collectin (e.g. mannose binding lectin, MBL) or ficolin recognition of carbohydrate motifs, which then activate MBL-associated serine proteases (MASPs). Alternative pathway activation is spontaneous or promoted by certain surfaces, and serves as an amplification loop of the other two pathways. All three pathways converge on C3 and C5 cleavage, leading to the terminal effector functions of inflammation, lysis, or opsonisation. Adapted from Dunkelberger and Song (2010).

C1q or MBL binding can lead to a conformational change that autocatalytically activates serine proteases contained within their complexes: C1r and C1s in the classical pathway or MBL-associated serine proteases (MASPs) in the lectin pathway. The serine proteases subsequently cleave C2 and C4 into two fragments: a small peptide (a) and a larger protein fragment (b). An internal thioester carbonyl becomes exposed on C4b after cleavage, which allows C4b to bind covalently to the activating target surface. C4b interacts with C2b (the larger fragment of C2 cleavage) to form the C3 convertase C4bC2b (historically known as C4bC2a).

In the alternative pathway, C3 undergoes low-level spontaneous hydrolysis to C3(H_2O) in a process called “tick-over”, which is increased by native C3 interactions

with altered surfaces such as microbes and plastic (Nilsson and Nilsson Ekdahl 2012; Andersson et al. 2002). C3(H_2O) binds Factor B and is subsequently cleaved by Factor D to form the alternative pathway C3 convertases: C3(H_2O)Bb and C3bBb. Properdin (also called Factor P) stabilises the alternative pathway convertases, and has been implicated in de novo alternative pathway activation on target surfaces (Spitzer et al. 2007). The alternative pathway also serves as an amplification loop for the other two pathways, and contributes a substantial proportion of complement activation in vivo (Dunkelberger and Song 2010).

Interestingly, additional mechanisms of complement activation involving various proteases have been described. In particular, proteases in the coagulation cascade have been implicated in complement activation by functioning as convertases, including factors II (thrombin), IXa, Xa, XIa, and plasmin (Amara et al. 2010). Moreover, Factor XII (Hageman Factor) is known to activate serine proteases in the C1 complex (Ghebrehiwet et al. 1983). This overlap between the complement and coagulation cascades suggests an important link between the two systems (Holers 2014; Dunkelberger and Song 2010). Other proteases not involved in coagulation have also been shown to act as C3 convertases, such as the blood pressure aspartic protease renin (Békássy et al. 2018) and the kallikrein family of serine proteases (Irmscher et al. 2018).

Pathways of complement activation typically converge on the cleavage of central complement component C3 into C3a anaphylatoxin (a proinflammatory molecule) and C3b. In a mechanism similar to C4 cleavage to C4b, C3 cleavage to C3b transiently exposes an internal thioester carbonyl that covalently binds to nearby target surfaces (Law and Levine 1977; Gadjeva et al. 1998) and opsonises or “tags” them for the attention of the immune system. In the terminal stage of complement activation, a C3b molecule can

be added to C3 convertases (C4bC2a or C3bBb) to generate C5 convertases, which then cleave C5 to C5a anaphylatoxin and C5b.

The complement cascade can terminate in three key effector functions: inflammation, lysis, and opsonisation. First, inflammation is enhanced through the binding of anaphylatoxins C3a and C5a to their G-protein coupled receptors (GPCRs) C3aR and C5aR (CD88) respectively. Second, direct lysis occurs through the assembly of the membrane attack complex (MAC), which consists of complement components C5b through to C9. Third, surfaces can be opsonised, which targets the tagged molecules to various CRs expressed on different cells.

The complement cascade is tightly regulated at key points since errant or excessive complement activation can also damage healthy host tissues. Degradation of C4b and C3b is mediated by soluble Factor I and requires cofactor activity of any one of the following: complement receptor 1 (CR1, or CD35) (Kinoshita, Lavoie, and Nussenzweig 1985), membrane cofactor protein (MCP, or CD46) (Sim et al. 1993), C4b-binding protein (C4BP) for C4b or Factor H for C3b (Wu et al. 2009) (**Figure 5.2A**).

C4b is cleaved by Factor I to fluid phase C4c and antigen-bound C4d via an iC4b intermediate (**Figure 5.3**) (Nagasawa, Ichihara, and Stroud 1980). C3b is first cleaved by Factor I to release C3f from covalently-bound iC3b, followed by a subsequent cleavage to release C3c from bound C3dg. C3dg can be digested by non-complement proteases to release C3g, leaving behind the covalently-bound limit fragment C3d (**Figure 5.4**). The products formed from the inactivation of C3b are preferentially recognised by other complement receptors: CR2 (CD21) (Kinoshita et al. 1990), CR3 (CD11b/CD18), CR4 (CD11c/CD18), and CR of the immunoglobulin superfamily (CRIg) (**Figure 5.5**).

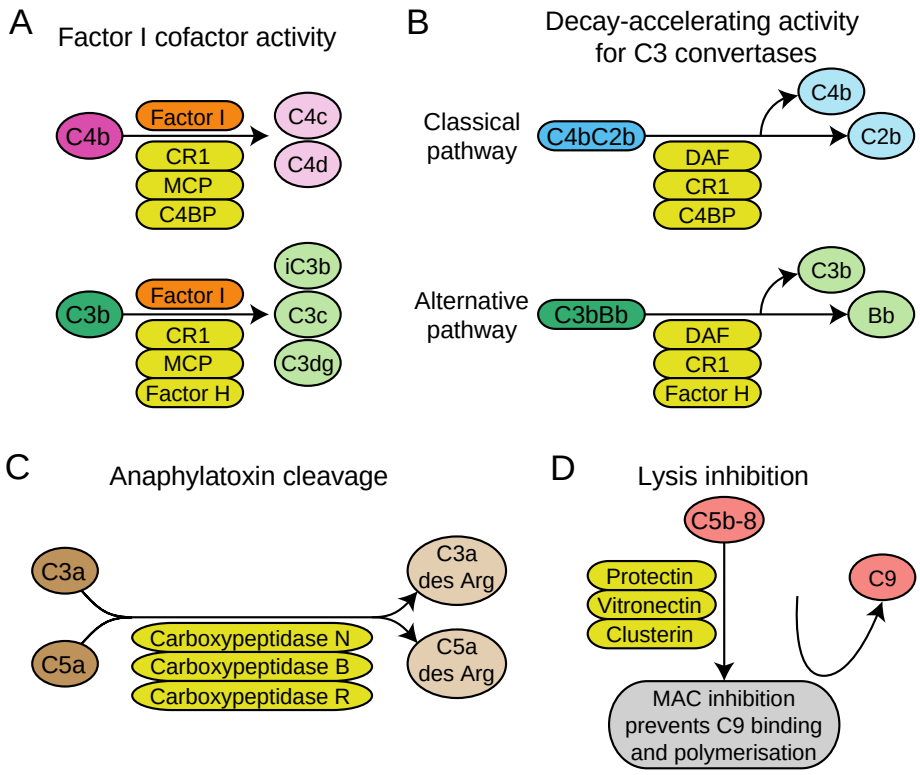


Figure 5.2: Negative regulation of complement activation. A) C4b and C3b are degraded by factor I, which requires cofactor activity of any one of the following: complement receptor 1 (CR1), membrane-cofactor protein (MCP), C4b-binding protein (C4BP) for C4b or factor H for C3b. B) Dissociation of C3 convertases C4bC2b and C3bBb are promoted by delay-accelerating factor (DAF), CR1, C4BP for C4bC2b or factor H for C3bBb. C) Anaphylatoxins are inactivated by carboxypeptidase cleavage. D) Membrane attack complex (MAC) formation is inhibited by protectin, vitronectin, or clusterin. Adapted from Dunkelberger and Song (2010).

Other regulators of complement activation can be found at all stages of the cascade. C1-inhibitor blocks cleavage of C4 and C2, while C2 receptor inhibitor trispanning (CRIT) prevents C2 cleavage. Further downstream, C3 convertase (C4bC2b and C3bBb) complex formation can be inhibited or dissociated by decay-accelerating factor (DAF, or CD55), CR1, C4BP for C4bC2b or factor H for C3bBb (**Figure 5.2B**). Sushi domain-containing protein 4 (SUSD4) is a more recently discovered protein that can also prevent C3 convertase formation (Holmquist et al. 2013). C3a and C5a anaphylatoxins are inactivated by carboxypeptidase cleavage, which prevents their binding to receptors (**Figure 5.2C**). MAC complex formation can be inhibited by protectin (CD59)

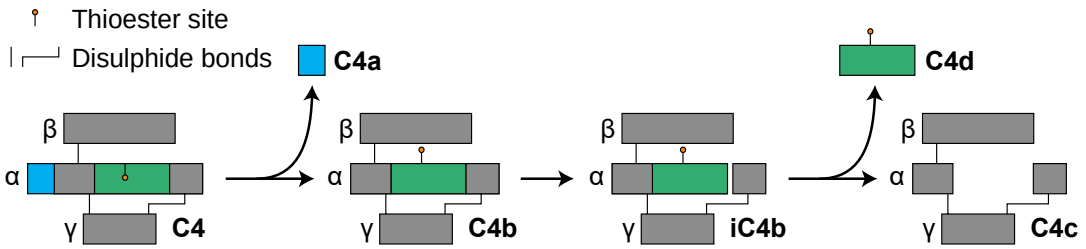


Figure 5.3: Cleavage of C4. C4 is cleaved to C4a and C4b by C1r/C1s serine proteases or MBL-associated serine proteases, which exposes a thioester site (circle) that allows covalent binding to activating surfaces. C4b is inactivated to iC4b by factor I and cofactors (Figure 5.2A) to ultimately form C4c and C4d terminal products. Adapted from Blom et al. (2015).

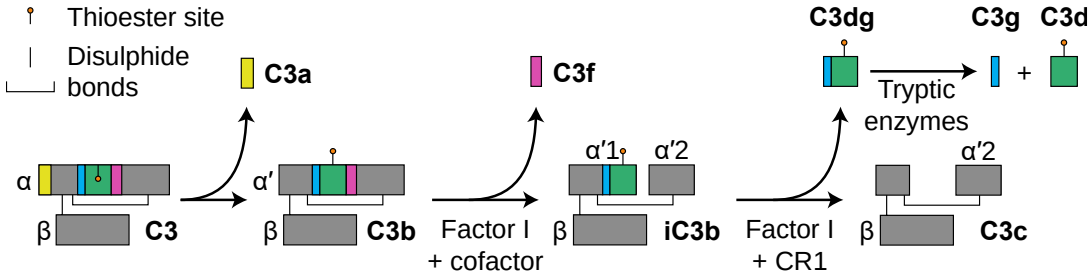


Figure 5.4: Cleavage of C3. C3 is cleaved by C3 convertases to C3a and C3b, which exposes a thioester site (circle) that allows covalent binding to activating surfaces. C3b is inactivated to iC3b by factor I and cofactors (Figure 5.2A) to remove the C3f peptide. Further inactivation by factor I and CR1 results in C3c and C3dg. C3dg can be cleaved by tryptic enzymes to C3g and C3d, which remains covalently bound to the surface. Adapted from Thurman et al. (2013).

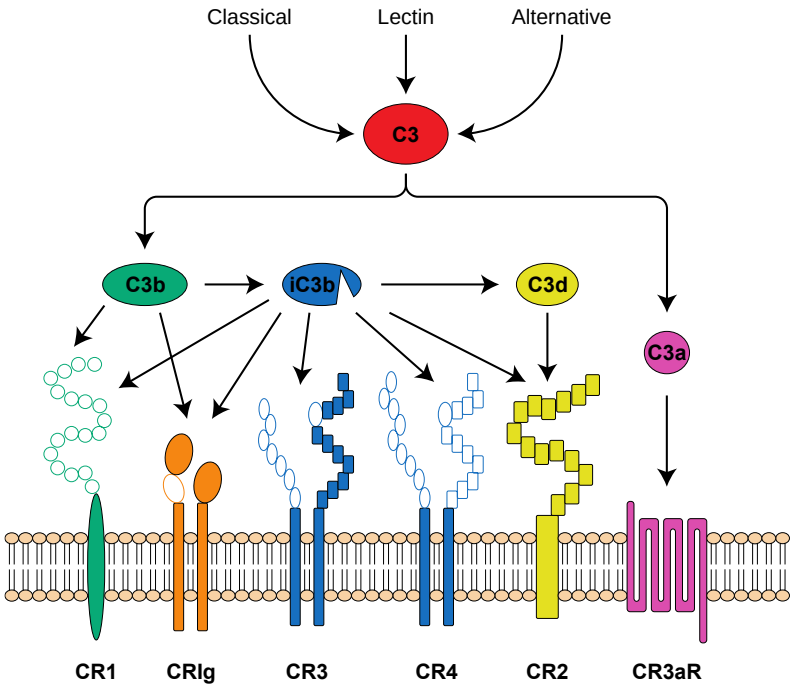


Figure 5.5: C3 activation products and their receptors. C3b is recognised by complement receptor 1 (CR1) and complement receptor of the immunoglobulin family (CRIg). After inactivation to iC3b, the ligand is recognised by CR1, CRIg, CR3, CR4 and CR2. Further cleavage to C3dg and C3d creates a ligand exclusively recognised by CR2. C3a is recognised by its receptor CR3aR. Adapted from Erdei et al. (2016).

(Meri et al. 1990), vitronectin (otherwise called protein S), or clusterin (SP-40,40) (**Figure 5.2D**). To add further complexity to complement regulation, the complement factor H-related (CFHR) protein family appear to block factor H binding and thus negate its protective effects in humans (Goicoechea De Jorge et al. 2013; Tortajada et al. 2013) and in mice (Antonioli et al. 2018).

5.1.4 Complement enhancement of antibody responses

Although the complement cascade has historically been considered to be part of the innate immune system, recent research indicates that complement also modulates adaptive immune responses, including antigen-presenting cell (APC), T cell and B cell functions (Killick et al. 2018; Merle et al. 2015). Of particular interest for this thesis is the role of complement in augmenting B cell function and antibody responses because mice immunised with HEL GA had a greater number of HEL-specific memory B cells than mice immunised with HEL mock and HEL PR (Section 4.2.9).

The interaction between C3d-containing fragments (iC3b, C3dg, and C3d) on opsonised antigen and CR2 expressed on B cells and follicular dendritic cells (FDCs) links complement activation with enhanced antibody responses (Morgan et al. 2005; Carroll and Isenman 2012). Anaphylatoxins released during complement activation can also influence B cell biology (Morgan et al. 2005; Dunkelberger and Song 2010). For example, C3a anaphylatoxin binding to MDA-modified proteins has been positively correlated with increased humoral immune responses (Veneskoski et al. 2011).

In B cells, CR2 associates with CD19 and CD81 (TAPA-1) to form the B cell co-receptor complex (Matsumoto et al. 1993). The co-receptor complex synergistically augments BCR-mediated cell signalling via CD19, which functions as an essential adaptor protein to recruit cytoplasmic signalling proteins to the membrane (Depoil et al. 2008).

Co-ligation of BCR and the co-receptor complex can decrease the B cell activation threshold by two orders of magnitude (Carter and Fearon 1992). Expression of HEL fused with up to three C3d tandem repeats (HEL-C3d) lowers the activation threshold of transgenic MD4 (HEL-specific) B cells in vitro and enhances immunogenicity in vivo (Dempsey et al. 1996). HEL-C3d also translocates the BCR and B cell co-receptor into lipid rafts for sustained signalling (Cherukuri et al. 2001).

Importantly, there are key differences in the expression and distribution of CRs between humans and mice. Human CR1 and CR2 are encoded by distinct genes (Jacobson and Weis 2008). In mice, CR1 and CR2 are alternative splice products of a single gene *Cr2* (Kurtz et al. 1990) and usually denoted as CR1/CR2 (CD35/CD21). The mouse-specific complement receptor 1-related protein y (Crry) is more similar in distribution and function to human CR1 (Y. U. Kim et al. 1995). Due to this distinction, the "molecular adjuvant" effect of CR1/CR2 originally observed in mice has recently been questioned in the human context (Kovács et al. 2021). Co-ligation of BCR and CR2 in primary human B cells using C3d molecules crosslinked to $F(ab')_2$ fragments was shown by Kovács et al. (2021) to inhibit rather than enhance CD69 expression, IL-6 secretion, proliferation, and antibody production. The authors suggested that this may be because CR2 complexed with CR1 rather than CD19, and CR1 is known to suppress human B cell activation (Fingeroth, Heath, and Ambrosino 1989; Józsi et al. 2002).

CR2 on FDCs within lymphoid tissues is crucial for the acquisition of larger (> 70 kDa) complement-opsonised antigens (Phan et al. 2007; Phan, Gray, and Cyster 2009), prolonged antigen retention and display (Mandels et al. 1980; Suzuki et al. 2009), presentation to germinal centre B cells (Suzuki et al. 2009), maintenance of memory B cells (Barrington et al. 2002), and antigen-specific IgG responses (Fang et al. 1998).

C3d-opsonised antigens acquired by CR2 on FDCs may thus enhance germinal centre formation with increased B cell affinity maturation, isotype switching, and memory B cell maintenance.

5.1.5 Measuring complement activation and opsonisation

Complement function is commonly assessed in vitro by haemolytic assays or enzyme-linked immunosorbent assays (ELISAs) (Oppermann and Würzner 2010). In haemolytic assays, the ability to activate the entire complement cascade (i.e. to the formation of the MAC) through the classical and alternative pathways is measured by the dilution of sera required for 50% lysis of antibody-coated erythrocytes. In ELISA, plates are coated with classical, lectin, and alternative pathway activators, and the formation of MAC is detected by antibodies specific to the complex (Seelen et al. 2005). Alternatively, deposition of other complement activation products can be detected by specific antibodies (Mollnes et al. 2007). The complement activation products include other complement complexes (C3bBb), relatively stable split products (C3b/iC3b/C3dg, C4d, Ba), or less stable split products (C3a, C4a, C5a, and Bb) (Section 5.1.3).

Serum is the fluid that remains after whole blood has been allowed to clot. Conversely, plasma is obtained when anticoagulants (such as EDTA, heparin and citrate) are added immediately after blood collection to prevent clotting, then centrifuged to separate the cells from plasma. For complement functional assays, serum is preferred to plasma because anticoagulants can decrease complement activity (Seelen et al. 2005; Lachmann 2010). EDTA prevents complement activation by chelating Ca^{2+} and Mg^{2+} (Mollnes, Garred, and Bergseth 1988; Troldborg et al. 2018), heparin enhances the activity of complement cascade inhibitors (Lachmann 2010), and coagulation factors cleave C3 if the factors are not inhibited by clotting (Amara et al. 2008).

Complement can be spontaneously activated in vitro (Mollnes, Garred, and Bergseth 1988; Mollnes et al. 2007; Oppermann and Würzner 2010), which has implications for functional testing. Sera should be harvested soon after venepuncture and not chilled before coagulation to prevent cold autoantibodies that can activate the classical pathway (Lachmann 2010). Sera should be aseptically collected but not sterile filtered, which could destroy complement activity (First Link UK, personal communication). Finally, sera should be stored at ultra-cold temperatures (−70 °C) until just before use (Mollnes et al. 2007; Oppermann and Würzner 2010). Variation in complement activity between samples may reflect blood processing issues or donor differences.

5.1.6 Chapter hypotheses and aims

Preliminary findings suggested that HEL GA may have increased binding to C1q and enhanced C3 opsonisation compared with HEL mock and HEL PR (Harris 2020). I hypothesised that increased C3 opsonisation of HEL GA could enhance B cell activation and antibody production. In addition, soluble factors other than complement may interact with HEL GA to drive increased T_H2 antibody responses in vivo.

In this chapter, I aimed to:

a) Confirm whether C1q has increased binding to HEL GA;
b) Verify if C3 opsonisation is increased on HEL GA;
c) Determine whether C3 opsonisation can increase B cell activation in vitro;
d) Determine if C3 is required for HEL GA anti-HEL IgG responses in vivo; and
e) Investigate whether other soluble factors have altered interactions with HEL GA.

5.2 Results

5.2.1 C1q binding to HEL GA

C1q classically binds to immune complexes containing IgM or IgG via its globular heads, although other targets bind to either the globular heads or collagen-like regions of C1q (Reid 2018). Interestingly, Chikazawa et al. (2016) reported that the human C1q (hC1q) collagen-like region could bind to AGEs directly and activate complement by the classical pathway. Preliminary work in our lab by Scarlett Harris found that biotinylated C1q (C1q-biotin) indeed bound more strongly to HEL GA compared with HEL mock and HEL PR (Harris 2020). Therefore, Scarlett and I repeated her experiments with greater statistical power using additional HEL mock, HEL GA and HEL PR samples that she had previously prepared.

We coated ELISA plates with HEL mock, HEL GA or HEL PR, as well as negative (BSA) and positive (human IgG1 monoclonal antibody) controls for C1q-biotin binding. After blocking, mouse or human C1q-biotin were titrated onto the targets and directly detected using streptavidin-horseradish peroxidase (strep-HRP). We observed significantly higher mouse and human C1q-biotin binding to HEL GA compared with binding to HEL mock and HEL PR (**Figure 5.6**).

In my own subsequent investigation, however, I observed that C1q-biotin non-specifically bound to negative control proteins. Mutation of both G236 and G237 to alanine in the fragment crystallisable (Fc) region of human IgG1 (hIgG1) almost completely abrogates binding by hC1q (Brinkhaus et al. 2020). I was gifted an angiotensin-converting enzyme 2 (ACE2)-hIgG1 fusion protein without (hIgG1-WT) and with (hIgG1-GAGA) the C1q-silent mutation (Herman Waldmann, University of Oxford). In the C1q-

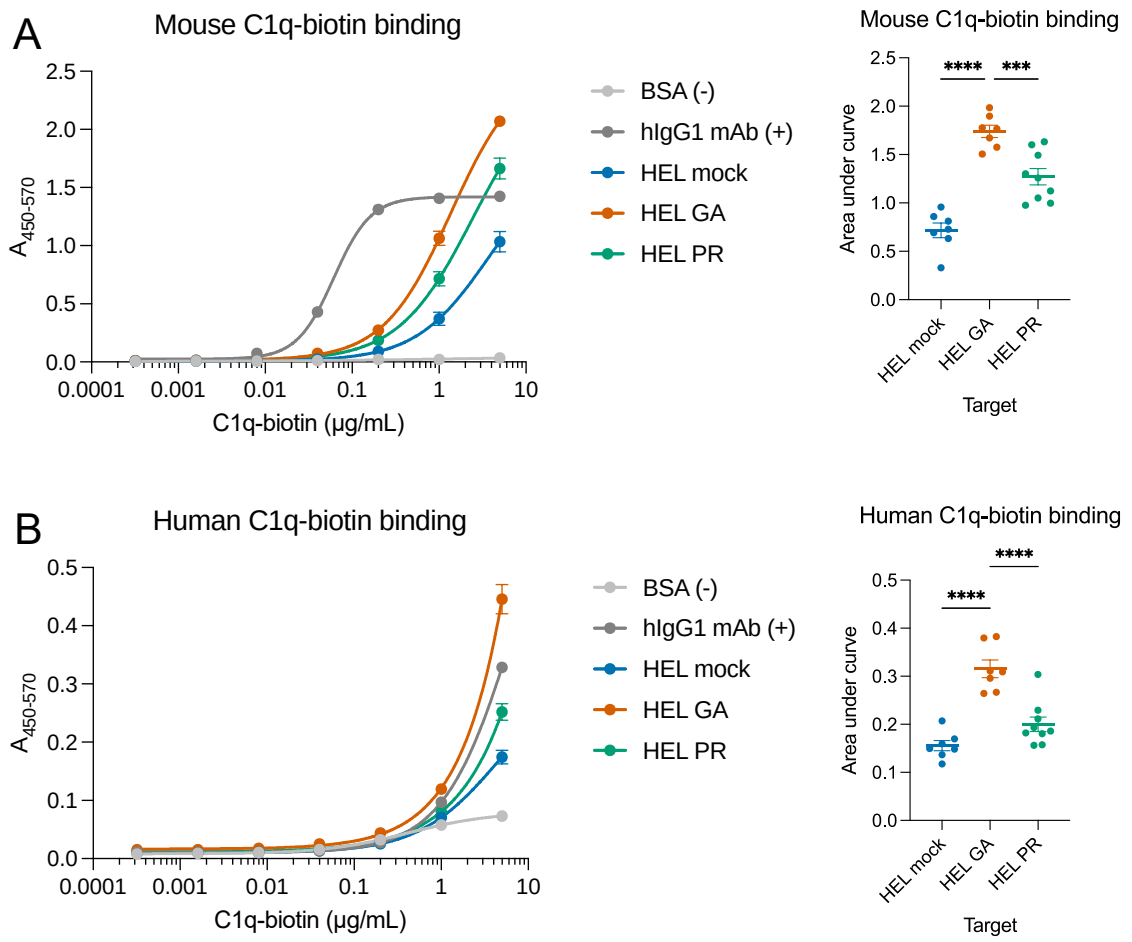


Figure 5.6: C1q-biotin binds more strongly to HEL GA compared with HEL mock and HEL PR. A) Mouse and B) human C1q-biotin binding ELISA. All data are mean ± SEM from 7–9 HEL samples (***p ≤ 0.001, ****p ≤ 0.0001; one-way ANOVA followed by Holm-Šídák's multiple comparisons test). The area under the curve was quantified for each sample and plotted as a single dot. Experiment conducted together with Scarlett Harris.

biotin binding assay (**Figure 5.7A**), hC1q-biotin bound to hIgG1-GAGA only slightly less than hIgG1-WT (**Figure 5.7B**). I also observed that hC1q-biotin seemed to bind more onto negative control BSA (**Figure 5.7B**) compared with earlier assays (**Figure 5.6B**).

Biotinylation of C1q has been reported to increase its hydrophobicity and non-specific binding to various cells (Storm, Loos, and Kaul 1996). Therefore, I re-tested the C1q binding assay using normal human sera as a source of hC1q and a commercial biotinylated anti-C1q antibody (anti-C1q-biotin) that recognised both mouse and human C1q

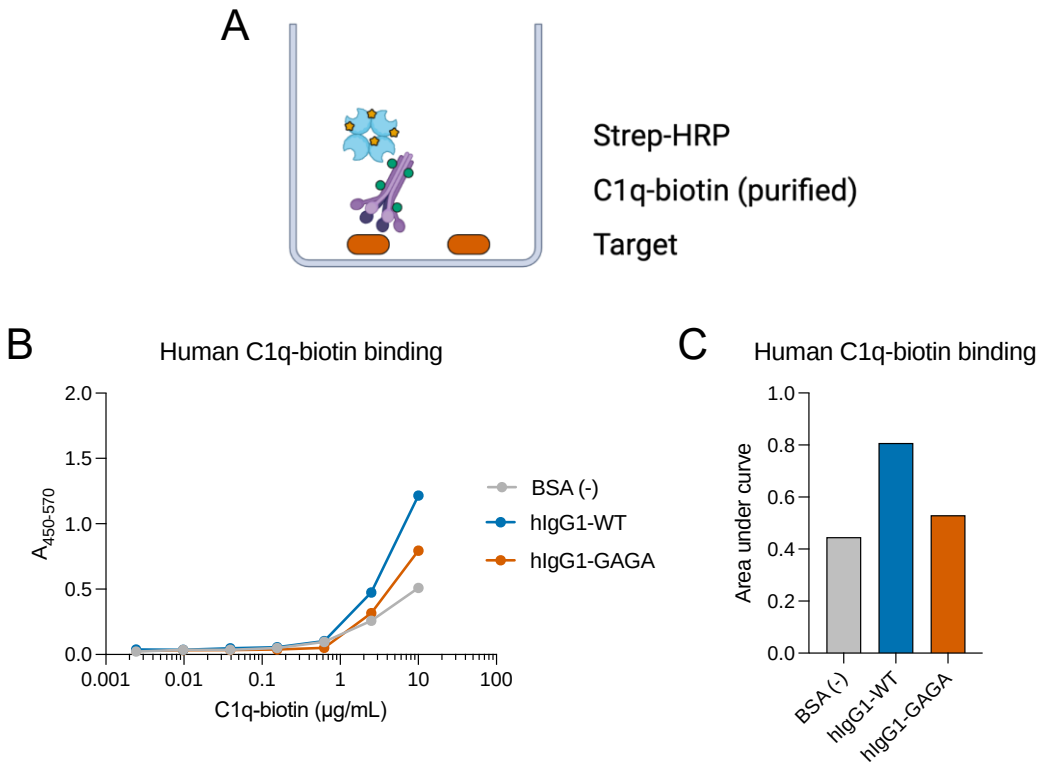


Figure 5.7: Human C1q-biotin appears to bind non-specifically to BSA and hIgG1-GAGA negative controls. Human C1q binding to the Fc region of hIgG1 is abrogated by the GAGA mutation. A) Schematic of C1q-biotin binding ELISA. ELISAs were blocked with 1% BSA in Veronal-buffered saline (VBS). B) Human C1q-biotin binding to hIgG1 constructs. C) Quantification of area under the curve. Sera diluted 1:40. Data from one experiment with single replicates.

for detection (**Figure 5.8A**). C1q from normal human sera bound selectively to hIgG1-WT and minimally to hIgG1-GAGA (**Figure 5.8B**). Heat inactivation of normal human sera completely abolished hC1q binding to hIgG1-WT. I also tested an old stock and freshly reconstituted stock of (unbiotinylated) purified hC1q. The old stock of purified hC1q bound both hIgG1-WT and IgG1-GAGA, whereas the new stock bound to only hIgG1-WT, suggesting that C1q degradation or aggregation could cause non-specific C1q binding. Interestingly, mouse C1q (mC1q) from normal mouse sera still bound to hIgG1-GAGA, suggesting that the mutation may be effective for silencing human C1q binding but not mouse C1q binding.

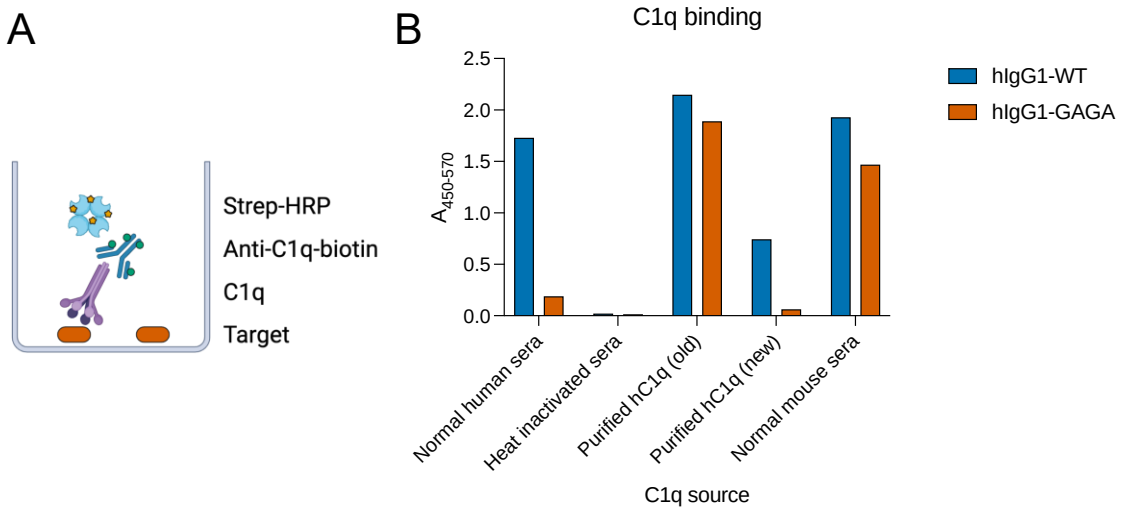


Figure 5.8: Old C1q stocks bind non-specifically to hIgG1-GAGA negative controls. A) Schematic of C1q binding ELISA with detection using anti-C1q-biotin. ELISAs were blocked with 1% BSA in VBS. B) Different sources of C1q were used to measure binding to hIgG1-WT and non-specific binding to hIgG1-GAGA. Sera diluted 1:40, purified human C1q used at 10 µg/mL. Data from one experiment with single replicates.

Next, I tested whether mouse C1q from normal mouse sera, as opposed to biotinylated purified mC1q (**Figure 5.6A**), could also bind better to HEL GA compared with HEL mock and HEL PR (**Figure 5.9A**). For negative controls, I included wells with no sera to determine non-specific anti-C1q-biotin binding to targets, and heat inactivated sera to determine whether signals were from heat-labile C1q. I coated plates with BSA as a negative control target, which bound only minimal amounts of mC1q. As a positive control target, I coated plates with BSA GA-modified for 7 d (BSA GA 7 d), which was previously shown to bind hC1q (Chikazawa et al. 2016) and in my assay showed high specific binding to mC1q (**Figure 5.9B**). Mouse IgM (mIgM) was also coated as another positive control target for mC1q binding.

Although there was high background from non-specific anti-C1q-biotin binding to mouse IgM, the signal was clearly increased in the presence of normal mouse sera and abrogated with heat inactivation, suggesting specific mC1q binding. In contrast, HEL

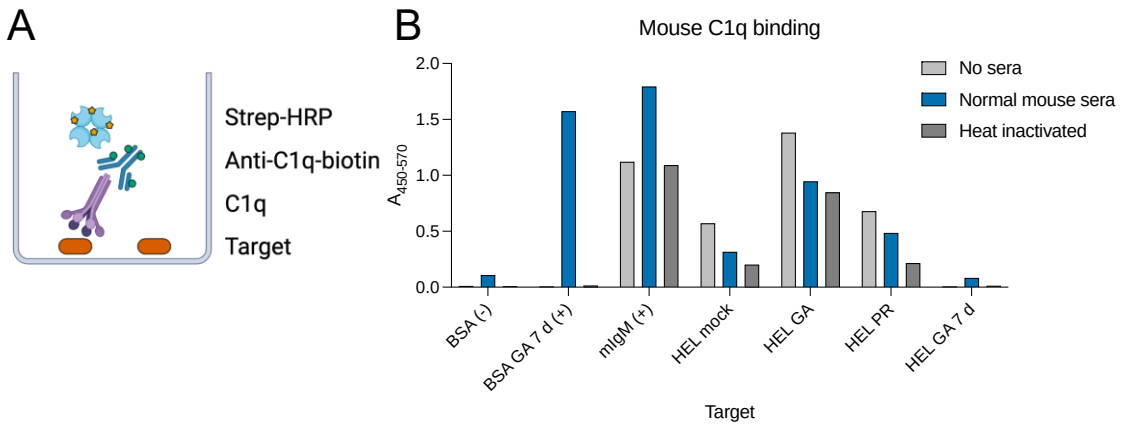


Figure 5.9: Mouse C1q binds specifically to BSA GA 7 d but does not bind to HEL. A) Schematic of C1q binding ELISA, with detection using anti-C1q-biotin. ELISAs were blocked with 1% BSA in VBS. B) Mouse C1q binding from normal mouse sera diluted 1:40. Signals from no sera control indicate non-specific anti-C1q-biotin binding, while heat inactivation should abrogate specific mouse C1q binding. Data from one experiment with single replicates.

mock, HEL GA and HEL PR all had non-specific anti-C1q-biotin binding but no increased signal upon incubation with normal mouse sera, suggesting no mC1q binding to HEL protein. Interestingly, anti-C1q-biotin appeared to bind directly to HEL GA more strongly than to HEL mock or HEL PR. HEL GA modified for 7 d (HEL GA 7 d) did not have background signal from anti-C1q-biotin or much specific mC1q binding. Further experimental repeats would be required to confirm these observations.

5.2.2 C3 activation and degradation product deposition on HEL GA

Complement activity is unstable and greatly affected by preparation conditions (Section 5.1.5). To determine whether the commercial human plasma-derived sera previously used in the lab was suitable for complement activation assays, I compared the capacity of different normal human sera sources to activate classical, lectin and alternative complement pathways. I purchased three other sources of normal human sera: off-the-clot male AB sera (Sigma), sterile-filtered off-the-clot sera, and non-filtered off-the-clot sera (both TCS Biosciences). I also prepared in-house off-the-clot sera from three donors.

Sera diluted 1:40 was added to ELISA plates coated with human IgM (hIgM) for classical pathway activation, mannan for lectin pathway activation, and zymosan for alternative pathway activation (**Figure 5.10**). Off-the-clot sera from Sigma and sterile-filtered sera from TCS performed poorly for complement activation in all three pathways. In-house sera had strong classical and lectin pathway activation, but lower levels of alternative pathway activation. TCS non-filtered sera and Sigma plasma-derived sera performed well for all three pathways, validating their use in complement activation assays.

Previous preliminary experiments in our lab found that HEL GA had increased C3 opsonisation compared with HEL mock and HEL PR (Harris 2020). Again, Scarlett Harris and I repeated her experiments with greater statistical power using a larger number of HEL mock, HEL GA and HEL PR samples that she previously prepared. We coated ELISA plates with HEL mock, HEL GA or HEL PR, as well as negative (BSA) and positive (human IgG1 monoclonal antibody or OxLDL) controls for complement activation. After blocking, mouse or commercial human plasma-derived sera containing C3 were added in Veronal buffered saline (VBS) and incubated at 37 °C for 1–2 h.

Our hypothesis was that C3d-opsonised antigens could enhance B cell activation through CR2 (Section 5.1.4) and therefore C3d deposition was measured using commercial anti-C3d antibodies. In hindsight, anti-C3d antibodies also recognise C3b and iC3b, which contain the C3d fragment that becomes exposed after C3 activation (**Figure 5.4**). Moreover, iC3b is the most likely C3 degradation product generated in our cell-free in vitro assay. Factor I and Factor H cleave C3b to iC3b, while the absence of CR1 (on cell membranes) means that iC3b is unlikely to be further degraded to C3d (**Figure 5.4**).

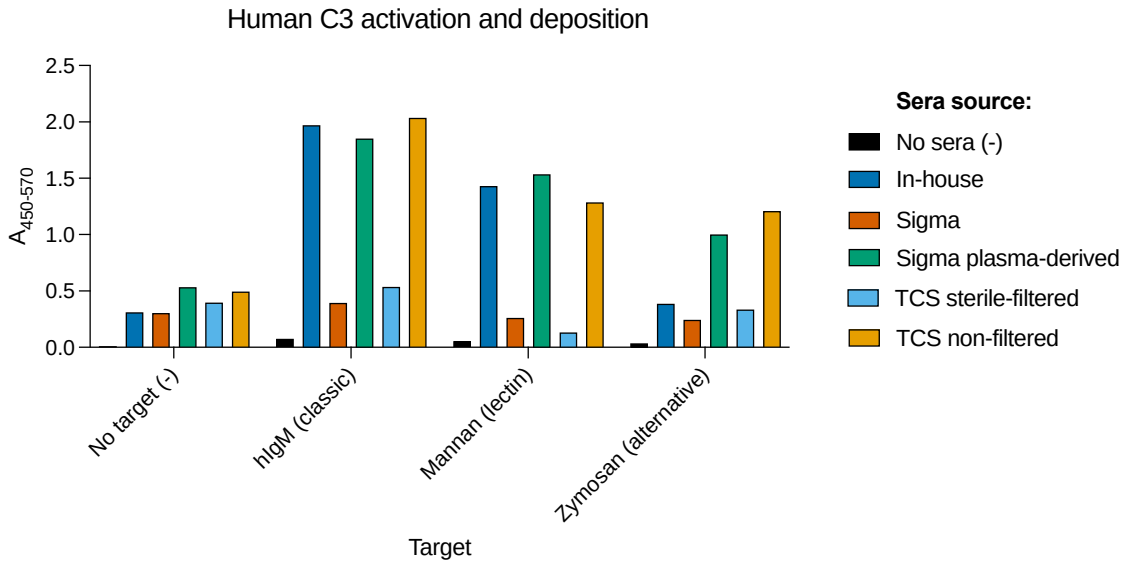


Figure 5.10: Complement activation via classical, lectin and alternative pathways differ between sources of normal human sera. Complement activation as measured by C3 degradation products detected by anti-C3d. Sera diluted 1:40. In-house sera (off-the-clot pooled from 3 donors), Sigma sera (male AB off-the-clot), Sigma plasma-derived sera (male AB plasma), TCS Biosciences sterile-filtered sera or TCS Biosciences non-filtered sera (pooled from 4 donors). All signals were abrogated by heat inactivation and EDTA (not shown). Data from one experiment with single replicates.

Nonetheless, anti-C3d antibodies can be used to measure C3 activation and opsonisation and we confirmed that there was significantly more mouse C3 degradation product deposition on HEL GA compared with HEL mock and HEL PR (**Figure 5.11A**). In contrast, human C3 degradation product deposition on HEL GA was significantly higher compared with HEL PR (**Figure 5.11B**). We observed modestly greater human C3 degradation product deposition on HEL GA compared with HEL mock that did not achieve the threshold for significance at the current statistical power.

5.2.3 In vitro MD4 B cell activation with complement from mouse sera

HEL GA appeared to increase complement activation and C3 degradation product deposition, at least in mice. I hypothesised that C3-opsonised HEL GA could bind CR2 in the B cell co-receptor complex to decrease the B cell activation threshold (Section 5.1.4).

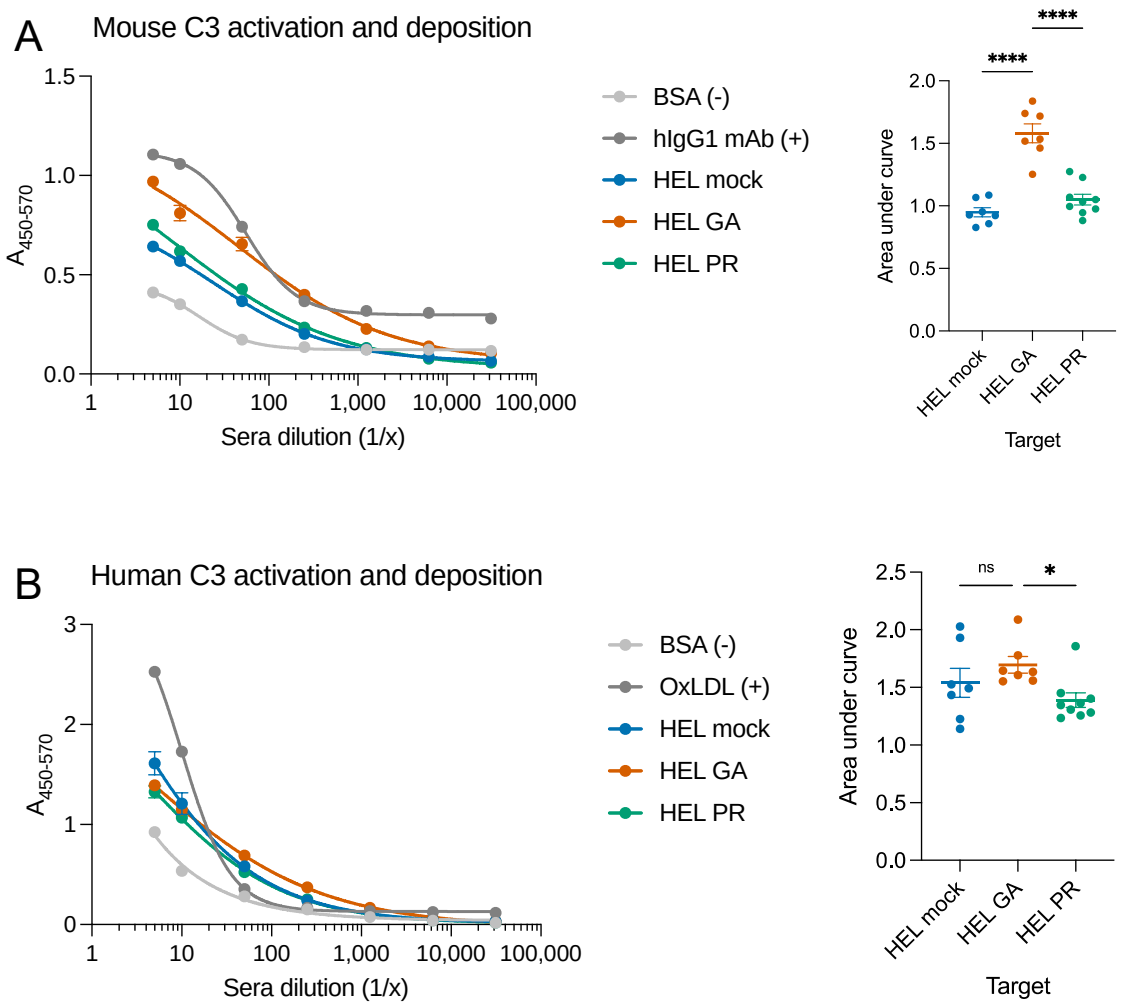


Figure 5.11: Mouse C3 activation and degradation product deposition on HEL GA is greater compared with HEL mock and HEL PR. A) Mouse and B) human C3 degradation product deposition from complement activation. Data are mean ± SEM from 7–9 HEL samples. Area under the curve was quantified for each sample and plotted as a single dot (*p ≤ 0.05, ****p ≤ 0.0001; one-way ANOVA followed by Holm-Šídák's multiple comparisons test). Experiment conducted together with Scarlett Harris.

Our lab had previously attempted to incorporate normal mouse sera as a source of complement in MD4 transgenic HEL-specific B cell assays (Harris 2020). Foetal bovine serum (FBS) used to supplement cell media was substituted with the equivalent concentration (10%) of normal mouse sera, but had anti-proliferative effects that were consistent with previous reports (Nelson and Shneider 1974; Müllbacher et al. 1985).

To overcome the anti-proliferative effects of normal mouse sera, I spiked in a lower percentage of normal mouse sera (≤ 5 %) to media supplemented with 10% heat-inactivated FBS. Naïve splenocytes were treated with anti-CD40 plus anti-IgM to

stimulate polyclonal B cell proliferation with or without normal mouse sera. The percentage of viable or activated ($CD69^+$ or $CD86^+$) B cells was measured with flow cytometry (**Figure 5.12A**). Lower concentrations of normal mouse sera (1%) did not greatly affect B cell viability or activation, while higher concentrations of normal mouse sera (5%) appeared to decrease B cell viability (**Figure 5.12B**). The effects of normal mouse sera on anti-CD40 and anti-IgM stimulated splenocyte proliferation were similar, because adding 5% normal mouse sera markedly decreased proliferation compared with 1% normal mouse sera (**Figure 5.12C**). Therefore, 1% normal mouse sera added to 10% FBS-supplemented cell media seemed to be most compatible with B cell activation and proliferation.

To eliminate any potential interference of FBS with mouse complement, I also tried replacing FBS with the chemically-defined supplement HL-1. However, naïve splenocytes cultured with HL-1 supplement proliferated in response to only B cell mitogenic stimulation (LPS, anti-CD40 plus anti-IgM) and not in response to any T cell mitogenic stimulation (PMA ionomycin, concanavalin A) (**Figure 5.13**). Since T cell proliferation was affected by HL-1, I decided to continue using FBS-supplemented media.

I then tested the effect of stimulating MD4 splenocytes with HEL mock, HEL GA or HEL PR in the presence or absence of co-stimulation and with or without 1% normal mouse sera (**Figure 5.14**). Without additional co-stimulation from anti-CD40 or LPS, normal mouse sera did not have much effect on proliferation. Surprisingly, for anti-CD40 co-stimulated splenocytes, normal mouse sera further increased proliferation to HEL proteins, while for LPS co-stimulated splenocytes, proliferation was essentially abolished.

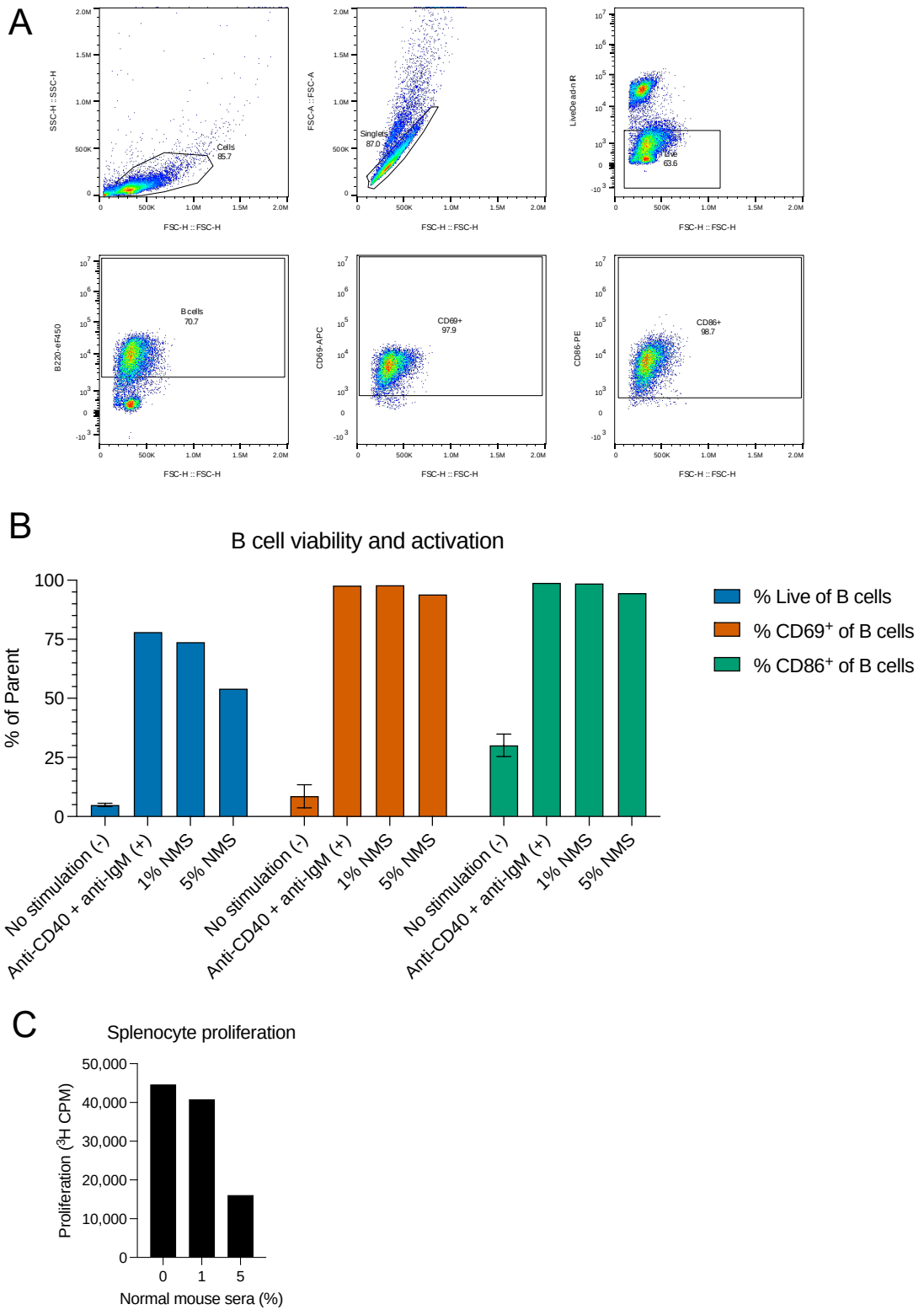


Figure 5.12: 1% normal mouse sera can be added as a source of complement for in vitro assays. Naïve splenocytes were stimulated with anti-CD40 plus anti-IgM for polyclonal B cell activation and cultured in 10% FBS-supplemented media with or without normal mouse sera. A) Flow cytometry gating to measure B cell viability and CD69/CD86 activation marker upregulation. Gates for CD69 and CD86 were set based on fluorescence minus one (FMO) controls. B) Percentage of viable and activated B cells quantified by flow cytometry. Data are mean ± SD of 3 technical replicates for no stimulation control. C) Splenocyte proliferation measured with ^{3}H thymidine incorporation.

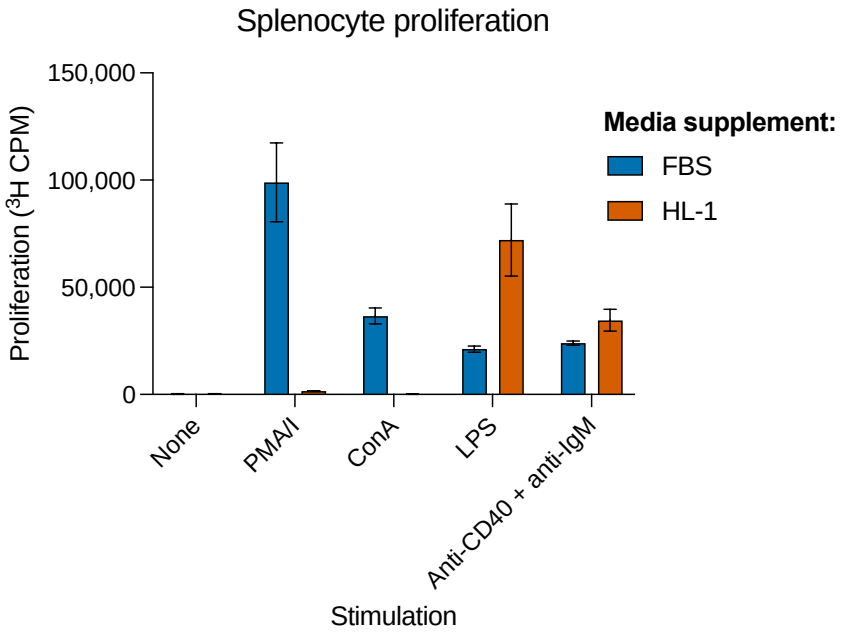


Figure 5.13: FBS cannot be substituted with HL-1 chemically-defined supplement for splenocyte proliferation assays. Splenocytes stimulated with T and B cell mitogens, with proliferation measured 3 d later. Data are mean ± SD of 2 technical replicates.

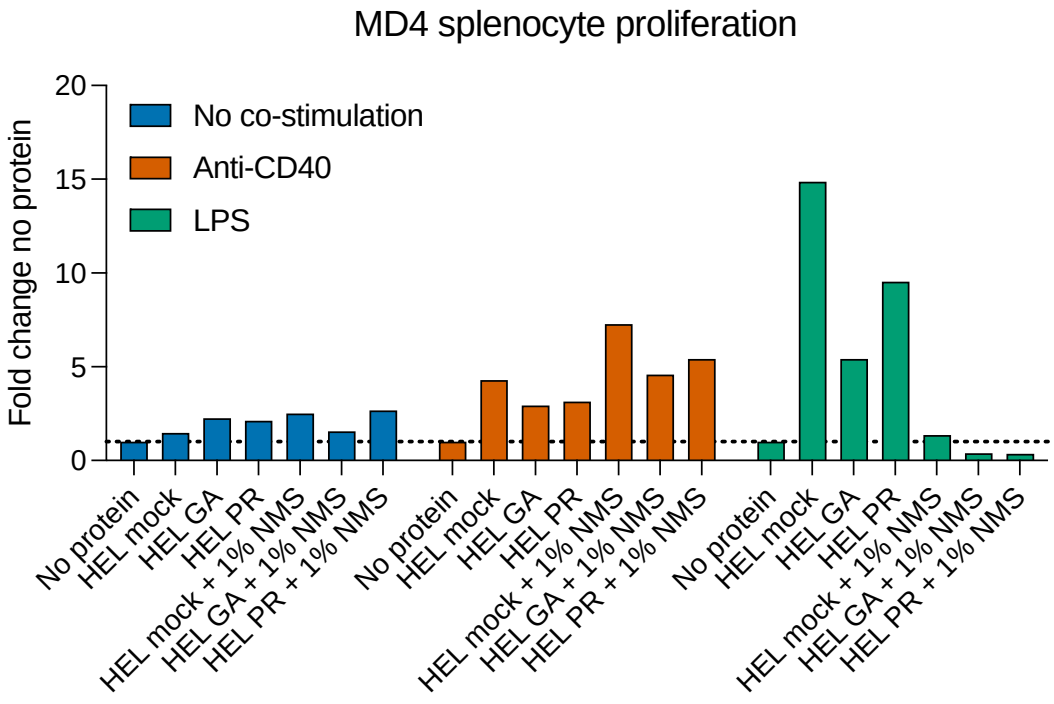


Figure 5.14: Normal mouse sera enhances anti-CD40 co-stimulation but negates LPS co-stimulation. Naïve MD4 splenocytes were stimulated with HEL mock, HEL GA or HEL PR and co-stimulated with anti-CD40 or LPS with or without 1% normal mouse sera for 3 d before measuring splenocyte proliferation. Proliferation expressed as fold change over no protein stimulation. Data from one experiment with single replicates. NMS = normal mouse sera.

MD4 splenocytes proliferated most when co-stimulated with HEL mock followed by HEL PR then HEL GA (similar to an earlier experiment in **Figure 4.23G**), and this trend was not changed by adding normal mouse sera (**Figure 5.14**). Overall, it appeared that normal mouse sera altered in vitro splenocyte proliferation depending on the type of co-stimulation, but similarly affected HEL mock, HEL GA and HEL PR responses, with more experimental repeats required to confirm the result. It was unclear if the effects on splenocyte proliferation were related to complement or to other factors in the sera.

5.2.4 IgG responses in C3-depleted mice immunised with HEL GA

In parallel with the in vitro experiments, I investigated the requirement of C3 for GA-mediated antibody production in vivo. Mice can be transiently depleted of C3 using cobra venom factor (CVF), which is a non-toxic protein structurally analogous to C3b. CVF binds factor B, which is cleaved by factor D to form a highly stable factor H-resistant C3 convertase (CVF,Bb) (Vogel and Fritzinger 2010). The CVF,Bb complex subsequently activates C3 via the alternative pathway and rapidly depletes C3 from the bloodstream within hours, and has been used for decades in research for this purpose (Vogel and Fritzinger 2010).

First, I determined whether I could deplete C3 in mice as previously reported (Pepys 1974). I injected two female BALB/c mice intraperitoneally (i.p.) with 800 mg/kg CVF (approximately 20 μg each), took bleeds every day over 7 d, and detected C3 using a commercial sandwich ELISA (**Figure 5.15A**). Before CVF administration, normal C3 levels were 987 μg/mL on average. 1 d post-CVF, C3 levels dropped to 5.7% of normal, then further to 5.1% after 2 d, before recovering to 7.0% after 3 d and 9.7% after 4 d. C3 levels then rapidly returned to normal over the next few days and on 7 d post-CVF C3

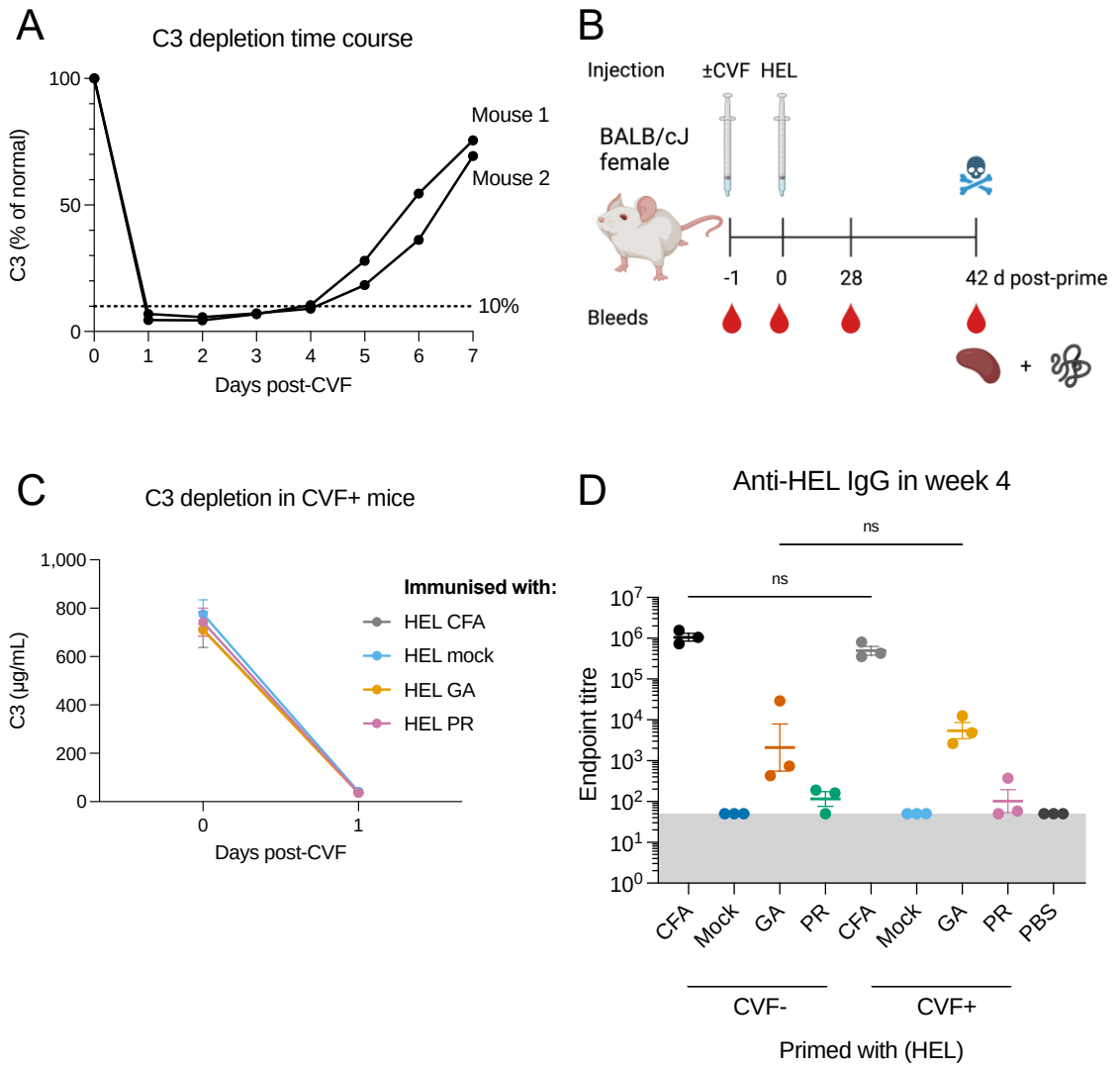


Figure 5.15: Transient depletion of complement C3 has no effect on anti-HEL IgG titres 4 weeks post-prime. A) C3 depletion time course after 800 mg/kg CVF administered i.p. in 2 female BALB/c mice. B) Bleed, immunisation and harvest schedule. C) All 12 CVF+ mice were C3-depleted on the day of HEL immunisation. C) No significant differences between CVF− and CVF+ mice for all immunisation groups. Sera were serially diluted starting at 1:50 and non-responding mice were plotted at the limit of detection (shaded in grey). Data are mean ± SEM (Kruskal-Wallis followed by Dunn's test).

levels were 72.4%. CVF can only be administered once because mice develop antibodies against CVF after a single exposure (Cochrane, Müller-Eberhard, and Aikin 1970; Pryjma and Humphrey 1975). I decided to administer CVF 1 d before priming to maximise interference with the primary immune response.

I set up a HEL immunisation experiment to compare anti-HEL IgG responses in female BALB/c mice depleted of C3 (CVF+) and non-depleted controls i.p. injected with

PBS (CVF−) (**Figure 5.15B**). After administering CVF, I verified that C3 was depleted in all CVF+ mice (**Figure 5.15C**). 1 d post-CVF, all mice were immunised subcutaneously (s.c.) with HEL mock, HEL GA, or HEL PR. Since C3 is important for antibody responses (Section 5.1.4), I also immunised mice with HEL emulsified in Complete Freund's Adjuvant (HEL CFA) as positive controls to test whether C3-depleted mice could produce anti-HEL responses. When I measured antibody responses 4 weeks post-prime, anti-HEL IgG titres in CVF− mice were highest in HEL CFA, variable for HEL GA, low for HEL PR and not detected in HEL mock immunised mice (**Figure 5.15D**). Surprisingly, anti-HEL IgG responses in CVF+ mice were very similar to CVF− mice, with no evidence of impaired antibody production.

I repeated the experiment and took additional bleeds at earlier time points (8, 10, 14 and 21 d post-prime) because Pepys (1974) showed that differences for ovalbumin (OVA) alum immunisation were greatest 8 d post-prime. I verified that C3 was depleted in CVF+ and not CVF− mice 1 d post-CVF (**Figure 5.16A**). I also measured C3 9 d post-CVF, and generally found no differences between CVF− and CVF+ mice, suggesting that depleted C3 had returned to normal by this time point. Interestingly, CVF− HEL CFA mice had significantly increased C3 levels compared with all other groups, suggesting that CFA immunisation could elevate C3 production. In contrast, C3 did not change between 1–9 d in CVF− mice immunised with non-adjuvanted HEL mock, HEL GA or HEL PR, suggesting that anti-HEL IgG responses in CVF− mice were not linked to C3.

Anti-HEL IgG responses 8 d post-prime appeared to be impaired in CVF+ HEL CFA mice compared with CVF− HEL CFA mice (**Figure 5.16B–C**, black compared with grey). The difference in antibody response between the two groups narrowed over time

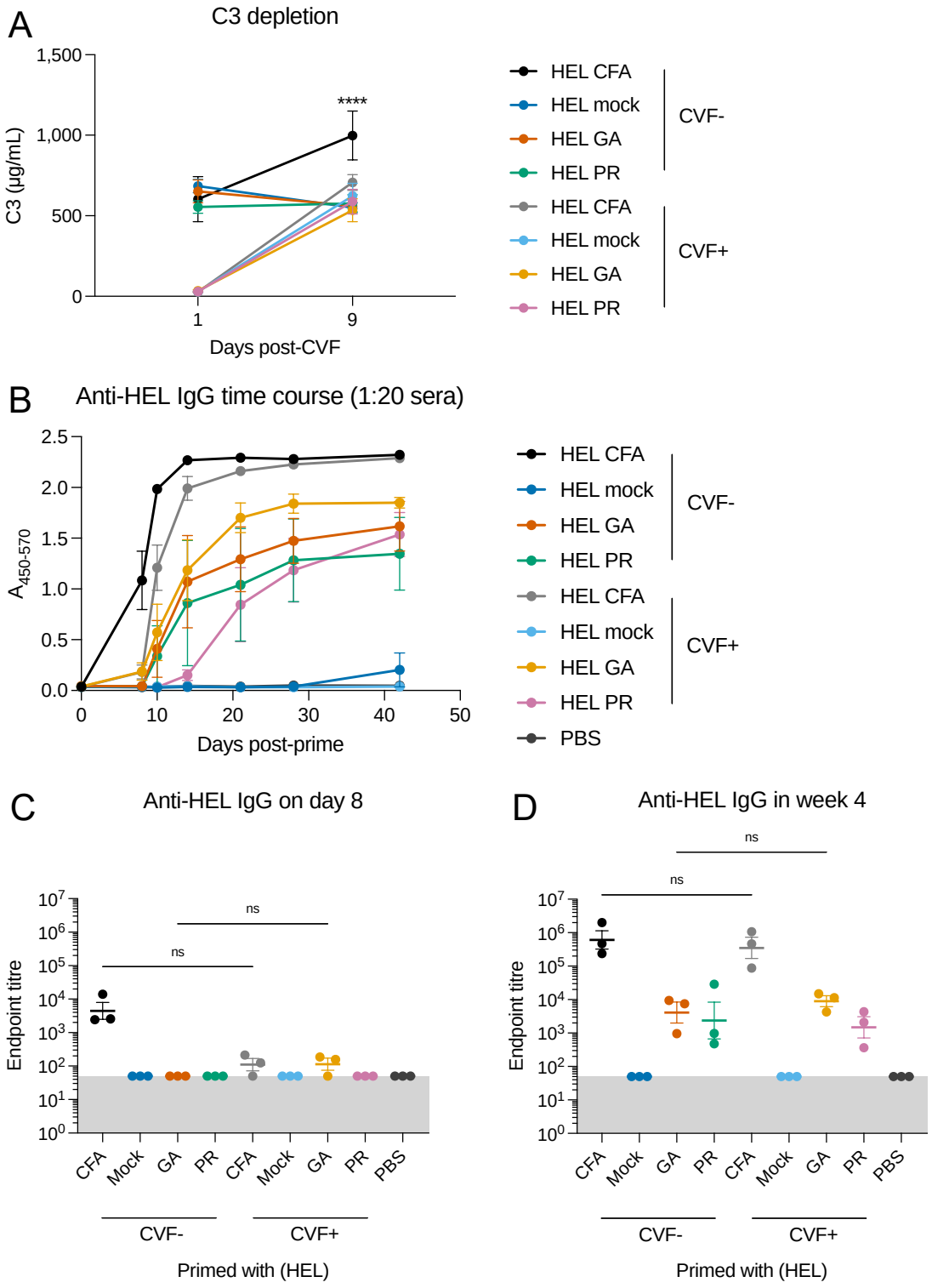


Figure 5.16: Transient depletion of complement C3 has early effects on anti-HEL IgG responses. A) C3 levels 1 d and 9 d post-CVF. C3 levels 9 d post-CVF were compared (****$p \leq 0.0001$; unpaired t test. B) Anti-HEL IgG responses measured over time. Sera diluted 1:20. Anti-HEL IgG titres C) 8 d post-prime and D) 4 weeks post-prime. Sera were serially diluted starting at 1:50 and non-responding mice were plotted at the limit of detection (shaded in grey). Data are mean ± SEM of 3 mice per group (Kruskal-Wallis followed by Dunn's test).

(**Figure 5.16B**) and no differences remained by week 4 (**Figure 5.16D**). In contrast, CVF+ HEL GA mice showed enhanced rather than impaired anti-HEL IgG titres compared with CVF− HEL GA mice 8 d post-prime (**Figure 5.16C**, orange compared with yellow). Further repeats of this experiment to obtain 8 mice per group would be required to detect the effect size observed with 80% power (calculated using G*Power).

In CVF− HEL GA mice, antibody responses were only detected 10 d post-prime, and remained slightly lower compared with CVF+ HEL GA mice throughout the experiment (**Figure 5.16B**). However, pooling anti-HEL IgG titres 4 weeks post-prime (**Figure 5.17A**) and terminal splenocyte recall responses 6 weeks post-prime (**Figure 5.17B**) from both CVF experiments confirmed that there were no significant differences between CVF− and CVF+ mice at later time points. Taken together, these results suggest that C3 may have a regulatory or suppressive rather than an immunogenic function in relation to GA-modified protein.

5.2.5 IgG responses in C3 knockout mice immunised with HEL GA

The CVF experiments performed in BALB/c mice were limited by C3 depletion for only a few days. Since anti-HEL IgG responses appeared to develop over a longer period than the first few days post-prime, I obtained C3 knockout ($C3^{-/-}$) mice to test the requirement of C3 for in vivo HEL GA immunogenicity. As with most transgenic and knockout mice, the strain was generated on a C57BL/6 (B6) background.

First, I determined whether anti-HEL IgG responses could be elicited in WT B6 mice, because our lab previously experienced difficulties generating antibody responses in the B6 strain. I immunised mice with 100 μg HEL mock, HEL GA or HEL PR (**Figure 5.18A**). In addition, I immunised control groups with either PBS or HEL CFA. 4 weeks

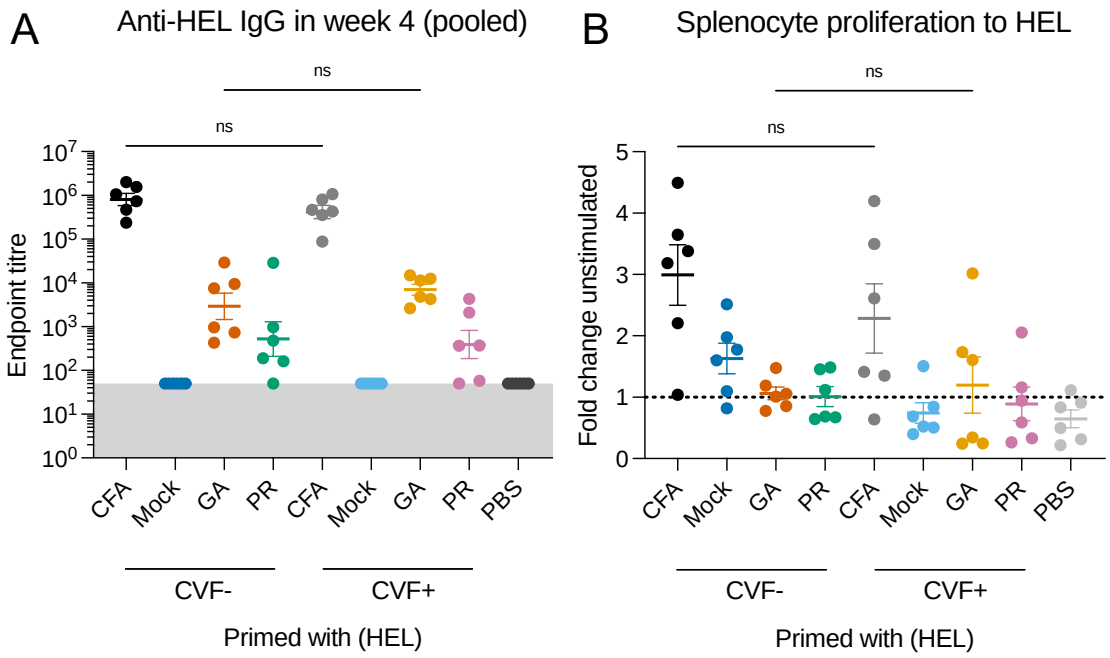


Figure 5.17: Transient depletion of complement C3 has no effect on later anti-HEL IgG titres or splenocyte responses. A) Anti-HEL IgG titres. Sera were serially diluted starting at 1:50 and non-responding mice were plotted at the limit of detection (shaded in grey). B) Splenocyte proliferation to HEL stimulation pooled from 2 independent experiments. Data are mean ± SEM of 6 mice per group (Kruskal-Wallis followed by Dunn's test for anti-HEL IgG titres; one-way ANOVA followed by Holm-Šídák's test for splenocyte proliferation).

after priming, only HEL CFA immunised mice developed anti-HEL IgG responses (**Figure 5.18B**). After homologous boosting with 50 µg, or boosting with HEL emulsified in Incomplete Freund's Adjuvant (HEL IFA) for positive control mice, anti-HEL IgG responses developed in all groups (**Figure 5.18C**). To avoid saturating responses in HEL mock and HEL PR groups, I decided to use 100 µg prime and 10 µg boosts for subsequent B6 experiments.

After the experiment in WT B6 mice, female $C3^{-/-}$ mice were functionally tested for complement activity and gifted by our collaborators Paul Morgan and Wioleta Zelek (University of Cardiff). I ordered a commercial strain of WT B6 mice as controls. The mice were primed with 100 µg HEL mock, HEL GA, HEL PR or HEL CFA/IFA and

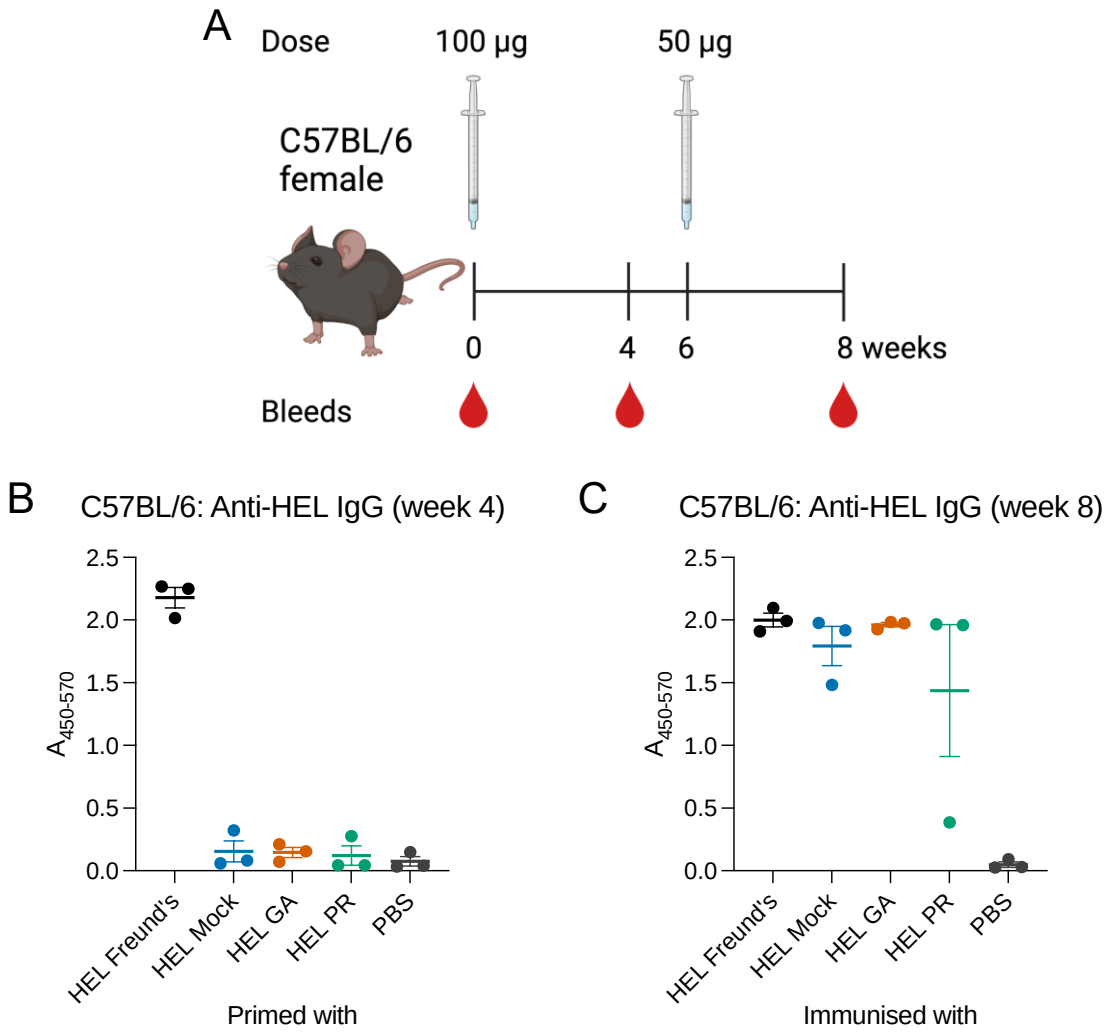


Figure 5.18: C57BL/6 mice can develop anti-HEL IgG responses from no-adjuvant HEL immunisations with high doses and boosting. A) Bleed and immunisation schedule. B) Anti-HEL IgG responses B) post-prime and C) post-boost. Sera diluted 1:20.

homologously boosted with 10 µg after four weeks, with antibody responses monitored weekly (**Figure 5.19**).

Positive control mice immunised with HEL CFA generally elicited maximum anti-HEL IgG and IgG1 responses by week 3 post-prime (**Figure 5.20A**). C3−/− mice immunised with HEL CFA tended to develop responses in week 2, while B6 mice immunised with HEL CFA had detectable responses starting in week 3, except for one B6

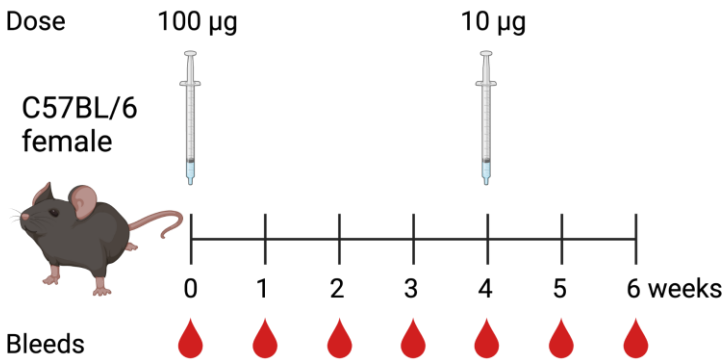


Figure 5.19: Bleed and immunisation schedule for the C3$^{-/-}$ experiment.

non-responder that only developed responses post-boost with HEL IFA. These results showed that C3$^{-/-}$ mice were capable of generating anti-HEL IgG responses.

In contrast, there were differences between C3$^{-/-}$ and B6 mice immunised with HEL GA and HEL PR. All three C3$^{-/-}$ mice immunised with HEL GA generated high anti-HEL IgG and IgG1 responses, whereas responses in B6 mice were more variable, with one high, low and non-responder (**Figure 5.20B**). Two C3$^{-/-}$ mice also generated responses to HEL PR immunisation post-boost, while B6 mice did not develop any responses (**Figure 5.20C**). As expected, mice immunised with HEL mock did not elicit anti-HEL IgG in either strain (**Figure 5.20D**).

When area under the curve was calculated for anti-HEL IgG responses in primed mice (i.e. up to week 4), HEL CFA and HEL GA responses in C3$^{-/-}$ mice were significantly higher than those in B6 mice (**Figure 5.20E**). The difference between C3$^{-/-}$ and B6 strains in HEL GA immunised mice was also maintained after boosting (**Figure 5.20F**). The increased anti-HEL IgG responses in C3$^{-/-}$ mice overall suggest that C3 may play an immunoregulatory rather than immunoenhancing role in general, not just in GA-mediated immunogenicity. Further experiment repeats to obtain 8 mice per group would provide sufficient power (80%) to detect the effect size observed (calculated using G*Power).

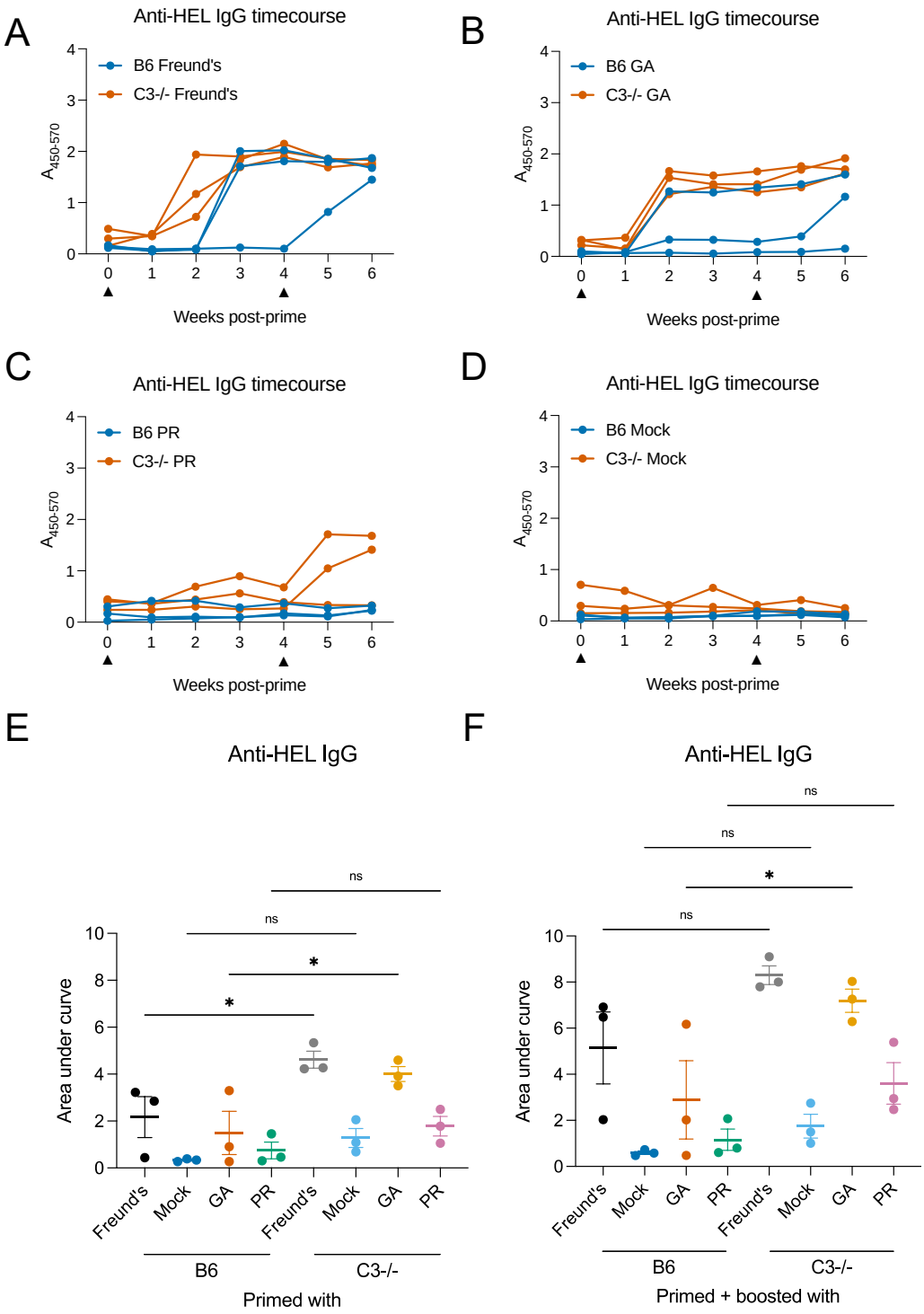


Figure 5.20: C3$^{-/-}$ mice have higher anti-HEL IgG responses compared with WT controls for HEL GA immunisation. WT B6 and C3$^{-/-}$ mice were primed (100 µg) and boosted (10 µg) at the times indicated with black triangles with A) HEL emulsified in CFA/IFA, B) HEL GA, C) HEL PR or D) HEL mock. Area under the curve calculated for anti-HEL IgG responses in E) primed mice (up to week 4) and in F) primed and boosted mice (up to week 6). Sera diluted 1:50. Data are mean ± SEM of 3 mice per group (*p ≤ 0.05, one-way ANOVA followed by Holm-Šídák's test).

5.2.6 Pull-down MS for HEL GA interaction partners in human sera

Since C3 was not required for HEL GA-induced antibody responses, I investigated other potential mechanisms for immunogenicity. Protein carbonyls promote type 2 cytokine secretion and antibody responses (Moghaddam et al. 2011), and extracellular proteins such as serum amyloid A (SAA1) and surfactant protein A (SP-A) have recently been shown to act as sPRRs to enhance type 2 immune responses (Section 5.1.1). SAA1 recognises conserved regions on dust mite fatty acid-binding proteins, which activates formyl peptide receptor 2 (FPR2) to promote the release of the type 2 cytokine IL-33 and allergic responses (Smole et al. 2020). SP-A and C1q have been shown to enhance type 2 macrophage responses (Minutti et al. 2017). Therefore, I performed a proteomics screen to identify potential interaction partners of HEL GA in sera that could be associated with GA-mediated type 2 immunity.

First, I prepared HEL bait conjugated to magnetic beads and considered two options for GA modification (**Figure 5.21A**). One option was to conjugate unmodified HEL to beads followed by GA treatment, but the beads themselves could also be affected. The other option was to conjugate previously modified HEL mock, HEL GA or HEL PR to beads, but modifications could be affected by chemical conjugation. I tested both methods, measuring the amount of conjugated protein with a bicinchoninic acid (BCA) assay and the amount of carbonylation with a DNPH assay (**Figure 5.21B**). Beads alone treated with GA had increased carbonylation, even though carboxylic acid-coated magnetic beads should not have any GA-modifiable groups. Conjugation of already modified HEL GA maintained its carbonylation and therefore I proceeded with the second option.

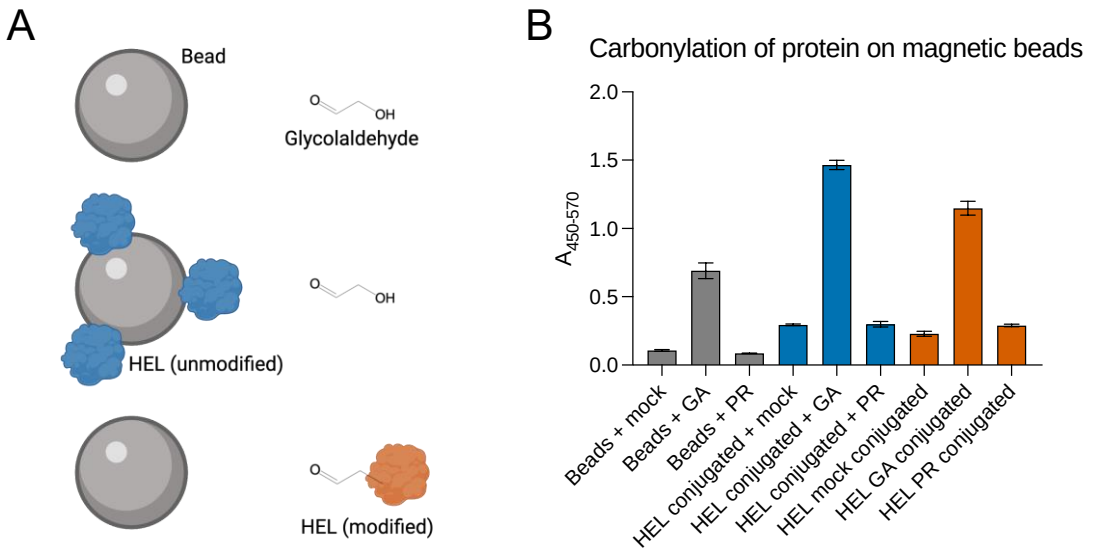


Figure 5.21: Magnetic beads become carbonylated after GA treatment. A) Schematic of protein conjugation to magnetic beads. Top: beads alone modified with GA. Middle: beads conjugated with HEL then modified with GA. Bottom: beads conjugated with already modified HEL GA. B) Carbonylation measured by DNPH ELISA. Data are mean ± SD of 3 technical replicates.

Next, I set up conditions for the pull-down assay. I used human (plasma-derived) sera because the human proteome is more comprehensively annotated. I tested different sera dilutions and bead concentrations, then visualised pulled-down proteins by sodium dodecyl sulphate–polyacrylamide gel electrophoresis (SDS-PAGE) (**Figure A.9**). Resuspending the beads in a larger volume of 400 µL PBS with 10× diluted sera (about 4 mg/mL) gave a suitable number of bands for tandem LC-MS (Marjorie Fournier, Advanced Proteomics Facility, personal communication). I also compared different buffers and detergents. While detergent reduced the amount of non-specific binding to magnetic beads, I opted to use VBS without detergent because detergents can interfere with MS (Marjorie Fournier, personal communication). I performed the pull-down experiment based on optimised conditions and used half of the samples for SDS-PAGE, and the other half for on-bead digest and tandem LC-MS (**Figure 5.22**).

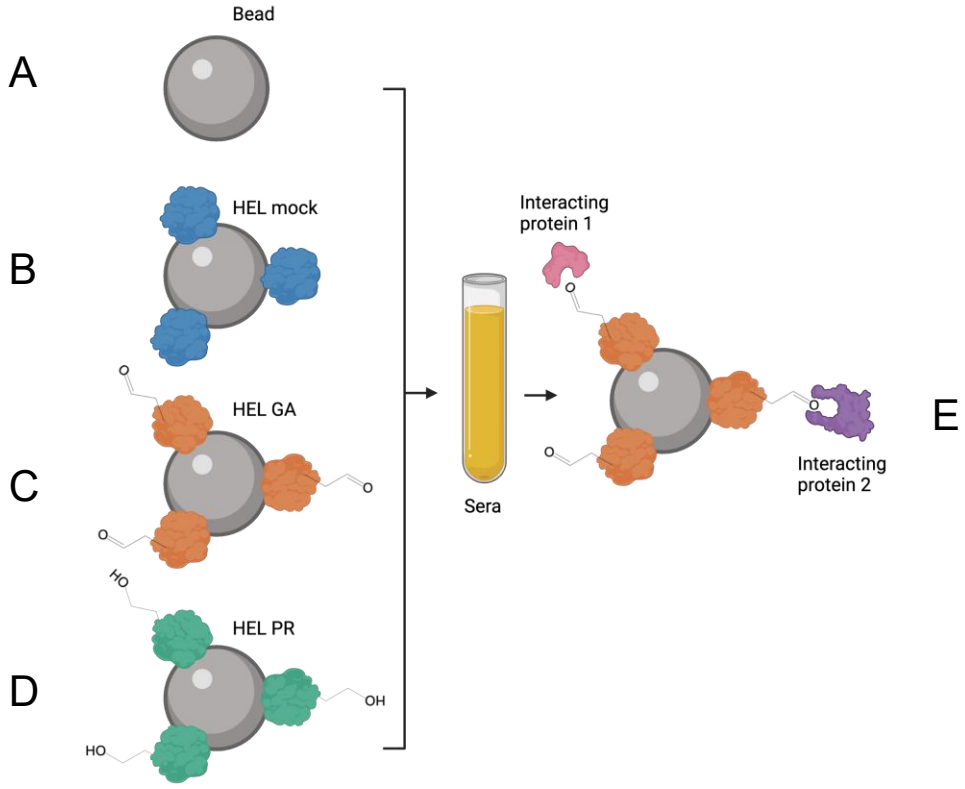


Figure 5.22: Overview of pull-down experiment. A) Beads control, B) HEL mock, C) HEL GA, and D) HEL PR conjugated magnetic beads. After incubation in human plasma-derived sera, E) magnetic beads were isolated with pulled-down proteins and analysed by either reducing SDS-PAGE or on-bead digest for tandem LC-MS.

Based on SDS-PAGE, there did not appear to be much non-specific protein binding to the magnetic beads (**Figure 5.23A**). Visually, there were no obvious differences between HEL mock, HEL GA and HEL PR, except for a slightly stronger band around 15 kDa that was likely to correspond to HEL GA. Surprisingly, in the MS samples the number of peptide spectrum matches (PSMs) for HEL protein detected in the HEL GA pull-down was more than four times less than that detected in the HEL mock and HEL PR pull-downs (**Figure 5.23B**).

Tandem LC-MS detected 249 pulled-down proteins (excluding HEL) after setting the false discovery rate (FDR) to 1% and removing known contaminants (performed by

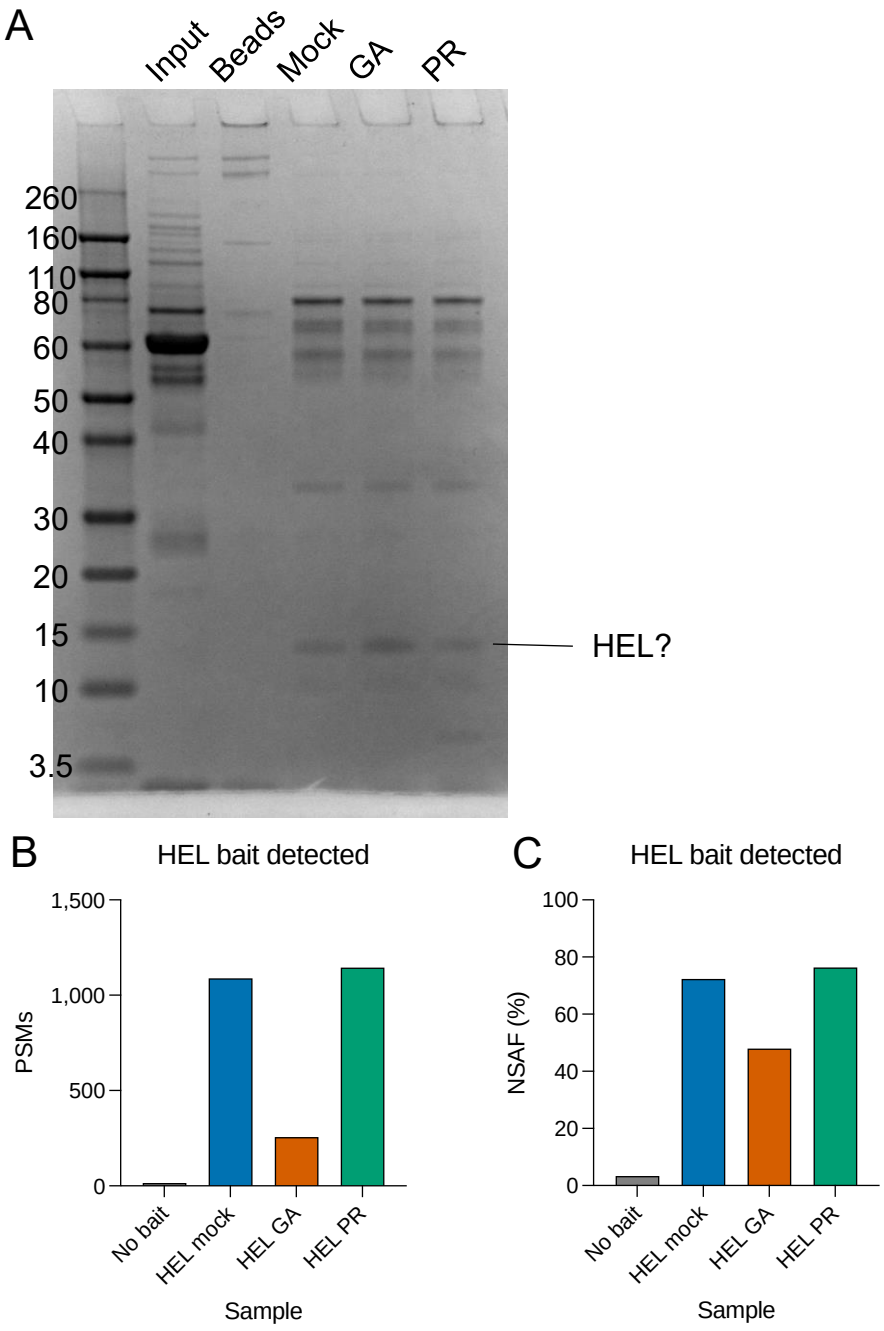


Figure 5.23: Less HEL bait is detected by tandem LC-MS in HEL GA pull-down despite being abundant in SDS-PAGE. A) Reducing SDS-PAGE of pulled-down proteins for each sample. HEL bait detected in tandem LC-MS samples expressed as B) the number of peptide spectrum matches (PSMs) or C) normalised spectral abundance factor (NSAF) values.

Marjorie Fournier). For each protein, the spectral abundance factor (SAF) was calculated by dividing the number of peptide spectrum matches (PSM) by protein length, then the SAF for each protein was normalised to the summed SAF of the entire sample (NSAF) (performed by Marjorie Fournier). Normalisation slightly improved the relative abun-

dance of HEL bait for comparisons between samples (**Figure 5.23C**). Using Perseus software (Tyanova et al. 2016), I log transformed (base 2) the NSAF values, imputed missing values based on the normal distribution, and performed hierarchical clustering based on Euclidean distance to determine which samples were most similar (**Figure 5.24**). Hierarchical clustering revealed that HEL mock and HEL PR pull-downs were more similar to one another than to HEL GA.

Since this pilot pull-down experiment was performed without replicates, it was not possible to determine statistically significant differences between the samples. Instead, I calculated the fold change (FC) of NSAF values to determine which proteins were differentially pulled-down in the HEL GA sample compared with HEL mock, HEL PR and the beads control. This narrowed the list to 60 proteins either enriched or depleted (> 1 FC) in the HEL GA sample, although 26 of these were low-abundance proteins detected with only one PSM (**Figure 5.25**, grey squares).

I then performed over-representation analysis (ORA) (Boyle et al. 2004) on the 60 differentially pulled-down proteins to determine whether particular biological processes or pathways were enriched compared with a list of background reference proteins, which I defined as the 249 proteins detected by tandem LC-MS. Using the online meta-database ConsensusDBPath (Kamburov et al. 2011) and the Database for Annotation Visualisation and Integrated Discovery (DAVID) (Jiao et al. 2012), I found that the 60 proteins were associated with some terms and pathways, but none were significantly enriched (data not shown). In contrast, when the entire human proteome was set as the reference, pathways relating to complement, innate immunity, coagulation, peptidase inhibition and activation were all significantly enriched (**Table A.1**). Human sera would have been a more appropriate background for the ORA, but I had not included a human serum input control sample in this experiment.

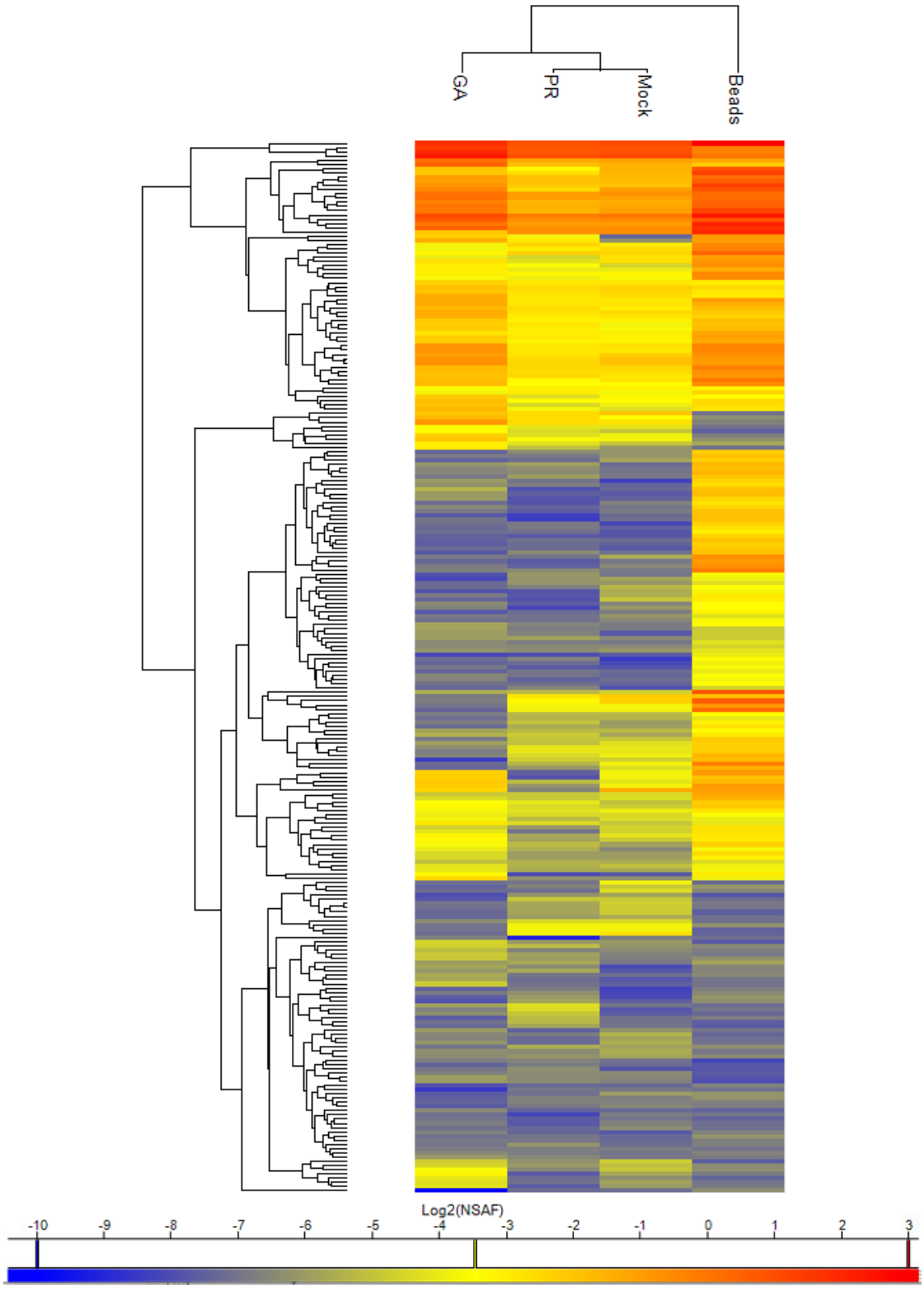


Figure 5.24: HEL mock and HEL PR pull-downs are more similar than to HEL GA. An initial list of 249 pulled-down proteins (excluding HEL) was generated by setting FDR < 1% and removing known contaminants (performed by Marjorie Fournier). SAF was calculated by dividing the number of PSMs by protein length, then normalised to the total SAF for each sample (NSAF) (performed by Marjorie Fournier). NSAF values were $\log_2$ transformed, missing values imputed based on normal distribution, and agglomerative hierarchical clustering was performed based on Euclidean distance and average-linkage.

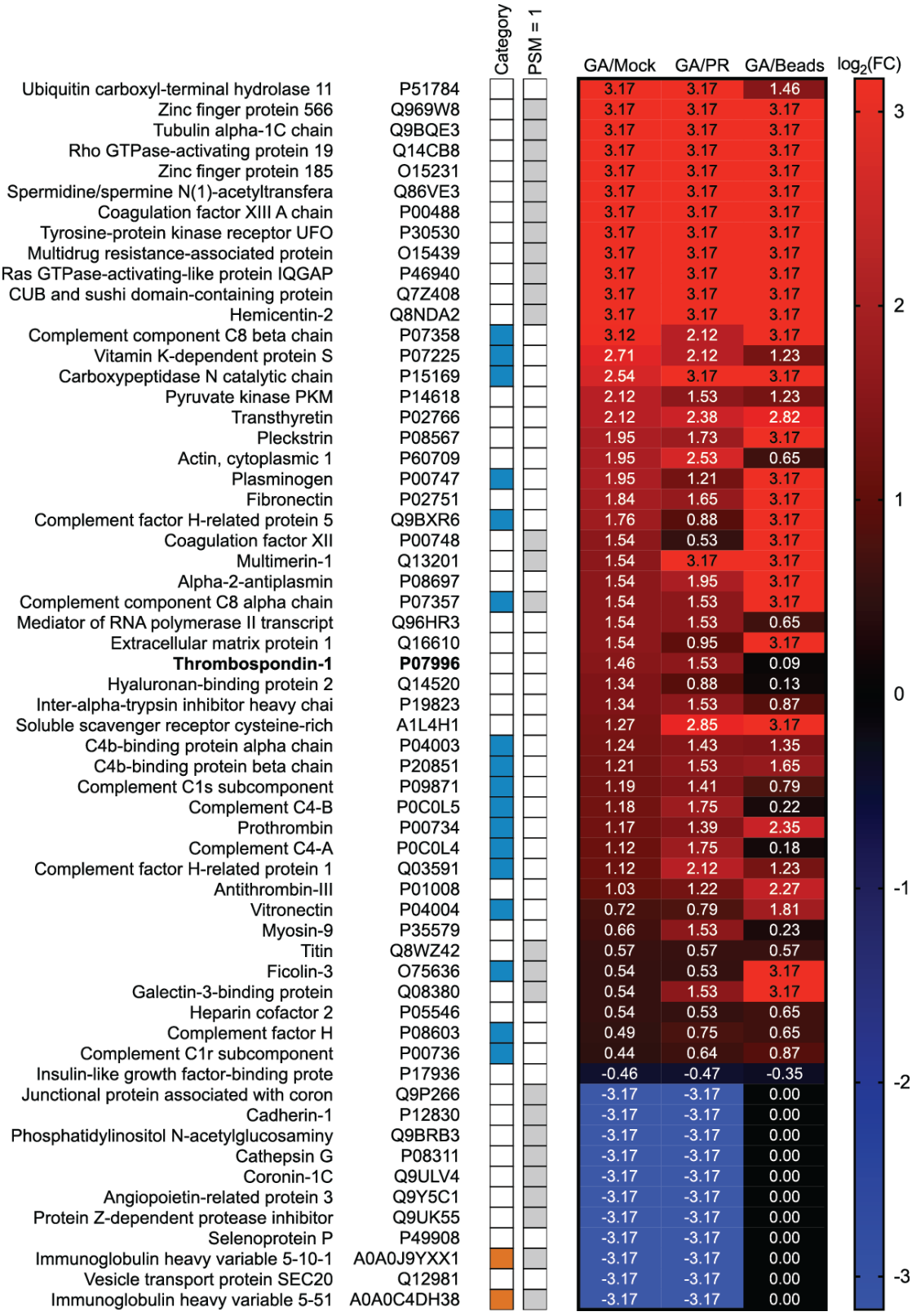


Figure 5.25: List of 60 proteins enriched (red) or depleted (blue) > 1 FC in HEL GA pull-down compared with HEL mock, HEL PR and beads. Log_2 transformed NSAF ratios of HEL GA over HEL mock, HEL PR or beads. Ratios with missing NSAF values (i.e. protein not detected in pull-down sample) were set to −3.17 and 3.17. Sorted descending on GA/Mock. Covariate bars indicate proteins i) classified as complement (blue), Ig (orange); or ii) detected with only 1 PSM (grey) in HEL GA (for enriched proteins) or HEL mock and HEL PR (for depleted proteins).

A further 80 proteins were enriched or depleted in HEL GA pull-down compared with HEL mock and HEL PR, but not in comparison with the beads control (**Figure 5.26**). I re-ran the ORA including these 80 proteins (140 proteins in total). ConsensusDBPath reported many gene ontology (GO) terms relating to immune and inflammatory responses as well as complement and protein activation were significantly enriched (**Table 5.1**). However, the complement cascade itself was not significantly enriched (q = 0.0651) **(Table 5.2**). DAVID functional analysis also pointed to complement activation and regulation, although these terms were again not significantly enriched (data not shown).

Since the complement pathway was potentially enriched in HEL GA pull-down and previous experiments suggested that complement activation was of interest, I separately analysed the 30 complement proteins detected by tandem LC-MS in further detail. Comparing the NSAF of all complement proteins showed that complement proteins were significantly more abundant in HEL GA pull-down compared with HEL mock and HEL PR (**Figure 5.27A**). In HEL GA pull-down, complement proteins comprised 15.1% of total proteins detected compared with 6-9% for all other conditions (**Figure 5.27B**).

23 complement proteins were more abundant in HEL GA pull-down compared with HEL mock and HEL PR, while only 4 were less abundant (**Figure 5.28**). In particular, initiators of the complement cascade C1r, C1s, C1q (subunits B and C), ficolin-2 and ficolin-3 as well as downstream proteins C4 and C3 were more abundant in HEL GA pull-down. Increased complement initiation appeared to recruit negative regulators of complement amplification, such as C4b-binding protein (C4BP), factor H and complement factor H related (CFHR) proteins 1 and 5. HEL GA pull-down was also enriched for C8 of the membrane attack complex (MAC), as well as MAC assembly inhibitors vitronectin (otherwise called protein S) and clusterin, which could explain the

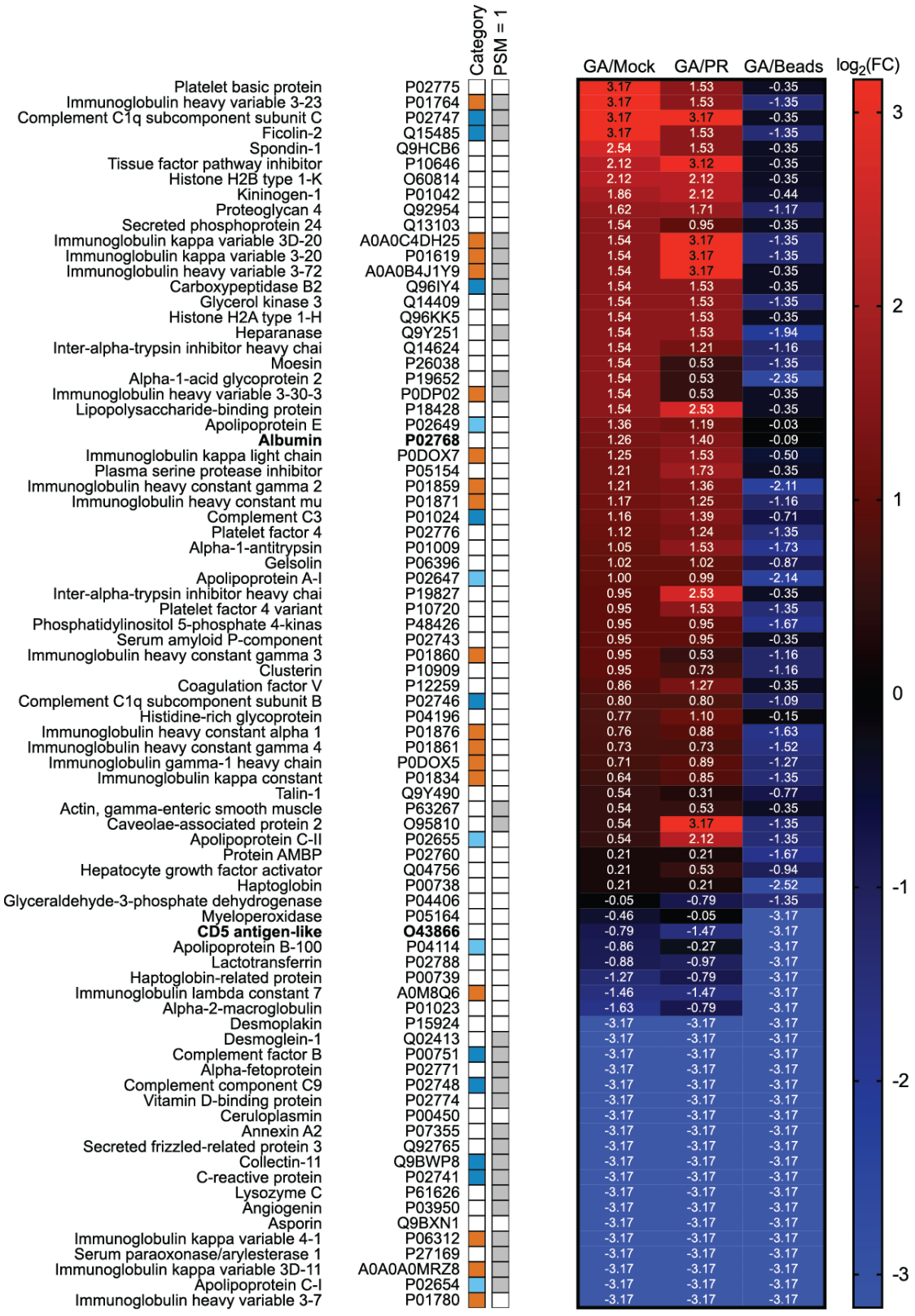


Figure 5.26: List of 80 proteins enriched (red) or depleted (blue) with > 1 FC in HEL GA pull-down compared with HEL mock and HEL PR (but not beads). Log_2 transformed NSAF ratios of HEL GA over HEL mock, HEL PR or beads. Ratios with missing NSAF values (i.e. protein not detected in pull-down sample) were set to −3.17 and 3.17. Sorted descending on GA/Mock. Covariate bars indicate proteins i) classified as complement (blue), Ig (orange), apolipoprotein (light blue); ii) detected with only 1 PSM (grey) in HEL GA (for enriched proteins) or HEL mock and HEL PR (for depleted proteins).

Table 5.1: ORA of pull-down hits compared with background show significant enrichment of gene ontology (GO) terms. 140 proteins with > 1 FC in HEL GA compared with HEL mock and HEL PR were analysed against a background reference of 249 initial proteins detected by MS using ConsensusDBPath.

GO Term		Category, Level	Set Size	Effective Size	Candidates Contained		p-value	q-value
GO:0072562	blood microparticle	CC 2	148	69	59	85.5%	2.20 E-09	1.30 E-07
GO:0006950	response to stress	BP 2	4192	142	98	69.0%	2.29 E-06	2.36 E-04
GO:0009605	response to external stimulus	BP 2	2572	114	81	71.1%	1.12 E-05	5.75 E-04
GO:0006959	humoral immune response	BP 3	402	73	57	78.1%	4.56 E-06	1.06 E-03
GO:0006956	complement activation	BP 3	195	59	47	79.7%	1.93 E-05	1.91 E-03
GO:0006952	defense response	BP 3	1876	110	78	70.9%	2.47 E-05	1.91 E-03
GO:0002253	activation of immune response	BP 2	759	67	51	76.1%	8.27 E-05	2.84 E-03
GO:0006954	inflammatory response	BP 4	842	75	58	77.3%	6.52 E-06	2.88 E-03
GO:0072376	protein activation cascade	BP 2	219	71	53	74.6%	1.49 E-04	3.84 E-03
GO:0002526	acute inflammatory response	BP 5	224	60	48	80.0%	1.17 E-05	4.32 E-03
GO:2000257	regulation of protein activation cascade	BP 4	122	44	37	84.1%	2.03 E-05	4.49 E-03
GO:0030449	regulation of complement activation	BP 5	121	43	36	83.7%	3.41 E-05	6.29 E-03
GO:0016485	protein processing	BP 5	345	59	59	100.0%	7.48 E-05	8.87 E-03
GO:0002920	regulation of humoral immune response	BP 5	144	44	36	81.8%	9.61 E-05	8.87 E-03

Table 5.2: ORA of pull-down hits compared with background does not show significant enrichment of GO pathways. 140 proteins with > 1 FC in HEL GA compared with HEL mock and HEL PR were analysed against a background reference of 249 initial proteins detected by MS using ConsensusDBPath.

Pathway	Source	Set Size	Effective Size	Candidates Contained		p-value	q-value
Regulation of Complement cascade	Reactome	127	39	33	84.6%	0.0002	0.0651
Complement cascade	Reactome	137	44	36	81.8%	0.0003	0.0651
Regulation of Insulin-like Growth Factor (IGF) transport and uptake by Insulin-like Growth Factor Binding Proteins (IGFBPs)	Reactome	124	25	22	88.0%	0.0010	0.1114
Post-translational protein phosphorylation	Reactome	107	21	19	90.5%	0.0012	0.1114

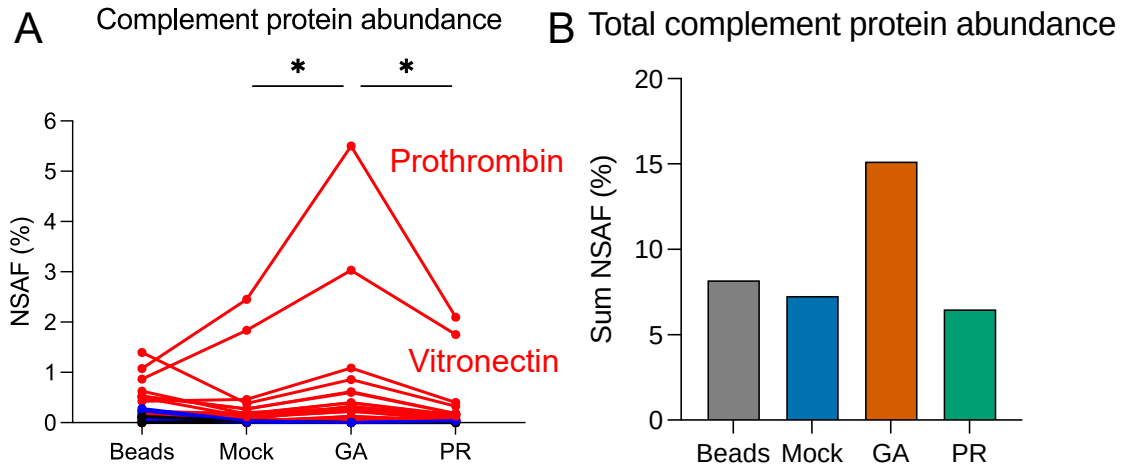


Figure 5.27: Complement proteins are most abundant in HEL GA pull-down. A) Individual NSAF values for 31 complement proteins in each pull-down sample. Each connected line represents a single protein either enriched (red), depleted (blue) or neither (black) in HEL GA pull-down compared with both HEL mock and HEL PR (*$p \leq 0.05$; repeated measures one-way ANOVA followed by Holm-Šídák's multiple comparisons test). B) Summed NSAF for the 31 complement proteins in each pull-down sample.

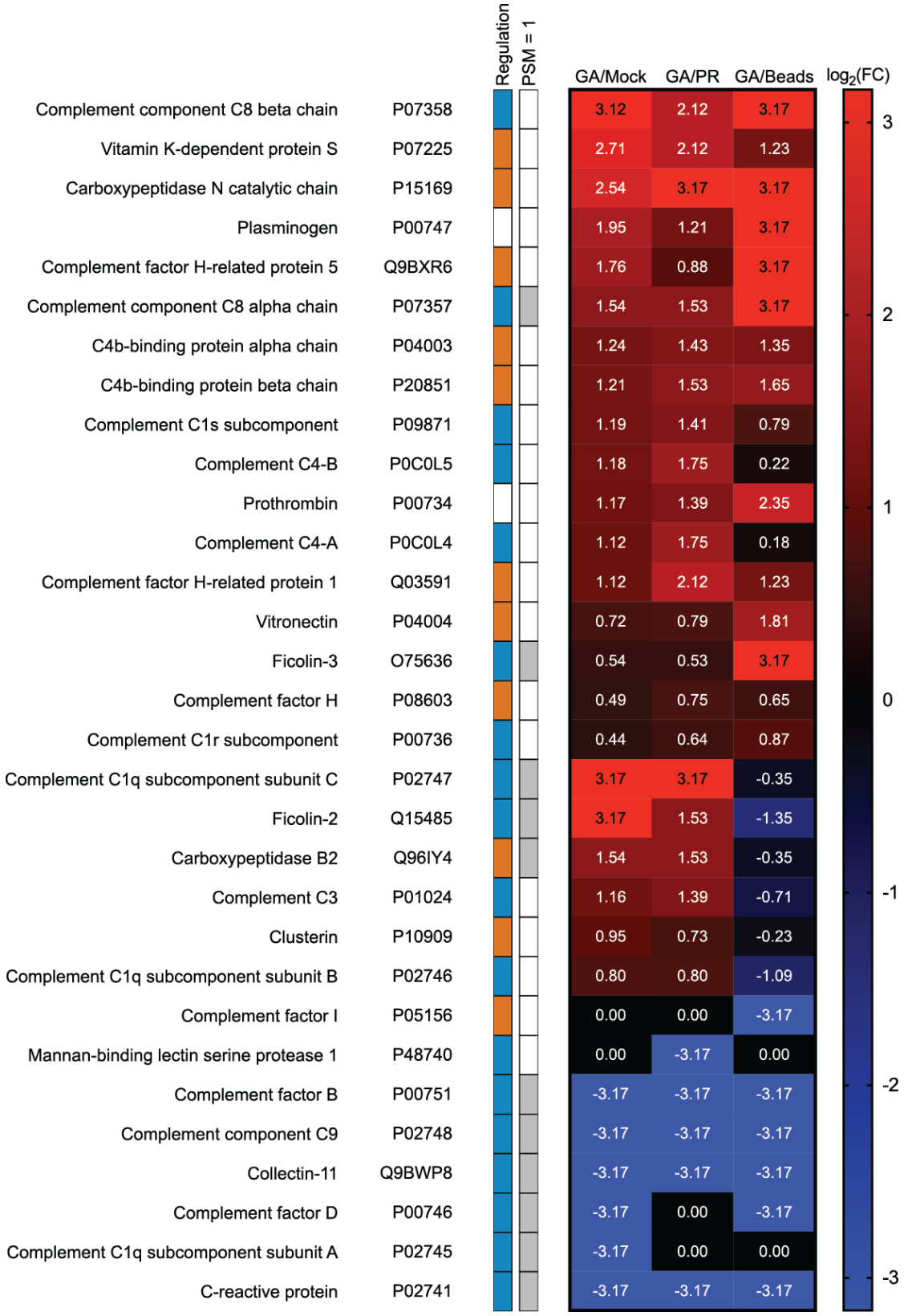


Figure 5.28: Complement activation is generally increased for HEL GA pull-down compared with HEL mock and HEL PR. 31 complement proteins detected by pull-down MS shown with $\log_2$ transformed NSAF ratios of HEL GA over HEL mock, HEL PR or beads. Ratios with missing NSAF values (i.e. not detected by MS) were set to −3.17 and 3.17. Sorted descending on GA/Mock. Covariate bars indicate proteins i) positive (blue) or negative (orange) regulators of complement cascade; or ii) detected with only 1 PSM (grey) in HEL GA (for enriched proteins) or HEL mock and HEL PR (for depleted proteins).

lower abundance of C9. HEL GA sample also recruited less factor B, which is involved in alternative complement activation. Although some proteins were most abundant on the beads control, they nonetheless showed differences between HEL GA compared with HEL mock and HEL PR pull-downs (e.g. C1q subunits B and C, C3). Together, these results suggest that HEL GA promotes increased complement activation and opsonisation.

I also analysed all immunoglobulins detected in the pull-down samples. Comparing the NSAF for all immunoglobulins did not show significant differences between HEL GA and HEL mock or HEL PR ($p = 0.0697$) (**Figure 5.29A**). Overall, immunoglobulins were highly abundant in beads control pull-down, comprising 35.2% of total proteins detected compared with 6.7% for HEL mock, 10.0% for HEL GA and 5.6% for HEL PR (**Figure 5.29B**). Interestingly, most immunoglobulin constant regions (IgG1, IgG2, IgG3, IgG4, IgM, IgA1 heavy chains and κ light chain) were enriched in HEL GA pull-down compared with HEL mock and HEL PR (**Figure 5.30**). In contrast, IgA2, λ light chains, J chain and immunoglobulin variable regions had no clear trends. These results suggested that specific immunoglobulin subclasses may have increased binding to HEL GA. A similar analysis was performed for apolipoproteins, which were slightly higher in HEL GA pull-down but not significantly compared with HEL mock and HEL PR (**Figure 5.31**).

Overall, the pull-down experiment suggested that HEL GA might stimulate increased complement activation and immunoglobulin binding. However, given the technical issues with unequal HEL bait (**Figure 5.23)**, I attempted co-immunoprecipitation (co-IP) instead and performed the experiment using normal mouse sera instead of normal human sera to correspond better with my in vivo results.

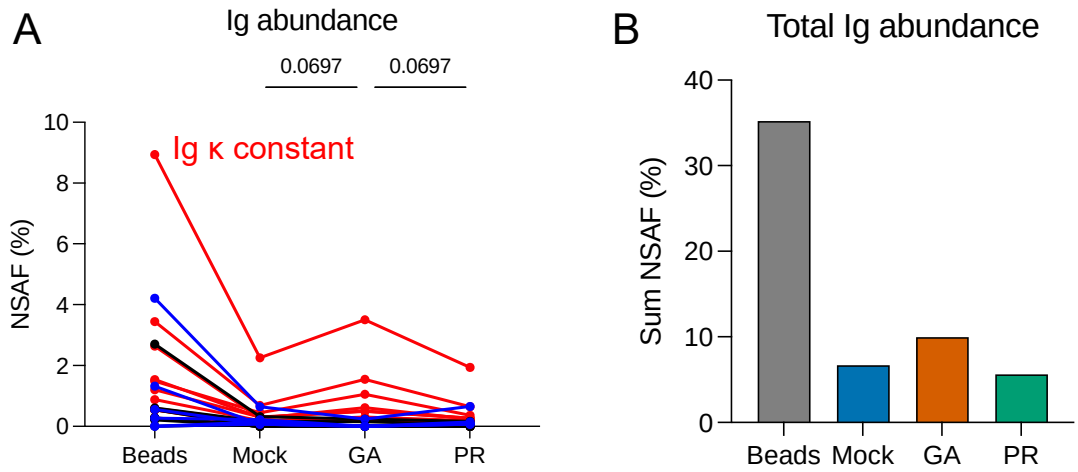


Figure 5.29: Immunoglobulins (Igs) are more abundant in beads control and HEL GA pull-down. A) Individual NSAF values for 31 Igs in each pull-down sample. Each connected line represents a single protein either enriched (red), depleted (blue) or neither (black) in HEL GA pull-down compared with both HEL mock and HEL PR (p-values indicated; repeated measures one-way ANOVA followed by Holm-Šídák's multiple comparisons test). B) Summed NSAF for the 31 Igs in each pull-down sample.

5.2.7 Co-IP MS for HEL GA interaction partners in mouse sera

I considered two well-characterised monoclonal mouse IgG1 anti-HEL antibodies for co-IP: HyHEL-10 that binds on the HEL surface over K96/K97 (PDB ID: 2DQJ, Shiroishi et al. 2007) (Section 4.2.10), and D1.3 (gifted from Xiaochao Xue) that may interact with K13/K116 (PDB ID: 1G7H, Sundberg et al. 2000).

First, I took into account any differences in binding to HEL mock, HEL GA and HEL PR by HyHEL-10 or D1.3. HEL mock, HEL GA or HEL PR were coated on ELISA plates at a constant concentration (1 μg/mL) and incubated with varying concentrations of HyHEL-10 or D1.3. Binding of anti-HEL monoclonal antibodies were detected using HRP-conjugated anti-mouse IgG1 secondary antibody. HyHEL-10 (**Figure 4.23A**) and D1.3 binding (**Figure 5.32A**) to HEL GA and HEL PR were higher compared with HEL mock. In comparison, when the amount of HEL mock, HEL GA or HEL PR coated onto plates was varied and HyHEL-10 or D1.3 added at a constant concentration (0.1 μg/mL),

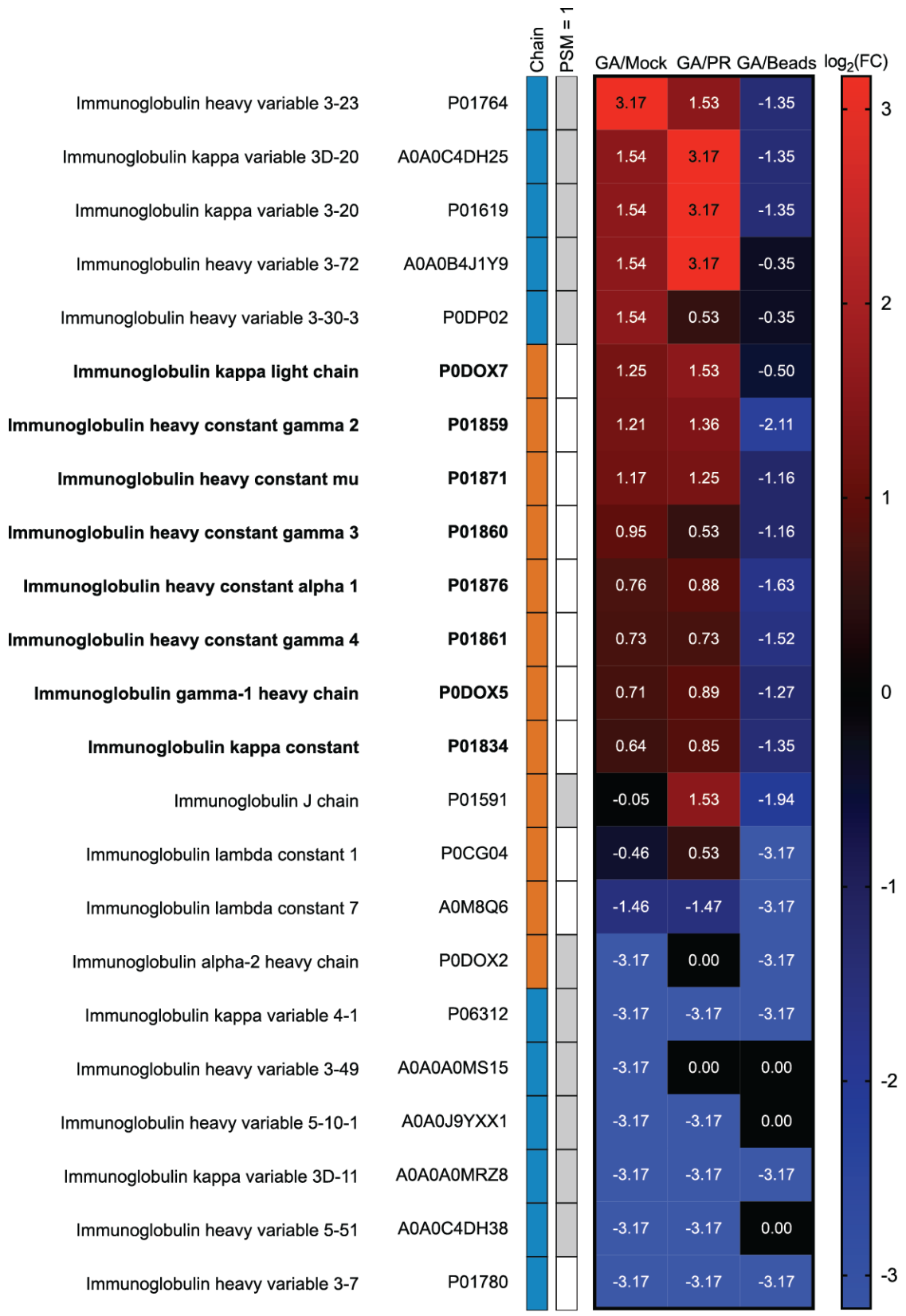


Figure 5.30: Many Ig constant regions are enriched in HEL GA pull-down compared with HEL mock and HEL PR. 23 (of 31) Ig proteins detected by pull-down MS shown with $\log_2$ transformed NSAF ratios of HEL GA over HEL mock, HEL PR or beads. Ratios with missing NSAF values (i.e. not detected by MS) were set to −3.17 and 3.17. Sorted descending on GA/Mock. Covariate bars indicate Ig with i) variable (blue) or constant (orange) regions; or ii) detected with only 1 PSM (grey) in HEL GA (for enriched proteins) or HEL mock and HEL PR (for depleted proteins). 8 Igs detected in only the beads sample not shown.

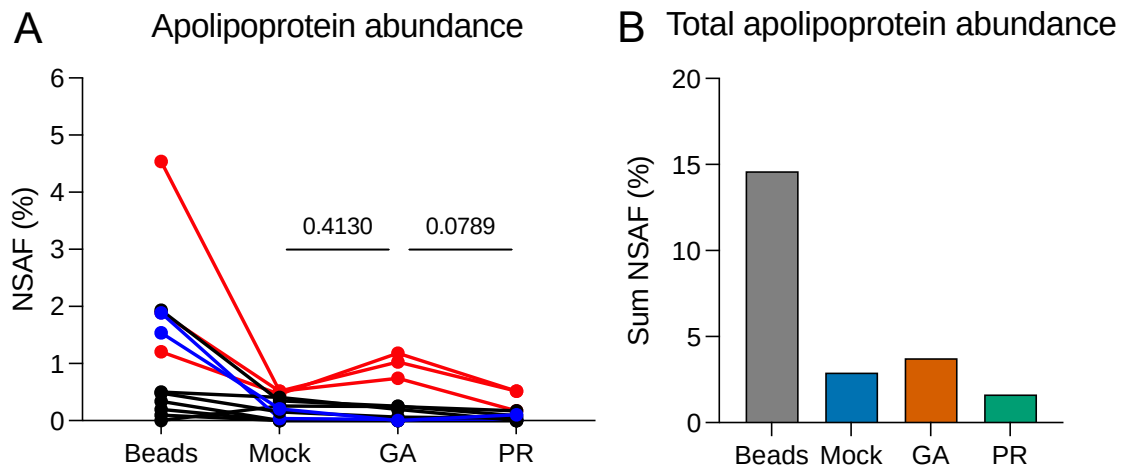


Figure 5.31: Apolipoproteins are more abundant in beads control and HEL GA pull-down. A) Individual NSAF values for 12 apolipoproteins proteins in each pull-down sample. Each connected line represents a single protein either enriched (red), depleted (blue) or neither (black) in HEL GA pull-down compared with both mock and PR (p-values indicated; repeated measures one-way ANOVA then Holm-Šídák's multiple comparisons test). B) Summed NSAF for the 12 apolipoproteins in each pull-down sample.

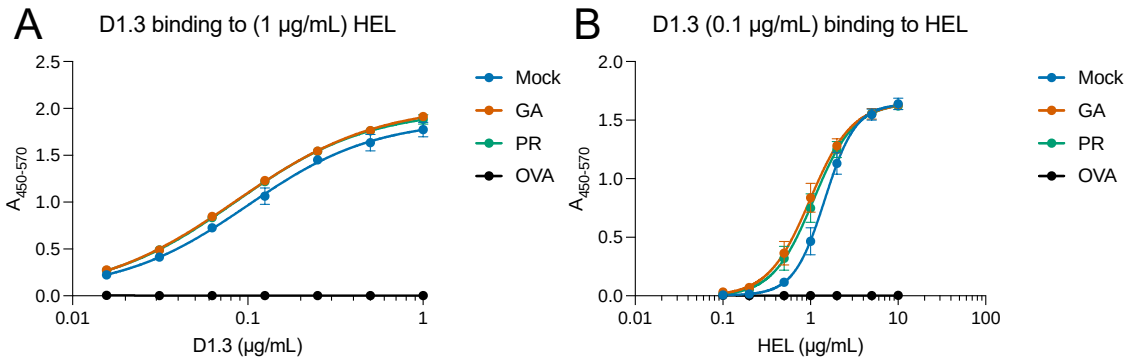


Figure 5.32: Monoclonal mouse IgG1 anti-HEL antibodies bind similarly to HEL GA and HEL PR. A) D1.3 titrated against 1 µg/mL HEL mock, HEL GA, HEL PR or OVA coated on ELISA plates. B) Varied amount of HEL mock, HEL GA, HEL PR, or OVA coated on ELISA plates incubated with 0.1 µg/mL D1.3. Data are mean ± SD of 3 technical replicates. See Figure 4.23A–B for HyHEL-10 data.

the results again showed that HyHEL-10 (**Figure 4.23B**) and D1.3 (**Figure 5.32B**) bound less to HEL mock compared with HEL GA and HEL PR.

Next, I conjugated HyHEL-10 and D1.3 separately onto magnetic beads and tested whether I could immunoprecipitate and elute HEL. I found that more HEL was eluted by immunoprecipitation using HyHEL-10 compared with D1.3 (**Figure 5.33**), and

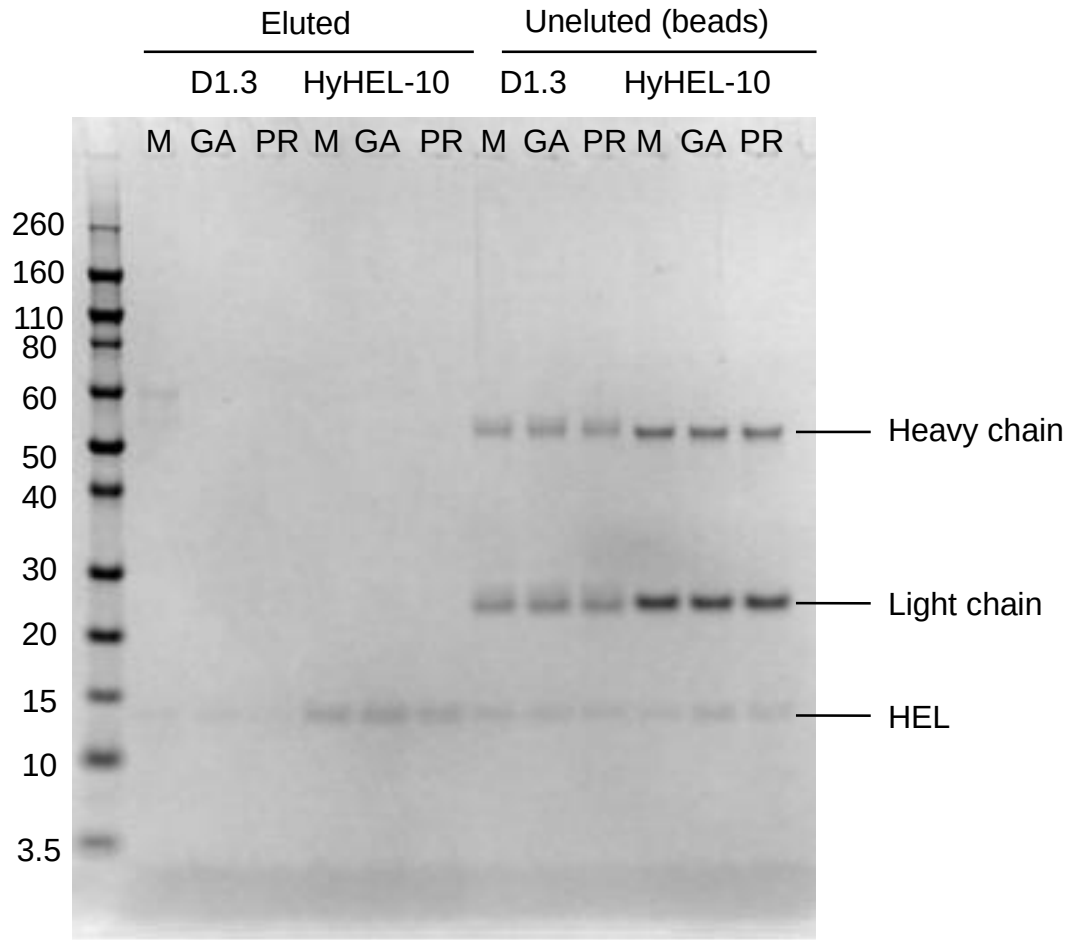


Figure 5.33: HEL immunoprecipitation and elution are more efficient using HyHEL-10 compared with D1.3. 0.3 mg magnetic beads conjugated with D1.3 or HyHEL-10 were incubated with 3 µg HEL mock (M), HEL GA or HEL PR at 4 °C for 1 h, washed, then eluted with 0.1 M glycine-HCl pH 2.5 (left half of gel). Magnetic beads were then boiled in LDS sample buffer with reducing agent to remove uneluted protein (right half of gel). Samples run on reducing SDS-PAGE and stained with a Coomassie-based dye.

decided to proceed with HyHEL-10 conjugated beads. In agreement with the ELISA binding results, there seemed to be slightly more HEL GA and HEL PR bound to HyHEL-10 conjugated beads compared with HEL mock, although the amount of HEL proteins actually eluted were similar.

I then set up a number of conditions to optimise co-IP of normal mouse sera proteins with HEL GA. I tested whether it was preferable to immunoprecipitate HEL bait first followed by sera incubation (**Figure 5.34A**, beads + HEL GA + sera) or to incubate

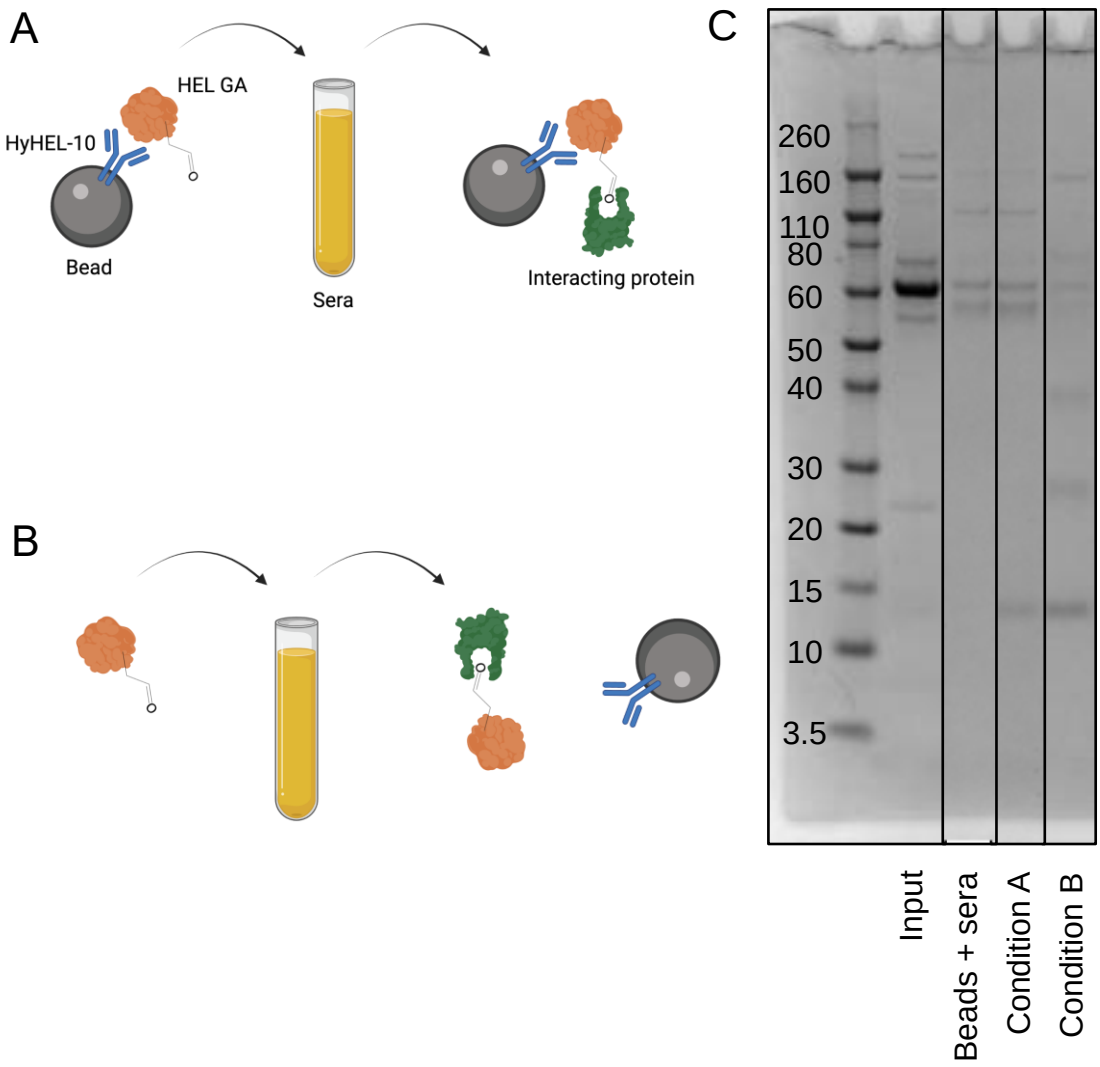


Figure 5.34: Co-IP after incubating HEL GA with normal mouse sera captures more proteins. A) HyHEL-10 conjugated magnetic beads were incubated with HEL GA at 4 °C for 1 h, washed, then incubated with 10× diluted normal mouse sera at 37 °C for 1 h. B) HEL GA was incubated in 10× diluted normal mouse sera, then HyHEL-10 conjugated magnetic beads were added at RT for 1 h. C) Beads were washed and proteins eluted with 0.1 M glycine-HCl pH 2.5. Samples were run on SDS-PAGE and stained with a Coomassie-based dye. Black outline indicates where the gel has been cropped for clarity.

HEL GA bait with sera first followed by co-IP (**Figure 5.34B**, HEL GA + sera + beads). Incubating HEL GA bait with sera first would maximise protein aldehyde interactions with serum proteins, but bound serum proteins could also block antibody epitopes to prevent co-IP. I found that incubating HEL GA bait with sera first did not prevent co-IP and therefore chose this approach (**Figure 5.34C**).

Having optimised conditions for the co-IP experiment, I incubated HEL mock, HEL GA and HEL PR bait proteins with fresh normal mouse sera pooled from two female BALB/c mice. I also prepared a no-HEL bait control to assess non-specific sera binding to HyHEL-10 conjugated beads, and an input serum control to calculate the degree of enrichment for co-immunoprecipitated proteins (**Figure 5.35**). The co-IP eluants were used to measure total protein concentration, run SDS-PAGE, and perform in-solution digest for tandem LC-MS.

The total protein concentration of co-IP eluants was lowest for no bait and highest for HEL GA eluant (**Figure 5.36A**). Total protein concentration seemed to correspond with the number of bands present in SDS-PAGE (**Figure 5.36B**). The gel also had three bands that seemed more prominent in HEL GA eluant compared with the HEL mock and HEL PR eluants. I excised and submitted the three bands for tandem LC-MS identification: the 30 kDa band was dimerised HEL, the 60 kDa band was mouse serum albumin (MSA), and the 160 kDa band could not be identified.

Tandem LC-MS data were analysed as for the pull-down experiment (Section 5.2.6). Again, less bait was detected in the HEL GA sample compared with the HEL mock and HEL PR eluants (**Figure 5.36C–D**), although there appeared to be similar amounts of HEL protein on the gel (**Figure 5.36B**). Besides HEL, 282 co-immunoprecipitated proteins were detected in the eluant after peptides were filtered to remove false hits (FDR = 1%) and known contaminants (performed by Marjorie Fournier). As for the pull-down tandem LC-MS data, SAF and NSAF were calculated for each protein, and Perseus software was used to log transform (base 2) NSAF, impute missing values, and perform hierarchical clustering. Hierarchical clustering suggested that HEL mock and HEL PR co-IP eluants were most similar to one another. The no HEL bait control was more similar to HEL mock and HEL PR, and HEL GA co-IP was the most different (**Figure 5.37**).

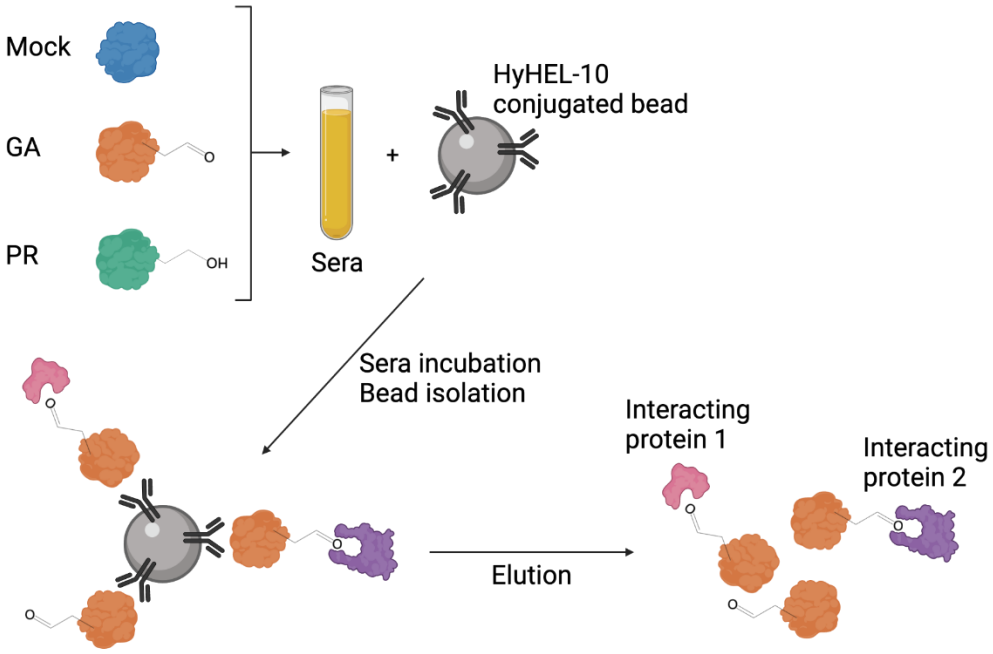


Figure 5.35: Overview of co-IP experiment. HEL mock, HEL GA or HEL PR bait were incubated in pooled normal mouse sera, then co-immunoprecipitated with HyHEL-10 conjugated magnetic beads. HEL mock, HEL GA or HEL PR were then eluted along with co-immunoprecipitated proteins. HyHEL-10 conjugated magnetic beads with no HEL bait was used as a control.

Next, I calculated NSAF ratios for HEL GA compared with HEL mock, HEL PR, no bait and input controls to find proteins enriched or depleted in HEL GA co-IP samples. 64 proteins were enriched or depleted > 1 FC in HEL GA co-IP relative to all other eluants (**Figure 5.38**). Interestingly, many ribosomal proteins and metabolic enzymes were enriched in the HEL GA eluant (**Figure 5.38**, green and pink squares), although most were detected with low abundance (PSM = 1).

The protein with the highest FC relative to HEL mock and detected with more than one PSM was thrombospondin-1 (TSP-1), which was also enriched from the human plasma-derived sera pull-down experiment (**Figure 5.25**). TSP-1 was highly enriched in HEL GA eluant relative to HEL mock eluant (14.8×), but less compared with HEL PR (1.2×) (**Figure 5.38**). Another promising hit was IgM heavy chain constant region, which

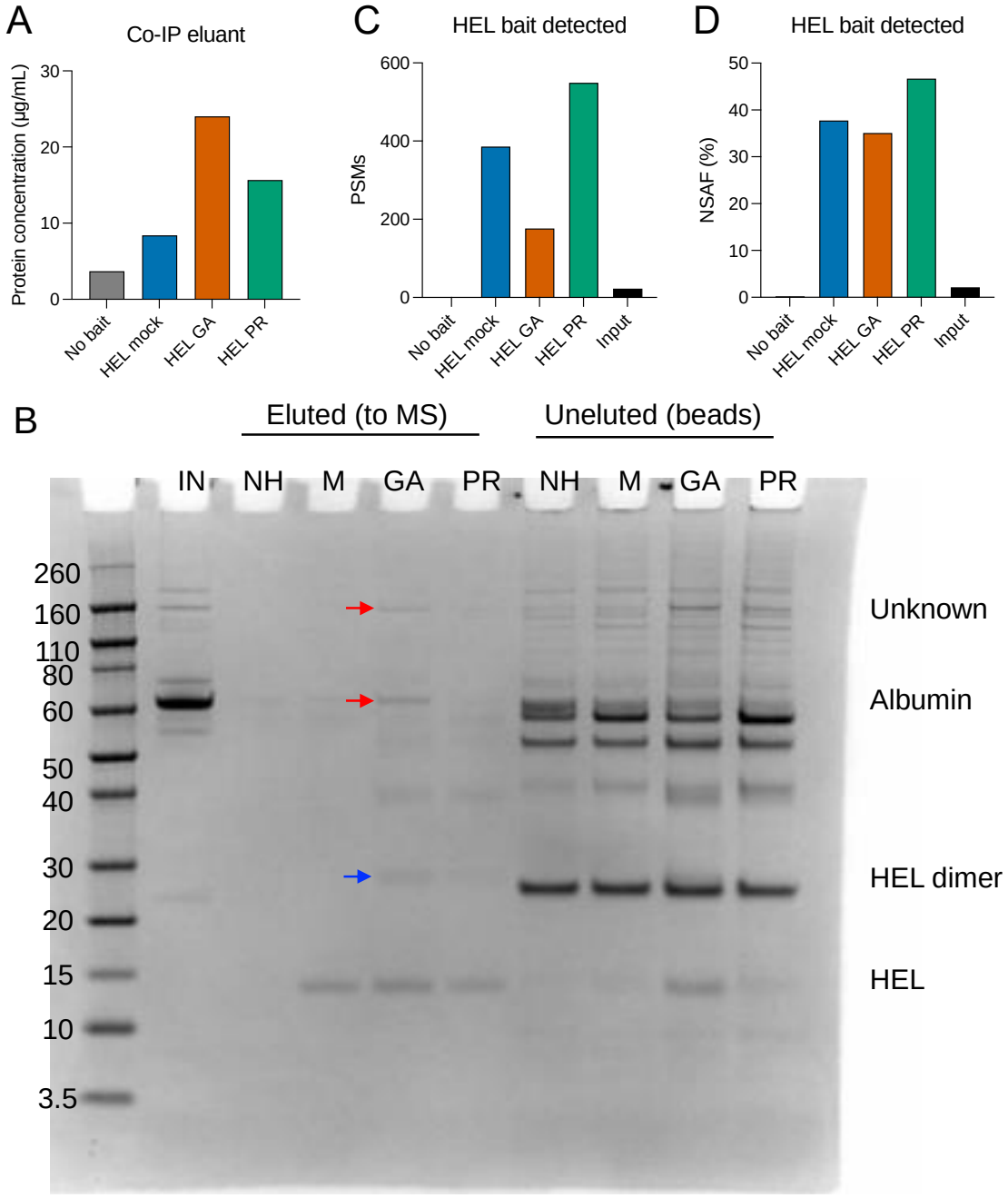


Figure 5.36: More proteins are co-immunoprecipitated but less HEL bait is detected by tandem LC-MS for HEL GA eluant compared with HEL mock and HEL PR eluants. A) Eluant protein concentration as measured by BCA assay. B) Eluants run on reducing SDS-PAGE and stained with a Coomassie-based dye. Arrows indicate bands that appear enriched by HEL GA bait, which were cut out and submitted for tandem LC-MS identification (result shown on right). IN = input control, NH = no HEL bait control, M = HEL mock. HEL bait detected in co-IP eluants by tandem LC-MS expressed as C) the number of PSMs or D) NSAF.

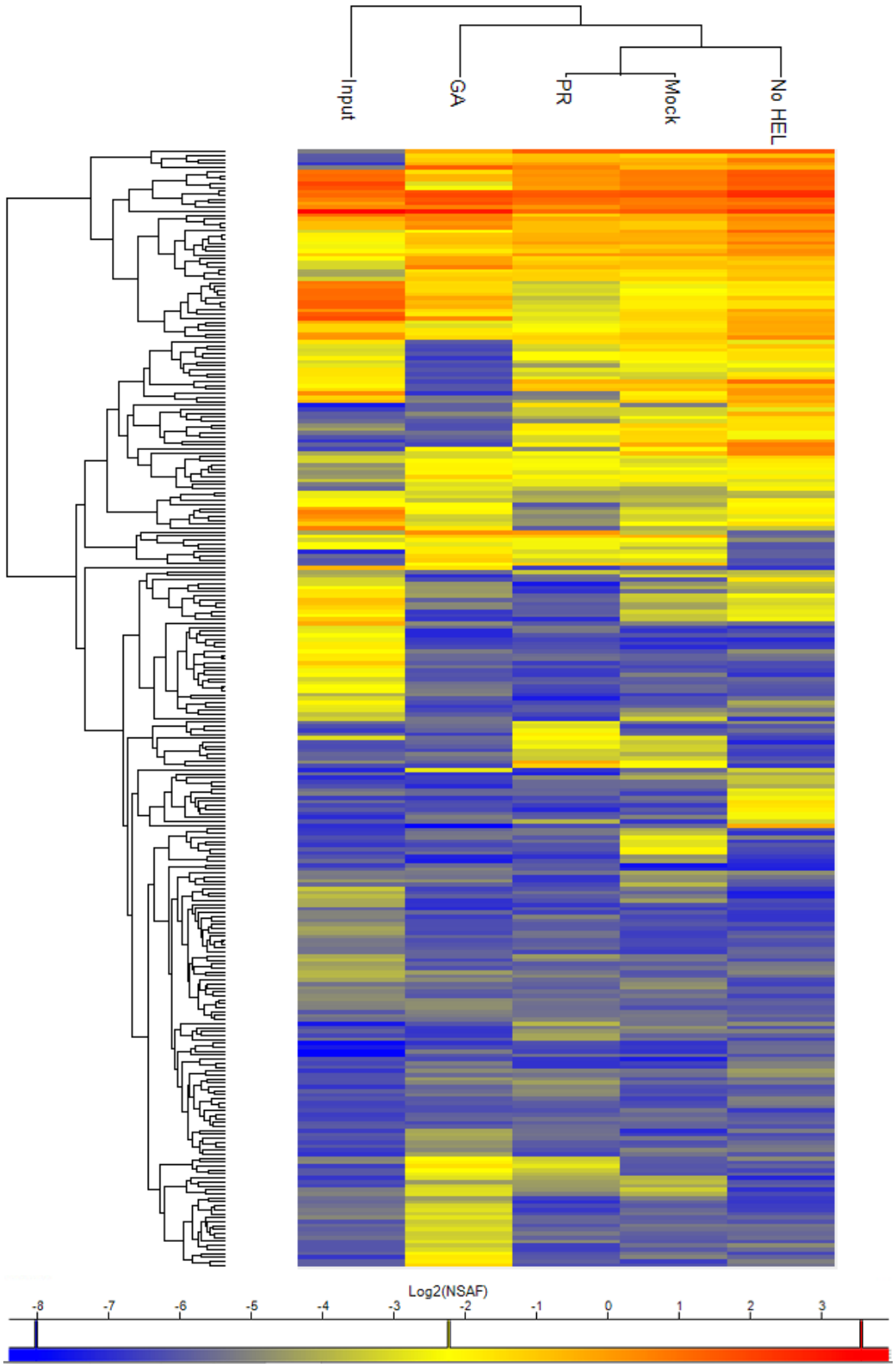


Figure 5.37: HEL mock and HEL PR co-IP are more similar compared with HEL GA. An initial list of 282 co-IP proteins (excluding HEL) was generated by setting FDR = 1% and removing known contaminants (performed by Marjorie Fournier). SAF was calculated by dividing the number of PSMs by protein length, then normalised to the total SAF for each sample (NSAF) (performed by Marjorie Fournier). NSAF values were $\log_2$ transformed, missing values imputed based on normal distribution, and agglomerative hierarchical clustering was performed based on Euclidean distance and average-linkage.

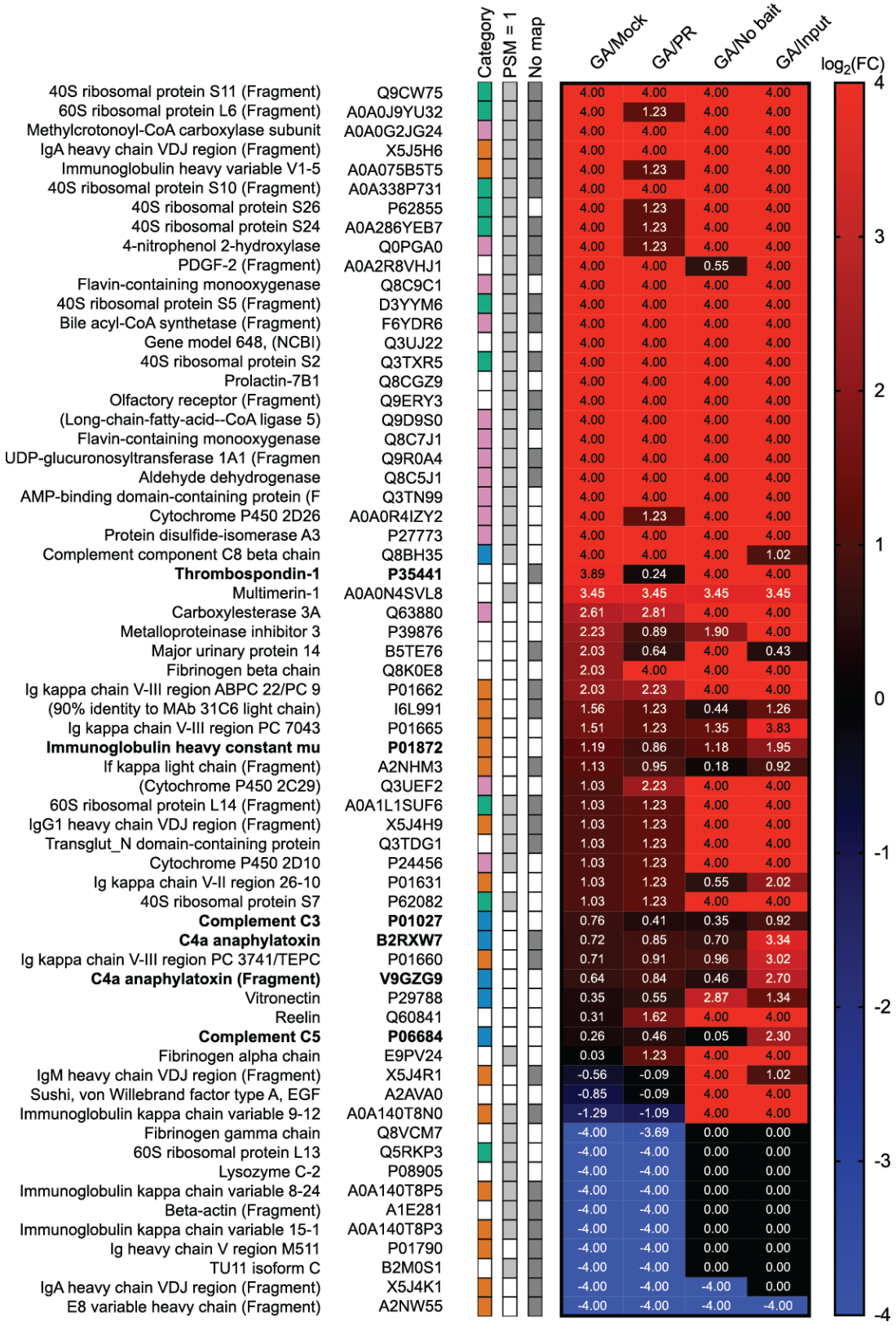


Figure 5.38: List of 64 proteins enriched (red) or depleted (blue) > 1 FC in HEL GA co-IP compared with HEL mock, PR, no bait and input controls. Log_2 transformed NSAF ratios of HEL GA over HEL mock, HEL PR, no bait or input controls. Ratios with missing NSAF values (i.e. protein not detected in co-IP sample) were set to −4 and 4. Sorted descending on GA/Mock. Covariate bars indicate proteins i) classified as complement (blue), Ig (orange), ribosome (green) or enzymes (pink); ii) detected with only 1 PSM (light grey) in HEL GA (for enriched proteins) or HEL mock and HEL PR (for depleted proteins); iii) not mapped in ConsensusDBPath (dark grey). Protein names in parentheses identified by similarity.

was enriched 2.3-fold compared with HEL mock and 1.8-fold compared with HEL PR. Other enriched proteins of interest were complement C4, C3, and C5, which again suggested increased complement activation by HEL GA. Although C4 is listed in the database as C4a anaphylatoxin, B2RXW7 is 99.8% identical to mouse complement C4-B (UniProt: P01029) and V9GZG9 is 93.1% identical with a cleaved N-terminal signal. In both cases, the sequence corresponding to C4a anaphylatoxin is intact, and thus these proteins are likely to be isoforms of complement C4-B rather than C4a anaphylatoxin.

A further 84 proteins were enriched by > 1 FC in HEL GA eluant compared with HEL mock and HEL PR eluants but not relative to no bait or input controls (**Figure 5.39**). Of these 84 proteins, 23 were more abundant in no bait control, 17 were more abundant in input sera, and 44 were more abundant in both. One of the 84 proteins was albumin, which was enriched in HEL GA eluant relative to HEL mock, HEL PR and no bait controls (consistent with the protein gel, **Figure 5.36B**), but albumin was already abundant in sera and not further enriched by HEL GA co-IP.

I then attempted ORA to determine enriched biological functions and pathways. However, only 148 out of 282 (52.5%) of detected mouse proteins could be mapped in ConsensusDBPath. In general, the mouse proteome was less well-annotated than the human proteome, and even contained uncharacterised proteins that could only be identified by similarity to other proteins. Instead, I analysed particular classes of proteins such as complement, immunoglobulins, ribosome and apolipoproteins.

Overall, there were no significant differences between HEL mock, HEL GA and HEL PR for complement proteins found in co-IP (**Figure 5.40A**). Of 29 complement proteins, 11 were more enriched and 11 were depleted in HEL GA compared with HEL

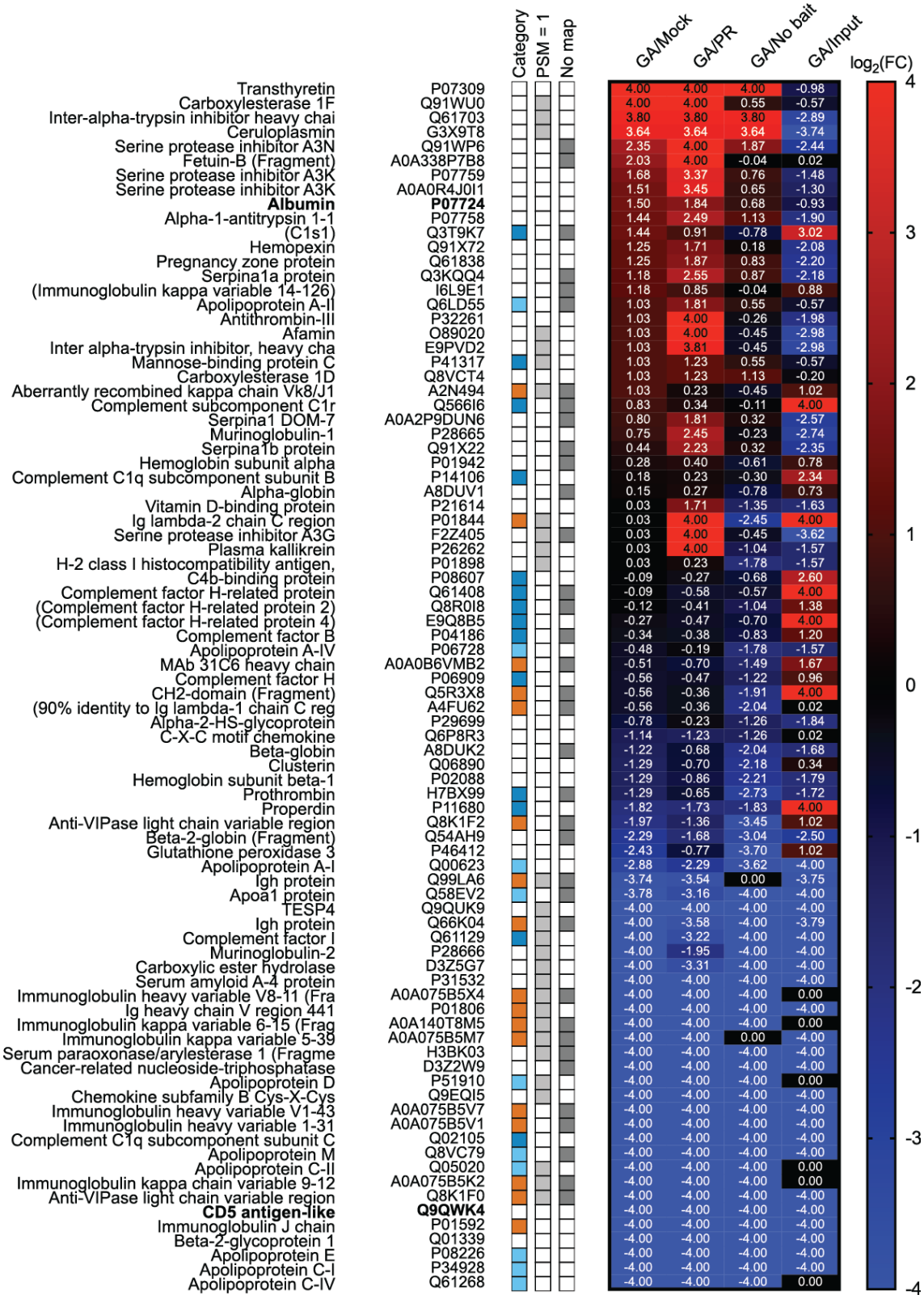


Figure 5.39: List of 84 proteins enriched (red) or depleted (blue) > 1 FC in HEL GA co-IP compared with HEL mock and HEL PR, but not relative to no bait or input controls. Log_2 transformed NSAF ratios of HEL GA over HEL mock, HEL PR, no bait or input controls. Ratios with missing NSAF values (i.e. protein not detected in co-IP sample) were set to −4 and 4. Sorted descending on GA/Mock. Covariate bars indicate proteins i) classified as complement (blue), Ig (orange) or apolipoprotein (light blue); ii) detected with only 1 PSM in HEL GA (for enriched proteins) or HEL mock and HEL PR (for depleted proteins); iii) not mapped in ConsensusDBPath. Proteins names in parentheses identified by similarity.

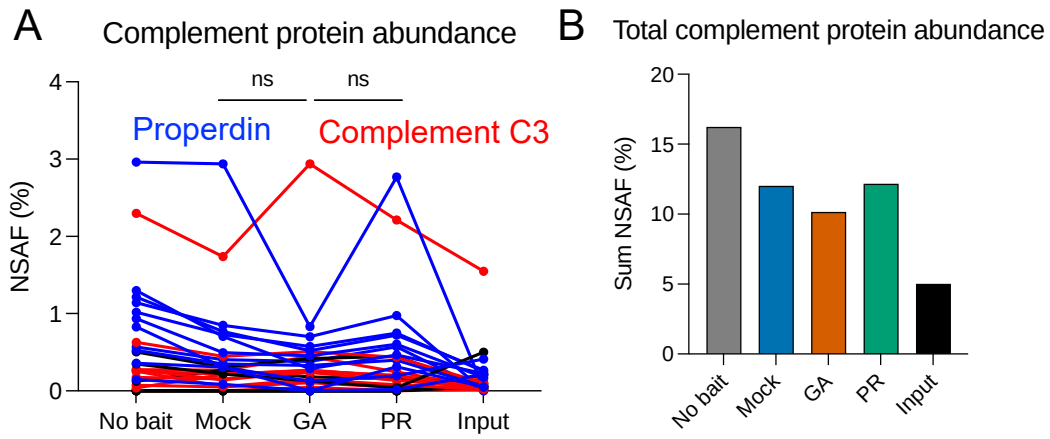


Figure 5.40: Complement proteins are least abundant in HEL GA co-IP. A) Individual NSAF values shown for 29 complement proteins. Each connected line represents a single protein either enriched (red), depleted (blue) or neither (black) in HEL GA co-IP compared with both HEL mock and HEL PR (repeated measures one-way ANOVA followed by Holm-Šídák's multiple comparisons test). B) Summed NSAF for the 29 complement proteins in each co-IP sample.

mock and HEL PR samples. C3 and properdin were highly abundant in the eluants relative to other complement proteins. In contrast to the pull-down results, HEL GA had the lowest amount of total complement proteins in the co-IP sample (**Figure 5.40B**).

For specific complement proteins, in HEL GA eluant there appeared to be increased C1s1, mannose-binding protein (MBP) subunit C, C1r, and C1q subunit B (but not subunits A or C) (**Figure 5.41**). However, these proteins were even more abundant in no HEL bait control, implying that beads with HyHEL-10 antibody were also binding C1 components. Downstream of complement initiation, enriched C4, C3 and C5 proteins in HEL GA relative to the other co-IP samples suggested increased complement activation. This complement activation did not appear to be mediated via the alternative pathway, since factor B and properdin were both depleted from HEL GA eluants. Negative regulators of complement amplification factor H and factor I were decreased in HEL GA sample. Finally, the presence of C8 (β-chain) and vitronectin in HEL GA sample suggested downstream effector function and inhibition respectively. Taken together, the pattern of

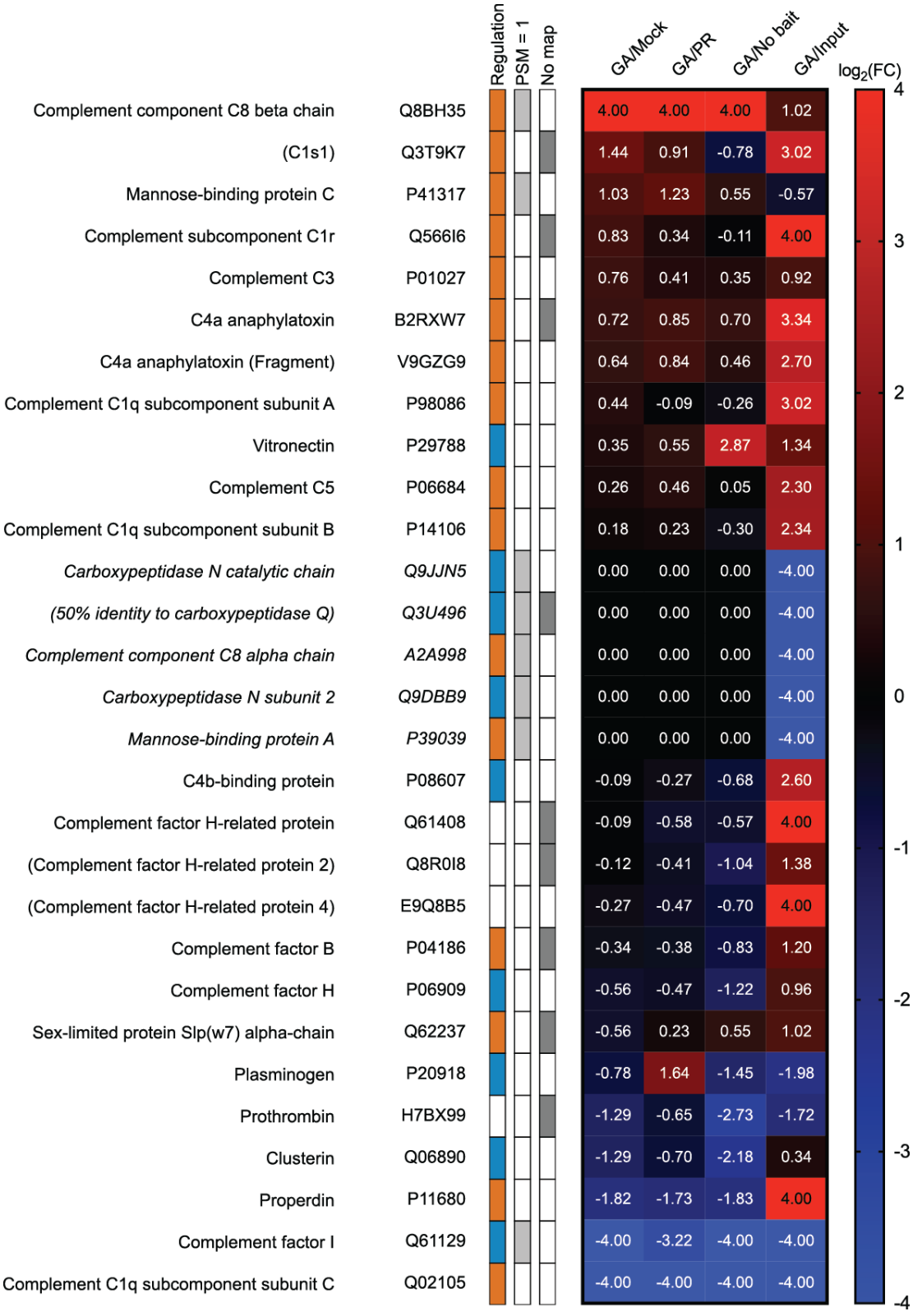


Figure 5.41: Increased classical or lectin complement activation and amplification in HEL GA co-IP compared with HEL mock and HEL PR. 29 complement proteins detected by co-IP MS shown with $\log_2$ transformed NSAF ratios of HEL GA over HEL mock, HEL PR, no bait and input controls. Ratios with missing NSAF values (i.e. not detected by MS) were set to −4 and 4. Sorted descending on GA/Mock. Covariate bars indicate proteins i) positive (blue) or negative (orange) regulators of complement cascade; ii) detected with only 1 PSM (light grey) in HEL GA (for enriched proteins) or HEL mock and HEL PR (for depleted proteins); iii) not mapped in ConsensusDBPath (dark grey). Protein names in parentheses identified by similarity, italicised proteins only detected in input sera.

complement protein enrichment and depletion suggested that HEL GA caused increased classical or lectin pathway but not alternative pathway initiation, and increased cascade amplification but terminated before MAC formation.

There were also no significant differences between HEL mock, HEL GA and HEL PR co-IP for immunoglobulins (**Figure 5.42A**). Of 48 immunoglobulins detected, 12 were more abundant and 22 were less abundant in HEL GA co-IP. The most striking result was the increase in IgM heavy constant levels in HEL GA eluant. As in the pull-down experiment, immunoglobulins were most abundant in no HEL bait control eluant followed by HEL GA (**Figure 5.42B**). In contrast to the pull-down experiment (where normal human sera were used), most peptides detected were mouse immunoglobulin variable rather than constant regions, and most could not be identified in online databases (**Figure 5.43**).

The presence of many proteins from the ribosome complex in HEL GA eluant suggested that ribosomes could preferentially interact with HEL GA bait. I compared the NSAF of all ribosome proteins in each sample, and found that ribosomal proteins were significantly enriched in HEL GA compared with HEL mock, and higher compared with HEL PR but not significant ($p = 0.1075$) (**Figure 5.44A**). Of the 15 ribosomal proteins detected, 9 were enriched and 1 was depleted in HEL GA co-IP. The relative total amount of ribosome protein was also highest in HEL GA eluant (**Figure 5.44B**). In contrast, apolipoproteins interacted significantly less with HEL GA compared with HEL mock, and less with HEL PR although again not statistically significant ($p = 0.2899$) (**Figure 5.45A**). Of the 12 apolipoproteins detected, only 1 was more abundant while 9 were less abundant in HEL GA co-IP. This corresponded with HEL GA co-IP having the lowest relative total amount of apolipoprotein detected (**Figure 5.45B**).

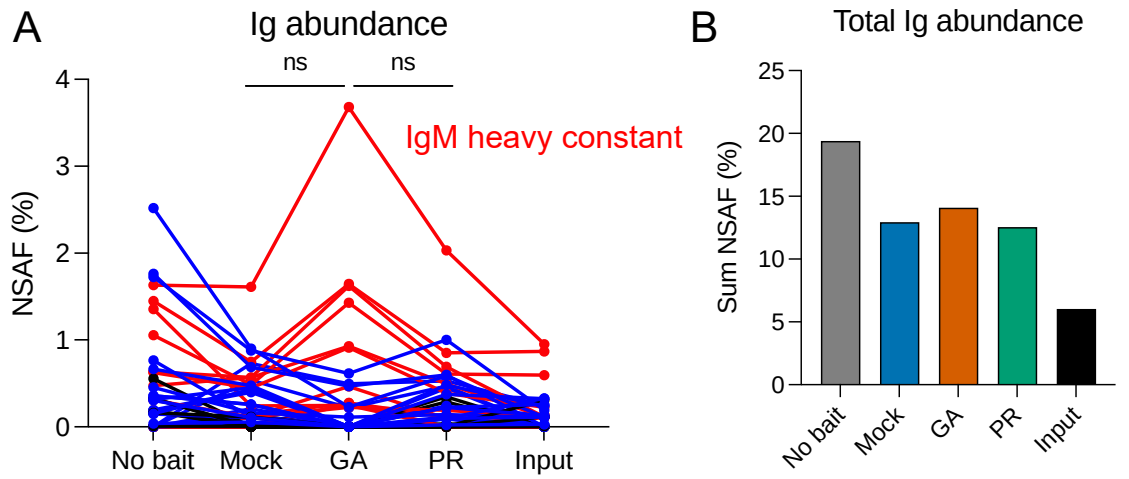


Figure 5.42: Immunoglobulins may be more abundant in no bait control and HEL GA co-IP. A) Individual NSAF values shown for 48 Igs. Each connected line represents a single protein either enriched (red), depleted (blue) or neither (black) in HEL GA co-IP compared with both HEL mock and HEL PR (repeated measures one-way ANOVA then Holm-Šídák's multiple comparisons test). B) Summed NSAF for the 48 Igs in each co-IP sample.

Finally, I determined whether there were any common hits between the pull-down and co-IP experiments. Out of 140 differentially pulled-down proteins from human plasma-derived sera and 148 differentially co-immunoprecipitated proteins from normal mouse sera, 35 proteins were common to both. Of these, 23 were similarly enriched or similarly depleted in both experiments, and 9 of these were detected with more than one PSM and with more abundance compared with input sera. The overlapping 9 proteins consisted of 5 complement proteins, 2 immunoglobulins, and 2 uncategorised proteins (**Table 5.3**). The uncategorised proteins were thrombospondin-1 (TSP-1) (enriched) and CD5 antigen-like (CD5L) (depleted).

5.2.8 Validation of immunoglobulin binding

Results from the pull-down and co-IP screens suggested that circulating IgM and IgG antibodies may bind more strongly to HEL GA compared with HEL mock and HEL PR. To follow up this observation, ELISA plates were coated with HEL mock, HEL GA or

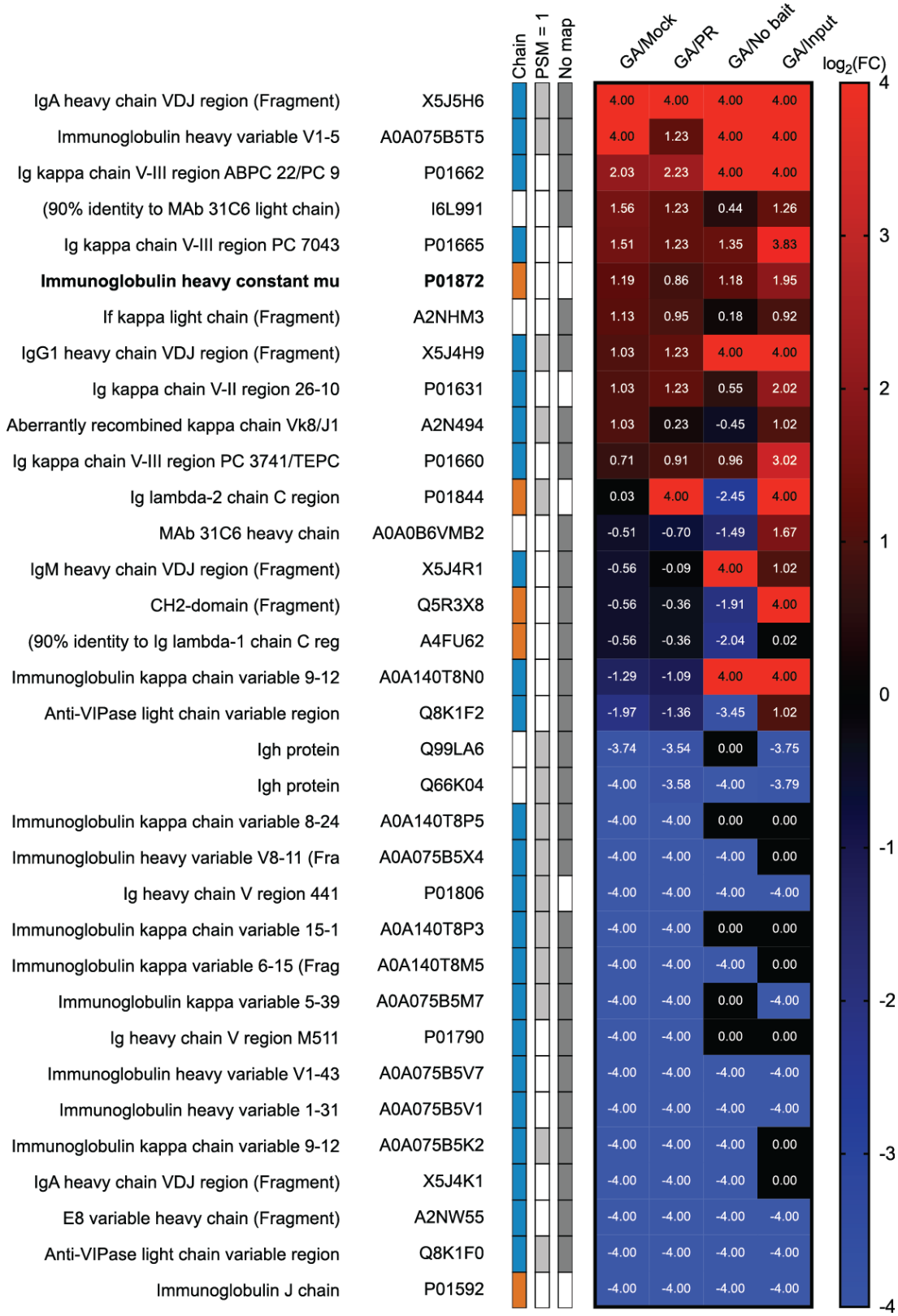


Figure 5.43: IgM constant region is enriched in HEL GA co-IP. 34 Igs detected by co-IP MS shown with $\log_2$ transformed NSAF ratios of HEL GA over HEL mock, HEL PR, no bait and input controls. Ratios with missing NSAF values (i.e. not detected by MS) were set to −4 and 4. Sorted descending on GA/Mock. Covariate bars indicate Ig with i) variable (blue) or constant (orange) regions; ii) detected with only 1 PSM (light grey) in HEL GA (for enriched proteins) or HEL mock and HEL PR (for depleted proteins); iii) not mapped in ConsensusDBPath (dark grey). Protein names in parentheses identified by similarity. 14 Igs detected only in no HEL bait and input controls not shown.

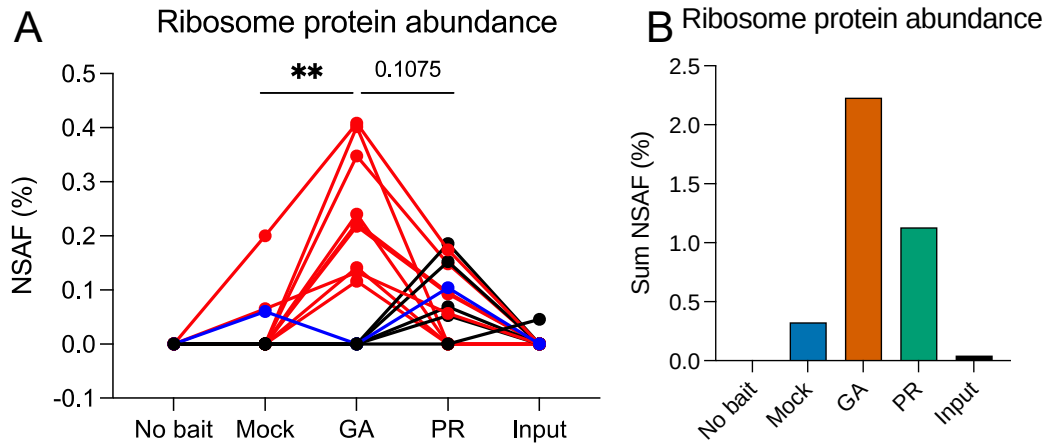


Figure 5.44: Ribosomal proteins are most abundant in HEL GA co-IP. A) Individual NSAF values shown for 15 ribosomal proteins. Each connected line represents a single protein either enriched (red), depleted (blue) or neither (black) in HEL GA co-IP compared with both HEL mock and HEL PR. Data were analysed with repeated measures one-way ANOVA followed by Holm-Šídák's multiple comparisons test. B) Summed NSAF for the 15 ribosomal proteins in each co-IP sample.

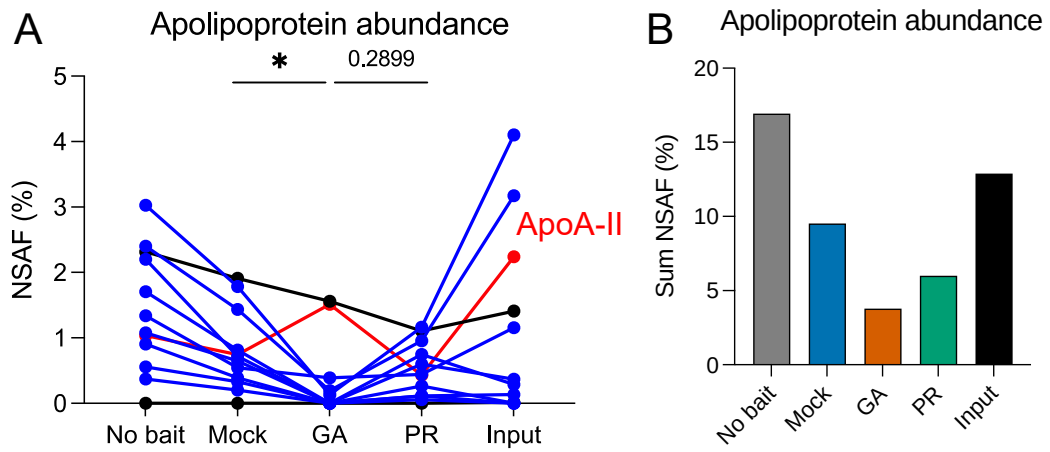


Figure 5.45: Apolipoproteins are least abundant in HEL GA co-IP. A) Individual NSAF values shown for 12 apolipoproteins. Each connected line represents a single protein either enriched (red), depleted (blue) or neither (black) in HEL GA co-IP compared with both HEL mock and HEL PR. Data were analysed with repeated measures one-way ANOVA followed by Holm-Šídák's multiple comparisons test. B) Summed NSAF for the 12 apoliproteins in each co-IP sample.

HEL PR and incubated with diluted normal mouse or human sera. Bound IgM and IgG were then detected using HRP-conjugated secondary antibodies. I observed slight increases in natural IgM antibody binding to HEL GA compared with HEL mock and HEL PR in pooled normal mouse sera (**Figure 5.46A**), as well as in-house off-the-clot human sera and TCS Biosciences non-filtered human sera (**Figure 5.46B**).

Table 5.3: Common hits between normal human sera pull-down and normal mouse sera co-IP. UniProt accession numbers provided for mouse proteins.

Protein	Accession	Class	Change
CD5 antigen-like	Q9QWK4		Down
Thrombospondin-1	P35441		Up
Complement C1q subcomponent subunit B	P14106	Complement	Up
Complement subcomponent C1r	Q566I6	Complement	Up
Complement C4-B	V9GZG9	Complement	Up
Complement C3	P01027	Complement	Up
Vitronectin	P29788	Complement	Up
Immunoglobulin heavy constant μ	P01872	Immunoglobulin	Up
Immunoglobulin κ light chain	A2NHM3	Immunoglobulin	Up

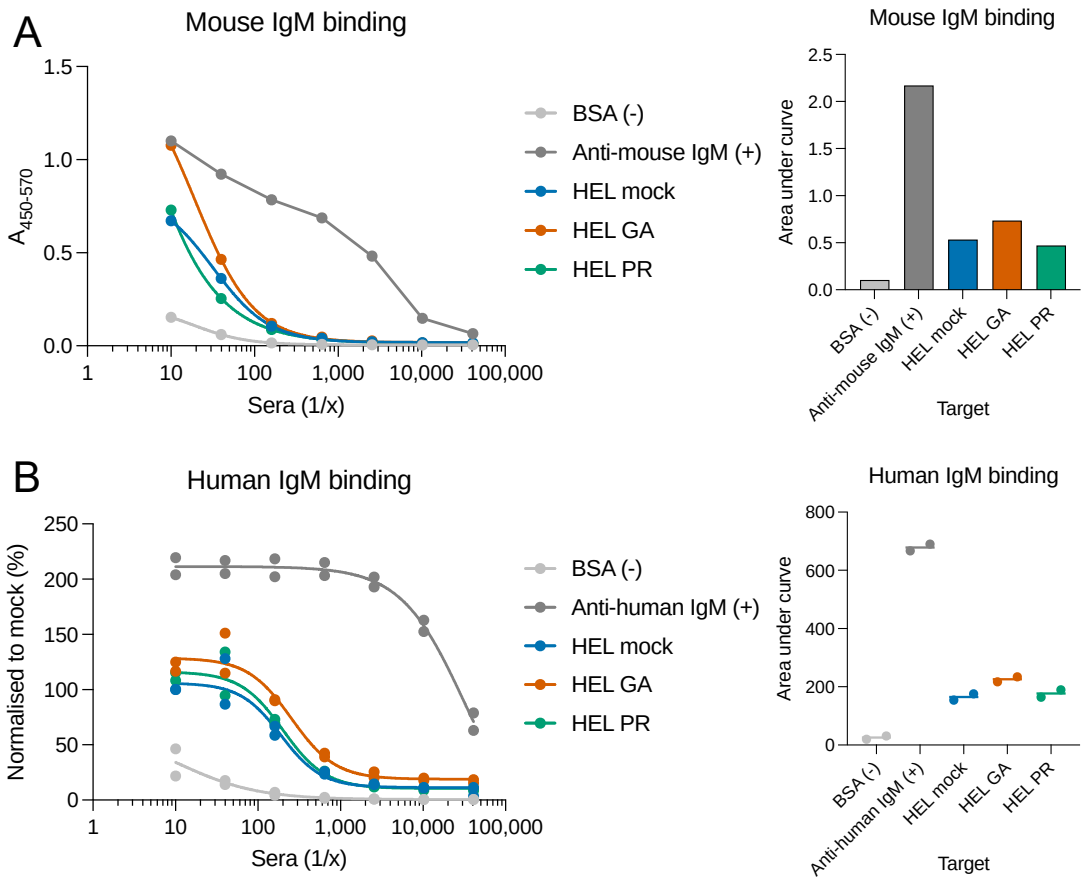


Figure 5.46: Natural IgM from sera may bind better to HEL GA compared with HEL mock and HEL PR. A) Normal mouse sera pooled from 3 mice and B) normal human sera were titrated onto targets and IgM binding was detected with HRP-conjugated secondary antibody. The area under the curve was quantified for each sample and plotted as a single dot.

In contrast, the signal detected in the mouse IgG binding ELISA did not titrate with sera concentration (**Figure 5.47A**). This indicated that IgG from normal mouse sera did not bind HEL, which would be consistent with the lack of anti-HEL IgG antibodies in naïve mice. Surprisingly, the background signal from (monoclonal rat IgG1) anti-mouse IgG secondary antibody was higher in HEL GA compared with HEL mock and HEL PR. Moreover, IgG antibodies in normal human sera recognised HEL, and also bound more strongly to HEL GA compared with HEL mock and HEL PR (**Figure 5.47B**).

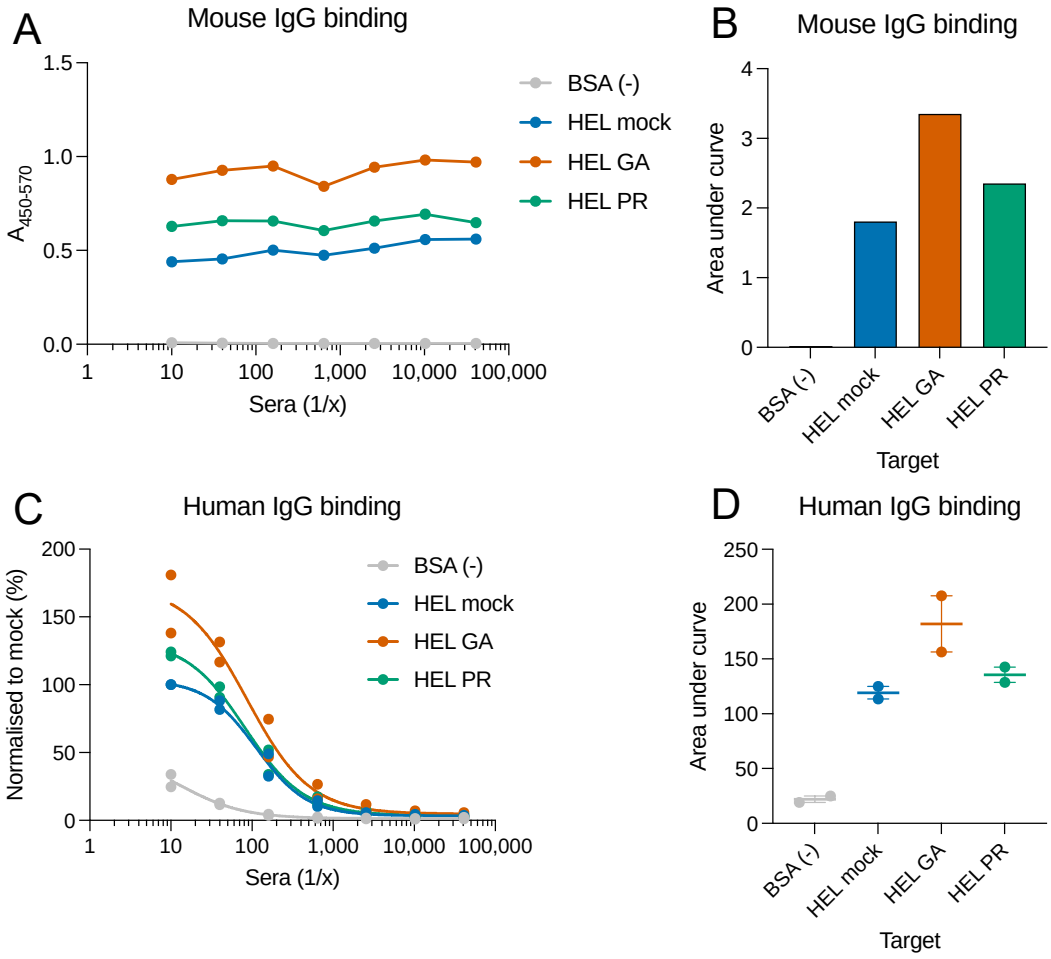


Figure 5.47: IgG from sera may bind better to HEL GA compared with HEL mock and HEL PR. A) Normal mouse sera pooled from 3 mice and B) normal human sera were titrated onto targets and IgG binding was detected with HRP-conjugated secondary antibody. The area under the curve was quantified for each sample and plotted as a single dot.

5.3 Discussion

5.3.1 Results summary

In this chapter, I investigated whether complement and other innate immune factors could mediate GA protein immunogenicity. ELISA binding assays, pull-down, and co-IP experiments suggested that C3 opsonisation may be enhanced for HEL GA compared with HEL mock and HEL PR. It was unclear whether complement activation was initiated by improved C1q binding to HEL GA.

Complement appeared to have an immunoregulatory role instead of an immunoenhancing role in GA-mediated immunogenicity. When normal mouse sera were added as a source of complement, MD4 splenocytes co-stimulated in vitro with HEL GA did not have enhanced B cell activation compared with HEL mock or HEL PR. Furthermore, C3-depleted and $C3^{-/-}$ mice showed heightened rather than dampened anti-HEL IgG responses compared with C3-functional mice.

Increased complement activation and natural IgM binding to HEL GA compared with HEL mock and HEL PR suggested that other innate immune pathways may be also activated by protein aldehydes. Finally, TSP-1 and CD5L were also identified as proteins of interest that interacted with HEL GA bait differently compared with HEL mock and HEL PR.

5.3.2 Non-specific C1q binding to HEL

Chikazawa et al. (2016) reported that the collagen-like region of C1q subunit A (C1qA) could interact with BSA GA 7 d directly via electrostatic interactions to initiate complement activation. Initially, we also observed enhanced binding of mouse and human C1q-biotin to HEL GA compared with HEL mock and HEL PR (**Figure 5.6**). However,

unbiotinylated C1q from normal mouse sera did not appear to bind HEL (**Figure 5.9B**), suggesting that HEL could be binding to biotin rather than to C1q.

The hypothesis that HEL directly binds to biotin and not to C1q is consistent with a reinterpretation of previous data from the lab (Harris 2020). In those experiments, un-biotinylated or biotinylated purified C1q were titrated on HEL mock, HEL GA, and HEL PR coated ELISA plates. Unbiotinylated C1q was detected with anti-C1q-biotin antibody (**Figure 5.8A**), while biotinylated C1q was directly detected using strep-HRP (**Figure 5.7A**). Anti-C1q-biotin was found to bind to HEL GA directly in the absence of purified C1q. Moreover, only biotinylated C1q showed dose-dependent binding to HEL mock, HEL GA and HEL PR.

Initially, I hypothesised that biotinylating C1q resulted in aggregation-induced non-specific binding. Assays performed with an old stock of (presumably aggregated) C1q but not freshly reconstituted stocks showed high non-specific binding to negative controls (**Figure 5.8B**). However, non-specific binding caused by biotinylation of C1q (and other proteins) has been demonstrated to be related to changes in protein hydrophobicity rather than sedimentation profile (i.e. aggregation) (Storm, Loos, and Kaul 1996).

An alternative explanation for non-specific C1q-biotin binding to HEL is that commercially purified HEL may be contaminated with avidin from egg white. The biotin-avidin interaction is one of the strongest non-covalent interactions in nature (Green 1963). The presence of avidin in HEL preparations could also explain why anti-C1q-biotin antibody can bind HEL directly (**Figure 5.9B**, no sera condition) and in a dose-dependent manner (Harris 2020). Conversely, the absence of avidin contamination in BSA could explain why C1q-biotin did not bind to BSA non-specifically (Chikazawa et al. 2016).

Given that both anti-C1q-biotin and C1q-biotin bind to HEL non-specifically in functional complement ELISAs, it is not yet clear whether C1q can bind to HEL GA. Pull-down and co-IP experiments suggested that C1q subunit B (C1qB), the subunit involved in Fc binding (Gaboriaud et al. 2012), was enriched in HEL GA compared with HEL mock and HEL PR samples (**Figure 5.28** and **Figure 5.41**). However, immunoglobulins were also enriched by HEL GA (**Figure 5.30** and **Figure 5.43**), suggesting that C1q could bind to HEL GA indirectly through immune complexes rather than directly as is the case for BSA GA 7 d.

The discrepancy of my result with the observations of Chikazawa et al. (2016) is likely to arise from the different GA modifications present on HEL GA 3 h and BSA GA 7 d. HEL GA 3 h is less extensively modified with GA-aldoamines, whereas BSA GA 7 d contains many more lysines and is likely to be extensively modified with complex AGEs such as GA-pyridine (**Figure 3.3**). Indeed, the different PTMs formed at the early and late stages of GA-modification have been shown to have different effects on scavenger receptor binding (Nagai et al. 2007).

To clarify the role of C1q in HEL GA complement activation, I sourced a non-biotinylated anti-C1q rat monoclonal antibody to overcome issues with non-specific biotin binding, and sera from C1q KO mice to determine whether C1q is required for C3 degradation product deposition. Future experiments could be performed using non-egg white derived model proteins such as mouse lysozyme and MSA.

5.3.3 Complement activation in mice and humans

Both normal mouse and human sera were used to test complement function in vitro. Although it would be ideal to use mouse sera because GA-mediated immunogenicity was

observed in immunised mice, mouse sera has considerable disadvantages in functional complement assays.

First, the mouse complement classical pathway is highly unstable and prone to spontaneous activation (Lachmann 2010). Second, the mouse genome is not well annotated compared with the human genome, which was evident from the lack of functional annotation for around half of the mouse proteins detected by co-IP (**Figure 5.38** and **Figure 5.39**). Third, few commercial mouse complement reagents are available (Mastellos et al. 2004). For functional complement ELISAs, specific monoclonal antibodies that recognise conformational neoepitopes are recommended to avoid detecting inactive native complement proteins (Mollnes et al. 2007; Oppermann and Würzner 2010). Our assays measured mouse C3 degradation product deposition using polyclonal goat anti-mouse C3d, as it was one of the few antibodies commercially available. The antibody was raised against recombinant mouse C3d and should be specific for activated C3. Nonetheless, to verify the mouse C3 degradation product deposition ELISA results I recently sourced a rat monoclonal antibody specific to mouse C3b/iC3b/C3c and not native C3 (Mastellos et al. 2004).

Although human complement reagents are readily available, we have not demonstrated GA-enhanced immunogenicity in humans. Moreover, normal human sera is not "naïve" and often contains antibodies against common model proteins developed after environmental exposure, which has been documented for BSA (Mogues et al. 2005). Target-bound IgG can activate complement through the classical pathway, which is an issue for assessing target-induced complement activation. Indeed, Chikazawa et al. (2016) used normal human sera to demonstrate that BSA GA 7 d could activate complement, but did not consider the effect of existing anti-BSA IgG antibodies. The human sera used in our lab also contained existing anti-HEL IgG antibodies (likely generated from dietary

exposure to eggs), while normal mouse sera did not (**Figure 5.47**). The presence of existing anti-HEL IgG could explain why human C3 degradation product deposition was much higher compared with mouse C3 degradation product deposition, and showed smaller differences between HEL mock, HEL GA and HEL PR (**Figure 5.11**). Proteins that are less likely to be encountered by humans, such as mouse lysozyme or MSA, could be used in future experiments to test the effect of GA protein modification on human complement activation.

Given the challenges with measuring bona fide complement activation, additional controls and multiple lines of evidence should be included in future experiments. For example, in complement activation ELISAs, EDTA can be added to prevent complement activation to demonstrate the specificity of monoclonal antibodies for activated rather than native complement proteins, and is preferable to heat inactivation that may expose conformational neoepitopes (Blom et al. 2015). Sera from complement knockout or depleted mice could be included as additional negative controls. Complement activation ELISAs should also titrate targets to demonstrate target-specific complement activation, since sera titrations could simply reflect spontaneous in vitro activation. Finally, complement activation could be confirmed by the presence of other activation complexes (e.g. MAC) or split products (e.g. C4b), some of which were indeed found in pull-down and co-IP experiments.

5.3.4 Comparison of pull-down and co-IP experiments

In both the pull-down and co-IP experiments, HEL GA had much less bait detected by tandem LC-MS compared with HEL mock and HEL PR samples (**Figure 5.23B–C** and **Figure 5.36C–D**). After the pull-down experiment, I hypothesised that conjugated HEL GA more readily detached from beads because it was slightly more abundant in SDS-

PAGE after bead boiling (**Figure 5.23A**), and therefore less available for on-bead digestion. However, HEL GA bait detection was only slightly improved by the co-IP approach.

In hindsight, the more probable explanation is that GA modification of lysines affects trypsin cleavage, which exclusively recognises lysine and arginine residues (Olsen, Ong, and Mann 2004). Indeed, issues with digesting lipoxidated (Liu, Minkler, and Sayre 2003) and glycated proteins (Lapolla et al. 2004) have been documented. Other enzymes that cleave less specifically, such as chymotrypsin, elastase, and proteinase K were used in those studies to overcome difficulties with digesting carbonylated proteins.

Given that the co-IP strategy did not resolve the issue with HEL GA bait protein detection, the pull-down approach is preferred for future repeat experiments. The HEL-specific mouse IgG1 antibody used for co-IP may actually inhibit C1q binding (Lilienthal et al. 2018) and interact with other serum components, which could affect the no-HEL bait control sample (**Figure 5.37**).

Non-specific interactions were also observed for the no-HEL bait control (i.e. beads only) in the pull-down experiment (**Figure 5.24**). The magnetic beads are made of iron oxide contained inside crosslinked polystyrene and coated with a hydrophilic layer of glycidyl ether and carboxylic acid groups (manufacturer's manual). Polymer surfaces can induce complement activation (Andersson et al. 2002), and indeed certain complement components such as C1qB, C1qC, ficolin-2, C3 and factor I were most abundant on the beads control sample (**Figure 5.28**). Beads coated with an irrelevant protein such as BSA may be a more suitable negative control. Finally, in addition to detecting proteins pulled-down by HEL-conjugated beads, the flow through could also be analysed for newly formed products such as C3 and C5 anaphylatoxins. This may provide further information about the serum factors activated by HEL GA.

5.3.5 Complement activation and immunogenicity

Complement C3 is thought to be required for normal antibody responses (Sörman et al. 2014). Therefore, I expected that $C3^{-/-}$ mice immunised with HEL CFA or HEL GA would have lower anti-HEL IgG responses compared with WT controls. However, my experiments with immunised $C3^{-/-}$ mice did not appear to have obvious defects in primary or secondary anti-HEL IgG production, since antibody responses in $C3^{-/-}$ mice were generally similar or higher than responses in WT mice (**Figure 5.20**).

One possible explanation is that the high dose (100 μg) HEL immunisation was sufficient to overcome C3 deficiency. $C3^{-/-}$ mice immunised intravenously with 3×10^7 plaque forming units (PFU) of bacteriophage ΦX 174 did not develop IgG responses, but IgG responses were partially restored with a 10-fold higher dose (Fischer et al. 1996). Moreover, studies showing that C3 is important for normal antibody responses have used more immunogenic molecules like sheep red blood cells (RBCs) (O'Neil et al. 1988) or microbes such as bacteriophage, (O'Neil et al. 1988; Fischer et al. 1996), influenza (Y.-J. Kim et al. 2018), herpes (Da Costa et al. 1999), and streptococcus B (Wessels et al. 1995). In contrast, Mener et al. (2018) observed that transfusion of mouse RBCs expressing human Kell (KEL) antigens into $C3^{-/-}$ mice elicited higher anti-KEL responses. The authors demonstrated that C3 deposition caused KEL antigen loss from RBCs, and concluded that C3 may negatively regulate antibody production against foreign antigens expressed on host cells.

HEL GA appeared to increase complement activation (C1qB, C1r, C4, C3, vitronectin) in vitro compared with HEL mock and HEL PR (**Figure 5.11, Figure 5.28** and **Figure 5.41**). However, $C3^{-/-}$ mice immunised with HEL GA had higher antibody responses compared with WT (**Figure 5.20**), suggesting that for HEL GA immunogenicity,

C3 was not immunoenhancing but rather immunoregulatory. This may be because C3 opsonisation is involved not only in positive regulation of B cell activation through iC3b/C3dg/C3d binding to CR2, but also in promoting phagocytosis and antigen clearance to prevent antibody responses (**Figure 5.5**). Moreover, a recent report showed that complement activation can produce fluid-phase C3d dimers, which can also interact with CR2 but appear to have B cell tolerogenic rather than stimulatory effects (Wahid et al. 2021). Other complement fragments, such as C1q, factor B and C4b, can also modulate B cell responses (Morgan et al. 2005).

The dual roles of complement in both enhancing and protecting against inflammation caused by damaged proteins are illustrated by MDA-modified proteins. Factor H can bind MDA-modified proteins to protect against excessive complement activation (Weismann et al. 2011). At the same time, C3a anaphylatoxin binding to MDA-modified proteins can increase inflammation and may be positively correlated with IgG antibody levels in vivo (Veneskoski et al. 2011).

Another complication that has not been explored in this thesis are sex differences in immune responses (Klein and Flanagan 2016). Previous experiments in our lab have typically used female mice to investigate immunogenicity (Section 3.2.1), but it is known that mouse complement is sexually dimorphic (Lachmann 2010). Future experiments should investigate the role of complement in male as well as female mice.

5.3.6 Potential protein interactions of interest with HEL GA

Although the pull-down and co-IP MS pilot experiments had single replicate samples using sera from different species, their preliminary results corroborated ELISA results and may provide insights into HEL GA interactions with serum proteins. The hierarchical

clustering of samples in both the pull-down and co-IP experiments agreed that HEL GA samples behaved differently to HEL mock and HEL PR (**Figure 5.24** and **Figure 5.37**).

A possible explanation could be that changing positively charged lysine residues to negatively charged carbonyls alters protein electronegativity, which may change electrostatic interactions with other proteins (Uchida 2013; Birts and Wilton 2021). For example, scavenger receptor recognition of ligands (Doi et al. 1993), C1qA and natural IgM recognition of GA-modified BSA (Chikazawa et al. 2016), and factor H binding to MDA-modified proteins (Hyvärinen et al. 2014) are mediated by negative charges.

Both the pull-down and co-IP experiments suggested that HEL GA increased immunoglobulin binding (IgM, Ig κ light chain). Prior experiments (Harris 2020) and my IgM binding ELISAs (**Figure 5.46**) seemed to confirm that natural IgM antibodies from naïve mouse and human plasma-derived sera bound more strongly to HEL GA compared with HEL mock and HEL PR. Indeed, natural IgM against AGE-modified proteins (Chikazawa et al. 2013), MDA-modified proteins (Palinski et al. 1990; Tsiantoulas et al. 2015) and HNE-modified proteins (Chou et al. 2009) have been documented in vivo and are thought to be important for neutralisation and clearance (Ryan, Nissim, and Winyard 2014; Binder 2010), suggesting that HEL GA could elicit additional immune protective mechanisms. IgM bound to HEL GA could also recruit C1q for complement activation.

Both MS experiments agreed that HEL GA enriched TSP-1 and depleted CD5L (**Table 5.3**). TSP-1 is a secreted multi-domain matricellular protein, exerting its many functions by binding to multiple receptors and proteins in the extracellular matrix (ECM) (Gutierrez and Gutierrez 2021; Isenberg and Roberts 2020; Lopez-Dee, Pidcock, and Gutierrez 2011). TSP-1 is mostly known for its anti-angiogenic properties, but is also involved in inflammation and immune modulation. TSP-1 interacts with numerous receptors, including scavenger receptor CD36 and CD47 (a “don’t eat me” signal), and can

convert transforming growth factor beta 1 (TGFβ1) from its latent form to its active form. CD5L, another pleiotropic protein, is mainly secreted by macrophages and belongs to the scavenger receptor cysteine-rich (SRCR) family (Sanchez-Moral et al. 2021). CD5L has mostly been studied as an anti-apoptosis protein, but also plays a key role in infectious and sterile inflammation. CD5L can act as a PRR by binding to DAMPs, and its main receptor is also scavenger receptor CD36.

There were some inconsistencies between the pull-down and co-IP experiments, and no conclusions could yet be drawn for certain hits. Overall, apolipoproteins were enriched in HEL GA pull-down (**Figure 5.31**) but depleted in HEL GA co-IP (**Figure 5.45**). Apolipoproteins have well-known functions in lipid transport and metabolism, but are also involved in innate immunomodulation (Cho and Seong 2009). Ribosome interactions with HEL GA were detected only in co-IP with normal mouse sera (**Figure 5.38** and **Figure 5.44**). This result was unexpected since ribosomes are intracellular, although ribosomes have recently been detected in the extracellular space (Tosar et al. 2020). Repeating the pull-down experiment using normal mouse sera with biological replicates would provide greater confidence about protein interaction leads that could underlie GA-mediated immunogenicity.

5.4 Conclusions

In this chapter, I investigated the role of innate immunity in mediating HEL GA immunogenicity. HEL GA interacted differently with normal mouse and human sera proteins compared with HEL mock and HEL PR, which was likely to be due to changes in electrostatic charge. The altered electrostatic interactions are consistent with an increase in complement activation and natural IgM binding as determined by ELISA, pull-down, and co-IP experiments.

Complement activation did not appear to enhance antibody responses, for example through the molecular adjuvant effects of C3d binding to CR2. In contrast, complement activation seemed to elicit immunoregulatory responses, because WT controls developed lower responses to HEL GA immunisation compared with C3-depleted and $C3^{-/-}$ mice. Increased natural IgM binding may also enhance the clearance of GA-modified proteins, as described for MDA, HNE, and AGE-modified proteins.

Overall, the results in this chapter suggest the activation of innate defence mechanisms in response to HEL GA immunisation. Pull-down and co-IP experiments revealed potentially interesting protein interactions with HEL GA that require further validation. The role of protein aldehydes in enhancing immunogenicity is yet to be elucidated.

Chapter 6

Discussion & Conclusion

6.1 Thesis summary

In this thesis, I aimed to characterise how protein aldehydes enhanced antibody responses to native carrier protein via modulation of the innate and adaptive immune systems.

In Chapter 3, I established that glycolaldehyde (GA) treatment could modify lysine residues with GA-aldoamines (protein aldehydes) and GA-pyridines (advanced glycation end-products, AGEs), depending on reaction conditions. Mice immunised with GA-aldoamine modified hen egg lysozyme (HEL) or its self-homologue mouse lysozyme (ML) elicited greater IgG antibody responses to the native carrier protein. Immunisation with post-reduced versions of GA-modified HEL or ML mostly abrogated the elevated responses.

In Chapter 4, I found that GA-modified HEL peptide and HEL protein could enhance in vitro antigen presentation to $CD4^+$ T cell hybridomas, but increased presentation was not abrogated by post-reduction. Moreover, I observed that GA modified HEL peptides and intact HEL protein at different sites and with possibly different chemistry.

Immunisation with GA-modified HEL peptide or HEL protein increased B cell memory responses but not in vivo $CD4^+$ T cell responses to native HEL protein.

In Chapter 5, I demonstrated that GA modification altered HEL interactions with many human and mouse serum proteins. Increased complement activation induced by immunisation with HEL GA appeared to have an immunoregulatory rather than immunoenhancing role in GA immunogenicity.

6.2 Intermediate aldehydes versus stable end-products

Stable end-products (i.e. either advanced glycation or lipoxidation end-products, EAGLEs) formed via protein carbonylation intermediates can be immunogenic by binding and/or activating innate immune receptors, and activate adaptive immunity as antigenic determinants recognised by T and B cell receptors. In contrast, the focus of my thesis was on how protein carbonylation *intermediates*, and specifically aldehydes, can increase immune responses to *native* protein rather than to neoepitopes on the modified protein.

Given the heterogeneity of non-enzymatic modification, however, it is very difficult to separate the effects of protein carbonylation from those of the stable end-products. Consequently, not many studies have attributed increased immunogenicity to the protein carbonyl intermediates without interference from the end-stage products. A few studies have attempted to distinguish between early and later stage products by using post-reduction or varying the extent of modification.

Takata et al. (1988) reported that macrophages efficiently took up bovine serum albumin (BSA) modified with 50 mM GA at 37 °C for 5 h and post-reduction did not abrogate uptake through scavenger receptor A (SR-A1). In contrast, BSA modified with GA in the presence of reducing agents to prevent formation of later stage AGEs was not taken up by macrophages, implying that later stage AGEs but not intermediate protein

aldehydes are critical for SR-A1 recognition. The extent of GA modification on BSA has also been positively correlated with SR binding and the rate of clearance from circulation (Nagai et al. 2007).

Similarly, low-density lipoprotein (LDL) extensively modified with GA or malondialdehyde (MDA) for longer periods of time or with higher concentrations of reactant showed decreased binding to the LDL receptor and increased recognition by SR-A (Haberland, Fogelman, and Edwards 1982; Haberland, Olch, and Folgelman 1984; Jinnouchi et al. 1998). These studies hypothesised that SR-A binding was positively correlated with the proportion of total lysines modified, but increased SR-A binding could also arise from the formation of more advanced PTMs. Finally, recent experiments in our lab also found no increase in bone marrow-derived dendritic cell (BMDC) uptake of 3 h GA-modified proteins, but much higher uptake for proteins extensively modified with glucose (Harris 2020).

Taken together, these studies could explain why proteins treated with GA then post-reduced with $NaBH_4$ remain somewhat immunogenic, particularly to T cells (**Figure 4.10**), and suggests that immunogenicity imparted by the aldehyde functional group and end-stage products may act through distinct mechanisms to enhance immunogenicity.

6.3 Alternative methods of protein aldehydation

In this thesis, the introduction of protein aldehydes was achieved by treating proteins with GA, which chemically modifies proteins on susceptible amino groups (Section 3.1.2). This investigation could be extended to introduce protein aldehydes by other reactive chemical species including oxidants (hypochlorous acid HOCl, peroxynitrate $ONOO^-$), lipoxidation by-products (4-hydroxy-2-nonenal HNE, acrolein, malondialdehyde MDA), carbohydrates (fructose, glyceraldehyde), certain reactive aldehyde species

(glutaraldehyde and succinimidyl 4-formylbenzoate SFB), and polyphenols with Cu^{2+} (Yamaguchi et al. 2021).

Indeed, our lab has demonstrated that proteins also become more immunogenic after treatment with HNE and MDA (Moghaddam et al. 2011). However, protein modification using chemical reactants is highly heterogeneous and the PTMs formed are often not-well characterised, making it extremely difficult to determine the effect of specific PTMs. Therefore, an important control is to treat proteins *subsequently* with sodium borohydride ($NaBH_4$) to reduce aldehydes to alcohols selectively (**Figure 3.2B**) and therefore distinguish between the effect of intermediate protein aldehydes and other modifications. However, Moghaddam et al. (2011) instead prepared HNE- and MDA-modified proteins *concurrently* with $NaBH_4$ (**Figure 3.2A**), which reduces aldehydes to alcohols but also prevents the formation of cross-linking and end-stage products.

Methods for protein modification that yield more homogeneous protein aldehydes will substantially help to determine the mechanism of aldehyde immunogenicity. Sodium (meta)periodate ($NaIO_4$) appears to introduce aldehydes more specifically than other chemical reactants by cleaving saccharides (Sklarz 1967), although under certain conditions $NaIO_4$ may also oxidise cysteine and methionine side chains (El-Mahdi and Melnyk 2013). Indeed, both Allison and Fearon (2000) and our lab (Moghaddam et al. 2011) have shown that $NaIO_4$-modified ovalbumin (OVA) increases immunogenicity. $NaIO_4$ can also introduce protein aldehydes by N-terminal cleavage of serine or threonine residues (Barlow, Guthrie, and Prior 1966; Geoghegan and Stroh 1992). However, protein aldehydes cannot be introduced to HEL using $NaIO_4$ because HEL does not contain any glycans and its N-terminal residue is lysine.

Interestingly, there are also naturally occurring enzymes that catalyse substrates to aldehyde-containing products. Fungi-derived galactose oxidase can cleave galactose-

containing glycans to introduce aldehydes (Novogrodsky and Katchalski 1973; Zheng et al. 1992), but again HEL does not have any glycans to modify. Lysyl oxidase (LOX) is an evolutionarily conserved copper-dependent amine oxidase that converts lysine to allysine (or α-aminadipic semialdehyde, AAS, **Figure 1.3A**) and in mammals is essential for cross-linking proteins of the extracellular matrix (ECM) (Grau-Bové, Ruiz-Trillo, and Rodriguez-Pascual 2015; Herchenhan et al. 2015). Formylglycine generating enzyme (FGE) is another evolutionarily conserved enzyme that converts cysteine residues to formylglycine. Formylglycine has a short aliphatic aldehyde that forms part of the catalytic site of sulfatases essential for activity (Landgrebe et al. 2003).

In the last two decades, there have been exciting developments in bioconjugation chemistry allowing different types of site-specific protein aldehyde (and ketone) tagging in defined locations with high purity and yields (Spears and Fascione 2016). Enzymes are used in vitro to convert residues directly or transfer site-specific aldehyde tags. FGE has been used to convert cysteine residues in CxPxR consensus sequences to formylglycine (Carrico, Carlson, and Bertozzi 2007), while protein farnesyl-transferase (PFTase) can install aldehyde-containing substrate analogues on the cysteine residue of CaaX sequences at a protein's C-terminus (Rashidian et al. 2010). *Escherichia coli*-derived lipoic acid ligase (Lp1A) mutants can incorporate aldehyde-containing substrate analogues on lysine side chains within the GFEIDKVWYDLDA acceptor sequence (Cohen, Zou, and Ting 2012), whereas tubulin tyrosine ligase (TTL) can install 3-formyl-L-tyrosine at a C-terminal tubulin-derived recognition sequence (Schumacher et al. 2015). Other strategies to introduce site-specific protein aldehydes include genetic incorporation of unnatural aldehyde-containing amino acids (Tuley et al. 2014), genetic incorporation of threonine-lysine dipeptide followed by $NaIO_4$ cleavage (Brabham et al. 2020), and epoxide ligand-directed affinity labelling followed by $NaIO_4$ cleavage (Song et al. 2020).

Although the bioconjugate chemistry approach may not be as physiologically relevant as protein modifications generated during oxidative and glycative stress, it provides a cleaner system for investigating the immune-activating role of reactive aldehydes in a site-specific manner and without potentially confounding end-product PTMs. However, some potential pitfalls are that multiple sites may need to be modified with protein aldehydes to observe immunogenic effects, since the extent of carbonylation and in vivo immunogenicity are positively correlated (Moghaddam et al. 2011). It should be noted that there are many types of protein aldehydes with different properties (Spears and Fascione 2016) that may have different effects in vivo. Moreover, some protein aldehydes are highly reactive and may concurrently exist in cyclic or cross-linked forms (Yamaguchi et al. 2021) that may not be preventable even after chromatographic separation.

6.4 Alternative model proteins

The nature and extent of protein modification is highly dependent on the protein, reactive species, and reaction conditions. HEL was investigated in this thesis because its relatively small size (14 kDa) made it particularly suitable for defining biochemical changes caused by GA, mapping T cell epitopes and studying peptide presentation. HEL is stable at a wide range of temperatures and pH, abundant in egg white, and readily available.

HEL has been extensively studied for the last century in various enzymatic, structural, and immunological studies (Johnson 1998). Many immunological tools are available, such as HEL-specific hybridomas and transgenic mice expressing soluble HEL (ML5 strain) (Goodnow et al. 1988), HEL-specific T cell receptors (TCRs) (3A9 TCR strain) (Ho et al. 1994) and HEL-specific B cell receptors (BCRs) (MD4 strain) (Mason, Jones, and Goodnow 1992). Future experiments could take advantage of HEL lysine and HEL

arginine mutants produced in our lab (**Table 3.3**). Since most GA modification occurs on lysine residues, this would allow us to control the amount of HEL carbonylation.

The key disadvantage of using HEL as a model protein is the protein's relatively low immunogenicity. HEL is intrinsically less immunogenic compared with larger proteins because it has fewer epitopes for T and B cell recognition. Moreover, HEL has only 6 lysines available for modification and lysine composition affects the extent of modification by GA (**Figure 3.22**). The effect of lysine composition on the degree of modification was also observed by the Thiele lab, who study DHP-lysines formed by malondialdehyde-acetaldehyde (MAA) modification (**Figure 1.6**). Under identical reaction conditions, each HEL molecule was modified with only one DHP-lysine (Willis et al. 2002) compared with 9 DHP-lysines on the larger protein BSA (Thiele et al. 1998).

Since IgG antibody responses appear to be correlated with the extent of carbonylation (Moghaddam et al. 2011) and the number of DHP-lysines (Willis et al. 2002), it could be advantageous to use a larger more modifiable protein to study protein aldehyde immunogenicity. Interestingly, the Thiele lab also found that less modification and lower doses directed antibody responses to native carrier protein only, while more modification and higher doses favoured antibody responses against both native protein and DHP-lysine (Thiele et al. 1998).

Experiments several decades ago demonstrated that C57BL/6 mice are particularly unresponsive to HEL immunisation (Hill and Sercarz 1975). Only 13 of 200 (6.5%) C57BL/6 mice immunised with 50 μg HEL emulsified in Complete Freund's Adjuvant (HEL CFA) generated anti-HEL plaque-forming cells (PFCs), and the few mice that responded had far fewer PFCs compared with other strains. Non-responsiveness to HEL in C57BL/6 mice was unrelated to dose, age or sex of the mice. Rather, the deficiency was related to HEL antigen processing and presentation to $CD4^+$ T cells in MHC haplotype

H-2^b mice (Manca et al. 1984; Kim and Jang 1992). Since most transgenic mouse strains are generated on a C57BL/6 background, it is problematic to use HEL as a model protein for such experiments. Indeed, previous members of the lab and I (**Figure 5.18B**) had difficulties detecting anti-HEL antibody responses in WT C57BL/6 mice.

Future experiments could use bovine ribonuclease (RNAse A), OVA or BSA as a model protein instead of HEL, especially in transgenic C57BL/6 mice. RNAse A is also a small 14 kDa protein, with 10 lysines and one N-glycan. The advantages of using RNAse A are that it is also a relatively small protein suitable for T cell studies and aldehydes can be introduced onto the N-glycan using $NaIO_4$. However, fewer immunological mouse tools have been developed for RNAse A.

OVA is the main protein found in egg white as a putative storage protein, and is one of two primary egg allergens, the other being ovomucoid. OVA is a 43 kDa protein with 20 lysines, 4 free cysteines, 1 N-glycan, and 2 phosphorylation sites. Like HEL, OVA is used extensively in immunological studies, with many OVA-specific hybridomas and strains of transgenic mice available. Due to its larger size and non-human glycan, OVA is intrinsically more immunogenic than HEL and has more than three times as many lysines available for modification.

Serum albumin primarily functions as a carrier protein but also has antioxidant properties and regulates osmotic pressure (Roche et al. 2008). Being the most abundant protein in vertebrate blood, serum albumin is particularly relevant in the context of oxidative stress, glycative stress and has been proposed as a biomarker for diabetes (Freitas, Ehlert, and Camargo 2017). Besides the low-density lipoprotein (LDL) protein complex, BSA and human serum albumin (HSA) have been extensively studied to assess the effects of EAGLEs (Ugur, Coffey, and Gronert 2012; Aldini et al. 2006; Temple, Yen, and Gronert 2006; Schalkwijk et al. 1999; Allarakha et al. 2015; Miyata 1997). BSA is a large

66 kDa protein with 59 lysines (of which 30−35 are free lysines, 5 times more than in HEL), 1 free cysteine, no glycans, and 10 phosphorylation sites. While there are fewer immunological tools for BSA, BSA has a long history of use as a conjugate carrier protein (G. T. Hermanson 2013).

6.5 Future prospects

The principal aim of my thesis was to define the mechanisms underpinning immune activation by protein aldehydes. I demonstrated that immunisation with aldehydated protein robustly stimulates B cells to produce antibodies against the native carrier protein. Based on this observation, there are several possible avenues for future investigation.

I investigated the role of complement components, in particular C3d as a potential B cell co-receptor activating factor. However, observations from C3-depleted and $C3^{-/-}$ mice do not support an immunoenhancing role for C3 in the context of aldehydated protein. Instead, the data suggest that complement components may have an immunosuppressive role and could protect against unwanted immune activation. The potential protective effects of complement in relation to protein aldehydes and similar damage-associated PTMs could be further investigated.

Since complement activation does not seem to underlie immune responses to protein aldehydes, it would be useful to continue exploring other mechanisms of innate immune activation. The unbiased proteomics approach to find serum proteins selectively associated with aldehydated proteins could yield further promising candidates and hypotheses. Similarly, systems vaccinology approaches looking at early transcriptional and cytokine responses after immunisation may shed more light on potential mechanisms.

T follicular helper (T_{FH}) cells are central to thymus-dependent B cell responses and their role has not yet been investigated in this project. Experiments to measure

germinal centre (GC) responses in draining lymph nodes could reveal a role for T_{FH}, GC B cells and follicular dendritic cells (FDCs) in GA-mediated immunogenicity. However, in light of the weak splenocyte memory recall responses observed with the current immunisation protocol, an appropriate protocol and immunogen dose would first need to be established to increase the likelihood of detecting rare T_{FH} cells.

Given that protein aldehydes are highly reactive, it is possible that the reactive aldehydes cross-link with endogenous proteins at the site of immunisation to form an antigen depot that enhances immunogenicity. Enzyme-linked immunosorbent assays (ELISAs) or immunohistochemistry could be used to investigate this hypothesis by assessing the propensity of GA-modified proteins to cross-link with other proteins, particularly structural proteins in the ECM. Mice could also be immunised with fluorescently labelled HEL for intravital imaging to determine whether HEL GA is removed from the site of injection or draining lymph nodes more slowly compared with controls immunised with HEL mock or HEL PR.

Finally, the generalisability of protein aldehyde immunogenicity could be tested with different model proteins and methods of cleanly introducing protein aldehydes, which would also help to elucidate the common mechanisms that underlie protein aldehyde immunogenicity.

Bibliography

Abeyrathne, E. D. N. S., Lee, H. Y., & Ahn, D. U. (2013). Egg white proteins and their potential use in food processing or as nutraceutical and pharmaceutical agents-A review. *Poultry Science*. https://doi.org/10.3382/ps.2013-03391

Acharya, A. S., & Manning, J. M. (1983). Reaction of glycolaldehyde with proteins: latent crosslinking potential of alpha-hydroxyaldehydes. *Proceedings of the National Academy of Sciences of the United States of America*. https://doi.org/10.1073/pnas.80.12.3590

Adrover, M., Vilanova, B., Muñoz, F., & Donoso, J. (2008). Kinetic study of the reaction of glycolaldehyde with two glycation target models. In *Annals of the New York Academy of Sciences*. https://doi.org/10.1196/annals.1433.008

Ahmed, N., & Furth, A. J. (1992). Failure of common glycation assays to detect glycation by fructose. *Clinical Chemistry*, *38*(7). https://doi.org/10.1093/clinchem/38.7.1301

Ahmed, R., & Gray, D. (1996). Immunological memory and protective immunity: Understanding their relation. *Science*, *272*(5258). https://doi.org/10.1126/science.272.5258.54

Akagawa, M. (2021). Protein carbonylation: molecular mechanisms, biological implications, and analytical approaches. *Free Radical Research*, *55*(4), 307–320. https://doi.org/10.1080/10715762.2020.1851027

Aldini, G., Gamberoni, L., Orioli, M., Beretta, G., Regazzoni, L., Facino, R. M., & Carini, M. (2006). Mass spectrometric characterization of covalent modification of human serum albumin by 4-hydroxy-trans-2-nonenal. *Journal of Mass Spectrometry*, *41*(9). https://doi.org/10.1002/jms.1067

Allarakha, S., Ahmad, P., Ishtikhar, M., Zaheer, M. S., Siddiqi, S. S., Moinuddin, & Ali, A. (2015). Fructosylation generates neo-epitopes on human serum albumin. *IUBMB Life*, *67*(5). https://doi.org/10.1002/iub.1375

Allen, J. C., Toapanta, F. R., Chen, W., & Tennant, S. M. (2020). Understanding immunosenescence and its impact on vaccination of older adults. *Vaccine*. https://doi.org/10.1016/j.vaccine.2020.11.002

Allison, M. E. D., & Fearon, D. T. (2000). Enhanced immunogenicity of aldehyde-bearing antigens: A possible link between innate and adaptive immunity. *European Journal of Immunology*, *30*(10), 2881–2887. https://doi.org/10.1002/1521-4141(200010)30:10<2881::AID-IMMU2881>3.0.CO;2-9

Amara, U., Flierl, M. A., Rittirsch, D., Klos, A., Chen, H., Acker, B., … Huber-Lang, M. (2010). Molecular Intercommunication between the Complement and Coagulation Systems. *The Journal of Immunology*, *185*(9). https://doi.org/10.4049/jimmunol.0903678

Amara, U., Rittirsch, D., Flierl, M., Bruckner, U., Klos, A., Gebhard, F., … Huber-Lang, M. (2008). Interaction between the coagulation and complement system. *Advances in Experimental Medicine and Biology*. https://doi.org/10.1007/978-0-387-78952-1_6

Amaya-Farfan, J., & Rodriguez-Amaya, D. B. (2021). The Maillard reactions. In *Chemical Changes During Processing and Storage of Foods*. https://doi.org/10.1016/b978-0-12-817380-0.00006-3

Amici, A., Levine, R. L., Tsai, L., & Stadtman, E. R. (1989). Conversion of amino acid residues in proteins and amino acid homopolymers to carbonyl derivatives by metal-catalyzed oxidation reactions. *Journal of Biological Chemistry*, *264*(6). https://doi.org/10.1016/s0021-9258(18)94071-8

Anderson, M. M., Hazen, S. L., Hsu, F. F., & Heinecke, J. W. (1997). Human neutrophils employ the myeloperoxidase-hydrogen peroxide-chloride system to convert hydroxy-amino acids into glycolaldehyde, 2-hydroxypropanal, and acrolein: A mechanism for the generation of highly reactive α-hydroxy and α,β-unsaturated aldehydes b. *Journal of Clinical Investigation*, *99*(3), 424–432. https://doi.org/10.1172/JCI119176

Andersson, J., Ekdahl, K. N., Larsson, R., Nilsson, U. R., & Nilsson, B. (2002). C3 Adsorbed to a Polymer Surface Can Form an Initiating Alternative Pathway Convertase. *The Journal of Immunology*, *168*(11), 5786–5791. https://doi.org/10.4049/jimmunol.168.11.5786

Annunziato, F., Romagnani, C., & Romagnani, S. (2015). The 3 major types of innate and adaptive cell-mediated effector immunity. *Journal of Allergy and Clinical Immunology*. https://doi.org/10.1016/j.jaci.2014.11.001

Antonioli, A. H., White, J., Crawford, F., Renner, B., Marchbank, K. J., Hannan, J. P., … Holers, V. M. (2018). Modulation of the Alternative Pathway of Complement by Murine Factor H–Related Proteins. *The Journal of Immunology*, *200*(1). https://doi.org/10.4049/jimmunol.1602017

Argirov, O. K., Lin, B., Olesen, P., & Ortwerth, B. J. (2003). Isolation and characterization of a new advanced glycation endproduct of dehydroascorbic acid and lysine. *Biochimica et Biophysica Acta (BBA) - General Subjects*, *1620*(1–3), 235–244. https://doi.org/10.1016/S0304-4165(03)00002-3

Bachmann, M. F., Rohrer, U. H., Kündig, T. M., Bürki, K., Hengartner, H., & Zinkernagel, R. M. (1993). The influence of antigen organization on B cell responsiveness. *Science*, *262*(5138). https://doi.org/10.1126/science.8248784

Baraibar, M. A., Liu, L., Ahmed, E. K., & Friguet, B. (2012). Protein oxidative damage at the crossroads of cellular senescence, aging, and age-related diseases. *Oxidative Medicine and Cellular Longevity*, *2012*. https://doi.org/10.1155/2012/919832

Barlow, C. B., Guthrie, R. D., & Prior, A. M. (1966). Periodate oxidation of amino-sugars. *Chemical Communications (London)*, (9). https://doi.org/10.1039/C19660000268

Barrington, R. A., Pozdnyakova, O., Zafari, M. R., Benjamin, C. D., & Carroll, M. C. (2002). B lymphocyte memory: Role of stromal cell complement and FcγRIIB receptors. *Journal of Experimental Medicine*, *196*(9). https://doi.org/10.1084/jem.20021110

Batista, F. D., & Harwood, N. E. (2009). The who, how and where of antigen presentation to B cells. *Nature Reviews Immunology*. https://doi.org/10.1038/nri2454

Békássy, Z. D., Kristoffersson, A. C., Rebetz, J., Tati, R., Olin, A. I., & Karpman, D. (2018). Aliskiren inhibits renin-mediated complement activation. *Kidney International*, *94*(4). https://doi.org/10.1016/j.kint.2018.04.004

Binder, C. J. (2010). Natural IgM antibodies against oxidation-specific epitopes. *Journal of Clinical Immunology*, *30*(SUPPL. 1), 56–60. https://doi.org/10.1007/s10875-010-9396-3

Binder, C. J., Hartvigsen, K., Chang, M. K., Miller, M., Broide, D., Palinski, W., … Witztum, J. L. (2004). IL-5 links adaptive and natural immunity specific for epitopes of oxidized LDL and protects from atherosclerosis. *Journal of Clinical Investigation*, *114*(3). https://doi.org/10.1172/JCI200420479

Binder, C. J., Papac-Milicevic, N., & Witztum, J. L. (2016). Innate sensing of oxidation-specific epitopes in health and disease. *Nature Reviews Immunology*, *16*(8), 485–497. https://doi.org/10.1038/nri.2016.63

Birts, C. N., & Wilton, D. C. (2021). Age, obesity and hyperglycaemia: Activation of innate immunity initiates a series of molecular interactions involving anionic surfaces leading to COVID-19 morbidity and mortality. *Medical Hypotheses*, *155*. https://doi.org/10.1016/j.mehy.2021.110646

Blom, A. M., Österborg, A., Mollnes, T. E., & Okroj, M. (2015). Antibodies reactive to cleaved sites in complement proteins enable highly specific measurement of soluble markers of complement activation. *Molecular Immunology*, *66*(2), 164–170. https://doi.org/10.1016/j.molimm.2015.02.029

Borbulevych, O. Y., Insaidoo, F. K., Baxter, T. K., Powell, D. J., Johnson, L. A., Restifo, N. P., & Baker, B. M. (2007). Structures of MART-126/27-35 peptide/HLA-A2 complexes reveal a remarkable disconnect between antigen structural homology and T cell recognition. *Journal of Molecular Biology*, *372*(5), 1123–1136. https://doi.org/10.1016/j.jmb.2007.07.025

Boyle, E. I., Weng, S., Gollub, J., Jin, H., Botstein, D., Cherry, J. M., & Sherlock, G. (2004). GO::TermFinder - Open source software for accessing Gene Ontology information and finding significantly enriched Gene Ontology terms associated with a list of genes. *Bioinformatics*, *20*(18). https://doi.org/10.1093/bioinformatics/bth456

Brabham, R. L., Keenan, T., Husken, A., Bilsborrow, J., McBerney, R., Kumar, V., … Fascione, M. A. (2020). Rapid sodium periodate cleavage of an unnatural amino acid enables unmasking of a highly reactive α-oxo aldehyde for protein bioconjugation. *Organic and Biomolecular Chemistry*, *18*(21). https://doi.org/10.1039/d0ob00972e

Brasel, K., De Smedt, T., Smith, J. L., & Maliszewski, C. R. (2000). Generation of murine dendritic cells from flt3-ligand-supplemented bone marrow cultures. *Blood*, *96*(9), 3029–3039. https://doi.org/10.1182/blood.v96.9.3029.h8003029_3029_3039

Braslavsky, S. E. (2007). Glossary of terms used in photochemistry 3rd edition: (IUPAC Recommendations 2006). *Pure and Applied Chemistry*. https://doi.org/10.1351/pac200779030293

Bretscher, P., & Cohn, M. (1970). A theory of self-nonself discrimination. *Science*, *169*(3950). https://doi.org/10.1126/science.169.3950.1042

Brinkhaus, M., Douwes, R. G. J., Bentlage, A. E. H., Temming, A. R., de Taeye, S. W., Tammes Buirs, M., … Vidarsson, G. (2020). Glycine 236 in the Lower Hinge Region of Human IgG1 Differentiates FcγR from Complement Effector Function. *The Journal of Immunology*, *205*(12), 3456–3467. https://doi.org/10.4049/jimmunol.2000961

Brown, G. D., Willment, J. A., & Whitehead, L. (2018). C-type lectins in immunity and homeostasis. *Nature Reviews Immunology*, *18*(6), 374–389. https://doi.org/10.1038/s41577-018-0004-8

Buss, H., Chan, T. P., Sluis, K. B., Domigan, N. M., & Winterbourn, C. C. (1997). Protein carbonyl measurement by a sensitive ELISA method. *Free Radical Biology and Medicine*, *23*(3), 361–366. https://doi.org/10.1016/S0891-5849(97)00104-4

Canfield, R. E. (1963). the Amino Acid Sequence of Egg White Lysozyme. *The Journal of Biological Chemistry*, *238*(8), 2698–2707. https://doi.org/10.1016/s0021-9258(18)67888-3

Carrico, I. S., Carlson, B. L., & Bertozzi, C. R. (2007). Introducing genetically encoded aldehydes into proteins. *Nature Chemical Biology*, *3*(6), 321–322. https://doi.org/10.1038/nchembio878

Carroll, M. C., & Isenman, D. E. (2012). Regulation of Humoral Immunity by Complement. *Immunity*, *37*(2), 199–207. https://doi.org/10.1016/j.immuni.2012.08.002

Carter, R. H., & Fearon, D. T. (1992). CD19: Lowering the Threshold for Antigen Receptor Stimulation of B Lymphocytes, *256*(April), 255–257.

Chand Bollineni, R., Fedorova, M., & Hoffmann, R. (2013). Qualitative and quantitative evaluation of derivatization reagents for different types of protein-bound carbonyl groups. *Analyst*, *138*(17), 5081–5088. https://doi.org/10.1039/c3an00724c

Chaplin, D. D. (2010). Overview of the immune response. *Journal of Allergy and Clinical Immunology*, *125*(2 SUPPL. 2). https://doi.org/10.1016/j.jaci.2009.12.980

Chavez, J., Wu, J., Han, B., Chung, W. G., & Maier, C. S. (2006). New role for an old probe: Affinity labeling of oxylipid protein conjugates by N′-aminooxymethylcarbonylhydrazino D-biotin. *Analytical Chemistry*, *78*(19), 6847–6854. https://doi.org/10.1021/ac0607257

Chen, D., Disotuar, M. M., Xiong, X., Wang, Y., & Chou, D. H. C. (2017). Selective N-terminal functionalization of native peptides and proteins. *Chemical Science*, *8*(4), 2717–2722. https://doi.org/10.1039/c6sc04744k

Chen, H. J. C., & Chung, F. L. (1996). Epoxidation of trans-4-hydroxy-2-nonenal by fatty acid hydroperoxides and hydrogen peroxide. *Chemical Research in Toxicology*, *9*(1). https://doi.org/10.1021/tx9501389

Chen, L., & Flies, D. B. (2013). Molecular mechanisms of T cell co-stimulation and co-inhibition. *Nature Reviews Immunology*. https://doi.org/10.1038/nri3405

Cherukuri, A., Cheng, P. C., Sohn, H. W., & Pierce, S. K. (2001). The CD19/CD21 complex functions to prolong B cell antigen receptor signaling from lipid rafts. *Immunity*, *14*(2), 169–179. https://doi.org/10.1016/S1074-7613(01)00098-X

Chikazawa, M., Otaki, N., Shibata, T., Miyashita, H., Kawai, Y., Maruyama, S., … Uchida, K. (2013). Multispecificity of immunoglobulin M antibodies raised against advanced glycation end products: Involvement of electronegative potential of antigens. *Journal of Biological Chemistry*, *288*(19), 13204–13214. https://doi.org/10.1074/jbc.M113.452177

Chikazawa, M., Shibata, T., Hatasa, Y., Hirose, S., Otaki, N., Nakashima, F., … Uchida, K. (2016). Identification of C1q as a Binding Protein for Advanced Glycation End Products. *Biochemistry*, *55*(3), 435–446. https://doi.org/10.1021/acs.biochem.5b00777

Chikazawa, M., Yoshitake, J., Lim, S. Y., Iwata, S., Negishi, L., Shibata, T., & Uchida, K. (2020). Glycolaldehyde is an endogenous source of lysine N-pyrrolation. *Journal of Biological Chemistry*, *295*(22), 7697–7709. https://doi.org/10.1074/jbc.RA120.013179

Cho, N. H., & Seong, S. Y. (2009). Apolipoproteins inhibit the innate immunity activated by necrotic cells or bacterial endotoxin. *Immunology*, *128*(1 PART 2). https://doi.org/10.1111/j.1365-2567.2008.03002.x

Cho, R. K., Okitani, A., & Kato, H. (1986). Polymerization of Acetylated Lysozyme and Impairment of Their Amino Acid Residues Due to α-Dicarbonyl and α-Hydroxycarbonyl Compounds. *Agricultural and Biological Chemistry*, *50*(6), 1373–1380. https://doi.org/10.1271/bbb1961.50.1373

Chondrogianni, N., Petropoulos, I., Grimm, S., Georgila, K., Catalgol, B., Friguet, B., … Gonos, E. S. (2014). Protein damage, repair and proteolysis. *Molecular Aspects of Medicine*, *35*(1), 1–71. https://doi.org/10.1016/j.mam.2012.09.001

Chou, M. Y., Fogelstrand, L., Hartvigsen, K., Hansen, L. F., Woelkers, D., Shaw, P. X., … Binder, C. J. (2009). Oxidation-specific epitopes are dominant targets of innate natural antibodies in mice and humans. *Journal of Clinical Investigation*, *119*(5). https://doi.org/10.1172/JCI36800

Cochrane, C. G., Müller-Eberhard, H. J., & Aikin, B. S. (1970). Depletion of plasma complement in vivo by a protein of cobra venom: its effect on various immunologic reactions. *J Immunol*, *105*, 55–69. https://doi.org/10.1016/0041-0101(71)90016-x

Cohen, J. D., Zou, P., & Ting, A. Y. (2012). Site-Specific Protein Modification Using Lipoic Acid Ligase and Bis-Aryl Hydrazone Formation. *ChemBioChem*, *13*(6). https://doi.org/10.1002/cbic.201100764

Coutinho, A., & Möller, G. (1973). B cell mitogenic properties of thymus-independent antigens. *Nature New Biology*, *245*(140). https://doi.org/10.1038/newbio245012a0

Crabb, J. W., O'Neil, J., Miyagi, M., West, K., & Hoff, H. F. (2002). Hydroxynonenal inactivates cathepsin B by forming Michael adducts with active site residues. *Protein Science*, *11*(4). https://doi.org/10.1110/ps.4400102

Crooke, S. N., Ovsyannikova, I. G., Poland, G. A., & Kennedy, R. B. (2019). Immunosenescence and human vaccine immune responses. *Immunity & Ageing*, *16*(1). https://doi.org/10.1186/s12979-019-0164-9

Crotty, S. (2014). T Follicular Helper Cell Differentiation, Function, and Roles in Disease. *Immunity*. https://doi.org/10.1016/j.immuni.2014.10.004

Da Costa, X. J., Brockman, M. A., Alicot, E., Ma, M., Fischer, M. B., Zhou, X., … Carroll, M. C. (1999). Humoral response to herpes simplex virus is complement-dependent. *Proceedings of the National Academy of Sciences of the United States of America*, *96*(22). https://doi.org/10.1073/pnas.96.22.12708

Dalle-Donne, I., Aldini, G., Carini, M., Colombo, R., Rossi, R., & Milzani, A. (2006). Protein carbonylation, cellular dysfunction, and disease progression. *Journal of Cellular and Molecular Medicine*. https://doi.org/10.1111/j.1582-4934.2006.tb00407.x

Dalle-Donne, I., Giustarini, D., Colombo, R., Rossi, R., & Milzani, A. (2003). Protein carbonylation in human diseases. *Trends in Molecular Medicine*, *9*(4), 169–176. https://doi.org/10.1016/S1471-4914(03)00031-5

Davis, C. A., H. Marder, and C. D. West. 1981. "Circulating Immune Complexes in Membranoproliferative Glomerulonephritis." *Kidney International* 20 (6). https://doi.org/10.1038/ki.1981.203.

Delamarre, L., Couture, R., Mellman, I., & Trombetta, E. S. (2006). Enhancing immunogenicity by limiting susceptibility to lysosomal proteolysis. *The Journal of Experimental Medicine*, *203*(9), 2049–2055. https://doi.org/10.1084/jem.20052442

Dempsey, P. W., Allison, M. E. D., Akkaraju, S., Goodnow, C. C., & Fearon, D. T. (1996). C3d of complement as a molecular adjuvant: Bridging innate and acquired immunity. *Science*, *271*(5247). https://doi.org/10.1126/science.271.5247.348

Depoil, D., Fleire, S., Treanor, B. L., Weber, M., Harwood, N. E., Marchbank, K. L., … Batista, F. D. (2008). CD19 is essential for B cell activation by promoting B cell receptor-antigen microcluster formation in response to membrane-bound ligand. *Nature Immunology*, *9*(1). https://doi.org/10.1038/ni1547

Doi, T., Higashino, K. I., Kurihara, Y., Wada, Y., Miyazaki, T., Nakamura, H., … Kodama, T. (1993). Charged collagen structure mediates the recognition of negatively charged macromolecules by macrophage scavenger receptors. *Journal of Biological Chemistry*, *268*(3). https://doi.org/10.1016/s0021-9258(18)53971-5

Drakesmith, H., O'Neil, D., Schneider, S. C., Binks, M., Medd, P., Sercarz, E., … Chain, B. (1998). In vivo priming of T cells against cryptic determinants by dendritic cells exposed to interleukin 6 and native antigen. *Proceedings of the National Academy of Sciences of the United States of America*. https://doi.org/10.1073/pnas.95.25.14903

Dunkelberger, J. R., & Song, W. C. (2010). Complement and its role in innate and adaptive immune responses. *Cell Research*, *20*(1), 34–50. https://doi.org/10.1038/cr.2009.139

Duryee, M. J., Freeman, T. L., Willis, M. S., Hunter, C. D., Hamilton, B. C., Suzuki, H., … Thiele, G. M. (2005). Scavenger receptors on sinusoidal liver endothelial cells are involved in the uptake of aldehyde-modified proteins. *Molecular Pharmacology*, *68*(5). https://doi.org/10.1124/mol.105.016121

El-Mahdi, O., & Melnyk, O. (2013). α-oxo aldehyde or glyoxylyl group chemistry in peptide bioconjugation. *Bioconjugate Chemistry*. https://doi.org/10.1021/bc300516f

Erdei, A., Sándor, N., Mácsik-Valent, B., Lukácsi, S., Kremlitzka, M., & Bajtay, Z. (2016). The versatile functions of complement C3-derived ligands. *Immunological Reviews*, *274*(1), 127–140. https://doi.org/10.1111/imr.12498

Fang, Y., Xu, C., Fu, Y. X., Holers, V. M., & Molina, H. (1998). Expression of complement receptors 1 and 2 on follicular dendritic cells is necessary for the generation of a strong antigen-specific IgG response. *Journal of Immunology (Baltimore, Md. : 1950)*, *160*(11).

Fearon, D. T., & Carter, R. H. (1995). The CD19/CR2/TAPA-1 complex of B lymphocytes: Linking natural to acquired immunity. *Annual Review of Immunology*. https://doi.org/10.1146/annurev.iy.13.040195.001015

Fearon, D. T., & Locksley, R. M. (1996). The instructive role of innate immunity in the acquired immune response. *Science*, *272*(5258). https://doi.org/10.1126/science.272.5258.50

Fedorova, M., Bollineni, R. C., & Hoffmann, R. (2014). Protein carbonylation as a major hallmark of oxidative damage: Update of analytical strategies. *Mass Spectrometry Reviews*. https://doi.org/10.1002/mas.21381

Fields, R., & Dixon, H. B. (1971). Micro method for determination of reactive carbonyl groups in proteins and peptides, using 2,4-dinitrophenylhydrazine. *The Biochemical Journal*, *121*(4), 587–589. https://doi.org/10.1042/bj1210587

Fingeroth, J. D., Heath, M. E., & Ambrosino, D. M. (1989). Proliferation of resting B cells is modulated by CR2 and CR1. *Immunology Letters*, *21*(4). https://doi.org/10.1016/0165-2478(89)90022-9

Fischer, M. B., Ma, M., Goerg, S., Zhou, X., Xia, J., Finco, O., … Carroll, M. C. (1996). Regulation of the B cell response to T-dependent antigens by classical pathway complement. *Journal of Immunology (Baltimore, Md. : 1950)*, *157*(2), 549–556.

Floor, E., Maples, A. M., Rankin, C. A., Yaganti, V. M., Shank, S. S., Nichols, G. S., … Williams, T. D. (2006). A one-carbon modification of protein lysine associated with elevated oxidative stress in human substantia nigra. *Journal of Neurochemistry*, *97*(2), 504–514. https://doi.org/10.1111/j.1471-4159.2006.03768.x

Freitas, P. A. C., Ehlert, L. R., & Camargo, J. L. (2017). Glycated albumin: A potential biomarker in diabetes. *Archives of Endocrinology and Metabolism*. https://doi.org/10.1590/2359-3997000000272

Fritzsche, S., Billig, S., Rynek, R., Abburi, R., Tarakhovskaya, E., Leuner, O., … Birkemeyer, C. (2018). Derivatization of methylglyoxal for LC-ESI-MS analysis—stability and relative sensitivity of different derivatives. *Molecules*, *23*(11). https://doi.org/10.3390/molecules23112994

Furuhata, A., Ishii, T., Kumazawa, S., Yamada, T., Nakayama, T., & Uchida, K. (2003). Nε-(3-methylpyridinium)lysine, a major antigenic adduct generated in Acrolein-modified protein. *Journal of Biological Chemistry*, *278*(49), 48658–48665. https://doi.org/10.1074/jbc.M309401200

Gaboriaud, C., Frachet, P., Thielens, N. M., & Arlaud, G. J. (2012). The human C1q globular domain: Structure and recognition of non-immune self ligands. *Frontiers in Immunology*, *2*(JAN), 1–8. https://doi.org/10.3389/fimmu.2011.00092

Gadjeva, M., Dodds, A. W., Taniguchi-Sidle, A., Willis, A. C., Isenman, D. E., & Law, S. K. A. (1998). The Covalent Binding Reaction of Complement Component C3. *Molecular Immunology*, *35*(6–7), 376. https://doi.org/10.1016/s0161-5890(98)90716-7

Gahmberg, C. G., & Andersson, L. C. (1977). Selective radioactive labeling of cell surface sialoglycoproteins by periodate-tritiated borohydride. *Journal of Biological Chemistry*, *252*(16). https://doi.org/10.1016/s0021-9258(17)40107-4

Gammon, G., Geysen, H. M., Apple, R. J., Pickett, E., Palmer, M., Ametani, A., & Sercarz, E. E. (1991). T cell determinant structure: Cores and determinant envelopes in three mouse major histocompatibility complex haplotypes. *Journal of Experimental Medicine*, *173*(3), 609–617. https://doi.org/10.1084/jem.173.3.609

Garred, P., Genster, N., Pilely, K., Bayarri-Olmos, R., Rosbjerg, A., Ma, Y. J., & Skjoedt, M. O. (2016). A journey through the lectin pathway of complement—MBL and beyond. *Immunological Reviews*. https://doi.org/10.1111/imr.12468

Gefen, T., Vaya, J., Khatib, S., Rapoport, I., Lupo, M., Barnea, E., … Pitcovski, J. (2015). The effect of haptens on protein-carrier immunogenicity. *Immunology*, *144*(1), 116–126. https://doi.org/10.1111/imm.12356

Geoghegan, K. F., & Stroh, J. G. (1992). Site-Directed Conjugation of Nonpeptide Groups to Peptides and Proteins Via Periodate Oxidation of a 2-Amino Alcohol. Application to Modification at N-Terminal Serine. *Bioconjugate Chemistry*, *3*(2). https://doi.org/10.1021/bc00014a008

Ghebrehiwet, B., Randazzo, B. P., Dunn, J. T., Silverberg, M., & Kaplan, A. P. (1983). Mechanisms of activation of the classical pathway of complement by Hageman factor fragment. *Journal of Clinical Investigation*, *71*(5). https://doi.org/10.1172/JCI110898

Glomb, M. A., & Monnier, V. M. (1995). Mechanism of protein modification by glyoxal and glycolaldehyde, reactive intermediates of the Maillard reaction. *Journal of Biological Chemistry*, *270*(17), 10017–10026. https://doi.org/10.1074/jbc.270.17.10017

Goicoechea De Jorge, E., Caesar, J. J. E., Malik, T. H., Patel, M., Colledge, M., Johnson, S., … Lea, S. M. (2013). Dimerization of complement factor H-related proteins modulates complement activation in vivo. *Proceedings of the National Academy of Sciences of the United States of America*, *110*(12). https://doi.org/10.1073/pnas.1219260110

Goodnow, C. C., Crosbie, J., Adelstein, S., Lavoie, T. B., Smith-Gill, S. J., Brink, R. A., … Basten, A. (1988). Altered immunoglobulin expression and functional silencing of self-reactive B lymphocytes in transgenic mice. *Nature*, *334*(6184). https://doi.org/10.1038/334676a0

Grace, P., Roberts, D. W., & Walker, J. D. (2003). QSARs for the skin sensitization potential of aldehydes and related compounds. *QSAR and Combinatorial Science*, *22*(2), 196–203. https://doi.org/10.1002/qsar.200390012

Grau-Bové, X., Ruiz-Trillo, I., & Rodriguez-Pascual, F. (2015). Origin and evolution of lysyl oxidases. *Scientific Reports*, *5*. https://doi.org/10.1038/srep10568

Green, N. M. (1963). Avidin. 1. The use of (14-C)biotin for kinetic studies and for assay. *The Biochemical Journal*, *89*(3), 585–591. https://doi.org/10.1042/bj0890585

Gribben, J. G., Devereux, S., Thomas, N. S. B., Keim, M., Jones, H. M., Goldstone, A. H., & Linch, D. C. (1990). Development of antibodies to unprotected glycosylation sites on recombinant human GM-CSF. *The Lancet*, *335*(8687). https://doi.org/10.1016/0140-6736(90)90665-R

Grimm, S., Ott, C., Hörlacher, M., Weber, D., Höhn, A., & Grune, T. (2012). Advanced-glycation-end-product-induced formation of immunoproteasomes: Involvement of RAGE and Jak2/STAT1. *Biochemical Journal*, *448*(1). https://doi.org/10.1042/BJ20120298

Grune, T., Merker, K., Jung, T., Sitte, N., & Davies, K. J. A. (2005). Protein oxidation and degradation during postmitotic senescence. *Free Radical Biology and Medicine*, *39*(9), 1208–1215. https://doi.org/10.1016/j.freeradbiomed.2005.06.009

Gutierrez, L. S., & Gutierrez, J. (2021). Thrombospondin 1 in Metabolic Diseases. *Frontiers in Endocrinology*, *12*(March), 1–12. https://doi.org/10.3389/fendo.2021.638536

Haberland, M. E., Fogelman, A. M., & Edwards, P. A. (1982). Specificity of receptor-mediated recognition of malondialdehyde-modified low density lipoproteins. *Proceedings of the National Academy of Sciences of the United States of America*, *79*(6 I). https://doi.org/10.1073/pnas.79.6.1712

Haberland, M. E., Olch, C. L., & Folgelman, A. M. (1984). Role of lysines in mediating interaction of modified low density lipoproteins with the scavenger receptor of human monocyte macrophages. *Journal of Biological Chemistry*, *259*(18), 11305–11311. https://doi.org/10.1016/s0021-9258(18)90863-x

Han, X., He, L., Xin, L., Shan, B., & Ma, B. (2011). PeaksPTM: Mass spectrometry-based identification of peptides with unspecified modifications. *Journal of Proteome Research*, *10*(7). https://doi.org/10.1021/pr200153k

Harding, F. A., Stickler, M. M., Razo, J., & DuBridge, R. B. (2010). The immunogenicity of humanized and fully human antibodies: Residual immunogenicity resides in the CDR regions. *MAbs*, *2*(3). https://doi.org/10.4161/mabs.2.3.11641

Harmel, R., & Fiedler, D. (2018). Features and regulation of non-enzymatic post-translational modifications. *Nature Chemical Biology*. https://doi.org/10.1038/nchembio.2575

Harris, S. L. (2020). *Immune system modulation by advanced glycation end products and their reactive intermediates (PhD thesis)*. University of Oxford.

Heilmann, M., Wellner, A., Gadermaier, G., Ilchmann, A., Briza, P., Krause, M., … Toda, M. (2014). Ovalbumin modified with pyrraline, a maillard reaction product, shows enhanced T-cell immunogenicity. *Journal of Biological Chemistry*, *289*(11), 7919–7928. https://doi.org/10.1074/jbc.M113.523621

Hensel, J. A., Khattar, V., Ashton, R., & Ponnazhagan, S. (2019). Characterization of immune cell subtypes in three commonly used mouse strains reveals gender and strain-specific variations. *Laboratory Investigation*, *99*(1). https://doi.org/10.1038/s41374-018-0137-1

Herchenhan, A., Uhlenbrock, F., Eliasson, P., Weis, M., Eyre, D., Kadler, K. E., … Kjaer, M. (2015). Lysyl oxidase activity is required for ordered collagen fibrillogenesis by tendon cells. *Journal of Biological Chemistry*, *290*(26). https://doi.org/10.1074/jbc.M115.641670

Hermanson, G. T. (2013). Chapter 19 - Vaccines and Immunogen Conjugates. In G. T. B. T.-B. T. (Third E. Hermanson (Ed.) (pp. 839–865). Boston: Academic Press. https://doi.org/https://doi.org/10.1016/B978-0-12-382239-0.00019-4

Hermeling, S., Crommelin, D. J. A., Schellekens, H., & Jiskoot, W. (2004). Structure-immunogenicity relationships of therapeutic proteins. *Pharmaceutical Research*. https://doi.org/10.1023/B:PHAM.0000029275.41323.a6

Hill, J. A., Southwood, S., Sette, A., Jevnikar, A. M., Bell, D. A., & Cairns, E. (2003). Cutting edge: The conversion of arginine to citrulline allows for a high-affinity peptide interaction with the rheumatoid arthritis-associated HLA-DRB1*0401 MHC class II molecule. *The Journal of Immunology*, *171*(2), 538–541. https://doi.org/10.4049/jimmunol.171.2.538

Hill, S. W., & Sercarz, E. E. (1975). Fine specificity of the H-2 linked immune response gene for the gallinaceous lysozymes. *European Journal of Immunology*, *5*(5). https://doi.org/10.1002/eji.1830050506

Hillson, W. R. (2013). *The role of thermal processing and protein oxidation in peanut allergy (PhD thesis)*. University of Oxford.

Ho, W. Y., Cooke, M. P., Goodnow, C. C., & Davis, M. M. (1994). Resting and anergic B cells are defective in CD28-dependent costimulation of naive CD4+ T cells. *Journal of Experimental Medicine*, *179*(5). https://doi.org/10.1084/jem.179.5.1539

Hodgkin, P. D., Heath, W. R., & Baxter, A. G. (2007). The clonal selection theory: 50 years since the revolution. *Nature Immunology*. https://doi.org/10.1038/ni1007-1019

Holers, V. M. (2014). Complement and its receptors: New insights into human disease. *Annual Review of Immunology*, *32*, 433–459. https://doi.org/10.1146/annurev-immunol-032713-120154

Holland, C. J., Cole, D. K., & Godkin, A. (2013). Re-directing CD4 + T cell responses with the flanking residues of MHC class II-bound peptides: The core is not enough. *Frontiers in Immunology*. https://doi.org/10.3389/fimmu.2013.00172

Holmquist, E., Okroj, M., Nodin, B., Jirström, K., & Blom, A. M. (2013). Sushi domain-containing protein 4 (SUSD4) inhibits complement by disrupting the formation of the classical C3 convertase. *FASEB Journal*, *27*(6). https://doi.org/10.1096/fj.12-222042

Hook, W. A., Carey, W. F., & Muschel, L. H. (1960). Alterations in Serum Lysozyme and Properdin Titers of Mice Following X-Irradiation or Treatment with Zymosan or Endotoxin. *The Journal of Immunology*, *84*(6), 569 LP – 575.

Horiuchi, S., Murakami, M., Takata, K., & Morino, Y. (1986). Scavenger receptor for aldehyde-modified proteins. *Journal of Biological Chemistry*, *261*(11), 4962–4966. https://doi.org/10.1016/s0021-9258(19)89199-8

Hyvärinen, S., Uchida, K., Varjosalo, M., Jokela, R., & Jokiranta, T. S. (2014). Recognition of malondialdehyde-modified proteins by the c terminus of complement factor h is mediated via the polyanion binding site and impaired by mutations found in atypical hemolytic uremic syndrome. *Journal of Biological Chemistry*, *289*(7). https://doi.org/10.1074/jbc.M113.527416

Insaidoo, F. K., Borbulevych, O. Y., Hossain, M., Santhanagopolan, S. M., Baxter, T. K., & Baker, B. M. (2011). Loss of T cell antigen recognition arising from changes in peptide and major histocompatibility complex protein flexibility: implications for vaccine design. *The Journal of Biological Chemistry*, *286*(46), 40163–40173. https://doi.org/10.1074/jbc.M111.283564

Irmscher, S., Döring, N., Halder, L. D., Jo, E. A. H., Kopka, I., Dunker, C., … Skerka, C. (2018). Kallikrein Cleaves C3 and Activates Complement. *Journal of Innate Immunity*, *10*(2). https://doi.org/10.1159/000484257

Isenberg, J. S., & Roberts, D. D. (2020). Thrombospondin-1 in maladaptive aging responses: A concept whose time has come. *American Journal of Physiology - Cell Physiology*, *318*(1), C45–C63. https://doi.org/10.1152/ajpcell.00089.2020

Ishii, T., Kumazawa, S., Sakurai, T., Nakayama, T., & Uchida, K. (2006). Mass spectroscopic characterization of protein modification by malondialdehyde. *Chemical Research in Toxicology*, *19*(1), 122–129. https://doi.org/10.1021/tx050231p

Ishii, T., Tatsuda, E., Kumazawa, S., Nakayama, T., & Uchida, K. (2003). Molecular basis of enzyme inactivation by an endogenous electrophile 4-hydroxy-2-nonenal: Identification of modification sites in glyceraldehyde-3-phosphate dehydrogenase. *Biochemistry*, *42*(12). https://doi.org/10.1021/bi027172o

Jacobson, A. C., & Weis, J. H. (2008). Comparative Functional Evolution of Human and Mouse CR1 and CR2. *The Journal of Immunology*, *181*(5). https://doi.org/10.4049/jimmunol.181.5.2953

Jaigirdar, S. A., & MacLeod, M. K. L. (2015). Development and function of protective and pathologic memory CD4 T cells. *Frontiers in Immunology*. https://doi.org/10.3389/fimmu.2015.00456

Janeway, C. A., & Medzhitov, R. (2002). Innate immune recognition. *Annual Review of Immunology*. https://doi.org/10.1146/annurev.immunol.20.083001.084359

Jang, Y. S., Mikszta, J. A., & Kim, B. S. (1994). T cell epitope recognition involved in the low-responsiveness to a region of hen egg lysozyme (46-61) in C57BL/6 mice. *Molecular Immunology*, *31*(11), 803–812. https://doi.org/10.1016/0161-5890(94)90018-3

Jensen, K. D. C., Sercarz, E. E., & Gabaglia, C. R. (2009). Altered peptide ligands can modify the Th2 T cell response to the immunodominant 161-175 peptide of LACK (Leishmania homolog for the receptor of activated C kinase). *Molecular Immunology*, *46*(3), 366–374. https://doi.org/10.1016/j.molimm.2008.10.024

Jiao, X., Sherman, B. T., Huang, D. W., Stephens, R., Baseler, M. W., Lane, H. C., & Lempicki, R. A. (2012). DAVID-WS: A stateful web service to facilitate gene/protein list analysis. *Bioinformatics*, *28*(13). https://doi.org/10.1093/bioinformatics/bts251

Jinnouchi, Y., Sano, H., Nagai, R., Hakamata, H., Kodama, T., Suzuki, H., … Horiuchi, S. (1998). Glycolaldehyde-modified low density lipoprotein leads macrophages to foam cells via the macrophage scavenger receptor. *Journal of Biochemistry*, *123*(6), 1208–1217. https://doi.org/10.1093/oxfordjournals.jbchem.a022062

Johnson, L. N. (1998). The early history of lysozyme. *Nature Structural Biology*. https://doi.org/10.1038/2917

Johnston-Carey, H. K., Pomatto, L. C. D., & Davies, K. J. A. (2016). The Immunoproteasome in oxidative stress, aging, and disease. *Critical Reviews in Biochemistry and Molecular Biology*. https://doi.org/10.3109/10409238.2016.1172554

Jones, V. E., & Leskowitz, S. (1965). Immunochemical study of antigenic specificity in delayed hypersensitivity. IV. The production of unresponsiveness to delayed hypersensitivity with a single antigenic determinant. *The Journal of Experimental Medicine*, *122*(3). https://doi.org/10.1084/jem.122.3.505

Josić, D., Buchacher, A., Kannicht, C., Lim, Y. P., Löster, K., Pock, K., … Stadler, M. (1999). Degradation products of factor VIII which can lead to increased immunogenicity. In *Vox Sanguinis* (Vol. 77). https://doi.org/10.1159/000056726

Józsi, M., Prechl, J., Bajtay, Z., & Erdei, A. (2002). Complement Receptor Type 1 (CD35) Mediates Inhibitory Signals in Human B Lymphocytes. *The Journal of Immunology*, *168*(6). https://doi.org/10.4049/jimmunol.168.6.2782

Kamala, T. (2007). Hock immunization: A humane alternative to mouse footpad injections. *Journal of Immunological Methods*, *328*(1–2), 204–214. https://doi.org/10.1016/j.jim.2007.08.004

Kamburov, A., Pentchev, K., Galicka, H., Wierling, C., Lehrach, H., & Herwig, R. (2011). ConsensusPathDB: Toward a more complete picture of cell biology. *Nucleic Acids Research*, *39*(SUPPL. 1). https://doi.org/10.1093/nar/gkq1156

Kapsenberg, M. L. (2003). Dendritic-cell control of pathogen-driven T-cell polarization. *Nature Reviews Immunology*. https://doi.org/10.1038/nri1246

Karlberg, A. T., Bergström, M. A., Börje, A., Luthman, K., & Nilsson, J. L. G. (2008). Allergic contact dermatitis - Formation, structural requirements, and reactivity of skin sensitizers. *Chemical Research in Toxicology*, *21*(1), 53–69. https://doi.org/10.1021/tx7002239

Kessler, M., Goldsmith, D., & Schellekens, H. (2006). Immunogenicity of biopharmaceuticals. *Nephrology Dialysis Transplantation*, *21*(suppl_5), v9–v12. https://doi.org/10.1093/ndt/gfl476

Killick, J., Morisse, G., Sieger, D., & Astier, A. L. (2018). Complement as a regulator of adaptive immunity. *Seminars in Immunopathology*, *40*(1), 37–48. https://doi.org/10.1007/s00281-017-0644-y

Kim, A. R., & Sadegh-Nasseri, S. (2015). Determinants of immunodominance for CD4 T cells. *Current Opinion in Immunology*. https://doi.org/10.1016/j.coi.2014.12.005

Kim, B. S., & Jang, Y. -S. (1992). Constraints in antigen processing result in unresponsiveness to a T cell epitope of hen egg lysozyme in C57BL/6 mice. *European Journal of Immunology*, *22*(3). https://doi.org/10.1002/eji.1830220322

Kim, Y.-J., Kim, K.-H., Ko, E.-J., Kim, M.-C., Lee, Y.-N., Jung, Y.-J., … Kang, S.-M. (2018). Complement C3 Plays a Key Role in Inducing Humoral and Cellular Immune Responses to Influenza Virus Strain-Specific Hemagglutinin-Based or Cross-Protective M2 Extracellular Domain-Based Vaccination. *Journal of Virology*, *92*(20). https://doi.org/10.1128/jvi.00969-18

Kim, Y. U., Kinoshita, T., Molina, H., Hourcade, D., Seya, T., Wagner, L. M., & Holers, V. M. (1995). Mouse complement regulatory protein crry/p65 uses the specific mechanisms of both human decay-accelerating factor and membrane cofactor protein. *Journal of Experimental Medicine*, *181*(1). https://doi.org/10.1084/jem.181.1.151

Kinoshita, T., Lavoie, S., & Nussenzweig, V. (1985). Regulatory proteins for the activated third and fourth components of complement (C3b and C4b) in mice. II. Identification and properties of complement receptor type 1(CR1). *The Journal of Immunology*, *134*(4).

Kinoshita, T., Thyphronitis, G., Tsokos, G. C., Finkelman, F. D., Hong, K., Sakai, H., & Inoue, K. (1990). Characterization of murine complement receptor type 2 and its immunological cross-reactivity with type 1 receptor. *International Immunology*, *2*(7). https://doi.org/10.1093/intimm/2.7.651

Klaus, A., Rau, R., & Glomb, M. A. (2018). Modification and Cross-Linking of Proteins by Glycolaldehyde and Glyoxal: A Model System. *Journal of Agricultural and Food Chemistry*, *66*(41), 10835–10843. https://doi.org/10.1021/acs.jafc.8b04023

Klein, S. L., & Flanagan, K. L. (2016). Sex differences in immune responses. *Nature Reviews Immunology*. https://doi.org/10.1038/nri.2016.90

Klose, C. S. N., & Artis, D. (2020). Innate lymphoid cells control signaling circuits to regulate tissue-specific immunity. *Cell Research*. https://doi.org/10.1038/s41422-020-0323-8

Kovács, K. G., Mácsik-Valent, B., Matkó, J., Bajtay, Z., & Erdei, A. (2021). Revisiting the Coreceptor Function of Complement Receptor Type 2 (CR2, CD21); Coengagement With the B-Cell Receptor Inhibits the Activation, Proliferation, and Antibody Production of Human B Cells. *Frontiers in Immunology*, *12*(April), 1–11. https://doi.org/10.3389/fimmu.2021.620427

Kumano-Kuramochi, M., Shimozu, Y., Wakita, C., Ohnishi-Kameyama, M., Shibata, T., Matsunaga, S., … Machida, S. (2012). Identification of 4-hydroxy-2-nonenal-histidine adducts that serve as ligands for human lectin-like oxidized LDL receptor-1. *Biochemical Journal*, *442*(1). https://doi.org/10.1042/BJ20111029

Kuriakose, A., Chirmule, N., & Nair, P. (2016). Immunogenicity of Biotherapeutics: Causes and Association with Posttranslational Modifications. *Journal of Immunology Research*, *2016*. https://doi.org/10.1155/2016/1298473

Kurtz, C. B., O'Toole, E., Christensen, S. M., & Weis, J. H. (1990). The murine complement receptor gene family. IV. Alternative splicing of Cr2 gene transcripts predicts two distinct gene products that share homologous domains with both human CR2 and CR1. *Journal of Immunology (Baltimore, Md. : 1950)*, *144*(9).

Lachmann, P. J. (2010). Preparing serum for functional complement assays. *Journal of Immunological Methods*, *352*(1–2), 195–197. https://doi.org/10.1016/j.jim.2009.11.003

Landgrebe, J., Dierks, T., Schmidt, B., & Von Figura, K. (2003). The human SUMF1 gene, required for posttranslational sulfatase modification, defines a new gene family which is conserved from pro- to eukaryotes. *Gene*, *316*(1–2). https://doi.org/10.1016/S0378-1119(03)00746-7

Lapolla, A., Fedele, D., Reitano, R., Aricò, N. C., Seraglia, R., Traldi, P., … Tonani, R. (2004). Enzymatic digestion and mass spectrometry in the study of advanced glycation end products/peptides. *Journal of the American Society for Mass Spectrometry*, *15*(4). https://doi.org/10.1016/j.jasms.2003.11.014

Laschtschenko, P. (1909). Uber die keimtötende und entwicklungshemmende Wirkung von Hühnereiweiß. *Zeitschrift Für Hygiene Und Infektionskrankheiten*, *64*(1), 419–427. https://doi.org/10.1007/BF02216170

Law, S. K., & Levine, R. P. (1977). Interaction between the third complement protein and cell surface macromolecules. *Proceedings of the National Academy of Sciences of the United States of America*, *74*(7). https://doi.org/10.1073/pnas.74.7.2701

Lemaitre, B., Nicolas, E., Michaut, L., Reichhart, J. M., & Hoffmann, J. A. (1996). The dorsoventral regulatory gene cassette spatzle/Toll/Cactus controls the potent antifungal response in Drosophila adults. *Cell*, *86*(6). https://doi.org/10.1016/S0092-8674(00)80172-5

Levine, R. L., Garland, D., Oliver, C. N., Amici, A., Climent, I., Lenz, A. G., … Stadtman, E. R. (1990). Determination of Carbonyl Content in Oxidatively Modified Proteins. *Methods in Enzymology*, *186*(C). https://doi.org/10.1016/0076-6879(90)86141-H

Li, D., & Wu, M. (2021). Pattern recognition receptors in health and diseases. *Signal Transduction and Targeted Therapy*, *6*(1), 1–24. https://doi.org/10.1038/s41392-021-00687-0

Lilienthal, G. M., Rahmöller, J., Petry, J., Bartsch, Y. C., Leliavski, A., & Ehlers, M. (2018). Potential of murine IgG1 and Human IgG4 to inhibit the classical complement and Fcγ receptor activation pathways. *Frontiers in Immunology*, *9*(MAY). https://doi.org/10.3389/fimmu.2018.00958

Liu, Z., Minkler, P. E., & Sayre, L. M. (2003). Mass spectroscopic characterization of protein modification by 4-hydroxy-2-(E)-nonenal and 4-oxo-2-(E)-nonenal. *Chemical Research in Toxicology*, *16*(7). https://doi.org/10.1021/tx0300030

Lopez-Dee, Z., Pidcock, K., & Gutierrez, L. S. (2011). Thrombospondin-1: Multiple paths to inflammation. *Mediators of Inflammation*, *2011*. https://doi.org/10.1155/2011/296069

Luckheeram, R. V., Zhou, R., Verma, A. D., & Xia, B. (2012). CD4 +T cells: Differentiation and functions. *Clinical and Developmental Immunology*. https://doi.org/10.1155/2012/925135

Lutz, M. B., Kukutsch, N., Ogilvie, A. L. J., Rößner, S., Koch, F., Romani, N., & Schuler, G. (1999). An advanced culture method for generating large quantities of highly pure dendritic cells from mouse bone marrow. *Journal of Immunological Methods*, *223*(1), 77–92. https://doi.org/10.1016/S0022-1759(98)00204-X

Madura, F., Rizkallah, P. J., Holland, C. J., Fuller, A., Bulek, A., Godkin, A. J., … Sewell, A. K. (2015). Structural basis for ineffective T-cell responses to MHC anchor residue-improved "heteroclitic" peptides. *European Journal of Immunology*, *45*(2), 584–591. https://doi.org/10.1002/eji.201445114

Manca, F., Clarke, J. A., Miller, A., Sercarz, E. E., & Shastri, N. (1984). A limited region within hen egg-white lysozyme serves as the focus for a diversity of T cell clones. *The Journal of Immunology*, *133*(4).

Mandels, T. E., Phippsi, R. P., Abbot, A., & Tew, J. G. (1980). The Follicular Dendritic Cell: Long Term Antigen Retention During Immunity. *Immunological Reviews*, *53*(1). https://doi.org/10.1111/j.1600-065X.1980.tb01039.x

Marcinkiewicz, J., Biedroń, R., Maresz, K., Kwaśny-Krochin, B., Bobek, M., Kontny, E., … Chain, B. (2004). Oxidative modification of type II collagen differentially affects its arthritogenic and tolerogenic capacity in experimental arthritis. *Archivum Immunologiae et Therapiae Experimentalis*, *52*(4), 284–291.

Mariño, L., Maya-Aguirre, C. A., Pauwels, K., Vilanova, B., Ortega-Castro, J., Frau, J., … Adrover, M. (2017). Glycation of Lysozyme by Glycolaldehyde Provides New Mechanistic Insights in Diabetes-Related Protein Aggregation. *ACS Chemical Biology*. https://doi.org/10.1021/acschembio.6b01103

Marshall, J. S., Warrington, R., Watson, W., & Kim, H. L. (2018). An introduction to immunology and immunopathology. *Allergy, Asthma and Clinical Immunology*. https://doi.org/10.1186/s13223-018-0278-1

Mason, D. Y., Jones, M., & Goodnow, C. C. (1992). Development and follicular localization of tolerant b lymphocytes in lysozyme/anti-lysozyme igm/lgd transgenic mice. *International Immunology*, *4*(2). https://doi.org/10.1093/intimm/4.2.163

Mastellos, D., Prechl, J. O., László, G., Papp, K., Oláh, E., Argyropoulos, E., … Erdei, A. (2004). Novel monoclonal antibodies against mouse C3 interfering with complement activation: Description of fine specificity and applications to various immunoassays. *Molecular Immunology*, *40*(16), 1213–1221. https://doi.org/10.1016/j.molimm.2003.10.019

Matsumoto, A. K., Martin, D. R., Carter, R. H., Klickstein, L. B., Ahearn, J. M., & Fearon, D. T. (1993). Functional dissection of the CD21/CD19/TAPA-1/Leu-13 complex of b lymphocytes. *Journal of Experimental Medicine*, *178*(4). https://doi.org/10.1084/jem.178.4.1407

McHeyzer-Williams, L. J., Malherbe, L. P., & McHeyzer-Williams, M. G. (2006). Helper T cell-regulated B cell immunity. *Current Topics in Microbiology and Immunology*. https://doi.org/10.1007/3-540-32636-7_3

McKenzie, A. N. J., Spits, H., & Eberl, G. (2014). Innate lymphoid cells in inflammation and immunity. *Immunity*. https://doi.org/10.1016/j.immuni.2014.09.006

Medzhitov, R., Preston-Hurlburt, P., Kopp, E., Stadlen, A., Chen, C., Ghosh, S., & Janeway, C. A. (1998). MyD88 is an adaptor protein in the hToll/IL-1 receptor family signaling pathways. *Molecular Cell*, *2*(2). https://doi.org/10.1016/S1097-2765(00)80136-7

Mellins, E. D., & Stern, L. J. (2014). HLA-DM and HLA-DO, key regulators of MHC-II processing and presentation. *Current Opinion in Immunology*, *26*(1), 115–122. https://doi.org/10.1016/j.coi.2013.11.005

Mener, A., Arthur, C. M., Patel, S. R., Liu, J., Hendrickson, J. E., & Stowell, S. R. (2018). Complement component 3 negatively regulates antibody response by modulation of red blood cell antigen. *Frontiers in Immunology*, *9*(JUN). https://doi.org/10.3389/fimmu.2018.00676

Meri, S., Morgan, B. P., Davies, A., Daniels, R. H., Olavesen, M. G., Waldmann, H., & Lachmann, P. J. (1990). Human protectin (CD59), an 18,000-20,000 MW complement lysis restricting factor, inhibits C5b-8 catalysed insertion of C9 into lipid bilayers. *Immunology*, *71*(1).

Merle, N. S., Noe, R., Halbwachs-Mecarelli, L., Fremeaux-Bacchi, V., & Roumenina, L. T. (2015). Complement system part II: Role in immunity. *Frontiers in Immunology*, *6*(MAY), 1–26. https://doi.org/10.3389/fimmu.2015.00257

Messele, T., Roos, M. T. L., Hamann, D., Koot, M., Fontanet, A. L., Miedema, F., … Rinke De Wit, T. F. (2000). Nonradioactive techniques for measurement of in vitro t-cell proliferation alternatives to the [3H]thymidine incorporation assay. *Clinical and Diagnostic Laboratory Immunology*, *7*(4). https://doi.org/10.1128/CDLI.7.4.687-692.2000

Miller, Y. I., Choi, S. H., Wiesner, P., Fang, L., Harkewicz, R., Hartvigsen, K., … Witztum, J. L. (2011). Oxidation-specific epitopes are danger-associated molecular patterns recognized by pattern recognition receptors of innate immunity. *Circulation Research*, *108*(2), 235–248. https://doi.org/10.1161/CIRCRESAHA.110.223875

Minutti, C. M., Jackson-Jones, L. H., García-Fojeda, B., Knipper, J. A., Sutherland, T. E., Logan, N., … Allen, J. E. (2017). Local amplifiers of IL-4Ra-mediated macrophage activation promote repair in lung and liver. *Science*, *356*(6342), 1076–1080. https://doi.org/10.1126/science.aaj2067

Miyata, S. (1997). Accumulation of pyrraline-modified albumin in phagocytes due to reduced degradation by lysosomal enzymes. *Journal of Biological Chemistry*, *272*(7). https://doi.org/10.1074/jbc.272.7.4037

Mlakar, A., Batna, A., Dudda, A., & Spiteller, G. (1996). Iron (II) ions induced oxidation of ascorbic acid and glucose. *Free Radical Research*, *25*(6). https://doi.org/10.3109/10715769609149074

Mogensen, T. H. (2009). Pathogen recognition and inflammatory signaling in innate immune defenses. *Clinical Microbiology Reviews*. https://doi.org/10.1128/CMR.00046-08

Moghaddam, A. E. (2001). *Increasing the immunogenicity of gp120 of HIV-1 by aldehyde modification (MSc thesis)*. Imperial College London.

Moghaddam, A. E., Gartlan, K. H., Kong, L., & Sattentau, Q. J. (2011). Reactive carbonyls are a major Th2-inducing damage-associated molecular pattern generated by oxidative stress. *The Journal of Immunology*, *187*(4), 1626–1633. https://doi.org/10.4049/jimmunol.1003906

Moghaddam, A. E., Olszewska, W., Wang, B., Tregoning, J. S., Helson, R., Sattentau, Q. J., & Openshaw, P. J. M. (2006). A potential molecular mechanism for hypersensitivity caused by formalin-inactivated vaccines. *Nature Medicine*, *12*(8), 905–907. https://doi.org/10.1038/nm1456

Mogues, T., Li, J., Coburn, J., & Kuter, D. J. (2005). IgG antibodies against bovine serum albumin in humans - Their prevalence and response to exposure to bovine serum albumin. *Journal of Immunological Methods*, *300*(1–2). https://doi.org/10.1016/j.jim.2005.01.022

Moheimani, F., Morgan, P. E., van Reyk, D. M., & Davies, M. J. (2010). Deleterious effects of reactive aldehydes and glycated proteins on macrophage proteasomal function: Possible links between diabetes and atherosclerosis. *Biochimica et Biophysica Acta - Molecular Basis of Disease*, *1802*(6), 561–571. https://doi.org/10.1016/j.bbadis.2010.02.007

Mollnes, T. E., Garred, P., & Bergseth, G. (1988). Effect of time, temperature and anticoagulants on in vitro complement activation: consequences for collection and preservation of samples to be examined for complement activation. *Clinical and Experimental Immunology*, *73*(3).

Mollnes, T. E., Jokiranta, T. S., Truedsson, L., Nilsson, B., Rodriguez de Cordoba, S., & Kirschfink, M. (2007). Complement analysis in the 21st century. *Molecular Immunology*, *44*(16), 3838–3849. https://doi.org/10.1016/j.molimm.2007.06.150

Mond, J. J., Vos, Q., Lees, A., & Snapper, C. M. (1995). T cell independent antigens. *Current Opinion in Immunology*, *7*(3). https://doi.org/10.1016/0952-7915(95)80109-X

Moon, J. J., Chu, H. H., Hataye, J., Pagán, A. J., Pepper, M., McLachlan, J. B., … Jenkins, M. K. (2009). Tracking epitope-specific T cells. *Nature Protocols*, *4*(4). https://doi.org/10.1038/nprot.2009.9

Moore, W. V., & Leppert, P. (1980). Role of aggregated human growth hormone (hGH) in development of antibodies to hGH. *Journal of Clinical Endocrinology and Metabolism*, *51*(4). https://doi.org/10.1210/jcem-51-4-691

Morgan, B. P., Marchbank, K. J., Longhi, M. P., Harris, C. L., & Gallimore, A. M. (2005). Complement: Central to innate immunity and bridging to adaptive responses. In *Immunology Letters* (Vol. 97). https://doi.org/10.1016/j.imlet.2004.11.010

Moss, C. X., Matthews, S. P., Lamont, D. J., & Watts, C. (2005). Asparagine deamidation perturbs antigen presentation on class II major histocompatibility complex molecules. *Journal of Biological Chemistry*, *280*(18), 18498–18503. https://doi.org/10.1074/jbc.M501241200

Müllbacher, A., Woodhams, C. E., Tomaska, L. D., Pereira, R. A., Ashman, R. B., & Blanden, R. V. (1985). Mouse serum as a medium supplement for murine immune responses in vitro. *Journal of Immunological Methods*, *76*(1), 17–26. https://doi.org/10.1016/0022-1759(85)90477-6

Muzio, M., Ni, J., Feng, P., & Dixit, V. M. (1997). IRAK (Pelle) family member IRAK-2 and MyD88 as proximal mediators of IL- 1 signaling. *Science*, *278*(5343). https://doi.org/10.1126/science.278.5343.1612

Nagai, R., Hayashi, C. M., Xia, L., Takeya, M., & Horiuchi, S. (2002). Identification in human atherosclerotic lesions of GA-pyridine, a novel structure derived from glycolaldehyde-modified proteins. *Journal of Biological Chemistry*, *277*(50), 48905–48912. https://doi.org/10.1074/jbc.M205688200

Nagai, R., Matsumoto, K., Ling, X., Suzuki, H., Araki, T., & Horiuchi, S. (2000). Glycolaldehyde, a reactive intermediate for adcanced glycation end products, plays an important role in the generation of an active ligand for the macrophage scavenger receptor. *Diabetes*, *49*(10), 1714–1723. https://doi.org/10.2337/diabetes.49.10.1714

Nagai, R., Mera, K., Nakajou, K., Fujiwara, Y., Iwao, Y., Imai, H., … Otagiri, M. (2007). The ligand activity of AGE-proteins to scavenger receptors is dependent on their rate of modification by AGEs. *Biochimica et Biophysica Acta - Molecular Basis of Disease*, *1772*(11–12), 1192–1198. https://doi.org/10.1016/j.bbadis.2007.09.001

Nagai, R., Shirakawa, J. ichi, Ohno, R. ichi, Hatano, K., Sugawa, H., Arakawa, S., … Nagai, M. (2016). Antibody-based detection of advanced glycation end-products: promises vs. limitations. *Glycoconjugate Journal*, *33*(4), 545–552. https://doi.org/10.1007/s10719-016-9708-9

Nagasawa, S., Ichihara, C., & Stroud, R. M. (1980). Cleavage of C4b by C3b inactivator: Production of a nicked form of C4b, C4b', as an intermediate cleavage product of C4b by C3b inactivator. *The Journal of Immunology*, *125*(2).

Nakamura, J., Shimomoto, T., Collins, L. B., Holley, D. W., Zhang, Z., Barbee, J. M., … Bultman, S. J. (2017). Evidence that endogenous formaldehyde produces immunogenic and atherogenic adduct epitopes. *Scientific Reports*, *7*(1). https://doi.org/10.1038/s41598-017-11289-8

Namiki, M., & Hayashi, T. (1975). Development of Novel Free Radicals during the Amino-Carbonyl Reaction of Sugars with Amino Acids. *Journal of Agricultural and Food Chemistry*, *23*(3), 487–491. https://doi.org/10.1021/jf60199a024

Nelson, D. S., & Shneider, C. N. (1974). Effect of normal mouse serum on mouse lymphocyte transformation in vitro. *European Journal of Immunology*, *4*(2), 79–86. https://doi.org/10.1002/eji.1830040205

Nilsson, B., & Nilsson Ekdahl, K. (2012). The tick-over theory revisited: Is C3 a contact-activated protein? *Immunobiology*. https://doi.org/10.1016/j.imbio.2012.07.008

Novogrodsky, A., & Katchalski, E. (1973). Induction of lymphocyte transformation by sequential treatment with neuraminidase and galactose oxidase. *Proceedings of the National Academy of Sciences of the United States of America*, *70*(6). https://doi.org/10.1073/pnas.70.6.1824

Nyström, T. (2005). Role of oxidative carbonylation in protein quality control and senescence. *EMBO Journal*, *24*(7), 1311–1317. https://doi.org/10.1038/sj.emboj.7600599

O'Neil, K. M., Ochs, H. D., Heller, S. R., Cork, L. C., Morris, J. M., & Winkelstein, J. A. (1988). Role of C3 in humoral immunity. Defective antibody production in C3-deficient dogs. *Journal of Immunology (Baltimore, Md. : 1950)*, *140*(6).

Obita, T., Ueda, T., & Imoto, T. (2003). Solution structure and activity of mouse lysozyme M. *Cellular and Molecular Life Sciences*, *60*(1). https://doi.org/10.1007/s000180300012

Obukhanych, T. V., & Nussenzweig, M. C. (2006). T-independent type II immune responses generate memory B cells. *Journal of Experimental Medicine*, *203*(2). https://doi.org/10.1084/jem.20052036

Oda, K., & Kitano, H. (2006). A comprehensive map of the toll-like receptor signaling network. *Molecular Systems Biology*. https://doi.org/10.1038/msb4100057

Okada, T., & Cyster, J. G. (2006). B cell migration and interactions in the early phase of antibody responses. *Current Opinion in Immunology*. https://doi.org/10.1016/j.coi.2006.02.005

Olsen, J. V., Ong, S. E., & Mann, M. (2004). Trypsin cleaves exclusively C-terminal to arginine and lysine residues. *Molecular and Cellular Proteomics*, *3*(6). https://doi.org/10.1074/mcp.T400003-MCP200

Oppermann, M., & Würzner, R. (2010). Modern determination of complement activation. *Seminars in Thrombosis and Hemostasis*, *36*(6), 611–619. https://doi.org/10.1055/s-0030-1262882

Oregioni, A., Stieglitz, B., Kelly, G., Rittinger, K., & Frenkiel, T. (2017). Determination of the pKa of the N-terminal amino group of ubiquitin by NMR. *Scientific Reports*, *7*. https://doi.org/10.1038/srep43748

Palinski, W., Yla-Herttuala, S., Rosenfeld, M. E., Butler, S. W., Socher, S. A., Parthasarathy, S., … Witztum, J. L. (1990). Antisera and monoclonal antibodies specific for epitopes generated during oxidative modification of low density lipoprotein. *Arteriosclerosis*, *10*(3). https://doi.org/10.1161/01.atv.10.3.325

Palm, N. W., & Medzhitov, R. (2009). Immunostimulatory activity of haptenated proteins. *Proceedings of the National Academy of Sciences of the United States of America*, *106*(12), 4782–4787. https://doi.org/10.1073/pnas.0809403105

Park, B. K., Sanderson, J. P., & Naisbitt, D. J. (2007). Drugs as haptens, antigens, and immunogens. *Drug Hypersensitivity*, 55–65. https://doi.org/10.1159/000104189

Parker, D. C. (1993). T cell-dependent B cell activation. *Annual Review of Immunology*. https://doi.org/10.1146/annurev.iy.11.040193.001555

Pasare, C., & Medzhitov, R. (2005). Control of B-cell responses by Toll-like receptors. *Nature*, *438*(7066). https://doi.org/10.1038/nature04267

Pepys, M. B. (1974). Role of complement in induction of antibody production in vivo. Effect of cobra factor and other C3-reactive agents on thymus-dependent and thymus-independent antibody responses. *J Exp Med*, *140*, 126–145.

Peters, N. C., Hamilton, D. H., & Bretscher, P. A. (2005). Analysis of cytokine-producing Th cells from hen egg lysozyme-immunized mice reveals large numbers specific for “cryptic” peptides and different repertoires among different Th populations. *European Journal of Immunology*, *35*(1), 56–65. https://doi.org/10.1002/eji.200425581

Phan, T. G., Gray, E. E., & Cyster, J. G. (2009). The microanatomy of B cell activation. *Current Opinion in Immunology*. https://doi.org/10.1016/j.coi.2009.05.006

Phan, T. G., Grigorova, I., Okada, T., & Cyster, J. G. (2007). Subcapsular encounter and complement-dependent transport of immune complexes by lymph node B cells. *Nature Immunology*, *8*(9). https://doi.org/10.1038/ni1494

Pizzimenti, S., Ciamporcero, E., Daga, M., Pettazzoni, P., Arcaro, A., Cetrangolo, G., … Barrera, G. (2013). Interaction of aldehydes derived from lipid peroxidation and membrane proteins. *Frontiers in Physiology*, *4 SEP*(September), 1–17. https://doi.org/10.3389/fphys.2013.00242

Porter, S. (2001). Human immune response to recombinant human proteins. *Journal of Pharmaceutical Sciences*. https://doi.org/10.1002/1520-6017(200101)90:1<1::AID-JPS1>3.0.CO;2-K

PrabhuDas, M. R., Baldwin, C. L., Bollyky, P. L., Bowdish, D. M. E., Drickamer, K., Febbraio, M., … El Khoury, J. (2017). A Consensus Definitive Classification of Scavenger Receptors and Their Roles in Health and Disease. *The Journal of Immunology*, *198*(10), 3775–3789. https://doi.org/10.4049/jimmunol.1700373

Pryjma, J., & Humphrey, J. H. (1975). Prolonged C3 depletion by cobra venom factor in thymus deprived mice and its implications for the role of C3 as an essential second signal for B cell triggering. *Immunology*, *28*(3).

Pulendran, B., Arunachalam, P. S., & O'Hagan, D. T. (2021). Emerging concepts in the science of vaccine adjuvants. *Nature Reviews Drug Discovery*, *20*(6), 454–475. https://doi.org/10.1038/s41573-021-00163-y

Quarsten, H., Molberg, Ø., Fugger, L., McAdam, S. N., & Sollid, L. M. (1999). HLA binding and T cell recognition of a tissue transglutaminase-modified gliadin epitope. *European Journal of Immunology*, *29*(8), 2506–2514. https://doi.org/10.1002/(SICI)1521-4141(199908)29:08<2506::AID-IMMU2506>3.0.CO;2-9

Radbruch, A., Muehlinghaus, G., Luger, E. O., Inamine, A., Smith, K. G. C., Dörner, T., & Hiepe, F. (2006). Competence and competition: The challenge of becoming a long-lived plasma cell. *Nature Reviews Immunology*. https://doi.org/10.1038/nri1886

Rashidian, M., Dozier, J. K., Lenevich, S., & Distefano, M. D. (2010). Selective labeling of polypeptides using protein farnesyltransferase via rapid oxime ligation. *Chemical Communications*, *46*(47). https://doi.org/10.1039/c0cc03305g

Ratanji, K. D., Derrick, J. P., Dearman, R. J., & Kimber, I. (2014). Immunogenicity of therapeutic proteins: Influence of aggregation. *Journal of Immunotoxicology*, *11*(2), 99–109. https://doi.org/10.3109/1547691X.2013.821564

Reid, K. B. M. (2018). Complement component C1q: Historical perspective of a functionally versatile, and structurally unusual, serum protein. *Frontiers in Immunology*, *9*(APR), 1–6. https://doi.org/10.3389/fimmu.2018.00764

Reis E Sousa, C. (2004). Activation of dendritic cells: Translating innate into adaptive immunity. *Current Opinion in Immunology*. https://doi.org/10.1016/j.coi.2003.11.007

Reynisson, B., Barra, C., Kaabinejadian, S., Hildebrand, W. H., Peters, B., Peters, B., … Nielsen, M. (2020). Improved Prediction of MHC II Antigen Presentation through Integration and Motif Deconvolution of Mass Spectrometry MHC Eluted Ligand Data. *Journal of Proteome Research*, *19*(6). https://doi.org/10.1021/acs.jproteome.9b00874

Rickert, R. C. (2005). Regulation of B lymphocyte activation by complement C3 and the B cell coreceptor complex. *Current Opinion in Immunology*. https://doi.org/10.1016/j.coi.2005.03.001

Roche, M., Rondeau, P., Singh, N. R., Tarnus, E., & Bourdon, E. (2008). The antioxidant properties of serum albumin. *FEBS Letters*. https://doi.org/10.1016/j.febslet.2008.04.057

Rogowska-Wrzesinska, A., Wojdyla, K., Nedić, O., Baron, C. P., & Griffiths, H. R. (2014). Analysis of protein carbonylation--pitfalls and promise in commonly used methods. *Free Radical Research*, *48*(10), 1145–1162. https://doi.org/10.3109/10715762.2014.944868

Roh, J. S., & Sohn, D. H. (2018). Damage-associated molecular patterns in inflammatory diseases. *Immune Network*. https://doi.org/10.4110/in.2018.18.e27

Rolla, R., Vay, D., Mottaran, E., Parodi, M., Traverso, N., Aricó, S., … Albano, E. (2000). Detection of circulating antibodies against malondialdehyde-acetaldehyde adducts in patients with alcohol-induced liver disease. *Hepatology*, *31*(4). https://doi.org/10.1053/he.2000.5373

Rosenberg, A. S. (2006). Effects of protein aggregates: An Immunologic perspective. *AAPS Journal*. https://doi.org/10.1208/aapsj080359

Ryan, B. J., Nissim, A., & Winyard, P. G. (2014). Oxidative post-translational modifications and their involvement in the pathogenesis of autoimmune diseases. *Redox Biology*. https://doi.org/10.1016/j.redox.2014.05.004

Sanchez-Moral, L., Ràfols, N., Martori, C., Paul, T., Téllez, É., & Sarrias, M. R. (2021). Multifaceted roles of CD5L in infectious and sterile inflammation. *International Journal of Molecular Sciences*, *22*(8), 1–14. https://doi.org/10.3390/ijms22084076

Scally, S. W., Petersen, J., Law, S. C., Dudek, N. L., Nel, H. J., Loh, K. L., … Rossjohn, J. (2013). A molecular basis for the association of the HLA-DRB1 locus, citrullination, and rheumatoid arthritis. *The Journal of Experimental Medicine*, *210*(12), 2569–2582. https://doi.org/10.1084/jem.20131241

Schaefer, L. (2014). Complexity of danger: The diverse nature of damage-associated molecular patterns. *Journal of Biological Chemistry*. https://doi.org/10.1074/jbc.R114.619304

Schalkwijk, C. G., Ligtvoet, N., Twaalfhoven, H., Jager, A., Blaauwgeers, H. G. T., Schlingemann, R. O., … Van Hinsbergh, V. W. M. (1999). Amadori albumin in type 1 diabetic patients: Correlation with markers of endothelial function, association with diabetic nephropathy, and localization in retinal capillaries. *Diabetes*, *48*(12). https://doi.org/10.2337/diabetes.48.12.2446

Schellekens, H. (2005). Factors influencing the immunogenicity of therapeutic proteins. *Nephrology Dialysis Transplantation*, *20*(SUPPL. 6). https://doi.org/10.1093/ndt/gfh1092

Schernthaner, G. (1993). Immunogenicity and allergenic potential of animal and human insulins. *Diabetes Care*. https://doi.org/10.2337/diacare.16.3.155

Schneider, S. C., Ohmen, J., Fosdick, L., Gladstone, B., Guo, J., Ametani, A., … Deng, H. (2000). Cutting Edge: Introduction of an Endopeptidase Cleavage Motif into a Determinant Flanking Region of Hen Egg Lysozyme Results in Enhanced T Cell Determinant Display. *The Journal of Immunology*, *165*(1), 20–23. https://doi.org/10.4049/jimmunol.165.1.20

Schroeder, H. W., & Cavacini, L. (2010). Structure and function of immunoglobulins. *Journal of Allergy and Clinical Immunology*, *125*(2 SUPPL. 2). https://doi.org/10.1016/j.jaci.2009.09.046

Schumacher, D., Helma, J., Mann, F. A., Pichler, G., Natale, F., Krause, E., … Leonhardt, H. (2015). Versatile and Efficient Site-Specific Protein Functionalization by Tubulin Tyrosine Ligase. *Angewandte Chemie - International Edition*, *54*(46). https://doi.org/10.1002/anie.201505456

Seelen, M. A., Roos, A., Wieslander, J., Mollnes, T. E., Sjöholm, A. G., Wurzner, R., … Daha, M. R. (2005). Functional analysis of the classical, alternative, and MBL pathways of the complement system: Standardization and validation of a simple ELISA. *Journal of Immunological Methods*, *296*(1–2), 187–198. https://doi.org/10.1016/j.jim.2004.11.016

Seidl, A., Hainzl, O., Richter, M., Fischer, R., Böhm, S., Deutel, B., … Macdougall, I. (2012). Tungsten-induced denaturation and aggregation of epoetin alfa during primary packaging as a cause of immunogenicity. *Pharmaceutical Research*, *29*(6). https://doi.org/10.1007/s11095-011-0621-4

Sercarz, E. E., Lehmann, P. V., Ametani, A., Benichou, G., Miller, A., & Moudgil, K. (1993). Dominance and crypticity of T cell antigenic determinants. *Annual Review of Immunology*, *11*, 729–766. https://doi.org/10.1146/annurev.iy.11.040193.003501

Shacter, E., Williams, J. A., Lim, M., & Levine, R. L. (1994). Differential susceptibility of plasma proteins to oxidative modification: Examination by western blot immunoassay. *Free Radical Biology and Medicine*, *17*(5), 429–437. https://doi.org/10.1016/0891-5849(94)90169-4

Shechter, I., Fogelman, A. M., Haberland, M. E., Seager, J., Hokom, M., & Edwards, P. A. (1981). The metabolism of native and malondialdehyde-altered low density lipoproteins by human monocyte-macrophages. *Journal of Lipid Research*, *22*(1). https://doi.org/10.1016/s0022-2275(20)34741-6

Shiroishi, M., Tsumoto, K., Tanaka, Y., Yokota, A., Nakanishi, T., Kondo, H., & Kumagai, I. (2007). Structural consequences of mutations in interfacial Tyr residues of a protein antigen-antibody complex: The case of HyHEL-10-HEL. *Journal of Biological Chemistry*, *282*(9). https://doi.org/10.1074/jbc.M605197200

Sicard, T., Kassardjian, A., & Julien, J. P. (2020). B cell targeting by molecular adjuvants for enhanced immunogenicity. *Expert Review of Vaccines*. https://doi.org/10.1080/14760584.2020.1857736

Sim, R. B., Day, A. J., Moffatt, B. E., & Fontaine, M. (1993). Complement Factor I and Cofactors in Control of Complement System Convertase Enzymes. *Methods in Enzymology*, *223*(C). https://doi.org/10.1016/0076-6879(93)23035-L

Sklarz, B. (1967). Organic chemistry of periodates. *Quarterly Reviews, Chemical Society*, *21*(1). https://doi.org/10.1039/qr9672100003

Smith-Gill, S. J., Mainhart, C. R., Lavoie, T. B., Rudikoff, S., & Potter, M. (1984). V(L)-V(H) expression by monoclonal antibodies recognizing avian lysozyme. *The Journal of Immunology (1950)*, *132*(2).

Smole, U., Gour, N., Phelan, J., Hofer, G., Köhler, C., Kratzer, B., … Wills-Karp, M. (2020). Serum amyloid A is a soluble pattern recognition receptor that drives type 2 immunity. *Nature Immunology*, *21*(7), 756–765. https://doi.org/10.1038/s41590-020-0698-1

Smole, U., Kratzer, B., & Pickl, W. F. (2020). Soluble pattern recognition molecules: Guardians and regulators of homeostasis at airway mucosal surfaces. *European Journal of Immunology*, *50*(5), 624–642. https://doi.org/10.1002/eji.201847811

Song, Y., Xiong, F., Peng, J., Fung, Y. M. E., Huang, Y., & Li, X. (2020). Introducing aldehyde functionality to proteins using ligand-directed affinity labeling. *Chemical Communications*, *56*(45). https://doi.org/10.1039/d0cc01982h

Sörman, A., Zhang, L., Ding, Z., & Heyman, B. (2014). How antibodies use complement to regulate antibody responses. *Molecular Immunology*, *61*(2), 79–88. https://doi.org/10.1016/j.molimm.2014.06.010

Spanneberg, R., Osswald, F., Kolesov, I., Anton, W., Radusch, H. J., & Glomb, M. A. (2010). Model studies on chemical and textural modifications in gelatin films by reaction with glyoxal and glycolaldehyde. *Journal of Agricultural and Food Chemistry*, *58*(6), 3580–3585. https://doi.org/10.1021/jf9039827

Spears, R. J., & Fascione, M. A. (2016). Site-selective incorporation and ligation of protein aldehydes. *Organic and Biomolecular Chemistry*, *14*(32), 7622–7638. https://doi.org/10.1039/c6ob00778c

Spicer, C. D., & Davis, B. G. (2014). Selective chemical protein modification. *Nature Communications*, *5*. https://doi.org/10.1038/ncomms5740

Spitzer, D., Mitchell, L. M., Atkinson, J. P., & Hourcade, D. E. (2007). Properdin Can Initiate Complement Activation by Binding Specific Target Surfaces and Providing a Platform for De Novo Convertase Assembly. *The Journal of Immunology*, *179*(4). https://doi.org/10.4049/jimmunol.179.4.2600

Stadtman, E. R., & Levine, R. L. (2000). Protein oxidation. In *Annals of the New York Academy of Sciences* (Vol. 899). https://doi.org/10.1111/j.1749-6632.2000.tb06187.x

Stavnezer, J. (1996). Immunoglobulin class switching. *Current Opinion in Immunology*, *8*(2). https://doi.org/10.1016/S0952-7915(96)80058-6

Steward, J. P., Ornellas, E. P., Beernink, K. D., & Northway, W. H. (1968). Errors in the technique of intraperitoneal injection of mice. *Applied Microbiology*, *16*(9), 1418–1419. https://doi.org/10.1128/aem.16.9.1418-1419.1968

Storm, D., Loos, M., & Kaul, M. (1996). Biotinylation of proteins via amino groups can induce binding to U937 cells, HL-60 cells, monocytes and granulocytes. *Journal of Immunological Methods*, *199*(1), 87–99. https://doi.org/10.1016/S0022-1759(96)00172-X

Sundberg, E. J., Urrutia, M., Braden, B. C., Isern, J., Tsuchiya, D., Fields, B. A., … Mariuzza, R. A. (2000). Estimation of the hydrophobic effect in an antigen-antibody protein-protein interface. *Biochemistry*, *39*(50). https://doi.org/10.1021/bi000704l

Suzuki, K., Grigorova, I., Phan, T. G., Kelly, L. M., & Cyster, J. G. (2009). Visualizing B cell capture of cognate antigen from follicular dendritic cells. *Journal of Experimental Medicine*, *206*(7). https://doi.org/10.1084/jem.20090209

Takata, K., Horiuchi, S., Araki, N., Shiga, M., Saitoh, M., & Morino, Y. (1988). Endocytic uptake of nonenzymatically glycosylated proteins is mediated by a scavenger receptor for aldehyde-modified proteins. *Journal of Biological Chemistry*, *263*(29), 14819–14825. https://doi.org/10.1016/s0021-9258(18)68112-8

Takeuchi, O., & Akira, S. (2010). Pattern Recognition Receptors and Inflammation. *Cell*, *140*(6), 805–820. https://doi.org/10.1016/j.cell.2010.01.022

Temple, A., Yen, T. Y., & Gronert, S. (2006). Identification of Specific Protein Carbonylation Sites in Model Oxidations of Human Serum Albumin. *Journal of the American Society for Mass Spectrometry*, *17*(8). https://doi.org/10.1016/j.jasms.2006.04.030

Terres, G., S. L. Morrison, and G. S. Habicht. 1968. "A Quantitative Difference in the Immune Response between Male and Female Mice." *Proceedings of the Society for Experimental Biology and Medicine* 127 (3). https://doi.org/10.3181/00379727-127-32768.

Théry, C., & Amigorena, S. (2001). The cell biology of antigen presentation in dendritic cells. *Current Opinion in Immunology*. https://doi.org/10.1016/S0952-7915(00)00180-1

Thiele, G. M., Duryee, M. J., Anderson, D. R., Klassen, L. W., Mohring, S. M., Young, K. A., … Mikuls, T. R. (2015). Malondialdehyde-acetaldehyde adducts and anti-malondialdehyde-acetaldehyde antibodies in rheumatoid arthritis. *Arthritis and Rheumatology*, *67*(3). https://doi.org/10.1002/art.38969

Thiele, G. M., Tuma, D. J., Willis, M. S., Miller, J. A., McDonald, T. L., Sorrell, M. F., & Klassen, L. W. (1998). Soluble proteins modified with acetaldehyde and malondialdehyde are immunogenic in the absence of adjuvant. *Alcoholism: Clinical and Experimental Research*, *22*(8), 1731–1739. https://doi.org/10.1111/j.1530-0277.1998.tb03973.x

Thurman, J. M., Kulik, L., Orth, H., Wong, M., Renner, B., Sargsyan, S. A., … Holers, V. M. (2013). Detection of complement activation using monoclonal antibodies against C3d. *Journal of Clinical Investigation*, *123*(5), 2218–2230. https://doi.org/10.1172/JCI65861

Toda, M., Hellwig, M., Henle, T., & Vieths, S. (2019). Influence of the Maillard Reaction on the Allergenicity of Food Proteins and the Development of Allergic Inflammation. *Current Allergy and Asthma Reports*, *19*(1). https://doi.org/10.1007/s11882-019-0834-x

Tortajada, A., Yébenes, H., Abarrategui-Garrido, C., Anter, J., García-Fernández, J. M., Martínez-Barricarte, R., … De Córdoba, S. R. (2013). C3 glomerulopathy-associated CFHR1 mutation alters FHR oligomerization and complement regulation. *Journal of Clinical Investigation*, *123*(6). https://doi.org/10.1172/JCI68280

Tosar, J. P., Segovia, M., Castellano, M., Gámbaro, F., Akiyama, Y., Fagúndez, P., … Cayota, A. (2020). Fragmentation of extracellular ribosomes and tRNAs shapes the extracellular RNAome. *Nucleic Acids Research*, *48*(22). https://doi.org/10.1093/nar/gkaa674

Troldborg, A., Jensen, L., Deleuran, B., Stengaard-Pedersen, K., Thiel, S., & Jensenius, J. C. (2018). The C3dg fragment of complement is superior to conventional C3 as a diagnostic biomarker in systemic lupus erythematosus. *Frontiers in Immunology*, *9*(MAR), 1–10. https://doi.org/10.3389/fimmu.2018.00581

Tsiantoulas, D., Perkmann, T., Afonyushkin, T., Mangold, A., Prohaska, T. A., Papac-Milicevic, N., … Binder, C. J. (2015). Circulating microparticles carry oxidation-specific epitopes and are recognized by natural IgM antibodies. *Journal of Lipid Research*, *56*(2). https://doi.org/10.1194/jlr.P054569

Tsujihata, Y., So, T., Chijiiwa, Y., Hashimoto, Y., Hirata, M., Ueda, T., & Imoto, T. (2000). Mutant Mouse Lysozyme Carrying a Minimal T Cell Epitope of Hen Egg Lysozyme Evokes High Autoantibody Response. *The Journal of Immunology*, *165*(7). https://doi.org/10.4049/jimmunol.165.7.3606

Tuley, A., Lee, Y. J., Wu, B., Wang, Z. U., & Liu, W. R. (2014). A genetically encoded aldehyde for rapid protein labelling. *Chemical Communications*, *50*(56). https://doi.org/10.1039/c4cc02000f

Tyanova, S., Temu, T., Sinitcyn, P., Carlson, A., Hein, M. Y., Geiger, T., … Cox, J. (2016). The Perseus computational platform for comprehensive analysis of (prote)omics data. *Nature Methods*. https://doi.org/10.1038/nmeth.3901

Uchida, K., Szweda, L. I., Chae, H. Z., & Stadtman, E. R. (1993). Immunochemical detection of 4-hydroxynonenal protein adducts in oxidized hepatocytes. *Proceedings of the National Academy of Sciences of the United States of America*, *90*(18), 8742–8746. https://doi.org/10.1073/pnas.90.18.8742

Uchida, Koji. (2013). Redox-derived damage-associated molecular patterns: Ligand function of lipid peroxidation adducts. *Redox Biology*, *1*(1), 94–96. https://doi.org/10.1016/j.redox.2012.12.005

Uchida, Koji, Sakai, K., Itakura, K., Osawa, T., & Toyokuni, S. (1997). Protein modification by lipid peroxidation products: Formation of malondialdehyde-derived N(ε)(2-propenal)lysine in proteins. *Archives of Biochemistry and Biophysics*, *346*(1), 45–52. https://doi.org/10.1006/abbi.1997.0266

Ugur, Z., Coffey, C. M., & Gronert, S. (2012). Comparing the efficiencies of hydrazide labels in the study of protein carbonylation in human serum albumin. *Analytical and Bioanalytical Chemistry*, *404*(5), 1399–1411. https://doi.org/10.1007/s00216-012-6235-9

Unno, Y., Sakai, M., Sakamoto, Y. I., Kuniyasu, A., Nagai, R., Nakayama, H., & Horiuchi, S. (2005). Glycolaldehyde-modified bovine serum albumin downregulates leptin expression in mouse adipocytes via a CD36-mediated pathway. *Annals of the New York Academy of Sciences*, *1043*, 696–701. https://doi.org/10.1196/annals.1333.080

Veneskoski, M., Turunen, S. P., Kummu, O., Nissinen, A., Rannikko, S., Levonen, A. L., & Hörkkö, S. (2011). Specific recognition of malondialdehyde and malondialdehyde acetaldehyde adducts on oxidized LDL and apoptotic cells by complement anaphylatoxin C3a. *Free Radical Biology and Medicine*, *51*(4). https://doi.org/10.1016/j.freeradbiomed.2011.05.029

Vidarsson, G., Dekkers, G., & Rispens, T. (2014). IgG subclasses and allotypes: From structure to effector functions. *Frontiers in Immunology*, *5*(OCT). https://doi.org/10.3389/fimmu.2014.00520

Vistoli, G., De Maddis, D., Cipak, A., Zarkovic, N., Carini, M., & Aldini, G. (2013). Advanced glycoxidation and lipoxidation end products (AGEs and ALEs): An overview of their mechanisms of formation. *Free Radical Research*, *47*(S1), 3–27. https://doi.org/10.3109/10715762.2013.815348

Vogel, C. W., & Fritzinger, D. C. (2010). Cobra venom factor: Structure, function, and humanization for therapeutic complement depletion. *Toxicon*, *56*(7), 1198–1222. https://doi.org/10.1016/j.toxicon.2010.04.007

Vos, Q., Lees, A., Wu, Z. Q., Snapper, C. M., & Mond, J. J. (2000). B-cell activation by T-cell-independent type 2 antigens as an integral part of the humoral immune response to pathogenic microorganisms. *Immunological Reviews*. https://doi.org/10.1034/j.1600-065X.2000.00607.x

Wahid, A. A., Dunphy, R. W., Macpherson, A., Gibson, B. G., Kulik, L., Whale, K., … van den Elsen, J. M. H. (2021). Insights Into the Structure-Function Relationships of Dimeric C3d Fragments. *Frontiers in Immunology*, *12*. https://doi.org/10.3389/fimmu.2021.714055

Walczewska, M., Ciszek-Lenda, M., Surmiak, M., Kozlowska, A., Jozefowski, S., & Marcinkiewicz, J. (2015). Impact of taurine on innate and adaptive immunity as the result of HOCL neutralization. *Advances in Experimental Medicine and Biology*, *803*, 109–120. https://doi.org/10.1007/978-3-319-15126-7_10

Wållberg, M., Bergquist, J., Achour, A., Breij, E., & Harris, R. A. (2007). Malondialdehyde modification of myelin oligodendrocyte glycoprotein leads to increased immunogenicity and encephalitogenicity. *European Journal of Immunology*, *37*(7), 1986–1995. https://doi.org/10.1002/eji.200636912

Walport, M. J. (2001). Complement. First of Two Parts. *New England Journal of Medicine*, *344*(14), 1058–1066.

Wang, J., Dauter, M., Alkire, R., Joachimiak, A., & Dauter, Z. (2007). Triclinic lysozyme at 0.65 Å resolution. *Acta Crystallographica Section D: Biological Crystallography*, *63*(12). https://doi.org/10.1107/S0907444907054224

Wang, J. H., & Reinherz, E. L. (2002). Structural basis of T cell recognition of peptides bound to MHC molecules. *Molecular Immunology*, *38*(14), 1039–1049. https://doi.org/10.1016/S0161-5890(02)00033-0

Wang, W., Singh, S. K., Li, N., Toler, M. R., King, K. R., & Nema, S. (2012). Immunogenicity of protein aggregates - Concerns and realities. *International Journal of Pharmaceutics*, *431*(1–2), 1–11. https://doi.org/10.1016/j.ijpharm.2012.04.040

Warnecke, A., Musunuri, S., N'diaye, M., Sandalova, T., Achour, A., Bergquist, J., & Harris, R. A. (2017). Nitration of MOG diminishes its encephalitogenicity depending on MHC haplotype. *Journal of Neuroimmunology*, *303*, 1–12. https://doi.org/10.1016/j.jneuroim.2016.11.008

Weber, D., Davies, M. J., & Grune, T. (2015). Determination of protein carbonyls in plasma, cell extracts, tissue homogenates, isolated proteins: Focus on sample preparation and derivatization conditions. *Redox Biology*, *5*, 367–380. https://doi.org/10.1016/j.redox.2015.06.005

Weismann, D., Hartvigsen, K., Lauer, N., Bennett, K. L., Scholl, H. P. N., Issa, P. C., … Binder, C. J. (2011). Complement factor H binds malondialdehyde epitopes and protects from oxidative stress. *Nature*, *478*(7367). https://doi.org/10.1038/nature10449

Wesche, H., Henzel, W. J., Shillinglaw, W., Li, S., & Cao, Z. (1997). MyD88: An adapter that recruits IRAK to the IL-1 receptor complex. *Immunity*, *7*(6). https://doi.org/10.1016/S1074-7613(00)80402-1

Wessels, M. R., Butko, P., Ma, M., Warren, H. B., Lage, A. L., & Carroll, M. C. (1995). Studies of group B streptococcal infection in mice deficient in complement component C3 or C4 demonstrate an essential role for complement in both innate and acquired immunity. *Proceedings of the National Academy of Sciences of the United States of America*, *92*(25). https://doi.org/10.1073/pnas.92.25.11490

Westman, E., & Harris, H. E. (2004). Alteration of an autoantigen by chlorination, a process occurring during inflammation, can overcome adaptive immune tolerance. *Scandinavian Journal of Immunology*, *59*(5), 458–463. https://doi.org/10.1111/j.0300-9475.2004.01428.x

Westman, E., Lundberg, K., & Erlandsson Harris, H. (2006). Arthritogenicity of collagen type II is increased by chlorination. *Clinical and Experimental Immunology*, *145*(2), 339–345. https://doi.org/10.1111/j.1365-2249.2006.03129.x

Weth, F., Schroeder, T., & Buxtorf, U. P. (1988). Determination of lysozyme content in eggs and egg products using SDS-gel electrophoresis. *Zeitschrift Für Lebensmittel-Untersuchung Und -Forschung*, *187*(6). https://doi.org/10.1007/BF01042386

Wieczorek, M., Abualrous, E. T., Sticht, J., Álvaro-Benito, M., Stolzenberg, S., Noé, F., & Freund, C. (2017). Major histocompatibility complex (MHC) class I and MHC class II proteins: Conformational plasticity in antigen presentation. *Frontiers in Immunology*. https://doi.org/10.3389/fimmu.2017.00292

Willis, M. S., Klassen, L. W., Tuma, D. J., Sorrell, M. F., & Thiele, G. M. (2002). Adduction of soluble proteins with malondialdehyde-acetaldehyde (MAA) induces antibody production and enhances T-cell proliferation. *Alcoholism: Clinical and Experimental Research*, *26*(1), 94–106. https://doi.org/10.1111/j.1530-0277.2002.tb02436.x

Willis, M. S., Thiele, G. M., Tuma, D. J., & Klassen, L. W. (2003). T cell proliferative responses to malondialdehyde-acetaldehyde haptenated protein are scavenger receptor mediated. *International Immunopharmacology*, *3*(10–11), 1381–1399. https://doi.org/10.1016/S1567-5769(03)00136-X

Wu, J., Wu, Y. Q., Ricklin, D., Janssen, B. J. C., Lambris, J. D., & Gros, P. (2009). Structure of complement fragment C3b-factor H and implications for host protection by complement regulators. *Nature Immunology*, *10*(7). https://doi.org/10.1038/ni.1755

Wuttge, D. M., Bruzelius, M., & Stemme, S. (1999). T-cell recognition of lipid peroxidation products breaks tolerance to self proteins. *Immunology*, *98*(2), 273–279. https://doi.org/10.1046/j.1365-2567.1999.00872.x

Xin, F., & Radivojac, P. (2012). Post-translational modifications induce significant yet not extreme changes to protein structure. *Bioinformatics*, *28*(22), 2905–2913. https://doi.org/10.1093/bioinformatics/bts541

Yakabe, S. (2010). ChemInform Abstract: One-Pot System for Reduction of Epoxides Using NaBH4, PdCl2 Catalyst, and Moist Alumina. *ChemInform*, *41*(40). https://doi.org/10.1002/chin.201040034

Yamaguchi, K., Itakura, M., Kitazawa, R., Lim, S. Y., Nagata, K., Shibata, T., … Uchida, K. (2021). Oxidative deamination of lysine residues by polyphenols generates an equilibrium of aldehyde and 2-piperidinol products. *Journal of Biological Chemistry*, *297*(3). https://doi.org/10.1016/j.jbc.2021.101035

Yan, L. J., & Forster, M. J. (2011). Chemical probes for analysis of carbonylated proteins: A review. *Journal of Chromatography B: Analytical Technologies in the Biomedical and Life Sciences*, *879*(17–18), 1308–1315. https://doi.org/10.1016/j.jchromb.2010.08.004

Yla-Herttuala, S., Palinski, W., Butler, S. W., Picard, S., Steinberg, D., & Witztum, J. L. (1994). Rabbit and human atherosclerotic lesions contain IgG that recognizes epitopes of oxidized LDL. *Arteriosclerosis and Thrombosis*, *14*(1). https://doi.org/10.1161/01.atv.14.1.32

Yoo, B. S., & Regnier, F. E. (2004). Proteomic analysis of carbonylated proteins in two-dimensional gel electrophoresis using avidin-flourescein affinity staining. *Electrophoresis*, *25*(9). https://doi.org/10.1002/elps.200405890

Yu, X., & Petersen, F. (2018). A methodological review of induced animal models of autoimmune diseases. *Autoimmunity Reviews*, *17*(5), 473–479. https://doi.org/10.1016/j.autrev.2018.03.001

Zalan, Z., Lazar, L., & Fulop, F. (2010). Chemistry of Hydrazinoalcohols and their Heterocyclic Derivatives. Part 1. Synthesis of Hydrazinoalcohols. *Current Organic Chemistry*, *9*(4). https://doi.org/10.2174/1385272053174949

Zhang, Z., Goldschmidt, T., & Salter, H. (2012). Possible allelic structure of IgG2a and IgG2c in mice. *Molecular Immunology*, *50*(3). https://doi.org/10.1016/j.molimm.2011.11.006

Zheng, B., Brett, S. J., Tite, J. P., Lifely, M. R., Brodie, T. A., & Rhodes, J. (1992). Galactose oxidation in the design of immunogenic vaccines. *Science*, *256*(5063). https://doi.org/10.1126/science.1598588

Appendix

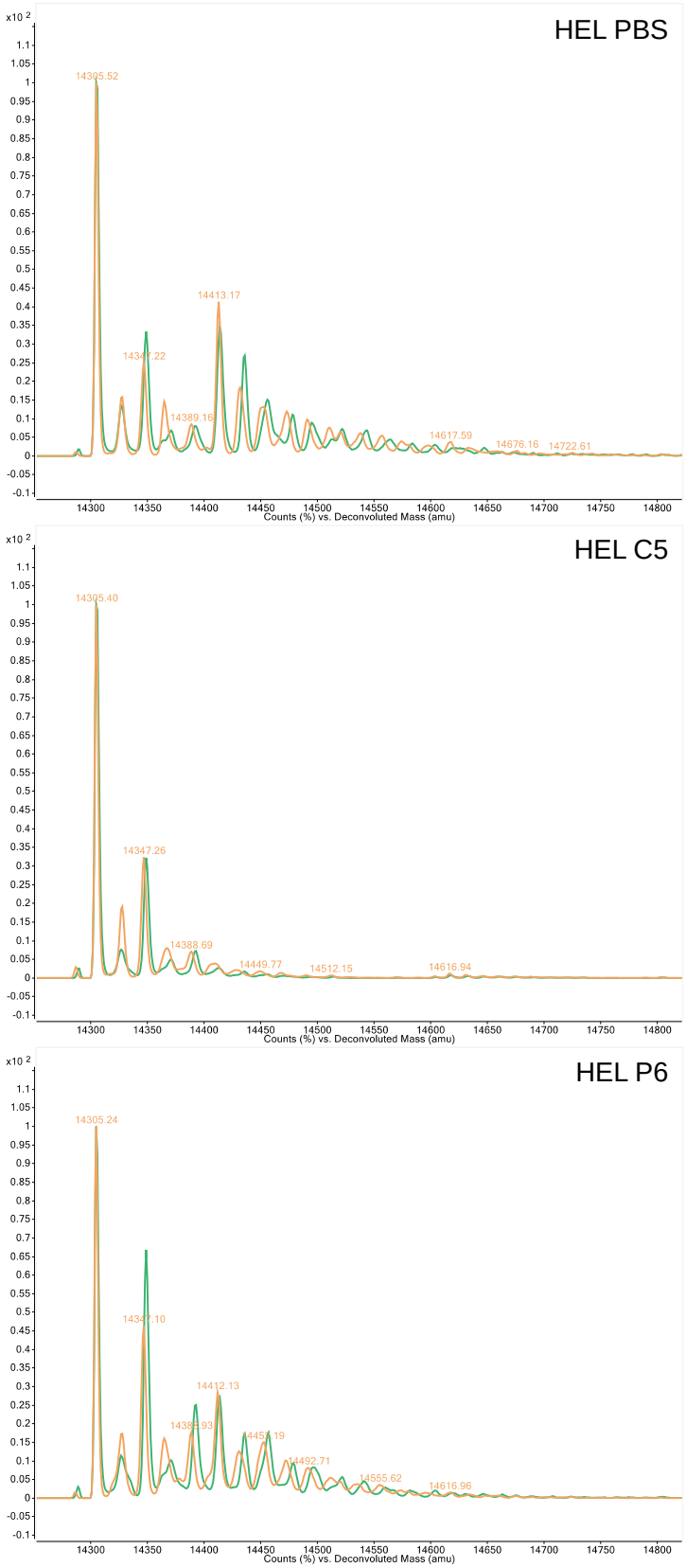


Figure A.1: Overlaid intact LC-MS spectra comparing HEL GA (orange) and HEL PR (green) samples. Slight shifts in certain peaks can be seen and suggest reduction of reactive carbonyl groups.

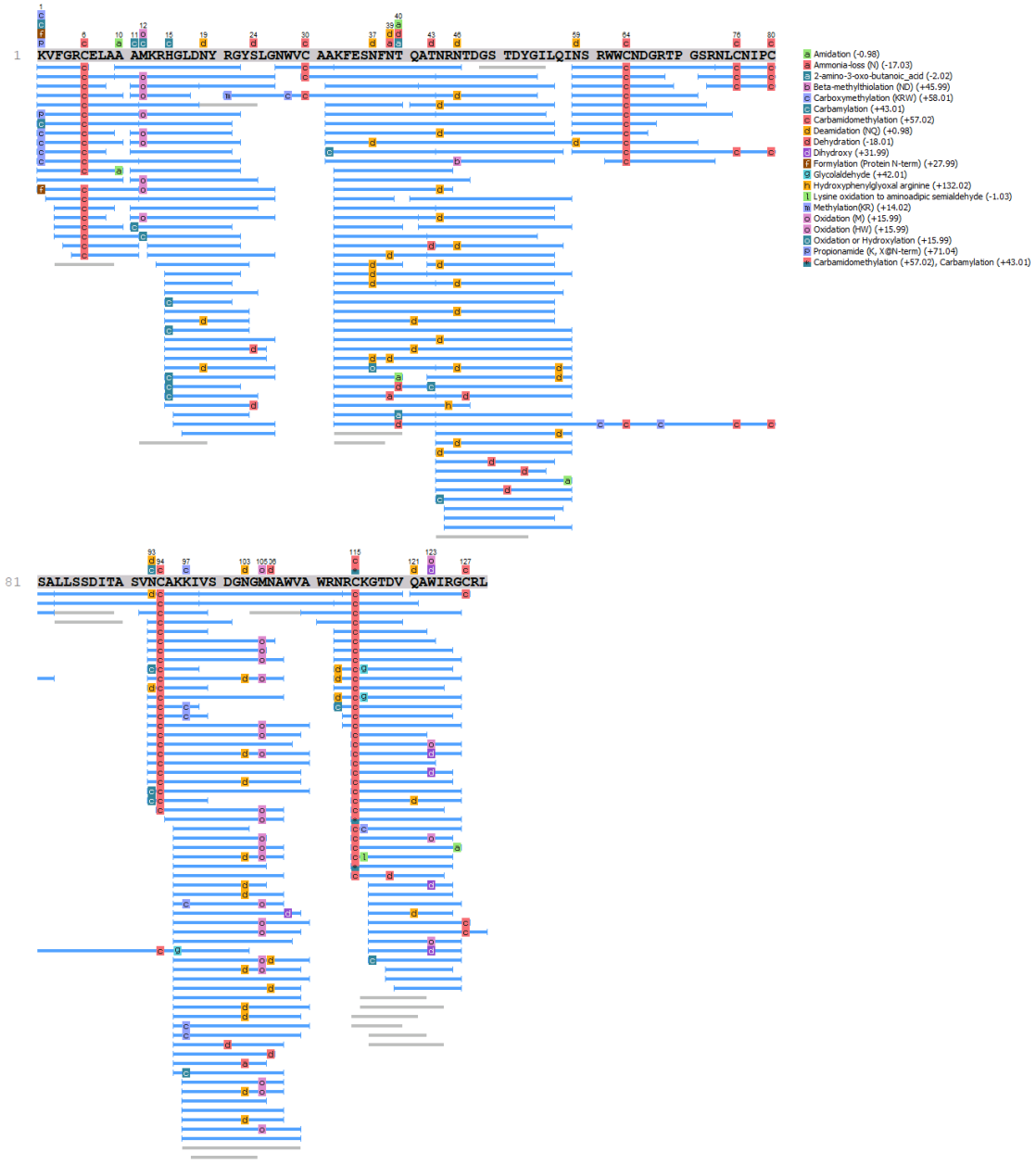


Figure A.2: Unbiased search for modifications detected with LC-MS/MS for HEL mock. PEAKS DB and PTM search tools were run to find peptides with both user-specified and unspecified modifications from the Unimod database. Blue lines represent unique PSMs. Detected PTMs are indicated on the blue lines. Confidently mapped PTMs appear above the protein sequence and their amino acid position is indicated. Samples prepared by Amin Moghaddam and analysed together with Iolanda Vendrell.

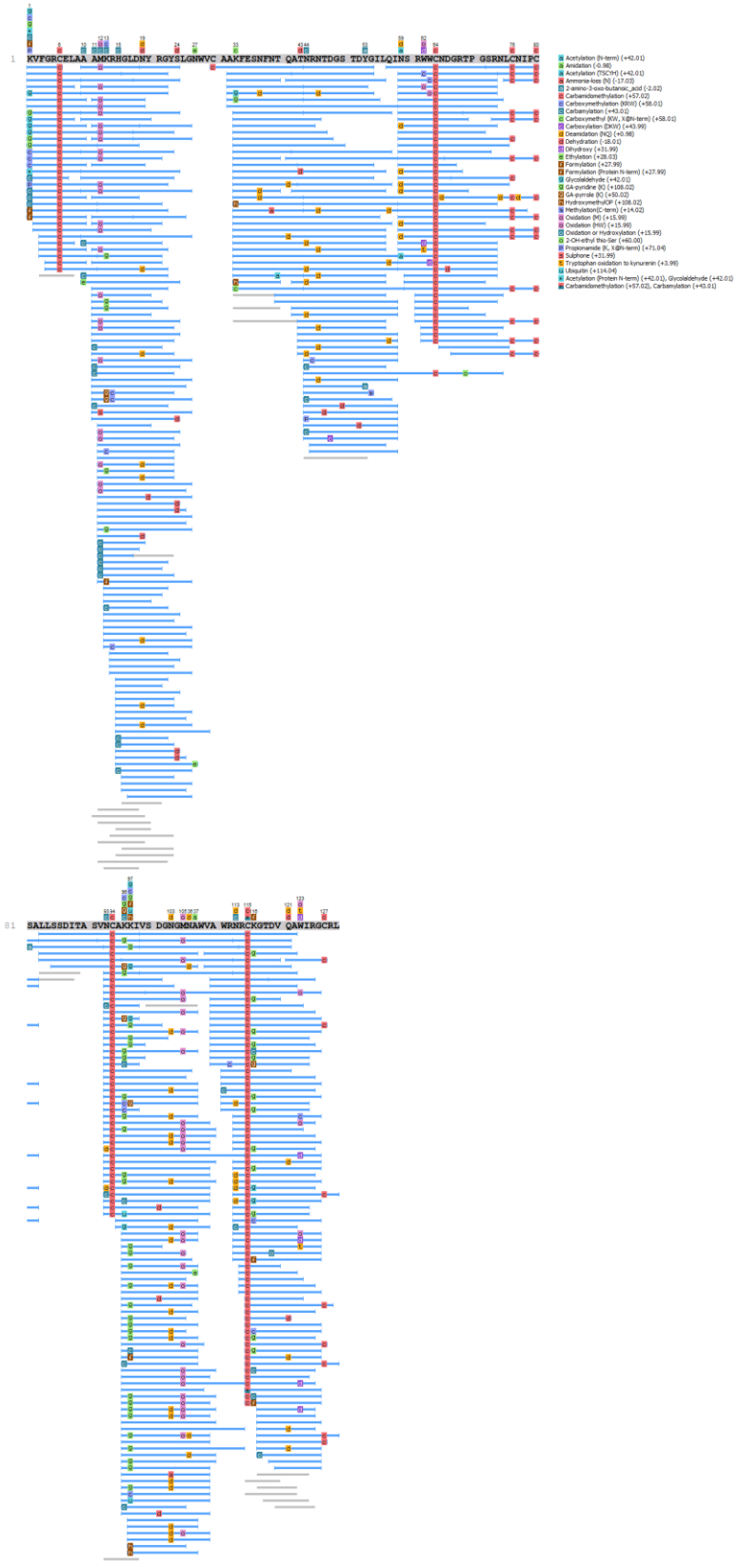


Figure A.3: Unbiased search for modifications detected with LC-MS/MS for HEL GA 3 h. PEAKS DB and PTM search tools were run to find peptides with both user-specified and unspecified modifications from the Unimod database. Blue lines represent unique PSMs. Detected PTMs are indicated on the blue lines. Confidently mapped PTMs appear above the protein sequence and their amino acid position is indicated. Samples prepared by Amin Moghaddam and re-analysed together with Iolanda Vendrell.

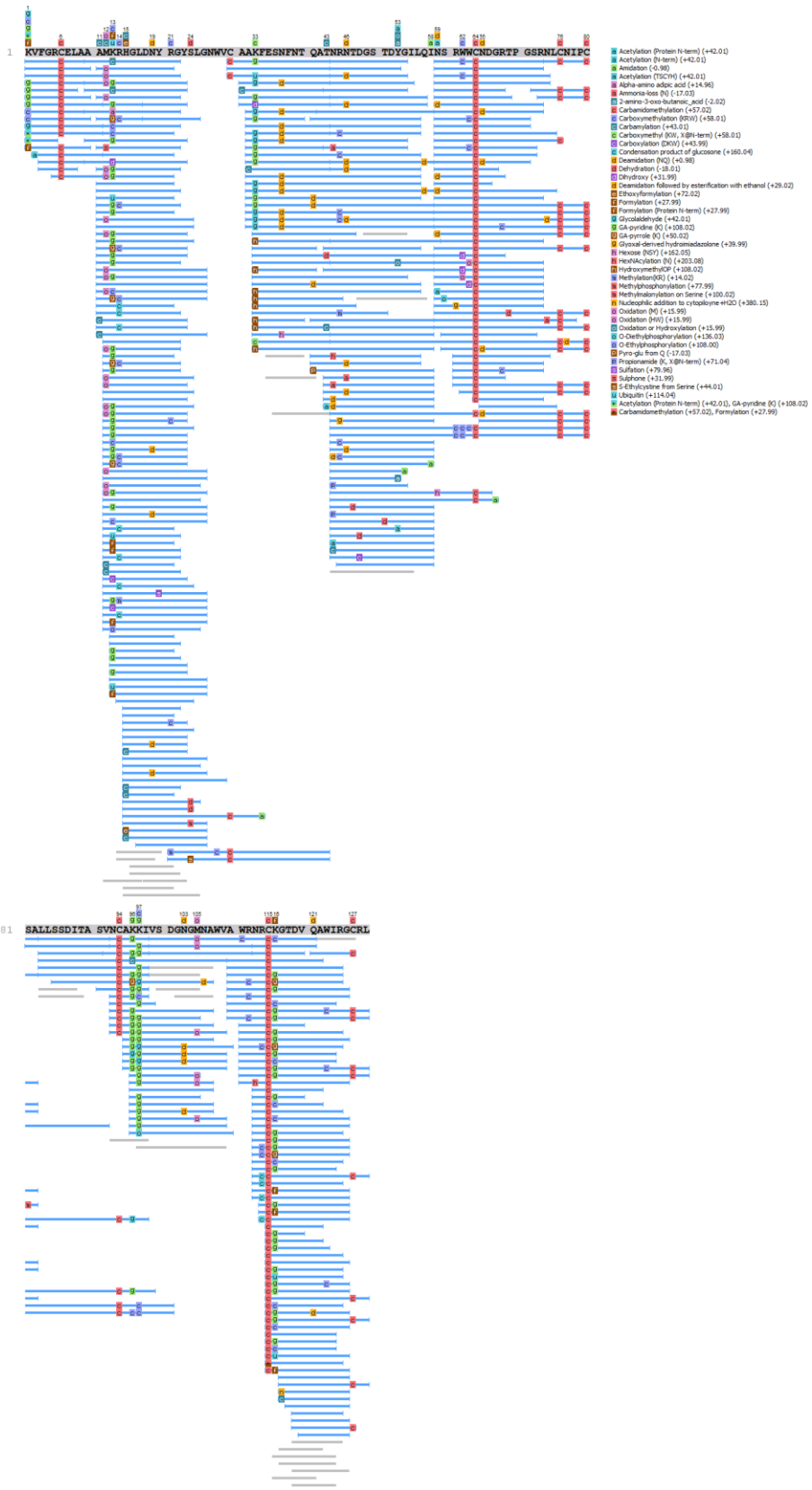


Figure A.4: Unbiased search for modifications detected with LC-MS/MS for HEL GA 7 d. PEAKS DB and PTM search tools were run to find peptides with both user-specified and unspecified modifications from the Unimod database. Blue lines represent unique PSMs. Detected PTMs are indicated on the blue lines. Confidently mapped PTMs appear above the protein sequence and their amino acid position is indicated. Samples prepared by Amin Moghaddam and re-analysed together with Iolanda Vendrell.

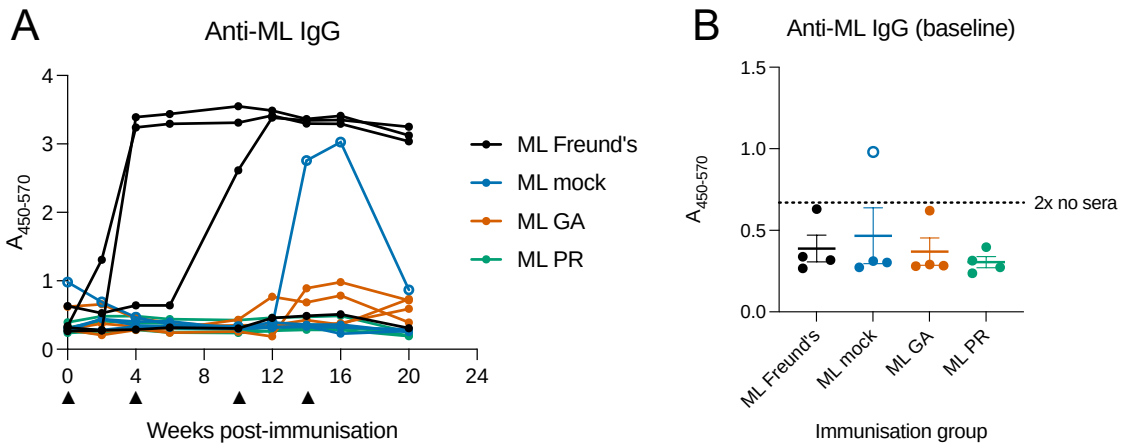


Figure A.5: Anti-ML IgG responses measured in the second ML immunisation experiment. A) Anti-ML IgG responses during the experiment with individual mice shown (n = 4 per group). B) Anti-ML IgG responses at baseline. Outlier immunised with ML mock shown with an empty circle. Sera diluted 1:50.

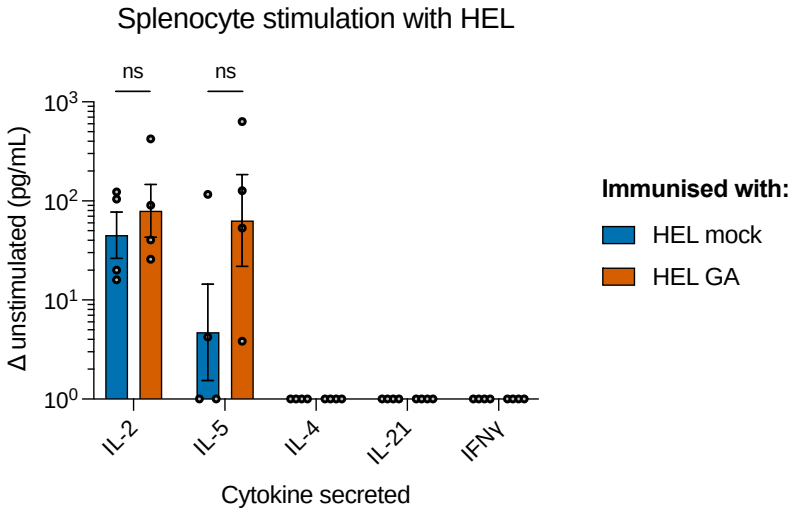


Figure A.6: Splenocytes from HEL mock and HEL GA primed mice have similar cytokine responses after native HEL protein stimulation. Splenocytes from mice primed with 10 µg HEL mock or HEL GA were stimulated with native HEL protein. Splenocyte cytokine secretion measured 3 d after stimulation, except for IL-4 measured 1 d after. Data are mean ± SEM from 4 mice (Mann-Whitney tests between HEL mock and HEL GA for each cytokine corrected for multiple comparisons using Holm-Šídák's method).

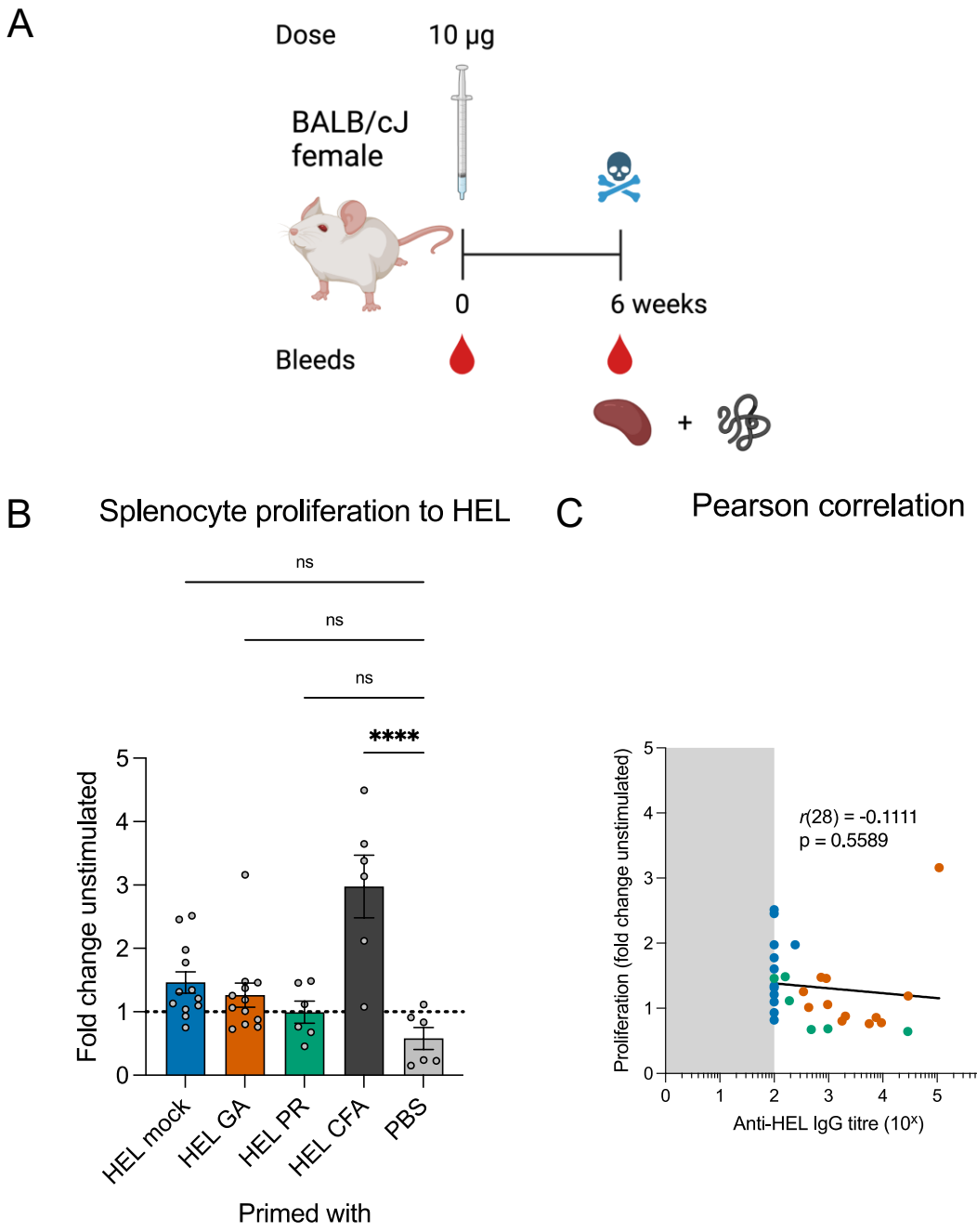


Figure A.7: HEL-specific splenocyte proliferation is not enhanced after priming with HEL GA compared with HEL mock and HEL PR, and does not correlate with anti-HEL IgG titre. A) Bleed, immunisation and harvest schedule. Splenocytes from mice primed with HEL mock, HEL GA, HEL PR, HEL CFA or PBS were stimulated with native HEL protein or left unstimulated with media only. B) Splenocyte proliferation as measured by ^{3}H thymidine incorporation, expressed as fold change over unstimulated splenocytes. Data are mean ± SEM from 6–12 primed mice across 3 independent experiments (one-way ANOVA followed by Holm-Šídák's multiple comparisons test). C) Pearson correlation analysis of splenocyte proliferation versus anti-HEL IgG titre of all mice in B) except PBS and HEL CFA. Each dot represents a single mouse. Anti-HEL IgG titres based on Figure 3.6. Sera were serially diluted starting at 1:100 and non-responding mice were plotted at the limit of detection (shaded in grey).

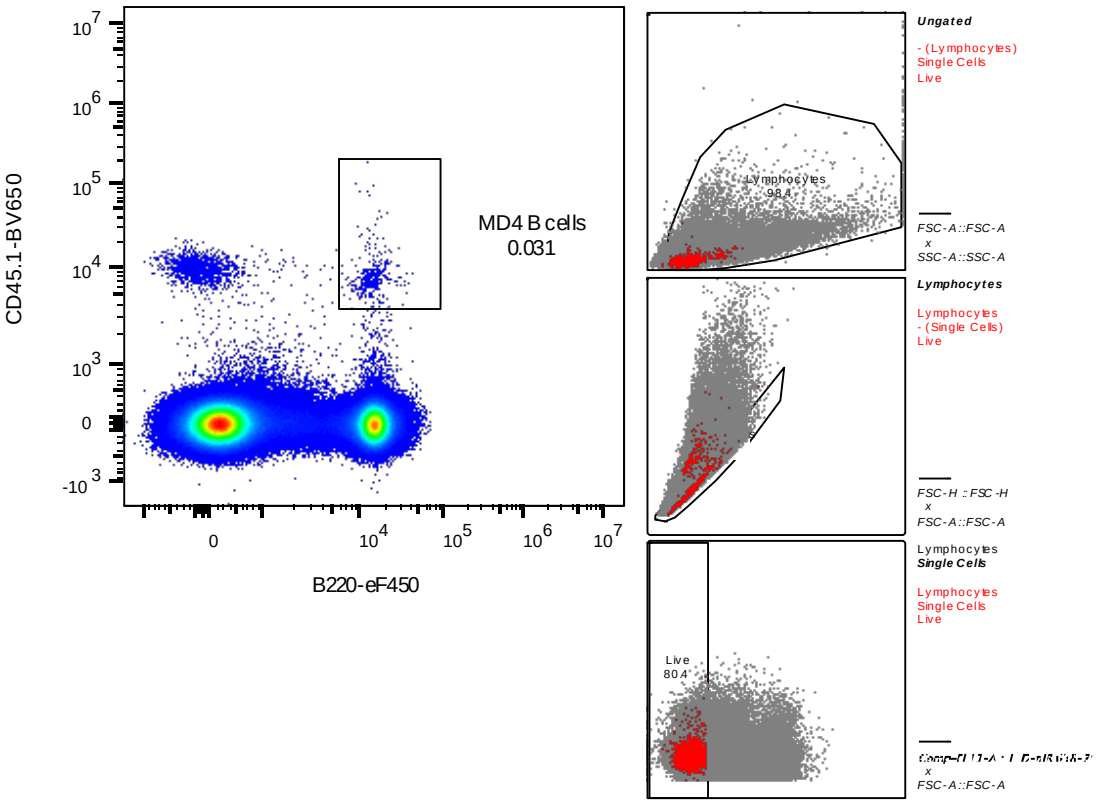


Figure A.8: Gating strategy for adoptively transferred MD4 B cells ($B220^{+}CD45.1^{+}$) in wild type (WT) B6 congenic hosts.

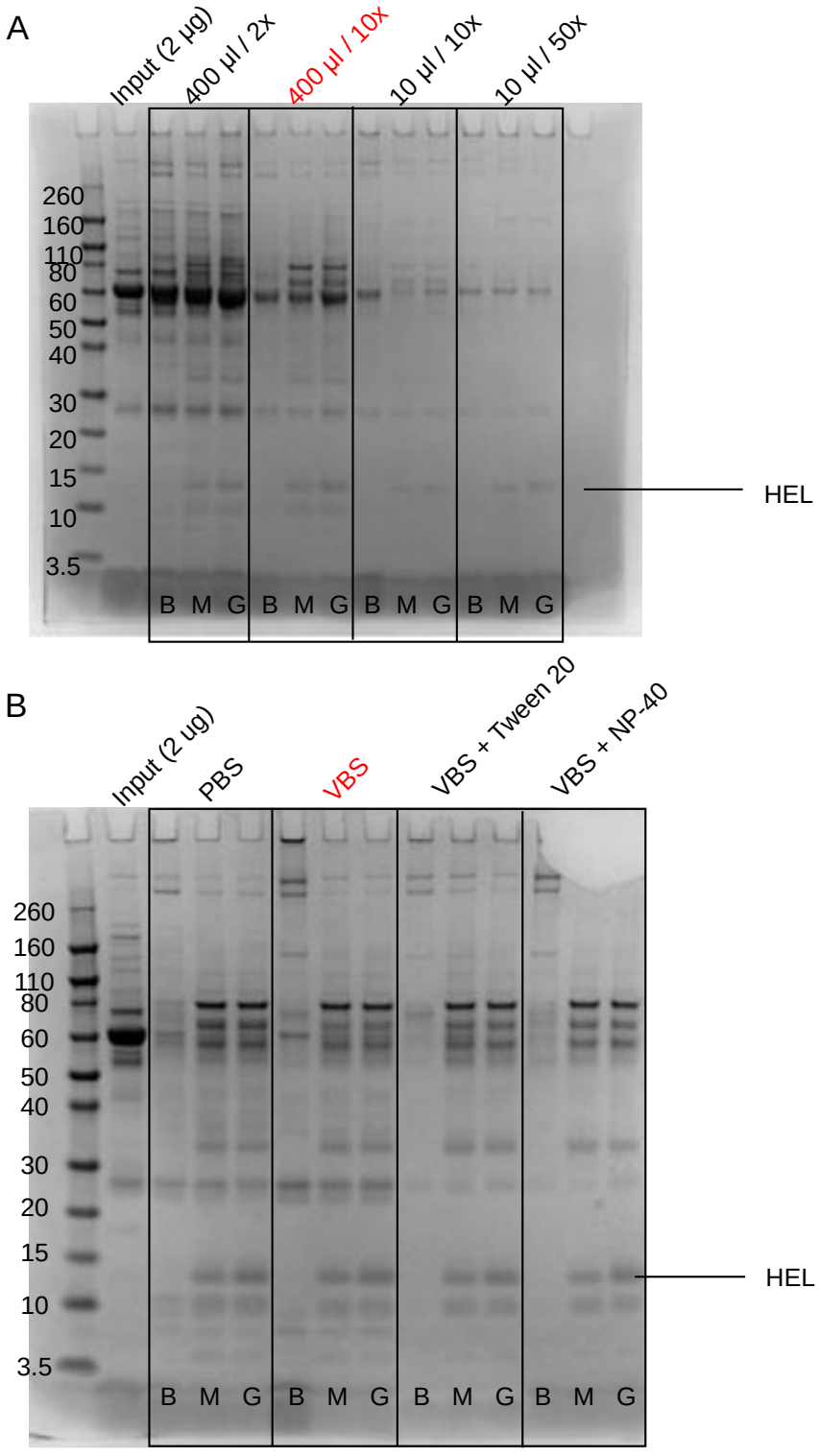


Figure A.9: Setting up conditions for the HEL mock, HEL GA and HEL PR pull-down experiment. 0.3 mg magnetic beads were incubated in the indicated volumes and dilutions of human plasma-derived sera in various buffers and detergents at RT for 1 h, washed and boiled in LDS sample buffer containing reducing agent, then run on SDS-PAGE and stained with a Coomassie-based dye. B = unconjugated beads, M = HEL mock conjugated beads, G = HEL GA conjugated beads.

Table A.1: Over representation analysis (ORA) of pull-down hits compared with background show significant enrichment of terms and pathways. 60 proteins with > 1 FC in HEL GA compared with HEL mock, HEL PR and beads were analysed against a background reference of the entire human proteome using DAVID. Top 10 annotation clusters shown. Annotation clusters containing terms with consistently low p-values have high enrichment scores (geometric mean of p-values in -log scale). Terms within each cluster were summarised for clarity and presented with the best q-value (corrected p-value).

Annotation Cluster	Cluster Enrichment Score	Best q-value
Complement and innate immunity	7.612079651	4.99E-23
Extracellular	14.85710349	2.73E-19
Coagulation	5.399829684	1.10E-09
Sushi-like domain	6.025744808	4.12E-09
EGF-like domain	4.489472942	2.22E-07
Endopeptidase inhibition	4.322087494	5.54E-07
Heparin binding	2.866143123	4.38E-06
Peptidase	4.520810289	5.74E-06
Immune response	2.782799793	4.23E-04